

PLANT SPECIES DETECTION AND CLASSIFICATION WITH IMAGE ANALYSES FOCUSSED ON DEEP LEARNING TECHNIQUES IN NATURAL ENVIRONMENTS

PhD Thesis



Sarah Brandt (*née* Kentsch)
United Graduate School of Agricultural Sciences - Yamagata University

Foreword

On the first view this thesis gigantic number of papers, pages, images and words and the reader might want to put the thesis away as it just seems to be too much. But before you, dear reader, put aside this heavy piece of a work, take a moment for reading this foreword and reconsider your decision. This study is composed of the main study, a side project, three kinds of forests, 13 studied sites, three methodologies, four seasons of data and three years of work. During my time as a PhD student, I was able to learn and practice the application of three completely different topics: Forestry science, Geographic Information Systems and deep learning. I had three years to learn to deal with the terms of all these fields and to understand all three sides, and I can say I made it. I dealt with scientists from three different specialities, communicated between them and focussed on the main goal of this study to finish a work, which might influence the field I am working in. (By the way, once during my studies, I had a lecture in geologic engineering, as student of geosciences, and the professor told us, when you put an engineer and a geologist together in a room and tell them to build a house: the engineer will talk about constructions and the geologist about soils and rocks, but both will not understand the other. So, believe me, it's kind of hard work to be the facilitator between three parties that do not really understand each other.

So, all the experiences I made and challenges I faced are part of this thesis. My goal with this study is to provide the necessary information to understand what I did and to follow the work.

Now dear reader, I want to explain you how this thesis is supposed to work. You will find an introduction and state of the art, which explains the study and their objectives. The following part is a long methodology chapter. It is composed of information of the three methodologies applied, important terms, which are needed to be understood and explanations about what we need and how to apply. This chapter contains the explanations for the forestry side of the work. In case you are from the forestry side, you may want to skip explanations about the structure of forests, tree species, diversity indices and how forests are classified. Explanations about image analysis and more precise deep learning are maybe completely new for you, terms like transfer learning, raster and Gaussian smoothing sounds like talking about the outer space. But fast forest inventories and automatic classification sounds like a dream for you, then you are most probably interested in getting a quick overview of terms and application in my image analysis and deep learning chapter. Perhaps you are not from forestry, but deep learning, then you are most probably an expert in you field and don't need any explanations on deep leaning. You are maybe sick of medical images and now want to apply your skills in the field of forestry, but you don't know anything about forests or what you can do to help with your expertise, please have a closer look at the forestry side of this study. Please, dear reader, do

not misunderstand me, you don't have to be from one of the mentioned fields, as long as you are interested in any aspect of this thesis you are invited to have a look into this.

As having said this also the single chapters focus on different topics: some more related to forestry, some to image analysis and some to deep learning. Each chapter has its own small introduction, methodology part, results part and discussion part. So, dear reader, you can pick a single chapter, read it and you will find all necessary information that you need to understand it. Again, when you want to know more, please refer to the methodology chapter. An exemption is my main topic, which are the last chapters of my thesis. Of course, you can also read single chapters there with a full understanding of what happened there, but this study is a comprehensive work of the different methodologies, which in the end work as one functional construction. Therefore, there is a separate chapter, which discusses the results of all results gathered for the study sites in the mixed forest in Shonai area.

To come to an end now, I hope I was able to explain you my idea behind this work. I hope, dear reader, you are now less afraid of the immense number of words lying in front of you. Take your time to check the table of content and find the piece of work, which interests you and have a look at it. I can promise you will not waste your time.

Table of contents

I.	List of Figures.....	10
II.	List of Tables.....	13
III.	Acknowledgements.....	15
IV.	Index of abbreviation.....	17
V.	Summary in English.....	19
VI.	Summary in Japanese.....	22
VII.	List of publications.....	24
	Chapter 1 Introduction.....	25
	Chapter 2 State-of-the-Art.....	30
	Chapter 3 Material and Methods.....	34
3.1	Climate.....	34
3.2	Japanese Forests.....	34
3.3	Japan forest policy.....	38
3.4	Forest types.....	39
3.4.1	Riparian forest.....	39
3.4.2	<i>Quercus</i> and <i>Fagus</i> forests.....	41
3.5	Composition of the research forest.....	43
3.5.1	Studied Sites.....	43
3.5.2	YURF - Top sites.....	47
3.6	Fieldwork.....	47
3.6.1	Tree species.....	48
3.7	Forest classification systems.....	62
3.8	Diversity measures.....	63
3.8.1	Species richness (<i>S</i>).....	64
3.8.2	Shannon index (<i>H</i>).....	64
3.8.3	Simpson index (<i>D</i>).....	64
3.8.4	Shannon Evenness.....	66
3.8.5	Hill numbers.....	66
3.8.6	Partitioning diversity.....	66
3.9	Data gathering.....	67
3.9.1	Georeferencing.....	68
3.10	Data Processing.....	69
3.10.1	Images.....	69

3.10.1.1	Image formats	69
3.10.1.2	Digital Elevation Models.....	70
3.10.3	Image Processing.....	71
3.10.3.1	Metashape.....	72
3.10.3.2	GIMP	73
3.11	Geographic information systems	73
3.11.1	ArcGIS	73
3.11.2	ArcGIS – Tools.....	74
3.12	Machine learning.....	80
3.12.1	Artificial Intelligence.....	80
3.12.2	Deep Learning.....	81
3.12.2.1	Convolutional Neural Networks	82
3.12.2.2	CNNs from an image point of view.....	82
3.12.2.3	Image analysis with computer vision	83
3.12.2.4	Deep learning techniques and settings	84
3.12.3	Multi-label patch classification using ResNet.....	86
3.12.4	Segmentation refinement using watersheds	88
3.12.5	Image segmentation using UNet	89
3.13	Evaluation Methods	89
Chapter 4	Tree species classification.....	93
Chapter 4.1	Assessing natural mixed forest composition, distribution and structure using field inventories.....	94
4.1.1	Problem definition.....	94
4.1.2	Data collection.....	95
4.1.2.1	Field surveys	95
4.1.3	Results	95
4.1.3.1	Species composition	95
4.1.3.2	Tree census.....	100
4.1.3.3	Tree species dominance	102
4.1.3.4	Field surveys and tree distributions	104
4.1.3.5	Forest diversity	108
4.1.3.6	Layering of mixed forests	109
4.1.4	Discussion	112
4.1.4.1	Challenges during the field work.....	112
4.1.4.2	Tree species distribution	113
4.1.4.3	Forest structure	117

4.1.4.4 Forest classification	119
4.1.4.5 Comparison of different riparian and mountain forests in Japan	120
4.1.5 Conclusion	122
Chapter 4.2 Tree species diversity in different kind of cold-temperate forests calculated on image-based analysis.....	123
4.2.1 Problem definition.....	123
4.2.2 Methodology	124
4.2.2.1 Data collection.....	124
4.2.2.2 Data processing	124
4.2.2.3 Image analysis	124
4.2.2.3.1 Census code.....	124
4.2.2.4 Species diversity	125
4.2.3 Results – Diversity	126
4.2.4 Discussion	137
4.2.4.1 Species distribution and abundances.....	137
4.2.4.2 Diversity indices.....	138
4.2.5 Conclusion	140
Chapter 4.3 Assessment of Forest composition and distribution with image analysis.....	141
4.3.1 Problem definition.....	141
4.3.2 Methodology	142
4.3.2.1 Image surveys and data preparation.....	142
4.3.2.2 Pixel counting code.....	142
4.3.2.3 GIS analysis	142
4.3.2.4 Data analysis.....	143
4.3.2 Results	145
4.3.2.1 Site characteristics.....	145
4.3.2.2 Forest area distribution	149
4.3.2.3 Forest composition and distribution	152
4.3.2.4 Tree counts and distribution	154
4.3.2.5 Canopy area, densities and relative dominance of tree species.....	154
4.3.2.6 Tree species frequencies and abundances.....	163
4.3.2.7 Forest main tree species areas.....	165
4.3.2.8 Area per tree	166
4.3.3 Discussion	168
4.3.3.1 Species composition	168
4.3.3.2 Species distribution	170

4.3.3.3	Tree canopy areas	171
4.3.3.4	Forest classification on image-based analysis	172
4.3.4	Conclusion	173
Chapter 4.4:	Analysis of Forest composition, diversity and structure with GIS applications	175
4.4.1	Problem definition	175
4.4.2	Methodology	177
4.4.2.1	Data collection and processing	177
4.4.2.2	Manual annotations	178
4.4.2.3	Point shapefiles	178
4.4.2.4	Application of ArcGIS tools	179
4.4.3	Results	181
4.4.3.1	Tree species composition	181
4.4.3.2	Tree species distribution	182
4.4.3.3	Image analysis – spatial tree species distribution	187
4.4.3.4	Large scale image analysis	192
4.4.4	Discussion	197
4.4.4.1	Surveying with GIS methods	197
4.4.4.2	Forest structure	199
4.4.4.3	Evaluation of spatial pattern in the data	200
4.4.4.3.1	Site-scale analysis	200
4.4.4.3.2	Large-scale analysis	202
4.4.5	Conclusion	203
Chapter 5	Semi-automatic counting of deciduous trees in images of a dense natural broadleaved forest – an evaluation	205
5.1	Introduction	205
5.1.1	Problem definition	206
5.2	Methodology	207
5.2.1	Study sites and field data	207
5.2.2	Data gathering	207
5.2.3	Data processing	208
5.2.4	Evaluation methods	210
5.3	Results	210
5.3.1	Field observations	210
5.3.2	Counting measures	211
5.4	Discussion	215
5.4.1	Time and technique consideration	216

5.4.2 Observations and difficulties	217
5.5 Conclusion	218
Chapter 6: Deep learning tree species classification.....	219
6.1: Computer vision and deep learning techniques for the analysis of UAV-acquired forest images, a transfer learning study	219
6.1.1 Introduction.....	219
6.1.2 Methodology	221
6.1.2.1 Data Acquisition	221
6.1.2.2 Problem definition.....	221
6.1.2.3 Data Processing and Annotation	222
6.1.2.4 Problem Formalisation	224
6.1.2.5 Multi-label Patch Classification Using ResNet.....	225
6.1.2.6 Segmentation Refinement using watersheds	226
6.1.2.7 Forest Orthomosaic Segmentation Using UNet	227
6.1.2.8 Experiments.....	228
6.1.2.9 Evaluation Methods.....	228
6.1.3 Results	229
6.1.3.1 Experiment 1: Transfer learning and multi-label patch classification	229
6.1.3.2 Experiment 2: Semantic segmentation	232
6.1.4 Discussion	235
6.1.5 Conclusion	237
6.2 Automatic tree species classification	238
6.2.1 Problem definition.....	238
6.2.2 Methodology	239
6.2.2.1 Data collection and processing.....	239
6.2.2.2 Manual annotations	240
6.2.2.3 Semantic segmentation with UNet	240
6.2.2.4 Evaluation	240
6.2.3 Results	241
6.2.3.1 Initial experiments.....	242
6.2.3.2 Experiment with 13 classes	244
6.2.3.3 Level 1 Segmentation	246
6.2.3.4 Semantic segmentation	248
6.2.4 Discussion	248
6.2.4.1 Misclassification	250
6.2.4.2 Over- and Underpredictions.....	251

6.2.5 Conclusion	252
Chapter 7 Invasive species - Two application examples of image analysis and deep learning.....	253
7.1 Introduction invasive species	253
7.2 State-of-the-Art	254
7.3 Coastal Forests	256
7.3.1 Methodology	256
7.3.1.1 Study site coastal forest and problem definition	256
7.3.1.2 Data processing	257
7.3.1.3 Deep learning methods	257
7.3.2 Results – Detection of invasive tree species in the coastal forest	258
7.3.3 Discussion	260
7.3.3.1 Data imbalance	260
7.3.3.2 Effects of coastal forests.....	260
7.3.3.3 Study assumptions and limitations	261
7.3.4 Conclusion	262
7.4 Analysis of UAV-acquired wetland orthomosaics using GIS, computer vision, computational topology and deep learning	263
7.4.1 Wetlands.....	263
7.4.1.1 Problem definition Blueberries	264
7.4.2 Study area.....	265
7.4.3 Description of the blueberry species.....	266
7.4.4 Data collection and pre-processing	268
7.4.4.1 Data processing using ArcGIS	268
7.4.5 Deep learning techniques.....	270
7.4.5.1 Deep learning architectures	270
7.4.5.2 Data augmentation and transfer learning.....	271
7.4.6 Evaluation	272
7.4.7 Results	273
7.4.7.1 Quantitative analysis of the blueberry invasion.....	274
7.4.7.2 Analysis of spread patterns	278
7.4.7.3 Deep learning results.....	281
7.4.7.3.1 Experiment 1: Assessment of deep learning architectures and settings	282
7.4.7.3.2 Experiment 2: Comparison of different networks.....	282
7.4.7.3.3 Experiment 3: Deep learning application	285
7.4.8 Discussion	287
7.4.8.1 Difficulties with data.....	287

7.4.8.2	Application in landscape management	288
7.4.8.3	Automatic masks generation.....	290
7.4.8.4	Contribution to invasive blueberry studies in wetlands.....	291
7.4.8.5	Deep learning studies	292
7.4.9	Opportunities, limitation and future works	292
7.4.10	Conclusion	293
Chapter 8	Discussion	294
8.1	Seasonal effects.....	294
8.2	Time consideration.....	296
8.3	Area and spatial resolution consideration	297
8.4	Benefits and difficulties during flights.....	299
8.5	Tree detection and classification of tree species using image and field data.....	300
8.5.1	Tree detection	300
8.5.2	Tree classification	302
8.6	Forest structure	307
8.6.1	Forest structures along rivers.....	307
8.6.2	Structures in Slope sites	309
8.7	Tree species distribution	310
8.8	Species diversities, disturbances and coexistence in Japanese forests	312
8.9	Forest classification bases on images and field surveys.....	315
8.10	Mixed forest classification.....	318
8.11	Automatic classification	319
8.11.1	Data issues.....	319
8.11.2	Comparison of deep learning setting and architectures.....	321
Chapter 9	Conclusion	323
VIII.	Reference list.....	325
IX.	Internet sources	347
X.	Appendix i – iv.....	351
XI.	Appendix A – N	355

I. List of Figures

FIGURE 1 OVERVIEW OF THE RESEARCH FLOW..... 28

FIGURE 2 OVERVIEW OF FORESTRY REMOTE SENSING APPLICATIONS (GUIMARÃES ET AL., 2020)..... 30

FIGURE 3 VEGETATION ZONES OF JAPAN (PIAZZA, 2007) 35

FIGURE 4 FOREST AREA IN PERCENT LOCATED IN DIFFERENT SLOPE ANGLES (MODIFIED AFTER LUNBÄCK ET AL., 2020) 36

FIGURE 5 DISTRIBUTION OF CONIFEROUS FORESTS (MAKIMOTO, 2019) 37

FIGURE 6 DISTRIBUTION OF BROAD-LEAVED FORESTS (MAKIMOTO, 2019) 37

FIGURE 7 COMPOSITION OF FOREST ECOSYSTEM BY DOMINANT TREE SPECIES (MAKIMOTO, 2019)..... 38

FIGURE 8 CHARACTERISTIC STRUCTURE OF RIPARIAN FOREST AREAS (NAIMAN, 1997). 39

FIGURE 9 LOCATION OF STUDY AREAS..... 46

FIGURE 10 THREE COMMUNITIES WITH DIFFERENT EVENNESS AT THE TOP AND DIAGRAMS OF THE SPECIES ABUNDANCE CORRESPONDING TO THE THREE COMMUNITIES ON THE BOTTOM. ([HTTPS://WWW.DAVIDZELENY.NET/ANADAT-R/DOKU.PHP/EN:DIV-IND](https://www.davidzeleeny.net/anadat-r/doku.php/en:div-ind), LATEST ACCESS 26. APRIL 2021) 65

FIGURE 11 EXAMPLE DIAGRAMS FOR THE SPECIES RICHNESS, SHANNON ENTROPY AND GINI-SIMPSON INDEX BASED ON THE SPECIES NUMBER AND UNEVENNESS ([HTTPS://WWW.DAVIDZELENY.NET/ANADAT-R/DOKU.PHP/EN:DIV-IND](https://www.davidzeleeny.net/anadat-r/doku.php/en:div-ind), LATEST ACCESS 26. APRIL 2021) 65

FIGURE 12 DIVERSITY PROFILES FOR THREE COMMUNITIES ([HTTPS://WWW.DAVIDZELENY.NET/ANADAT-R/DOKU.PHP/EN:DIV-IND](https://www.davidzeleeny.net/anadat-r/doku.php/en:div-ind), LATEST ACCESS 26. APRIL 2021) 67

FIGURE 13 EXAMPLE IMAGES OF DSM AND DTM. THE UPPER IMAGE SHOWS A SKETCH, WHERE THE RED LINE SHOWS THE DSM AND THE BLUELINE THE DTM. THE BOTTOM IMAGE SHOWS HOW THE DTM AND DSM OF A REAL-WORLD EXAMPLE ([HTTPS://WWW.GISRESOURCES.COM/CONFUSED-DEM-DTM-DSM/](https://www.gisresources.com/confused-dem-dtm-dsm/), LATEST ACCESS 15. MARCH 2021)..... 71

FIGURE 14 GENERAL WORKFLOW IN METASHAPE, WHERE FIRST THE ACQUIRED IMAGES ARE INPUTTED, THEN ALIGNED TO CREATE FIRST A SPARE, THEN A DENSE POINT CLOUD. THE DENSE POINT CLOUD IS THE BASIS TO GENERATE THE ORTHOMOSAIC, DSM AND THE DTM (GUIMARÃES ET AL., 2020)..... 72

FIGURE 15 THE EQUATION USED FOR CALCULATING THE KERNEL DENSITY OF POINTS..... 74

FIGURE 16 IN- AND OUTPUT OF THE TOOL COLLECT EVENTS, WHEREBY THE OUTPUT SHOWS THE WEIGHED POINTS BY HAVING DIFFERENT RADII ([HTTPS://PRO.ARCGIS.COM/EN/PRO-APP/LATEST/TOOL-REFERENCE/SPATIAL-STATISTICS/COLLECT-EVENTS.HTM](https://pro.arcgis.com/en/pro-app/latest/tool-reference/spatial-statistics/collect-events.htm), LATEST ACCESS 14. MARCH 2021) 75

FIGURE 17 EXAMPLE OF A HOT SPOT ANALYSIS OF A POINT SHAPEFILE. RED ARE THE SIGNIFICANT HOT SPOTS; WHILE BLUE ARE THE SIGNIFICANT COLD SPOTS, WHILE DARKER COLOURS REPRESENT A HIGHER CONFIDENCE INTERVAL ([HTTPS://PRO.ARCGIS.COM/EN/PRO-APP/LATEST/TOOL-REFERENCE/SPATIAL-STATISTICS/OPTIMIZED-HOT-SPOT-ANALYSIS.HTM](https://pro.arcgis.com/en/pro-app/latest/tool-reference/spatial-statistics/optimized-hot-spot-analysis.htm), LATEST ACCESS 14. MARCH 2021) 75

FIGURE 18 EXAMPLE OF FILTER OUTPUT USING A LOW PASS FILTER WITH A 3 X 3 KERNEL, [HTTPS://PRO.ARCGIS.COM/EN/PRO-APP/LATEST/TOOL-REFERENCE/SPATIAL-ANALYST/HOW-FILTER-WORKS.HTM](https://pro.arcgis.com/en/pro-app/latest/tool-reference/spatial-analyst/how-filter-works.htm), LATEST ACCESS 03. FEBRUARY 2021 76

FIGURE 19 EXAMPLE OF TWO RECTANGLE KERNELS AND THE INCLUDED AND PROCESSED CELLS. ([HTTPS://PRO.ARCGIS.COM/EN/PRO-APP/LATEST/TOOL-REFERENCE/SPATIAL-ANALYST/FOCAL-STATISTICS.HTM](https://pro.arcgis.com/en/pro-app/latest/tool-reference/spatial-analyst/focal-statistics.htm), LATEST ACCESS 03. FEBRUARY 2021) 77

FIGURE 20 EXAMPLE OF THE TOOL FOCAL STATISTICS AND HOW IT CONVERTS THE INPUT RASTER INTO AN OUTPUT RASTER. ([HTTPS://PRO.ARCGIS.COM/EN/PRO-APP/LATEST/TOOL-REFERENCE/SPATIAL-ANALYST/FOCAL-STATISTICS.HTM](https://pro.arcgis.com/en/pro-app/latest/tool-reference/spatial-analyst/focal-statistics.htm), LATEST ACCESS 03. FEBRUARY 2021) 77

FIGURE 21 THE IMAGE SHOWS THE SURFACE SCANNING WINDOW AS A 3 X 3 MATRIX. THE CALCULATION IS PERFORMED FOR PIXEL E, WHILE A TO I ARE THEIR CONSIDERED NEIGHBOURS ([HTTPS://PRO.ARCGIS.COM/EN/PRO-APP/LATEST/TOOL-REFERENCE/3D-ANALYST/HOW-SLOPE-WORKS.HTM](https://pro.arcgis.com/en/pro-app/latest/tool-reference/3d-analyst/how-slope-works.htm), LATEST ACCESS 09. FEBRUARY 2021) 77

FIGURE 22 ASPECT DIRECTIONS AND THEIR COLOUR DISTRIBUTION USED BY ARCGIS 78

FIGURE 23 THE FUNCTION OF THE ARCGIS TOOL NEAR AND HOW IT WORKS WITH DIFFERENT INPUT FEATURE CLASSES ([HTTPS://PRO.ARCGIS.COM/EN/PRO-APP/LATEST/TOOL-REFERENCE/ANALYSIS/NEAR.HTM](https://pro.arcgis.com/en/pro-app/latest/tool-reference/analysis/near.htm), LATEST ACCESS 14.03.2021).... 78

FIGURE 24 EXAMPLE OF SUMMARIZING FEATURES IN POLYGONS. FIRST ROW: POINTS IN POLYGONS; SECOND ROW: LINES IN POLYGONS; THIRD ROW: POLYGONS IN POLYGONS ([HTTPS://PRO.ARCGIS.COM/EN/PRO-APP/LATEST/TOOL-REFERENCE/BIG-DATA-ANALYTICS/SUMMARIZE-WITHIN.HTM](https://pro.arcgis.com/en/pro-app/latest/tool-reference/big-data-analytics/summarize-within.htm), LATEST ACCESS 12.04.2021) 80

FIGURE 25 DIAGRAM PLOTTING THE DIFFERENT FIELDS OF AI. THE BOXES WITH THE GREEN TEXT ARE WAYS HUMAN INTELLIGENCE IS USED AND THEY ARE PLACED CLOSE TO THE PART OF HOW AI CAN COPY HUMAN INTELLIGENCE..... 80

FIGURE 26 EXAMPLES OF KERNELS, WHICH IDENTIFY DIFFERENT FEATURE MAPS (LÓPEZ-JIMÉNEZ, 2019)..... 81

FIGURE 27 INFLUENCE OF TRANSFER LEARNING ON THE PERFORMANCE OF A NETWORK (BROWNLEE, 2017) 86

FIGURE 28 MODEL COMPLEXITY PLOTTED AGAINST THE ERROR (HTTPS://ZAHIDHASAN.GITHUB.IO/2020/10/13/BIAS-VARIANCE-TRADE-OFF-AND-LEARNING-CURVE.HTML , LATEST ACCESS 19. MARCH 2021)	92
FIGURE 29 STRUCTURE OF THE TREE SPECIES CLASSIFICATION CHAPTER. THE STARS INDICATE THE DIFFERENT SUBCHAPTERS	93
FIGURE 30 STRUCTURE OF THE CHAPTER FIELD INVENTORIES WITH THE FOCUS ON FOREST COMPOSITION, DISTRIBUTION AND STRUCTURE	94
FIGURE 31 INVESTIGATED FIELD SURVEY AREA (APPROX.) FOR SLOPE SITES	98
FIGURE 32 SPECIES DISTRIBUTION IN THE THREE CONSIDERED SITES: RIPARIAN (TOP), TERRACE (MIDDLE), SLOPE (BOTTOM). THE X-AXIS: THE TREE SPECIES; THE Y-AXIS: TREE COUNTS PER SPECIES.....	99
FIGURE 33 LOCATION OF THE TREES ON ISLAND OF SITE 1.....	101
FIGURE 34 ORTHOMOSAIC OF SITE 1, WITH THE PURPLE SURROUNDED AREA OF THE SAMPLE PLOT 1. IN BLACK STRIPS, THE LOCATION OF JUGLANS AILANTIFOLIA TREES IS MARKED, IN GREY STRIPS THE LOCATION OF AESCULUS TURBINATA, IN THE BLUE CIRCLE PHELLODENDRON AMURENSE TREE, IN RED.....	101
FIGURE 35 TREE SPECIES, WHICH ACCOUNTS 95 % OF ALL TREES	104
FIGURE 36 FIELD SURVEY OF SITE 1, DIGITALISED IN ARCGIS PRO	105
FIGURE 37 FIELD SURVEY OF SITE 12, DIGITALISED IN ARCGIS PRO	106
FIGURE 38 LAYERING OF THE FOREST	110
FIGURE 39 SPECIES ABUNDANCE FOR ALL 13 SITES.....	136
FIGURE 40 RELATIONSHIP BETWEEN THE SPECIES RICHNESS AND THE AREA IN HECTARE	136
FIGURE 41 FILTERED DEM OF SITE 2, WHICH WAS PROCESSED IN ARCGIS PRO.....	146
FIGURE 42 ASPECT OF SITE 2 GENERATED WITH ARCGIS PRO BASED ON THE DEM, WHICH WAS FILTERED AND SMOOTHENED BEFORE	147
FIGURE 43 SLOPE MAP OF SITE 2 GENERATED BY ARCGIS PRO ON THE BASIS OF THE FILTERED AND SMOOTHENED DEM	148
FIGURE 44 SKETCH OF THE SURFACE TYPES IN RIPARIAN AREAS. THE ABBREVIATIONS USED ARE: LFC = LOW-FLOW CHANNEL, AC = ACTIVE CHANNEL, FP = FLOODPLAIN, SC = SECONDARY CHANNEL, T = TERRACE, VW = VALLEY WALL AND AF = ACTIVE/INACTIVE ALLUVIAL FAN (GRANT ET AL.).....	149
FIGURE 45 AREA DISTRIBUTIONS FOR ALL COUNTED PIXEL (WITHOUT THE ROI) AND THE ONES BELONGING TO THE ROI IN THE LEFT FIGURES AND THE DISTRIBUTIONS OF TREES, UNDERSTORY VEGETATION, GROUND, RIVER AND RIVERBED WITHIN THE ROI SHOWN IN THE RIGHT FIGURES.....	151
FIGURE 46 COUNTS PER SPECIES FOR THE DIFFERENT SITES, WHICH ARE CONSIDERED: TOP, SLOPE, TERRACE AND RIPARIAN SITES..	156
FIGURE 47 DETAILED COUNTS FOR THE CONSIDERED SITES SEPARATED: RIPARIAN, TERRACE AND SLOPE SITES. IN EACH DIAGRAM, THE COUNTS PER SITE ARE SHOWN	158
FIGURE 48 INFORMATION ABOUT THE TREE DENSITIES 18 TREE SPECIES CLASSES. NOTE THAT THE TWO OCCURRING SALIX SPECIES WERE GROUPED TOGETHER IN THIS GRAPHIC, AS WELL AS THE SMALL-LEAVED ACER SPECIES	159
FIGURE 49 FREQUENCY OF MAIN SPECIES OF ALL SITES.....	164
FIGURE 50 CANOPY AREA PER TREE FOR ALL SITES, DIVIDED INTO SPECIES WHICH MAINLY OCCUR IN RIPARIAN AND TERRACE SITES (A) AND SPECIES THAT MAINLY OCCUR IN TERRACE AND SLOPE SITES (B).....	167
FIGURE 51 OVERVIEW OF STUDY.....	176
FIGURE 52 GENERATED POINT SHAPEFILES AND MAPS, AN OVERVIEW.....	178
FIGURE 53 COUNT MAP (LEFT), SPECIES MAP WITHOUT ORTHOMOSAIC (MIDDLE) AND WITH ORTHOMOSAIC (RIGHT) OF SITE 1	184
FIGURE 54 SPECIES COUNTS FOR SITE 1 AND SITE 6, AUTOMATICALLY GENERATED BY ARCGIS.....	185
FIGURE 55 SITE 5 TREE SPECIES MAP AND TREE SPECIES SURVEY MAP	186
FIGURE 56 TREE SPECIES DISTRIBUTIONS DEPENDENT ON THE DISTANCE TO THE RIVER AND THE HEIGHT	189
FIGURE 57 THREE MAPS OF SITE 1, THE RESULTS OF: HOT SPOT ANALYSIS, COUNTING IN A FISHNET GRID AND DENSITY MEASURES (16 M).....	191
FIGURE 58 DISTRIBUTION OF PTEROCARYA RHOIFOLIA, ACER MONO MAXIM AND JUGLANS AILANTIFOLIA IN THE SOUTHERN SITES OF YURF	194
FIGURE 59 DISTRIBUTION OF AESCULUS TURBINATA, QUERCUS MONGOLICA AND JUGLANS AILANTIFOLIA IN THE NORTHERN SITES OF YURF	195
FIGURE 60 HOT SPOT ANALYSIS MAPS FOR THREE EXAMPLES, JUGLANS AILANTIFOLIA IN THE SOUTHERN SITES, ACER MONO MAXIM IN THE NORTHERN SITES AND THE RIPARIAN – TERRACE HOT SPOT MAP	196
FIGURE 61 LOCATION OF THE STUDY AREA YURF. THE LEFT IMAGE SHOWS THE LOCATION IN JAPAN, THE MIDDLE IMAGE SHOWS THE LOCATION OF YURF AND THE RIGHT IMAGE THE STUDY SITES.....	208

FIGURE 62 EXAMPLE DATA (EXAMPLE SITE 1). FROM LEFT: THE DEM, THE SUMMER ORTHOMOSAIC, THE WINTER ORTHOMOSAIC AND THE SUMMER ORTHOMOSAIC WITH THE SELECTED PARTS.	209
FIGURE 63 WORKFLOW FOR THIS STUDY.....	209
FIGURE 64 TREE TOP ANNOTATIONS FOR S1A. FROM LEFT: ANNOTATIONS BASED ON THE SUMMER IMAGE, ANNOTATIONS BASED ON THE WINTER IMAGE AND THE FIELD DATA OVERLAYED ON THE SUMMER IMAGE.	213
FIGURE 65 S1B WITH THE ANNOTATIONS SEPARATED INTO CANOPY LAYER TREES, UNDERSTORY AND YOUNG TREES.	216
FIGURE 66 OVERVIEW OF THE CONTRIBUTION	220
FIGURE 67 LOCATION OF THE SITES WHERE DATA WAS ACQUIRED. THE MIDDLE UPPER MAP SHOWS THE LOCATION OF THE STUDY AREA IN JAPAN, WHEREBY YURF IS MARKED AS ORANGE POINT. THE MAP ALSO CONTAINS THE (ORANGE) AREA OF YURF. THE FIVE IMAGES AT THE RIGHT SHOW REPRESENTATIVE ORTHOMOSAIC FOR EACH SITE	222
FIGURE 68 EXAMPLE OF A WINTER ORTHOMOSAIC. EXAMPLES OF PATCHES EACH CONTAINING A SINGLE DIFFERENT CLASS.....	223
FIGURE 69 EXAMPLE IMAGES OF DIFFICULTIES FACED WITH THE DATA. IMAGES ARE EXAMPLES OF THE MIXED FOREST.....	224
FIGURE 70 ALGORITHM PIPELINE	225
FIGURE 71 A SMALL SECTION (PATCH) OF A WINTER ORTHOMOSAIC. PATCH OF AN RGB IMAGE AS CAPTURED BY THE UAV (LEFT). MASK WITH THE ANNOTATIONS SHOWING THE CLASS OF EACH PIXEL (MIDDLE), IN THIS CASE BLUE PIXELS BELONG TO THE "EVERGREEN" CLASS, YELLOW PIXELS TO THE "VOID" CLASS. THIS MASK SERVES AS THE GROUND TRUTH FOR THE SEMANTIC SEGMENTATION FORMALISATION. SUPERPOSITION OF THE TWO PREVIOUS IMAGES (RIGHT). CONSEQUENTLY, THE GROUND TRUTH FOR THIS PATCH WAS THE LIST [RIVER, UNCOVERED, EVERGREEN] FOR THE MULTI-LABEL CLASSIFICATION FORMALISATION.	225
FIGURE 72 (A) TOTAL AGREEMENT (TA), (B) ACCUMULATED VALUE OF TOTAL AGREEMENT WITH FALSE POSITIVES (TAFP), (C) PARTIAL AGREEMENT (PA), (D) ACCURACY (ACC), (E) SENSITIVITY (SENS), AND (F) SPECIFICITY (SPEC) FOR WINTER ORTHOMOSAIC DATA. PATCH SIZE IS 150. FROZEN MODELS END WITH AN F, UNFROZEN MODELS WITH UNF.....	231
FIGURE 73 EXAMPLES OF THE DIFFERENT TYPES OF PROBLEMS SOLVED WITH DL (DIEZ ET AL., 2021).....	241
FIGURE 74 A) THE FOLLOWING PLOT REPRESENTS THE DISTRIBUTION OF THE SPECIES PER MOSAIC. THEREFORE, ALL COLUMNS SHOULD SUM UP TO 100% B) THE FOLLOWING PLOT REPRESENTS THE DISTRIBUTION OF THE SPECIES OF A GIVEN MOSAIC (ALL LINES SHOULD SUM UP TO 100%)	243
FIGURE 75 PRECISION MATRIX A) ALL SITES (LEFT) B) SPECIFIC SITES (RIGHT).....	244
FIGURE 76 RECALL MATRIX A) ALL SITES (LEFT) B) SPECIFIC (RIGHT)	245
FIGURE 77 CONFUSION MATRICES ONLY SITE 1 TO 13 A) ALL SITES (LEFT) B) SPECIFIC (RIGHT)	245
FIGURE 78 CONFUSION MATRICES A) TRAINING WITH 13 ORTHOMOSAICS AND 5 CLASSES (TOP) B) TRAINING WITH ALL ORTHOMOSAICS AND 5 CLASSES (MIDDLE) C) TRAINING WITH ALL ORTHOMOSAICS AND 11 CLASSES (BOTTOM)	247
FIGURE 79 GROUND TRUTH (LEFT) AND SEGMENTATION RESULT OF THE NETWORK (RIGHT).....	249
FIGURE 80 EXAMPLE OF THE COASTAL FOREST MOSAIC. EXAMPLES OF PATCHES EACH CONTAINING A SINGLE DIFFERENT CLASS	258
FIGURE 81 EXAMPLE OF THE COASTAL FOREST. MOSAIC WITH MARKED BLACK LOCUST AREAS (LEFT); EXAMPLE OF JAPANESE BLACK PINE TREES (MIDDLE); EXAMPLE OF BLACK LOCUST TREES (RIGHT)	259
FIGURE 82 RESULTS FOR THE MLP CLASSIFICATION OF THE COASTAL FOREST MOSAIC FOR THREE LEARNING RATES (LR). PIE CHARTS SHOW, TOTAL AGREEMENT (TA), TOTAL AGREEMENT WITH FALSE POSITIVES (TAFP), PARTIAL AGREEMENT (PA). THE BAR CHARTS SHOW CLASSIFICATION MEASURE FOR THE "BLACK LOCUST" AND "OTHER TREES" CLASSES: SENSITIVITY OR TRUE POSITIVE RATE (SENS), SPECIFICITY OR TRUE NEGATIVE RATE (SPEC) AND ACCURACY (ACC).....	259
FIGURE 83 LOCATION OF THE STUDY AREA IN THE NORTH OF GERMANY. IN THE UPPER RIGHT PART OF THE FIGURE THE STUDY SITES ARE MARKED WITH DIFFERENT COLOURS. THE BOTTOM RIGHT PART AN EXAMPLE ORTHOMOSAIC IS SHOWN WITH DETAIL OF THE DIFFERENT CLASSES	266
FIGURE 84 WORKFLOW OF THE CHAPTER. GRAY IS THE DATA BASE; PURPLE BOXES SHOW SOFTWARE/PROGRAMS USED IN THIS STUDY; WHITE BOXES WITH A BLUE OUTLINE ARE GENERATED FILES; DARK BLUE ARE PROCESSES USED FOR THE DL CLASSIFICATION AND DETECTION; LIGHT BLUE ARE TOOLS IN ARCGIS.....	267
FIGURE 85 IMAGE ANALYSIS WORKFLOW. CONSISTS OF TWO PARTS, THE MANUAL APPROACH USING MANUAL ANNOTATION, GIS AND PERSISTENT HOMOLOGY AND THE AUTOMATIC APPROACH USING DL AND SEGMENTATION TO ANALYSE THE BLUEBERRY INVASION	274
FIGURE 86 DISTRIBUTION OF ANNOTATED CLASSES FOR THE ORTHOMOSAICS B1 TO B3.....	275
FIGURE 87 DISTRIBUTION OF THE AREA AND HEIGHT VALUES OF BLUEBERRY BUSHES. FROM TOP TO BOTTOM: AREA, MAXIMUM HEIGHT AND MEDIAN HEIGHT.....	277

FIGURE 88 DENSITY MAP FOR THE BLUEBERRY SPECIES FOR THE SITES B1 TO B3. AREAS OF LOW DENSITIES ARE MARKED IN GREEN AND HIGH DENSITIES ARE RED COLOURED. A GRADIENT BETWEEN GREEN AND RED REPRESENTS VALUES OF MEDIUM DENSITY. WHITE POINTS MARK THE LOCATION OF THE BLUEBERRY BUSHES.....	280
FIGURE 89 THE PERSISTENT HOMOLOGY IS PLOTTED BY RADIUS AGAINST THE REGION. FOUR FUSED REGIONS WERE CONSIDERED: 1 %, 10 %, 50 % AND 90 % AND ALL SITES ARE PLOTTED	281
FIGURE 90 TPR (A) AND ACCURACY(B) RESULTS OF DIFFERENT TESTS FOR THE BLUEBERRY CLASS WITH F = FROZEN AND UNF = UNFROZEN NETWORK SETTINGS. ADDITIONALLY: DATA AUGMENTATION OR LOSS FUNCTION WEIGHTING WITH FNOA AND UNFNOA AND WITH LOSS FUNCTION WEIGHTING, FW AND UNFW, WITH FUNCTION WEIGHTING AND INTENSIVE USE OF DATA AUGMENTATION, FHA AND UNFHA (CABEZAS ET AL. 2020).....	283
FIGURE 91 TPR (A) AND ACCURACY (B) RESULTS OF THE NETWORK COMPARISON. NETWORKS: ALEXNET, RESNET50, RESNET152, VGG, DENSENET, RESNEXT, WIDERESNET (CABEZAS ET AL., 2020).....	284
FIGURE 92 COMPARISON OF RESNET50, RESNET152, VGG, DENSENET, RESNEXT, WIDERESNET TPRS	285
FIGURE 93 ORTHOMOSAIC B1 IS IMAGED WITH A COMBINATION OF THE MANUAL ANNOTATIONS (BLACK MARKED SPOTS), THE COARSE MASK (DARK GREY) AND THE REFINED MASK (LIGHT GREY). THE RED BOX WAS ZOOMED IN TO SHOW A DETAILED VIEW ON THE IMAGE AND MASKS	286
FIGURE 94 SIX CHARACTERISTIC IMAGES FROM THE FOREST. A) AN IMAGE OF AN AESCULUS TURBINATA TREE IN THE SPRING SEASON, B) ALBIZIA JULIBRISSIN IN EARLY SUMMER, C) AESCULUS TURBINATA WITH THEIR FLOWER IN EARLY SUMMER, D) PRUNUS SPECIES WITH CHARACTERISTIC COLOURING IN AUTUMN, E) ACER SPECIES IN AUTUMN AND F) FAGUS CRENATA IN AUTUMN	295
FIGURE 95 EXAMPLE IMAGES OF A) BETULA B) FRAXINUS C) TILIA D) SALIX	303
FIGURE 96 A) MIX OF SHRUB AND UNDERSTORY VEGETATION; B) JUGLANS WITH DRY LEAVES; C) MAGNOLIA WITH A CLIMBING PLANT; D) MAGNOLIA WITH DRY LEAVES; E) OAK TREE AND G) SAME TREE WITH HIGHER RESOLUTION; F) DARK LEAVED BEECH TREE AND H) WITH HIGHER RESOLUTION	305
FIGURE 97 SALIX JESSENSIS (A, C, E, G) AND SALIX SERISSAEFOLIA (B, D, F, H), WITH LEAVE IMAGES IN THE FIRST AND SECOND ROW, HIGH RESOLUTION IMAGES (APPROX. 1.3 CM/PIX) IN THE THIRD ROW AND NORMAL RESOLUTION IMAGES (APPROX. 2,73 CM/PIX)	306
FIGURE 98 FOREST PROFILE WITH CHARACTERISTIC TREE DISTRIBUTION.....	311
FIGURE 99 WALK PATH FOR THE FIELD INVENTORY IN SITE 3	317

II. List of Tables

TABLE 1 CHARACTERISTIC SPECIES IN QUERCUS MONGOLICA FORESTS IN TOHOKU AREA (OKITSU, 2003).....	42
TABLE 2 TREE SPECIES DESCRIPTIONS	49
TABLE 3 CONFUSION MATRIX FOR A CLASSIFICATION OF DECIDUOUS VS CONIFEROUS TREES. (IMAGES MODIFIED AFTER HTTPS://WWW.FREEPIK.COM/FREE-VECTOR/TREE-ICONS-PACK_813723.HTM , LATEST ACCESS 16. MARCH 2021).....	90
TABLE 4 IDENTIFIED TREE SPECIES IN THE FIELD, WITH THEIR SCIENTIFIC NAMES, FAMILY, GENERA AND LAYER. THE LAYERS CANOPY (C), SUBCANOPY (SC), UNDERSTORY (U) AND SHRUB (S) WERE ASSIGNED TO EACH SPECIES.	96
TABLE 5 COMPARISON FIELD PLOT (SITE 1) WITH WHOLE STUDY SITE 1	100
TABLE 6 DIVERSITY AND EVENNESS VALUES CALCULATED ON THE BASIS OF THE FIELD COUNTS.....	109
TABLE 7 THE CALCULATED SUM FOR THE LAYERS: CANOPY, SUBCANOPY, UNDERSTORY AND SHRUB ARE PRESENTED FOR EACH SITE .	112
TABLE 8 IMAGE-BASED TREE COUNTING.....	127
TABLE 9 CALCULATED DIVERSITY INDICES FOR ALL SITES.....	130
TABLE 10 CALCULATED SIMILARITIES BETWEEN ALL SITES, DIVIDED INTO RIPARIAN AND SLOPE SITES (HORN INDEX).....	131
TABLE 11 CALCULATED ALPHA DIVERSITY FOR THE RIPARIAN SITES	132
TABLE 12 CALCULATED ALPHA DIVERSITY FOR THE SLOPE SITES.....	132
TABLE 13 CALCULATED BETA DIVERSITY FOR THE RIPARIAN SITES	133
TABLE 14 CALCULATED BETA DIVERSITY FOR THE SLOPE SITES.....	134
TABLE 15 SITE CHARACTERISTICS WITH AREA CALCULATIONS, STEM DENSITIES AND SPECIES RICHNESS FOR THE STUDY SITES.....	152
TABLE 16 IDENTIFIED TREE SPECIES, FAMILIES AND GENERA	152
TABLE 17 RELATIVE DOMINANCE FOR THE RIPARIAN, TERRACE AND SLOPE SITES, AS WELL AS THE TOTAL IN %	160

TABLE 18 SPECIES IDENTIFIED FROM IMAGES WITH THE FOLLOWING PARAMETERS: CANOPY AREA (CA), TREE COUNTS (TC), RELATIVE DENSITY, DENSITY AND DENSITY PER HA	162
TABLE 19 DOMINANT SPECIES FOR THE SLOPE SITES, WHEREBY THE FIRST ROW CONTAINS THE MOST FREQUENT ONES, THE SECOND FREQUENT ONES IN THE SECOND ROW AND THE THIRD FREQUENT IN THE THIRD ROW. WHEN THE VALUES OF THE RELATIVE DOMINANCE WERE LESS THAN 1% DIFFERENT BETWEEN TWO SPECIES, THEY WERE BOTH COUNTED.....	163
TABLE 20 MAIN SPECIES WITH THE FOLLOWING PARAMETER: FREQUENCY, DENSITY, ABUNDANCE, DOMINANCE AND IMPORTANCE VALUE	165
TABLE 21 RESULTS FOR THE FIRST APPROACH, SUMMARIZING THE AUTOMATIC AND REAL COUNTS. (ORTHOMOSAIC=MOSAIC).....	212
TABLE 22 RESULTS FOR THE SECOND APPROACH, SUMMARIZING THE COUNTING'S IN SUMMER AND WINTER IMAGES, AS WELL AS THE COMPARISON TO THE FIELD COUNTING.	213
TABLE 23 COUNTS EXCLUDING THE UNDERSTORY VEGETATION AND/OR YOUNG TREES, AS WELL AS THE CALCULATED ACCURACY FOR WINTER AND SUMMER IMAGES.	214
TABLE 24 COMPARISON OF SEMANTIC SEGMENTATION APPROACHES FOR THE "DECIDUOUS" CLASS IN WINTER ORTHOMOSAICS (WM*). THE FIRST HALF OF THE TABLE CONTAINS THE RESULTS FOR THE UNET MODEL, THE SECOND HALF CONTAINS RESULTS FROM THE PATCH BASED MULTI-LABEL RESNET CLASSIFIER. THE FIRST COLUMN CONTAINS THE SIZE OF THE PATCHES USED. ROWS MARKED "COARSE" USE ONLY THE RESNET CLASSIFIER WHILE ROWS MARKED "REFINED" ALSO USE WATERSHED REFINEMENT. LAST TWO COLUMNS ARE THE AVERAGE VALUES (AVG) BETWEEN ALL ORTHOMOSAICS AND BETWEEN ORTHOMOSAICS OF SITE 1.	233
TABLE 25 COMPARISON OF SEMANTIC SEGMENTATION APPROACHES FOR THE "EVERGREEN" CLASS IN WINTER ORTHOMOSAICS (WM*). THE FIRST HALF OF THE TABLE CONTAINS THE RESULTS FOR THE UNET MODEL, THE SECOND HALF CONTAINS RESULTS FROM THE PATCH BASED MULTI-LABEL RESNET CLASSIFIER. THE FIRST COLUMN CONTAINS THE SIZE OF THE PATCHES USED. ROWS MARKED "COARSE" USE ONLY THE RESNET CLASSIFIER WHILE ROWS MARKED "REFINED" ALSO USE WATERSHED REFINEMENT. LAST TWO COLUMNS ARE THE AVERAGE VALUES (AVG) BETWEEN ALL ORTHOMOSAICS AND BETWEEN ORTHOMOSAICS OF SITE 1.	235
TABLE 26 COMPARISON WITH STATE-OF-THE-ART METHODS	236
TABLE 27 SPECIES LABELLING AND AREA CALCULATIONS OF SITE ROIS	242
TABLE 28 ACCURACIES REACHED FOR THE EXPERIMENTS	246
TABLE 29 AREA AND COUNTING MEASURES OF BLUEBERRY BUSHES DETECTED IN THE ORTHOMOSAICS	276
TABLE 30 CLUSTERING RESULTS BASED ON POINT SHAPEFILES OF THE SITES.....	279
TABLE 31 NUMERICAL EVALUATION OF THE REFINEMENT STEP OF THE DNN. THE ROWS MARKED "REFINED" STAND FOR THE ALGORITHM AFTER REFINEMENT WHILE THE ROWS MARKED "COARSE" CORRESPOND TO THE ALGORITHM WITHOUT REFINEMENT FOR EACH OF THE THREE STUDIED MOSAICS. THE DICE COEFFICIENT AS WELL AS THE RATIO OF BLUEBERRY PIXELS IN THE GROUND TRUTH COVERED BY EACH OF THE TWO MASKS IS PRESENTED	286

III. Acknowledgements

I want to thank all my supervisors, **Larry Lopez**, **Yoshimura-sensei** and **Tsou-sensei** who supported me during my PhD time, gave me advice and guided me on the long way to the PhD degree. I want to thank Larry Lopez, for giving me the change working on a topic, which was completely new for me, which needed me to learn so much more. I want to thank Larry Lopez, for introducing me to Yago Diez. My work on this topic was the most awesome experience in my life. Doing the PhD in Japan was the best ever happened to me, even though there were some up and downs (but who can say that everything always was smooth).

I want to thank **Yago Diez**. Doing a PhD, working on the same topic for three years, facing several challenges, getting stuck in the middle and from time to time just feeling bad is something I think every PhD candidate faces at some point. But I can say I was very lucky, because I had you. When we were working hard you said: "Thank you for your hard work" or when you told me that you appreciate my work and that you are happy working with me. It is only a couple of words but for me it meant so much. It gave me a super good feeling and nothing could stop my smile on those days and it let me feel that I can face every challenge in my life. You gave me trust when I thought I cannot do it. When you corrected my papers, you always started with: You will not gonna like it. And yes, I never liked it! But with your help and guidance I was able to publish papers in very good Journals and I always saw (afterwards of course 😊) that your recommendations made my work better, made me better. I want to thank you for improving me and my work. But not only in research I could always count on you, but also when I had trouble in my life. I could always ask you for advice and you always helped me overcoming the depression, in which I stuck from time to time. Thank you for never letting me down and always being there for me. I am happy, that life brought us together. Thank you so much!

Ich möchte zuallererst **Alex** danken, der an meiner Seite nun schon so viele Jahre steht! Nach meinem Abschluss wusste ich nicht wohin und ich hatte das Gefühl meinen Weg nicht zu finden. Durch deine Reise nach Japan, lieber Alex, hast du es mir nicht leicht gemacht, aber ich weiß, dass du mir damit nur den Weg gezeigt hast den ich gehen soll. Durch dich bin ich den für mich damals schwersten Weg meines Lebens angetreten, habe mich in ein Abenteuer gestürzt von dem ich dachte, dass ich daran scheitern würde. Ich habe ein Thema begonnen, von dem ich nichts wusste. Ich habe alles zurückgelassen, was ich gekannt habe und was mir Sicherheit gegeben hat. Heute weiß ich, dass dies alles nötig war, um der Mensch zu werden der ich heute bin. Durch dich und deine Liebe zu Japan wie auch Schnee, habe ich Vertrauen in mich und meine Fähigkeiten gewonnen. Durch dich habe ich das schönste und größte Abenteuer meines Lebens gewagt. Ich möchte mich hiermit für all das bedanken. Danke, dass du immer zu mir gestanden hast. Danke, dass du mir immer

in den Hintern getreten hast. Danke, dass du immer an mich geglaubt hast. Danke, dass du immer für mich da warst. Ich hoffe, dass wir auch weiterhin füreinander da sein werden, uns motivieren, wenn wir antriebslos sind, wir uns stärken, wenn wir glauben schwach zu sein und einfach glücklich in ein neues gemeinsames Leben zu starten. Danke, Alex, dass du immer für mich da bist und mich immer unterstützt. Ich liebe dich über alles.

I want to thank **Luca** and **Hanna**, who I met first in Japan. I am thankful to meet you during my PhD time, you filled my life with happiness and fun. You showed me again how to live, when I was stuck in my work. You both made Alex and my life another advantage and I don't want to forget any day we spend together. I am sorry Luca, but Hanna, you know you became the second most important person in my life not only because of the magic number 1 hour 11 minutes 😊 but because you became a person in my life, I want to be together with. I hope you will still be a part of my life and I will be there for you as you be there for me. Please never stop complaining with me. Thank you, my beloved friend!

Ich möchte meiner **Familie** danken, Mama, Papa, Fabian und Dennis, den Menschen die mich zu dem gemacht haben was ich heute bin. P.S. lieber Fabian, schön dass du da bist, aber meine Mama wäre mir lieber 😊. Immer seid ihr für mich da gewesen und habt mich unterstützt. Ihr habt mich aufgefangen, wenn ich im freien Fall war und ihr habt mir Kraft geschenkt, wenn ich kraftlos war. Ihr habt mir immer beigestanden und mir mit Rat und Tat zur Seite gestanden. Ich weiß, dass ich mich immer auf euch verlassen kann und dass ihr immer für mich da sein werdet. Danke, dass ihr mich auf meinem Weg unterstützt, bestärkt und geleitet habt. Vielen Dank und ich habe euch lieb!

I want to thank you, **Ha Trang**. As my laboratory neighbour, we spend a lot of time together and I enjoyed it. Talking and drinking coffee, discussing research and challenges in our life's. I loved that you introduced me to Vietnamese coffee and to so many culinary experiences. Thank you for being my friend and special thanks for supporting me handing in my thesis. Also, I want to thank all my laboratory members who helped and supported me and my work, with special thanks to **Felix, Fabian W., Kazushi, Kohei, Cho** and **Herve**. I want to thank **Arifa** and **Uemura-sensei**, who supported me during my time in Japan. I got to know both of you early and you influenced my life as a PhD student. I want to thank you that I could always ask you for advice and support to my make my study and my life in Japan the best experience.

IV. Index of abbreviation

Accuracy	ACC
Average	AVG
Convolutional Neutral Networks	CNN
Deciduous	Dec
Deep Learning	DL
Deep Neutral Networks	DNN
Digital Elevation Model	DEM
Evergreen	Ev
False Negatives	FN
False Positives	FP
Frozen	F
Frozen no Augmentation	FNOA
Frozen with loss function weighting and augmentation	FH
Frozen with loss function weighting	FW
Ground Control Points	GCP
Ground Sampling Distance	GSD
Learning Rate	LR
Multi-Label Patch	MLP
No Agreement	NA
Neural networks	NN
Orthomosaic	Mosaic
Partial Agreement	PA
Rectified Linear Units	ReLU
Red, green, blue	RGB
ResNet50	RN50
Sensitivity	SENS
Specificity	SPEC
Total Agreement	TA
Total Agreement with False Positives	TAFP
True Negatives	TN

True Positives	TP
Unfrozen	UNF
Unfrozen no Augmentation	UNFNOA
Unfrozen with loss function weighting and augmentation	UNFHA
Unfrozen with loss function weighting	UNF W
Unmanned Aerial Vehicles	UAV
Winter orthomosaic	wM
Yamagata University Research Forest	YURF

V. Summary in English

Forests, with an area of 4.15 billion hectares, cover large areas of the earth surface and provide essential economic, environmental and social services, like balancing carbon cycles, conserve biodiversity and regulate fresh water supplies. Human disturbances and climate change affect forest ecosystems, their growth and resilience. Changing forest stresses and changes in the ecosystem increased the demand of accurate forest information. This is especially important in Japan, due to the sheer magnitude and complexity of the forest area, composed of natural mixed broadleaved deciduous forests.

Traditionally, information about forests has been collected using expensive and work-intensive field inventories collecting data about tree species compositions, distributions and forest structures by identifying trees and counting them. These and further information are needed to do sustainable forest management and monitoring of the ecosystems. Challenging environments restricted forest inventories to be conducted in small field plots and data were scaled-up to forest stand levels. In natural mixed forests small field plots were found to be less representative for the forests studied.

In recent years Unmanned Aerial Vehicles (UAVs) have become very popular as they represent a simple and inexpensive way to do automated flied surveys by gathering high resolution data of large forested areas. Among the many sensors that UAVs can carry, RGB cameras are fast, cost-effective and make the data gathering and interpretation easy, as they do not need intensive calibrations or pre-processing. With spatial resolution of less than 1 m, canopy structures and even leave structures can be identified, so that tree species classification can be performed from images. In addition, deep learning (DL) has also been catching more attention in the field of forestry. In particular as a way to include the knowledge of forestry experts into automatic software pipelines, to deal with tree detection, tree health or tree species classification. The increasing numbers of studies performed in forestry using DL together with improving software and data availability increased the need of such kind of studies in Japan's forests.

In this study three methodologies were applied to characterise and evaluate natural mixed forests in Japan regarding their tree species composition, distribution and structure: Field surveys, Image analysis with GIS application and DL. These three methodologies were used for the main analysis of the Yamagata University Research Forest (YURF) sites, as one aspect was that the DL results needed to be evaluated regarding their accuracy compared with field inventories. The other aspect was that the collected images could further be used for image analysis with Geographic Information Systems (GIS). Therefore, field data were collected in the traditional way of classifying tree species and counting them in the field. Data were collected for seven sites with distribution and survey maps, while for three Slope

sites only tree counting information were provided. For the total of 13 sites, image analyses were performed using manual annotations and GIS applications generating tree survey, tree distribution, density, count, hot spot, DEMs, aspect and slope maps for the different sites and tree species. In total, 70 tree species were identified in the field, while 41 species classes were identified from the images. Field and image results were analysed regarding biodiversity, densities, frequencies and dominant tree species in the different considered sites. Results of the image analyses and the field analyses were similar, when canopy and subcanopy species were considered; differences were mainly found for understory vegetation and shrubs, which were hardly identifiable from images. Significant differences occurred only in the Slope sites, where small *Quercus mongolica* and *Fagus crenata* trees were covered by canopy layer species, but still dominated those forests, according to the field data. The image data identified several species as dominant, depending on the observed site (*Magnolia obovata*, small-leaved *Acer*, *Acer mono maxim* and *Quercus mongolica*). In Riparian and Terrace sites, *Juglans ailantifolia*, *Pterocarya rhoifolia*, *Salix* species and *Acer* species dominated the sites. Biodiversity measures indicated a higher diversity when field data were used, in contrast to image data. While the Shannon diversity values ranged between 1.73 and 2.39 (with the evenness ranging between 55 % and 82 %) for the image analysis results, it ranged between 2.14 and 2.76 (evenness: 71 % - 84 %). Layering of the forest was better classified with the field data, as all layers could be easily identified, while most of the lower vegetation could not be identified from images. The forest sites were classified based on the layering and the dominance of tree species, while the dominance of canopy areas was used for the classification. Riparian and Terrace sites were *Juglans ailantifolia* forests with *Pterocarya rhoifolia* and *Salix* as co-dominant species. According to the results of the image analyses, *Juglans ailantifolia*, *Acer* species, *Magnolia obovata* and *Quercus mongolica* were the dominant species, which confirmed the field analysis, but with a different order (small-leaved *Acer* and *Quercus mongolica* were the majority). The evaluation of the images with GIS tools enhanced the visibility of important aspects hidden in the data, and spatial information could be easily extracted and interpreted. Generally, image analyses of tree canopy areas provided more accurate information than tree counting, as dense canopy areas hampered counting. To evaluate semi-automatic counting, field data, DEMs, summer and winter images were used to count tree species. Highest accuracies were reached when counting was performed on winter images, while small and young trees still remained challenging to count.

The main aim was to classify plant species automatically with DL techniques. Therefore, data were gathered in the 13 sites in the YURF in four seasons and over three years, as well as in the coastal forest near Sakata city and in Lichtenmoor, a wetland area in Germany. The 13 sites in YURF were divided into Riparian, Terrace and Slope sites. All images were processed with Metashape to produce orthomosaics and DEMs (Digital Elevation Models). In a first step, DL was applied to a simple example of classifying trees with leaves versus trees without leaves (deciduous vs. evergreen) in winter images,

to assess the effect of transfer learning and DL architectures (ResNet50 and UNet). In this approach also multi-label patch (MLP) classification versus semantic segmentation were studied, breaking the orthomosaics into image patches. The results showed that transfer learning is necessary to achieve satisfactory outcome with MLP classification of deciduous versus evergreen trees. In the winter orthomosaic dataset the improvement from no transfer learning to transfer learning from a general-purpose dataset was 9.78 %. Furthermore, the ResNet50 architecture showed a high performance with better results than the UNet. The results indicated already that data balancing is an important topic. The study of invasive blueberry species, endangering sensitive wetland environments and black locusts invading into coastal forests, were two more application-oriented examples, with an easier problem definition: Classifying target species in a natural green environment. The ResNet50 architecture was used with transfer learning to detect black locust trees in an evergreen coniferous black pine forest with a 75 % of True Positives (TP) and 9 % False Positives (FP) while the detection of native trees achieved 95 % TP and 10 % FP. Detections of invasive blueberry bushes were performed with ResNet50, transfer learning and unfrozen weights with True Positive Values (TPV) of 93.83 % and an Overall Accuracy (OA) of 98.83 %. A refinement of the result masks reached a Dice of 0.624. Image analyses were performed to produce maps of blueberry location, distribution and spread in each study site, as well as bush height and area information. A preliminary study of different DL networks, transfer learning, the use of data augmentation and loss functions and settings were tested for the detection of invasive blueberry species. The challenge of the data was the imbalance, as invasive species had fewer individuals than natural occurring plants. In this study of state-of-the-art DL architectures, the best results were obtained with the ResNeXt architecture (93.75 True Positive rate), and 98.11 % accuracy for the Blueberry class with ResNet50; Densenet and wideResNet calculated similar results. The knowledge, gained with easy examples, was then applied to automatic tree species classification in natural mixed forest. The DL approaches for the automatic species classification in YURF are not finished, yet, but promising. Some classes were already classified well, reaching accuracies of approximately 80 %.

This study provides an efficient and effective methodology to study forests and other natural environments, like wetlands, using different techniques: field surveys, image analyses and DL. Automatic generated results showed high accuracies and indicated the applicability of the methodology in different fields. Image analyses extract the most important information of aerial images, depending on the study focus. Field data captured a lot of information that could not be extracted from images, and therefore the methodology set provided new and important insights into forest environments.

VI. Summary in Japanese

地球上で41億5,000万ヘクタールの森林は、地表の広い範囲を占め、炭素循環の調整、生物多様性を保全、水供給など、経済的、環境的、社会的に不可欠なサービスを提供しています。人為的な攪乱や気候変動は、森林生態系における成長や回復力に影響を与えます。従来、森林に関する情報は、コストと労力のかかる毎木調査によって収集されてきました。毎木調査は通常小規模なフィールドプロットで行われ、そのデータを用いて森林レベルにスケールアップされてきました。しかし、日本に多く分布している天然生広葉樹林は非常に複雑であるため、小さなフィールドプロットでは調査対象の森林をあまり代表していないという問題が生じていました。

近年、UAV（Unmanned Aerial Vehicle：無人航空機）が森林調査において用いられるようになってきました。UAVが搭載できるRGBカメラは集中的なキャリブレーションや前処理を必要としないため、データの収集と解釈が容易です。また、1m以下の空間分解能で、林冠構造や葉の構造まで識別できるため、画像から樹種分類を行うことが可能です。

本研究では、現地調査、GISを用いた画像解析、ディープラーニングという3つの方法論を用いて、日本の天然生混合林の樹種構成、分布、構造を特徴づけ、評価した。山形大学研究林（YURF）の合計13サイトにおいて、フィールドデータを取得し、GISアプリケーションを用いて画像解析を行いました。その結果、合計でフィールドデータからは70種の樹木が確認され、画像データを用いた深層学習からは41種のクラスが特定されました。林冠種を考慮した場合、画像分析とフィールド分析の結果は類似していましたが、下層植生と低木において両結果に差異が生じ、画像からはほとんど識別できませんでした。生物多様性の指標は、画像データとは対照的に、フィールドデータを使用した場合に高い多様度を示した。画像解析の結果では、シャノン多様性指数が1.73～2.39（均等性は55%～82%）であったのに対し、2.14～2.76（均等性は71%～84%）であった。森林の階層構造に関して、画像からは下層においては識別できませんでした。溪畔林に設置したサイトは、実際にはオニグルミが優占する森林で、サワグルミが共優占種であったが、画像分析の結果によると、オニグルミ、カエデ属、ホオノキ、ミズナラが優占種であると認識され、優占度の順序が異なっていました。GISツールを使って画像を評価することで、データに隠れていた重要な側面が見えやすくなり、空間情報を簡単に抽出して解釈することができました。

一般的に、樹冠が密集していると個体数推定が困難になることが知られています。そこで、フィールドデータ、DEM、夏季および冬季の画像を用いて樹木個体数の正確な評価を半自動解析によりおこないました。その結果、冬の画像でカウントを行った場合に最も高い精度が得られましたが、小さい木や若い木のカウントは依然として困難でした。

次に深層学習技術を用いて植物種を自動的に分類するために、YURFの13のサイト、酒田市近郊の海岸林や、ドイツの湿地帯でもデータを収集しました。すべての画像はMetashapeで処理され、オルソモザイクとDEM（Digital Elevation Models）を作成しました。まず、冬の画像で葉のある木とない木（落葉樹と常緑樹）を分類するという簡単な例に深層学習を適用し、伝達学習と深層学

習のアーキテクチャ（ResNet50とUNet）の効果を評価しました。このアプローチでは、マルチレベルパッチ（MLP）分類とセマティックセグメンテーションについても検討しました。その結果、MLPによる落葉樹と常緑樹の分類で満足いく結果を得るためには、転移学習が必要であることがわかりました。冬のオルソモザイクのデータセットでは、転移学習を行わなかった場合と、汎用データセットからの転移学習を行った場合の改善率は9.78%でした。さらに、ResNet50アーキテクチャは、UNetよりも優れた結果を示し、高い性能を発揮しました。ResNet50アーキテクチャを伝達学習とともに使用して、常緑針葉樹のクロマツ林におけるニセアカシアの木を検出したところ、真陽性(TP)が75%、偽陽性(FP)が9%であったのに対し、在来種の木を検出ではTPが95%、FPが10%となりました。

本研究では、森林や湿地帯などの自然環境を調査するための効率的かつ効果的な方法論を、現地調査、画像解析、深層学習などのさまざまな手法を用いて提供することができました。自動生成された結果は高い精度を示し、さまざまな分野での方法論の適用可能性を示しました。画像解析では、調査対象に応じて航空画像の中から最も重要な情報を抽出します。フィールドデータは、画像からは抽出できない多くの情報を捉えているため、この方法論セットは、森林環境に関する新たな重要な洞察を提供するものだと考えられます。

VII. List of publications

- (1) Diez, Y.; **Kentsch, S.**; López Caceres, M L.; Nguyen, H.; Serrano, D.; Roure, F.: Comparison of Algorithms for Tree-top Detection in Drone Image Mosaics of Japanese Mixed Forests. 10.5220/0009165800750087, March 2020
- (2) **Kentsch, S.**; Lopez Caceres, M.L.; Serrano, D.; Roure, F.; Diez, Y. Computer Vision and Deep Learning Techniques for the Analysis of Drone-Acquired Forest Images, a Transfer Learning Study. *Remote Sens.*, 12, 1287. <https://doi.org/10.3390/rs12081287>, April 2020
- (3) **Kentsch S.**; Karatsiolis S.; Kamilaris A.; Tomhave L.; Lopez C., L.M.: Identification of Tree Species in Japanese Forests Based on Aerial Photography and Deep Learning. In: Kamilaris A., Wohlgemuth V., Karatzas K., Athanasiadis I.N. (eds) *Advances and New Trends in Environmental Informatics. Progress in IS.* Springer, Cham. https://doi.org/10.1007/978-3-030-61969-5_18, July 2020
- (4) Diez Y., **Kentsch S.**, C. Lopez L.M., Moritake K., Nguyen H., Serrano D., Roure F.: A Preliminary Study on Tree-Top Detection and Deep Learning Classification Using Drone Image Mosaics of Japanese Mixed Forests. In: De Marsico M., Sanniti di Baja G., Fred A. (eds) *Pattern Recognition Applications and Methods. ICPRAM 2020. Lecture Notes in Computer Science*, vol 12594. Springer, Cham. https://doi.org/10.1007/978-3-030-66125-0_5, December 2020
- (5) Cabezas, M.; **Kentsch, S.**; Tomhave, L.; Gross, J.; Caceres, M.L.L.; Diez, Y. Detection of Invasive Species in Wetlands: Practical DL with Heavily Imbalanced Data. *Remote Sens.*, 12, 3431. <https://doi.org/10.3390/rs12203431>, October 2020
- (6) **Kentsch, S.**; Cabezas, M.; Tomhave, L.; Groß, J.; Burkhard, B.; Lopez Caceres, M.L.; Waki, K.; Diez, Y. Analysis of UAV-Acquired Wetland Orthomosaics Using GIS, Computer Vision, Computational Topology and Deep Learning. *Sensors*, 21, 471. <https://doi.org/10.3390/s21020471>, January 2021
- (7) Nguyen, H.T.; Lopez Caceres, M.L.; Moritake, K.; **Kentsch, S.**; Shu, H.; Diez, Y. Individual Sick Fir Tree (*Abies mariesii*) Identification in Insect Infested Forests by Means of UAV Images and Deep Learning. *Remote Sens.*, 13, 260. <https://doi.org/10.3390/rs13020260>, January 2021
- (8) Diez, Y.; **Kentsch, S.**; Fukuda, M.; Caceres, M.L.L.; Moritake, K.; Cabezas, M. Deep Learning in Forestry Using UAV-Acquired RGB Data: A Practical Review. *Remote Sens.*, 13, 2837. <https://doi.org/10.3390/rs13142837>, July 2021

Chapter 1 Introduction

One-third of the total land area are covered by forests, in numbers around 4.15 billion hectares, of which most of them are in mountainous areas. Forests provide essential ecosystem services like biodiversity conservation and water supply (Lunbäck et al., 2020) and are regulators of the planet's climate, as they influence carbon and water cycles and are one of the most important carbon sinks (Lunbäck et al., 2020). Contrary, changes in climate conditions or ecosystem changes influence forest ecosystems by causing several disturbances and stresses for plant communities, which further influence ecosystem functions and processes (Makimoto, 2019). Therefore, the study of potential influences or impacts of climate on forests need to be studied. Egli & Höpke (2020) pointed out, that forest efficiencies and resiliency are often directly connected with species richness and thus the accurate mapping needs to be performed to accurately assess forest inventories and biodiversity.

Fukamachi et al. (2020) and Makimoto (2019) have pointed out that forest monitoring systems are needed to accurately gain long-term data about forest changes and dynamics. Accurate information about forests and ecosystems in general are crucial for forestry management, protection and research (Onishi & Ise, 2021). Providing the required information demands analyses of different forest areas, as those vary strongly regarding their canopy levels, ages, basal areas and biomass (Haq et al., 2020).

Foresters conduct conventional field surveys, which require man-power, expert knowledge, experience, time and economical resources. With field surveys, vegetation information about the plant numbers, species, morphology, age and distribution are gathered achieving a high accuracy of information. Forests located in mountainous areas are challenging, which are sometimes not even accessible. Therefore, field surveys are usually provided only rarely and only for small areas, which are especially for mixed natural forests that are not necessarily representative. Makimoto et al. (2019) further indicated that different field survey methods increase the difficulties in evaluation forests on a regional or even global scale, so they demand further a standard methodology for evaluating forests. Decreasing the number of those manual inventories can be performed by automatization of plant species classification with remote sensing, which has been identified as an important tool in forest science (Nezami et al., 2020).

Remote sensing monitoring is already a well-studied area (Fassnacht et al. 2016, Gini et al. 2018, Franklin 2018), but extracting textural information, classifying single tree species are still challenging in natural environments because of the differences between plant species and stand conditions (Diez et al., 2021). Based on the selected sensor relevant features of trees can be extracted like shape, colour intensity, leaf properties and spectral responses, but also geometric features of trees and canopies (Nezami et al., 2020).

Unmanned aerial vehicles (UAVs) have become an important tool for remote sensing studies in forest areas. The benefit of these small and light-weighted tools is that they can be used in all environments, flexible and with low costs, while the operating of the machine is easy. Additionally, apps like DJI Go enables automated flights, which provide a standardized acquisition of data. The low flight altitude allows the gathering of high-resolution images, can be easily cooperated into photometric workflows and computer vision techniques (Diez et al., 2021). Satellite images, where the level of resolution allows biomass estimations or vegetation classifications e.g., cannot be used for single tree detections or classifications Fujimoto et al. (2019). High resolution images acquired by UAVs with spatial resolutions of 0.2 – 3.0 m can be used for detailed characterisations of tree species, as canopy structures or even leaves can be identified (Onishi & Ise, 2021). They can be further used for detailed analyses of species compositions and forests structures, as well as obtaining information about the state of forest ecosystems and their monitoring (Schiefer et al., 2020). Geographic Information Systems (GIS) can extract information out of images. Important results can be obtained with GIS techniques by reducing the complexity contained in the images (using different image interpretation strategies) and the findings can be presented in elaborate visualizations (Heipke et al., 2000). GIS analysis need digitalized data, which are still labour intensive and time-consuming when annotations need to be performed by hand.

Recent developments in Artificial Intelligence (AI) and increasing computational power enabled the use of Deep Learning (DL) in the broad field of forestry research. Data availability and free software make DL accessible for forest researchers. The basis of this technology are computers, that learn characteristics of plant species and identify patterns in images to detect and classify the species in images. A simple application in image analysis is object detection, where the location of a plant species shall be provided. Another approach is image classification with DL techniques means that images will be labelled automatically, by identifying the object in the foreground and the background. A final approach is semantic segmentation, where each pixel in an image gets assigned to a class based on probabilities. Consequently, DL has become a powerful tool to analyse forest images, which will accelerate and improve forestry research by providing robust and fast algorithms that allows the processing of large datasets (Diez et al., 2021).

Still, these technologies are rarely used because of several challenges: the complexity of natural ecosystems with steep slopes, dense understory vegetation and canopy areas and the need of accurate reference material, which enables the comparison of field data with results of image analysis. Furthermore, experts in the fields of forestry, image analysis and DL are required to provide high quality results as pointed out by Diez et al. (2021). Furthermore, the alignment of gathered field data and remote sensing images provides several difficulties and is often not considered (Kattenborn et al.,

2020). Most studies use manual annotations to provide information about the accuracy of DL networks or separately conducted fieldwork, while a direct comparison between DL and field gathered data are not conducted.

This study was conducted under the supervision of experts from each mentioned field in the area of Northern Honshu, Japan, which makes the work unique for this research field. To the best of my knowledge, this study belongs to the first studies using DL with UAV gathered RGB data to classify tree species of mixed forests in Japan.

The basis of this study was the mixed forest in Shonai area, represented in the Yamagata University Research Forest (YURF). The forest is composed of a mixture of different forest patches, composed of natural and planted tree species, which grow along the rivers, on the slopes and the top of the mountain. There were previous studies performed in YURF, which analysed species occurrence in different forest patches, but there is no information provided about the composition and structure of the different kind of forests. Due to the complexity of mixed forests, there are also no detailed studies provided on which species occurs where, if they are minor or dominant or if there are relationships and interactions between tree species. For such kind of information, the different forests patches with their varying characteristic need to be analysed, which has to be done in a large-scale to achieve superior structures and interactions. This requires a fast, efficient and standardized methodology, which can be provided with the use of UAVs, image analysis and specifically DL, which was studied in detail with this work. A combination of field gathered data and image analysis with GIS methodologies provides unique insights in the studied forests sites, which are representative of cold temperate mountainous forests of Shonai area. Additionally, DL techniques were studied and evaluated for the use in forestry under the consideration of aspects like the applicability, time consideration and accuracy, especially in relation to precise field surveys. With such a methodology, study areas do not need to be localised and focussed on a small number of trees anymore, while extrapolation need to be performed to scale the gathered information up for regional analyses. Instead, UAV-acquired images in combination with DL can be used to reduce significantly surveying time, to increase study areas and provide accurate information without extrapolations.

This study also used the developed techniques for applications, in coastal forests and wetlands to provide information about the transferability of the studied methodology. In both cases, invasive species were studied, which invaded into natural environments. First, invasive Black locust trees in Black pine coastal forests were studied, then a blueberry species, which invaded into sensitive wetlands in Germany. The benefit of these studies was that they provide useful insights into the application of DL and how to handle it, while the main focus is on the detection of only one species. Still, the main focus of this work were tree species classifications. For this approach, seasonality was

used to first classify deciduous and coniferous trees in winter images and later perform species classifications in summer images.

In this study, the incorporation of all the mentioned techniques from remote sensing, GIS, computer vision, computational topology and artificial intelligence allows to characterise vegetation on a large scale, with minimum disturbances and required man-power, incorporating expert knowledge. To the best of my knowledge, this is the first study that includes a large dataset, and the use of different techniques in combination with UAV acquired data to increase the understanding of vegetations in natural environments, with a specific focus on automatic classifications a high number of tree species.

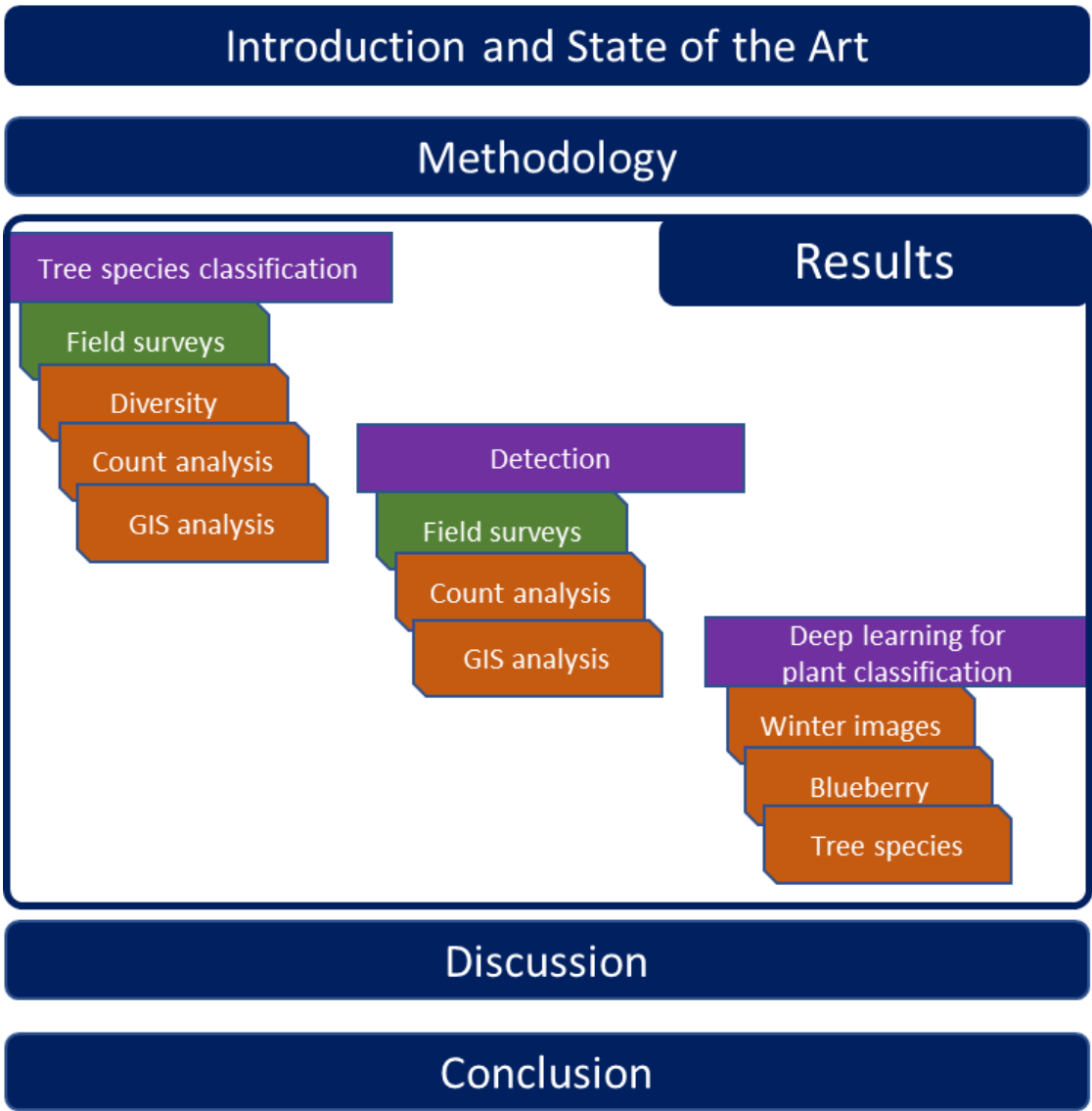


Figure 1 Overview of the research flow

The developed and presented methodology had the following objectives as the basis to gain a deeper knowledge about mixed forests.

- i. Develop low cost and low time demanding methodologies for forest ecosystem analysis.
- ii. Evaluate the composition, distribution and structure of mixed natural forests in Shonai area.
- iii. Characterise mixed forests with the use of the state-of- the-art GIS and DL technologies.

Hence, the development of an image analysis methodology for forestry research is presented with this study. The thesis the structure, first presenting YURF data analysed with field and image data and finally automatic DL classification (Figure 1). Gathered field data will be presented first, followed by diversity measures based on image analysis. Later, image analysis will be presented first only using GIS, then with a detailed comparison between the gathered field data and results of tree detection in image. At last, DL results will be presented first applying it to tree classification (winter images and tree species classification) and then the application for studying invasive species. Note that the invasive species chapter contains a GIS image analysis and a DL part, while the DL chapter explains tools, software and settings which benefits DL studies. In the end, this thesis provides a completed methodology, which can be applied in forestry research, as well as in other natural environments.

Chapter 2 State-of-the-Art

The development and usability of inexpensive and easy-to-use UAVs offered the possibility to cover large areas with high resolution images, which have been used in agriculture (Grenzdörffer & Teichert, 2008; Raparelli et al., 2019) and forestry (Diez et al., 2021; Natesan et al., 2019; Gambella et al., 2016) studies. UAVs, depending on their size, can be equipped with sensors such as LIDAR, multi- or hyperspectral sensors. Natesan et al. (2020) pointed out that those sensors are expensive and need a precise calibration. Furthermore, DL applications are known to work better with RGB images than with LIDAR, etc. RGB images can be directly gathered by cost-effective UAVs, as the cameras are usually already attached. Additionally, the images can be used for image analysis without costly pre-processing. Therefore, this study only considered RGB images acquired from UAVs.

Recently, with the development and progress in computer science, DL has become popular with the use of RGB images (Diez et al., 2021). Data can be processed with high capabilities of computers allowing the processing of big datasets. With the increasing potential of computers and the expansion of DL to research in agriculture and forestry applications have increased immensely.

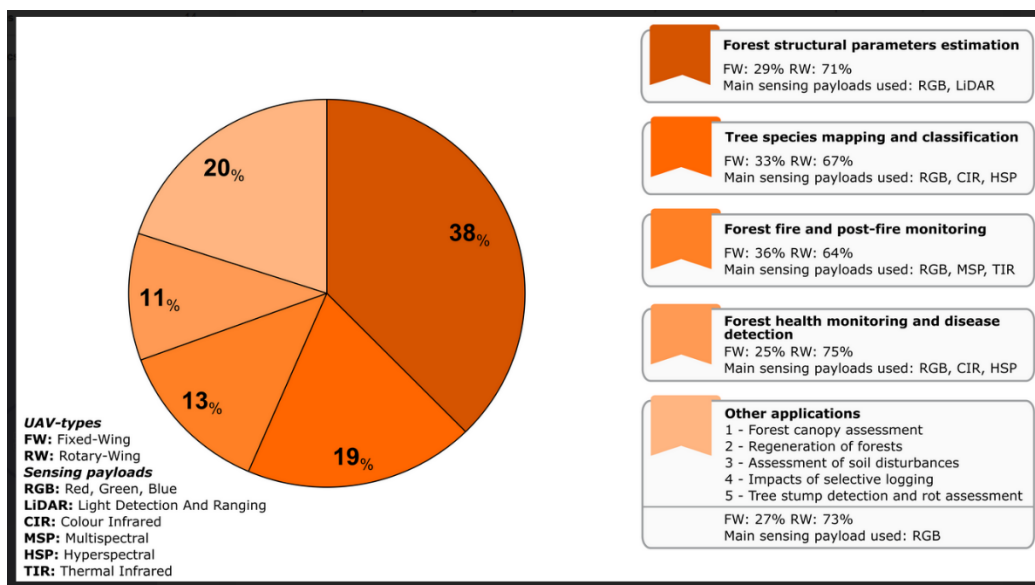


Figure 2 Overview of forestry remote sensing applications (Guimarães et al., 2020)

Figure 2 summarised studies conducted with remote sensing until 2020 in the different forestry fields. There were six types of sensors and two kinds of UAVs which were used: fixed- and rotary-wing types. Studies in the field of forest structural parameters, tree species classification and mapping, forest fires and health monitoring are the main applications using remote sensing, of which a small field additionally uses DL techniques.

There is a small number of pioneering studies in the field of DL in forestry research with UAV acquired RGB images, but only two of them were conducted in Japan (Onishi & Ise, 2018 and Fujimoto et al.,

2019). The studies, which will be presented in the following paragraphs showed the potential of the methodology proposed in this study to transform the way forest science research is carried on by developing algorithms that allow the extraction of important forest information.

Studies use orthomosaics and Digital Elevation Models (DEMs) built from UAV-acquired images to locate and classify different tree species. The starting point for this kind of research was detection of individual trees, meaning the identification of locations of trees within forestry images. Tree top annotations or the use of bounding boxes around trees are the common methodologies (Diez et al., 2020, Ocer et al., 2020), which can be combined with tree crown delineation or pixel-wise segmentations. The results can be used for tree counting or tree classifications.

Chadwick et al. (2020) used Mask R-CNN to detect coniferous trees in a mixed forest with deciduous trees under leaf-less conditions. The high number of trees and occurring densities together in the environment of a valley in the Rocky Mountains provided an interesting example of DL in forestry research (Diez et al., 2021). The authors applied transfer learning with the COCO and Balloons dataset to train a Mask R-CNN network with different settings of the network, like using it frozen. Further, F1-scores were used to evaluate the performance of the network. Best results were achieved with a reported precision of 0.98 and a recall of 0.85, which means that the network produced less false positives but 15 % of the trees were missed by the network. In a second attempt the estimation of tree heights was in good agreement with field measurements. Another tree detection study was offered by Ocer et al. (2020), detecting conifers in flat forests and urban areas with a small number of images (256 training images). The authors were specifically interested in detections using different image resolutions in training and testing images. Here, also a Mask R-CNN was trained and a precision of 0.90 was achieved when tested with different images and resolutions. While the precision value stood stable for all tested images, the recall varied between 0.82 and 0.91 with the best results achieved with similar images and the same resolution for training and testing. This indicated that different resolutions have a significant impact on detection results.

The main contributions of the two papers are the demonstration that DL can be used for practical applications for individual tree detection and how the studied algorithms can be used. The behaviour of DL models, when different resolutions are used, is of main interest, because most forests are located in mountainous areas, where slopes are the reason for significantly varying image resolutions. Those studies also indicated the usually small amount of available data in forestry research, which need to be addressed when DL is used for analyses. The presented methodologies still struggle in detecting all trees, even when only coniferous trees were analysed. Coniferous trees are beneficial for detection purposes as their cone-shaped canopy is easy to recognise in comparison to broad-leaved canopies.

A precise classification of detected trees is the aim of every study, as it is crucial to understand forest compositions, distributions and structures, but it is also needed for further analysis like biomass estimations. Therefore, studies that focus on tree species classifications will be presented in the following paragraphs.

The most interesting studies are the ones from [Onishi & Ise \(2018 and 2021\)](#) and [Fujimoto et al. \(2019\)](#), as they were performed in Japan. The study of [Fujimoto et al. \(2019\)](#) was performed in coniferous plantation in a mountainous area. Orthomosaics and normalized DEMs were used, DEMs from which the floor was extracted to increase the detectability of tree tops with an iterative local maxima algorithm. A watershed algorithm was applied to segment tree canopy areas, which were then used as input for a ResNet200 network and initialised with ImageNet weights. It seemed that the tree top algorithm and the classification were performed separately based on the presented tree counts, which decreased its practical use. The classification was performed by separating 591 trees into 90 % training and 10 % testing set. An increase in data was performed on the training dataset by applying data augmentation. In the end, precisions of 0.848 and 0.821 were achieved for cypress and cedar with a recall of 0.856 and 0.811. In a second attempt a carbon dynamic simulation was performed. In comparison, [Onishi & Ise \(2018 and 2021\)](#) published two works based on an image collection in an experimental forest, which was partially natural and partially managed. The considered area was a mix of planted coniferous and natural broad-leaved trees in a flat area. The studies considered six tree classes and one non-tree class in orthomosaics of two seasons. At first, tree detections were performed using ArcGIS to construct a terrain model, while the commercial eCognition software was used to detect individual trees. A manual correction was performed before a central squared-patch around the detected tree tops and was cut out of the orthomosaic. These patches were used to train different networks: AlexNet, VGG ResNet18 and ResNet152, which were trained before with the ImageNet database. A further comparison between the ResNet152 and the classical machine learning technique SVM (Structure from motion) was performed. The evaluation was done using F1-scores reaching 0.955 and 0.885 on average for autumn and summer images.

Other studies focussed on semantic segmentation to solve the problem of species classifications, instead of considering individual trees. In semantic segmentation each pixel in images was classified and sorted into the considered categories. The benefit of semantic segmentations is that the algorithms can be directly used, but counting and tree canopies extraction cannot be performed easily. While there were several studies published ([Morales et al., 2018](#), [Ferreira et al, 2020](#), [Haq et al. 2020](#)), the focus of my research was on the studies of [Schiefer at al. \(2019\)](#) and [Kattenborn et al. \(2020\)](#): [Kattenborn et al. \(2019, 2020\)](#) presented two works where several datasets were considered. One of the datasets contained images of two invasive species, of which one was a pine tree that invaded into

natural forests. The pine tree was mixed with a species called *Nothofagus*. Orthomosaics were cut into tiles and data augmentation was applied before the dataset was divided into 80 % training and 20 % validation/testing using a random split. A UNet was then trained, achieving a classification accuracy of 0.87 for the pine class. The study used a simple example, achieving good results but suffering from data leakage problems (Diez et al., 2021). In the study of 2020, another presented case study classified two tree species. A CNN was trained to predict cover areas in patches cut from the previously built orthomosaic, while the height information was used, too. The training and validation sets were divided 2/3 and 1/3. Correlations between predicted and real cover were evaluated with a correlation coefficient reaching values of 0.61 and 0.82.

The study presented by Schiefer et al. (2019) is one of the most complex works in this area with a total of nine considered tree species, five coniferous and four deciduous trees, three genus classes and two other classes. Data were gathered in two sites: a well-managed mountainous area and a flat broad-leaved forest. Images for a total of 51 orthomosaics were gathered and nDSMs were generated. For the production of the nDSMs airborne laser scanners were used to extract floor regions. The data were considered as 3 channel (RGB) and 4 channel (RGB and the height of the DSM), which were divided into tiles. The tiles were separated into 90 % training and 10 % testing to train a UNet network. The best results were performed with tiles of a size 128 and 256 pixels achieving 0.89 overall pixel accuracies. Classes which were less frequent reached only 0.67, while frequent classes reached 0.897. Furthermore, the authors considered different pixel resolutions in their discussion.

Most of the presented papers were published in the last years, which represent the state of forestry research with DL using UAV-acquired RGB images. Furthermore, most studies were performed analysing coniferous trees or only one or two tree species. Studies in mixed forests, especially in dense forest areas in mountainous environments, need to consider a higher number of tree species, face challenges like steep mountains and varying image resolutions. A completed workflow, which is applicable in several environments, from image gathering, over processing and detecting until the final classification, needs to be achieved. The published information was used in this study to overcome some of the mentioned challenges and perform tree species classification in natural environments.

Chapter 3 Material and Methods

This chapter focusses on the methodologies used in this study. As the study is a combination of forestry, geoinformatics and computer sciences, it combines methodologies of three different fields. Detailed explanations are given to ensure that readers with different scientific fields can follow the work and gain enough background knowledge to understand this study.

3.1 Climate

Global and regional climate conditions affect tree species composition, distribution and structure in forests. The over 3000 km long north-south extension of Japan induced the differentiation into several climate zones, which means that studying forests in different areas is essential to understand the structure of the forests. In the south the climate is mainly sub-tropical, in higher longitudes warm-temperate, followed by cool temperate and boreal in the north of Japan (Makimoto, 2019).

Generally, Japan is divided into two major climate zones, the Japan Sea side and the Pacific Ocean side. The main study area (YURF) is located close to the North-eastern Japan Sea, which influences the climatic conditions of this area by heavy snowfalls in winter, strong winds and heavy precipitation in the July and August (Ohno, 2008). These conditions influence species compositions in forests.

The location in the northern part of Honshu positions this forest in the cool-temperate climate zone. The climate conditions present an annual mean air temperature of 13.4 °C representing a cold region environment. The forest is affected by summer and winter monsoons, which results in mean annual precipitation of 2500 mm, the lowest precipitation is approximately 130 mm per month. Half of the precipitation falls as snow during the winter month, so the climate is humid. A cumulative solar radiation of approximately 3000 MJ/m² and the cumulative sunlight hours per year with 730 hours are common.

The mentioned climate conditions of Japan are the reason, why the study area is located in the cool-temperate broadleaf climate zone, which indicates that the tree species composition is influenced by a large distribution of beech and oak trees (Figure 3).

3.2 Japanese Forests

Two-thirds of Japan is covered by forests, which is approximately 25 Mha (Makimoto, 2019). Based on the climate zones, forests belong to one of five forest types: Alpine zone forests, sub-frigid forests, cool temperate forests, warm temperate forests and sub-tropical forests. The forests, usually, follow

climate zones from the North to the South, but there is also a west – east difference of forest types, as the high mountains in the centre in Japan influence the climate (Piazza, 2007). A detailed distribution can be seen in Figure 3.

Therefore, it can be said that Japanese forests show a high biodiversity. In the southern area of Japan, in subtropical forests, mainly Mangroves can be found, in temperate zones broad-leaved and evergreen trees and in sub-frigid and sub-alpine forests mainly coniferous trees are distributed.

Forests in Japan are mainly distributed in mountainous areas and mostly with steep slopes. The study of Lunbäck et al. (2020) provided further information about the forest area on slopes with a different steepness. Figure 4 shows a comparison between the location on slopes of forests world-wide and in Japan. It can be seen, that there are only 45.2 % of the forests in flat areas (0 – 15°) and more than 50 % in steeper slopes, which is higher than for most areas of the world.

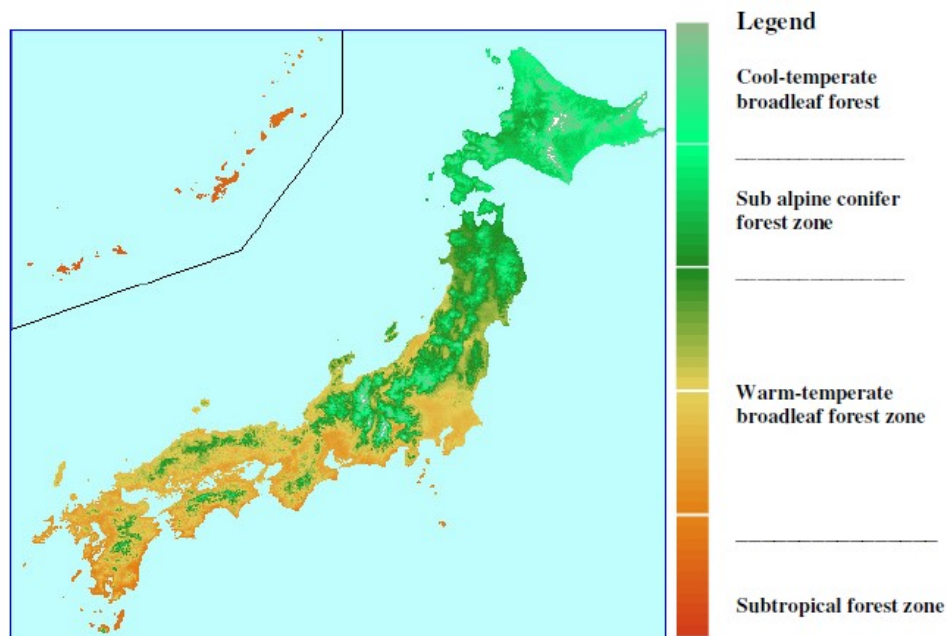


Figure 3 Vegetation zones of Japan (Piazza, 2007)

While in countries like USA or Russia the forests are mainly in flat areas, Europe, Oceania and Asia have 30 – 40 % of their forests in steep areas, whereby Japan has with more than 50 % one of the highest values. This distribution of forest areas is an important factor when it comes to management tasks, surveying and providing information about the forest status.

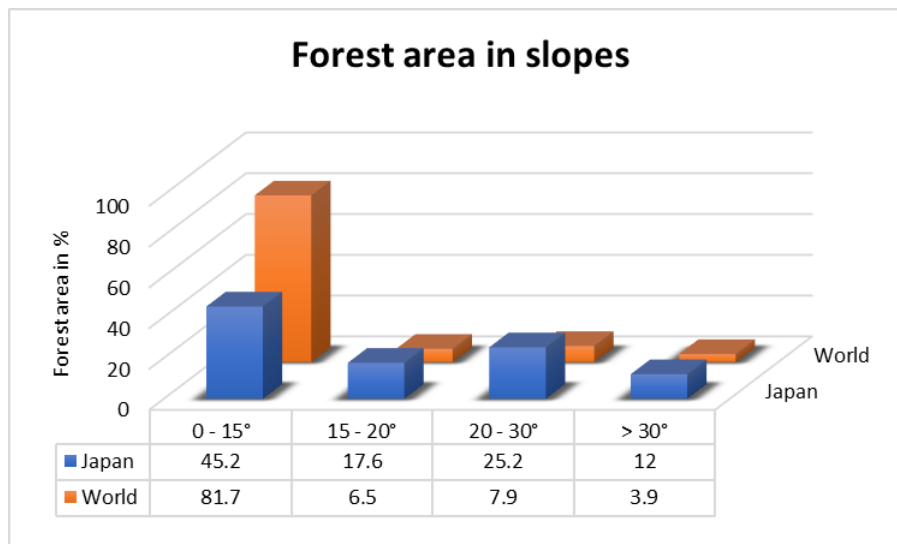


Figure 4 Forest area in percent located in different slope angles (Modified after Lunbäck et al., 2020)

It was estimated that 54 % of Japan's forests are natural forests. In 1951, only 20 % forest were planted, while the number increased to 40 % in 2012. This whole forest area is divided into 50 % coniferous trees and 44 % broad-leaved trees (Makimoto, 2019). Coniferous trees are composed of 20 % Japanese cedar (*Cryptomeria japonica*) and 10 % Japanese cypress (*Chamaecyparis obtuse*), while the number of Larch (*Larix kaempferi*) is significantly higher than Japanese cypress when only planted trees are counted. The main purpose of the several forest plantations is to provide wood for timber production and biomass power plants. Another category of forests in Japan are coastal forests, which are man-made forests that play an important function of protection from wind, sand movements and tsunamis. A third category are natural forests, which are retaining biodiversity, but nowadays also considered as source for biomass power plant. For broad-leaved forests it is known that 10 % are composed of Japanese oak (*Quercus ssp.*) and 4 % beech (*Fagus crenata*).

The following figures, provide an overview of the species distributed in different areas of Japan. Figure 5 shows the distribution of coniferous species. Spruce and fir trees are mainly distributed in the North, while cedar, larch and red pine trees are distributed in Honshu and cedar in the South. In the region of the study area, mainly cedar and larch were planted.

In comparison, Figure 6 provides less information regarding the species composition. The map focuses mainly on oak and beech trees; all other deciduous forests were not further specified. Therefore, it is only known that deciduous forests are distributed all over Japan, while beech and oak forests are mainly distributed along the western coast of Honshu. In comparison to the previously mentioned Figures, Figure 7 includes relative numbers of coniferous and broad-leaved tree species.

It can be seen, that out of the 50% coniferous trees, planted cedar and cypress are the main species, which can be found in Japan. Considering the broad-leaved trees, also in this figure only the species oak

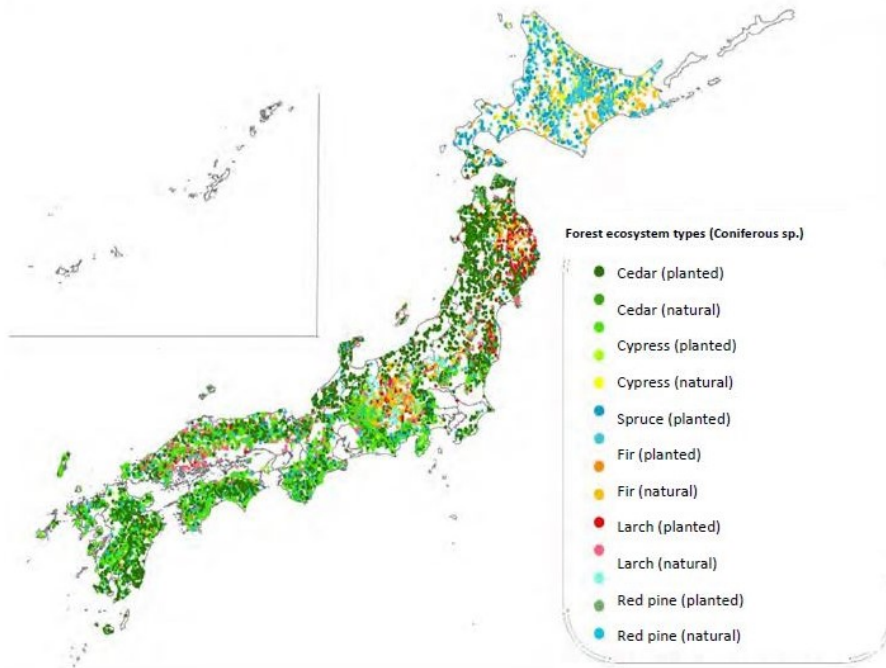


Figure 5 Distribution of coniferous forests (Makimoto, 2019)

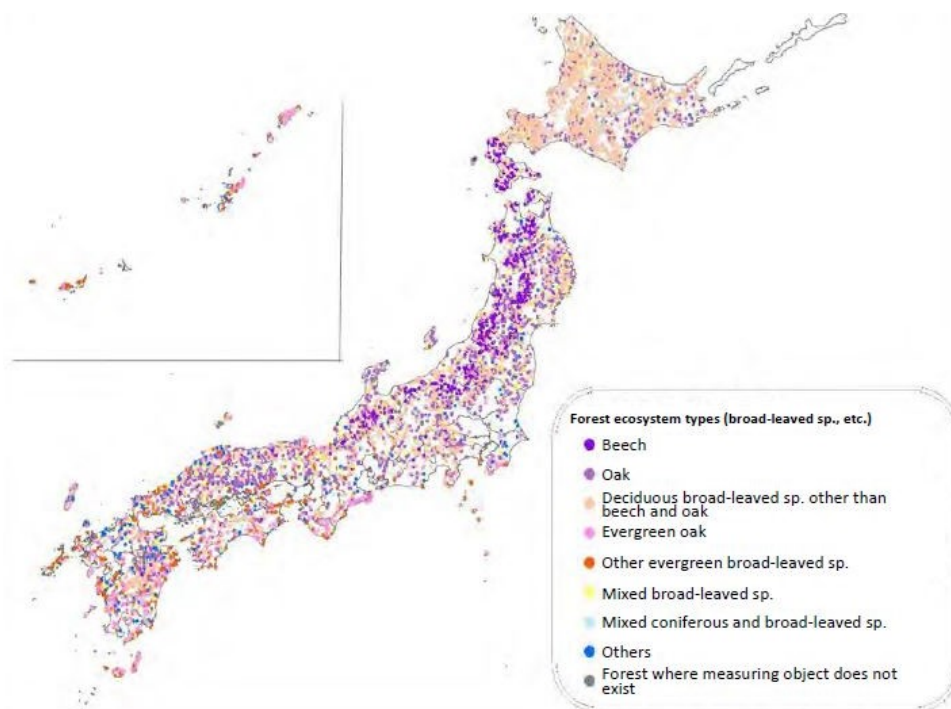


Figure 6 Distribution of broad-leaved forests (Makimoto, 2019)

and beech are mentioned by name. Except those, the broad-leaved trees are classified into mixed species, no dominant species and species other than beech and oak. It occurred that there are more information provided for the planted species than the natural forests and more for coniferous trees than mixed broad-leaved forests.

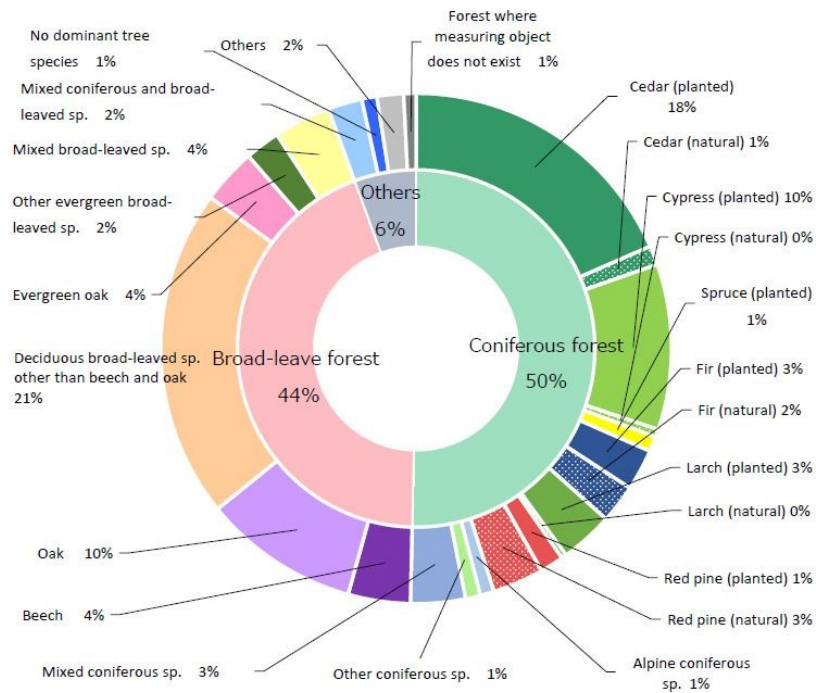


Figure 7 Composition of forest ecosystem by dominant tree species (Makimoto, 2019)

3.3 Japan forest policy

In general, Japan forest policy aims at preserving forests for socio-economic and environmental benefits (Makimoto, 2019). Field surveys are carried out every five years to gather information about the status, health and the population in forests. These surveys are conducted in around 13,000 sites to analyse effects of disturbances, climate change, infestations and invasions (Makimoto, 2019). Additionally, the delivery of information is essential to increase the public understanding about the importance of forests.

There are several factors which have to be considered when forests are analysed. Biodiversity is one of the most important factors, since forests contain a substantial proportion of species, which enables the forest ecosystem to respond to natural and anthropogenic disturbances. Diversity can be significantly influenced by disturbances which can result in species decline or even extinction. Sufficient habitat sizes, structural diversity and protection measures are necessary to preserve diversity (Makimoto, 2019).

Another indicator for the health of the forest is the number of native tree species, which helps to understand changes in ecosystems and relationships between species (Makimoto, 2019). The report of native species further indicated exotic plants which distribute in natural environments and outline invasive plant species invading natural ecosystems. Diseases or infections need to be monitored as

well, because they can alter the forest structure significantly and lead to a significant reduction or loss of forest areas on the one hand but could be on the other hand a mechanism for regeneration.

Preservation of forests needs the collection of accurate data, which demands time and money. The study of cheaper and more efficient methodologies to gather information should be the aim to continue and achieve the ambitious goals of Japan's forest policy.

3.4 Forest types

There are three types of forests introduced in the following two chapters. The first chapter considers riparian forests, which occurs mainly in lowland areas and along rivers. The second chapter summarises *Quercus* and *Fagus* mixed forests.

3.4.1 Riparian forest

Riparian forests refer to vegetations along rivers and streams, have an expansion from the active floodplains to the uplands (Naiman et al., 1998) and are in the transition zone between terrestrial and aquatic environments (Sakio & Tamura, 2008). Forest vegetation develops on fluvial terraces and debris flows, which are formed in or along rivers (Ohno, 2008) and vary in their longitudinal and lateral structure (Naiman et al., 1998). Therefore, riparian forests are often characterised as diverse mosaics in large landscapes (Figure 8).

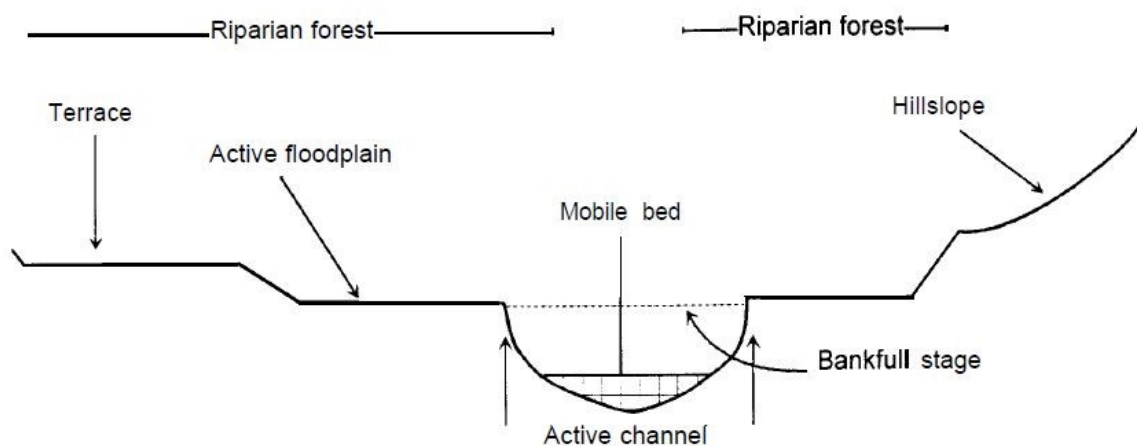


Figure 8 Characteristic structure of riparian forest areas (Naiman, 1997).

The biodiversity of riparian forests provides essential ecosystem services and is of great importance for ecological functions (Sakio & Tamura, 2008). Their diverse ecosystem is structurally and floristically complex, provides high rates of nutrient cycling and productivity (Naiman et al., 1998). The forest

influences microclimate conditions and biochemical cycles and directly affect the stream environment. Water and soil temperatures are regulated by the forest and have a direct influence on air and surface temperature.

The development of soils in different locations and influences the diversity of the forest additionally. Usually, soil conditions are rocky with a small amount of fine soil particles, which are influenced by sedimentation and erosion, especially in the active channels, where vegetation colonizes extensively and resists the shear stress of flowing water and physical disturbances, the soils are initially poor (Naiman et al., 1998). An organic layer is formed by organic matter of decomposing vegetation and increases the fertility of the soil (Ohno, 2008). Further, riparian forests offer good conditions for tree species regarding the location, because they have a high input of nutrients and sediment movement due to water dynamics (Miyawaki & Washitani, 2003).

Riparian forests are strongly affected by topographic and hydrologic factors, which influence the composition of forests (Fukamachi et al., 2020). There are several disturbance systems affecting the forest such as floods, landslides and slope failures (Fukamachi et al., 2020). Those disturbances can vary in frequency and magnitude. The destruction of forests, regeneration and change in tree species vary with the heterogeneous topography. The disturbances are responsible for the high diversity of forests, since they provide diverse habitats, offer several species ideal niche conditions and enhance species richness (Sakio et al., 2002). Riparian forests further provide a heterogeneous microenvironment, which increases the ecological niches and therefore the species richness (Masaki et al., 2008). Vegetations, growing in these areas, show morphological, physiological and reproductive adaptations to survive in the unstable environment conditions (Naiman et al., 1998). It can be said, that physical processes initialize vegetation spread and growth, but species interactions and survival strategies adapted to riparian areas form the characteristic mosaic of vegetation structure (Naiman et al., 1998). Plants need to be well adapted when they grow in riparian areas, and need several morphological, physiological and reproduction adaptations to survive the harsh environment (Naiman et al., 1998). Sakio & Tamura (2008) summarised several riparian forests and their characteristic tree species. Throughout Japan the dominant species in riparian forests are different kinds of *Salix*, *Alnus* and *Fraxinus* species, as well as *Pterocarya rhoifolia*, *Cercidiphyllum japonicum*, *Fagus crenata* and *Aesculus turbinata*. *Salix* trees in particular are invaders, endures and resisters after all kinds of disturbances and therefore well adapted in these environments.

Riparian forests are complex ecosystems with various interactions between the forest structure and composition and reactions to disturbances (Naiman et al., 1998). A riparian forest is therefore difficult to characterise and detailed analysis are necessary to identify the kind of riparian forest. Further, an

overview of species composition and structure is needed to give the forest a label and the possibility to characterise them properly.

3.4.2 *Quercus* and *Fagus* forests

Quercus and *Fagus* forests belong to the cold-temperate forests, which show a high tree species density and occurring genera, similar to the ones occurring in Europe and North America. Additionally, these forest types in cold-temperate forests are divided into *Fagus japonica*, *Fagus crenata*, *Quercus serrata* and *Quercus mongolica*, while there is another cold-temperate forest (*Abies-sachalinensis-quercus mongolica* forest), which is not considered in this study. The forests are distributed in the lowland of northern Japan: Tohoku region and southern Hokkaido (Okitsu, 2003). Also, there is a division between the forests in the South and the North and between forests in the Japan sea side and the Pacific side. Several studies pointed out that there are significant differences between these sides according to the climate conditions (Hukusima et al., 2013; Okitsu, 2003; Ohno 1991, Sasaki 1970). Furthermore, the literature provides several categories and groupings of *Fagus* and *Quercus* forests. Ohno (1991) identified a combination of 20 natural forest communities with 55 related subgroups in the area of northern Honshu. A general overview for the *Fagus* and *Quercus* forests is given in the following section.

Fagus crenata forests are composed of *Fagus crenata*, *Viburnum furcatum*, *Quercus mongolica*, *Acer japonicum*, *Acer palmatum* and *Lindera umbellata*, which differ slightly when they are located on the Japan sea side or the Pacific side (Okitsu, 2003). As there are several subcategories of *Fagus* forests, Sasaki (1970) generalised them and pointed out that the species coexisting with *Fagus* are *Acer mono*, *Acer sieboldianum*, *Fraxinus sieboldiana*, *Tilia japonica*, *Quercus mongolica* var.

grosseserrata, *Acanthopanax sciadophylloides*, *Kalopanax septemlobus*, *Acer rufinerve*, *Magnolia obovata*, *Sorbus alnifolia* etc., with all of them reaching heights of 30 m. The shrub layer is usually composed of *Lindera membranacea*, *Viburnum furcatum*, *Hamamelis japonica* var. *obtusata*, *Rhododendron albrechtii*, *Acer japonicum* etc., with heights ranging between 2 and 3 m. This forest type distributes usually between elevations of 500 and 1800 m. Sasaki (1970) pointed out that the lower boundary varies depending on the climate conditions while *Fagus* forests can occur from 200 m in North of Honshu.

Sasaki (1970) further concluded that in regions lower than 200 m *Fagus* forests form a secondary forest with one of the subgroups *Quercus mongolica* var. *grosseserrata*, *Quercus serrata*, *Quercus dentata* and *Castanea crenata*. Therefore, forests develop from lowland *Quercus* forests to *Fagus* forests in highlands. *Quercus mongolica* forests are dominated by *Quercus mongolica*, *Kalopanax pietus*, *Acer mono*, *A. japonicum*, *Tilia japonicum*, *Fraxinus languniosa* and *Prunus sargentii* (Okitsu, 2003). A

species that occurs in these types of forests, additionally, is *Camellia japonica* (Sasaki, 1970). For the Japan sea side of Tohoku, Ohno (1991), the community group *Quercus mongolica* *vat. grosserrata-Fagus crenata* is identified for lower altitude regions, as considered in this study. In the case of *Quercus mongolica* forests, Okitsu (2003) pointed out, that the forest type is not well classified and needs to be further conducted.

According to Okitsu (2003) these forest types distribute between 500 to 1700 m, while Ohno (1991) specified that the group of *Quercus mongolica* *vat. grosserrata-Fagus crenata* occurred mostly in lowlands and the lower montane belt (average altitudes of 400 m).

The mentioned studies summarised a couple of studies to provide an overview of Japan cold-temperate forests, which will help to classify and evaluate the forest in Shonai (Table 1).

Table 1 Characteristic species in *Quercus mongolica* forests in Tohoku area (Okitsu, 2003)

Region*	NT	NT	SH	SH	SH	SH	SH	NH	NH	NH
Running no. **	1	2	3	4	5	6	7	8	9	10
<i>Quercus mongolica</i>	4	4	5	4	3	5	4	5	5	5
<i>Kalopanax pictus</i>	+	.	+	1	2	2	2	2	+	.
<i>Acer mono</i>	.	+	2	+	2	.	2	+	1	1
<i>Acer japonicum</i>	1	2	+	.	.	.	+	.	+	.
<i>Tilia japonica</i>	+	+	+	+	2	.	+	.	.	.
<i>Fraxinus lamuginosa</i>	+	2	+	+	2	.	+	.	.	.
<i>Sorbus alnifolia</i>	2	.	+	.	.	+	+	.	+	.
<i>Prunus sargentii</i>	1	+	.	+	.	.	.	+	+	+
<i>Carpinus cordata</i>	+	3	+	.	+	.
<i>Magnolia obovata</i>	.	+	1	.	.	.	+	.	+	.
<i>Rhus trichocarpa</i>	+	.	1	+	+
<i>Cornus controversa</i>	.	+	+	.	.	.	+	.	.	+
<i>Prunus ssiori</i>	.	.	+	.	+	.	+	.	+	.
<i>Acer palmatum</i>	.	.	+	+	3	.	+	+	.	.
<i>Maackia amurensis</i>	1	+	.	+	+	.
<i>Abies sachalinensis</i>	1	1	.	.	+
<i>Magnolia kobus</i>	.	.	+	+	.	.	+	.	.	.
<i>Fagus crenata</i>	2	+
<i>Viburnum furcatum</i>	2	1
<i>Viburnum wrightii</i>	1	+
<i>Corylus sieboldiana</i>	+	+
<i>Acer rufinerve</i>	+	+
<i>Morus bombycis</i>	.	.	+	+	.	.
<i>Betula ermanii</i>	3	+
<i>Phellodendron amurense</i>	2	+
<i>Ulmus laciniata</i>	+	.	+	.	.	.
<i>Cephalotaxus harringtonia</i>	1	2	.	.	.
<i>Tilia maximowicziana</i>	1	+	.
<i>Ulmus propinqua</i>	+	1	.
<i>Sorbus commixta</i>	+	+
<i>Sasamorpha borealis</i>	1	5
<i>Sasa paniculata</i>	.	.	.	5	5	4	5	4	1	5

*: NT – northern Tohoku, SH – southern Hokkaido, NH – northern Hokkaido

** : 1, 2 – Iwate prefecture (Takeda & Ikuta 1986), 3 – Chitose (Tatewaki 1961b), 4 – Shiraoi (Tatewaki 1961b), 5 – Shizunai (Kojima 1982), 6 – Maruyama, Sapporo (Tatewaki 1958c), 7 – Nopporo (Tatewaki & Igarashi 1973), 8, 9 – Yobito, Abashiri (Tatewaki 1961c), 10 – Teshio (Tatewaki & Igarashi 1971)

3.5 Composition of the research forest

The research area for this study is located on the main Island of Japan, Honshu. The area is part of Yamagata prefecture, located in the northern part of the island. In the western side of this prefecture is the Faculty of Agriculture of Yamagata University in Tsuruoka city. Yamagata University owns a Research Forest (YURF), which is used for forestry investigations. YURF is located around 26 km south of the faculty in the northern part of the Asahi Mountains, part of the Echigo Mountain Range and the Wasada River Basin, covers an area of 753 ha and is crossed from north to south by the Wasada River (38°33'21"N 139°51'42"E). The highest elevation is around 860 m, based on a relief with steep slopes, ranging between 30 and 44 degrees, whereby approximately 50 % of the slopes are steeper than 30 degrees.

Generally, the mixed forest is composed by deciduous broad-leaved and coniferous trees [22]. The climate conditions and the location of YURF are responsible for the dominance of beech (*Fagus crenata*) forests in this area. Beech forests are mainly observed in the higher altitude areas and often mixed with Mongolian oak (*Quercus mongolica*), Japanese Bigleaf Magnolia (*Magnolia obovata*), Maple species (*Acer palmatum*, *Acer japonica*, *Acer rufinerve*) and Monarch birch (*Betula maximowicziana*). In lower altitudes mixed forests are composed by Mizugi (*Cornus controversa*), Maple (*Acer pictum*), Japanese lime (*Tilia japonica*, *Tilia maximowicziana*), Loose-flower Hornbeam and Aohada (*Carpinus laxiflora* and *Ilex macropoda*). The distribution and dominance of these species is less studied. On the bottom of the mountain most areas in the forest are close to the river and characterised as riparian forest type. The main species, which can be found, are Japanese wingnuts (*Pterocarya rhoifolia*), Japanese walnut (*Junglans ailantifolia*), Tochinoki (*Aesculus turbinata*) and *Salix* species (*Salix jessoensis*, *Salix serissaefolia*). Furthermore, the forest is composed of several deciduous shrub species like *Lindera umbellata* and *Hamamelis japonica* (Lopez, 2014). The forest is further composed of three planted tree species: Japanese cedar (*Cryptomeria japonica*), Japanese cypress (*Chamaecyparis obtuse*) and larch (*Larix kaempferi*). Those species replaced the natural mixed forests in lower regions, especially beech forests were replaced by Japanese cedar plantations (Lopez, 2014). A total number of 108 families, 293 genus and 335 species have been identified in the University Forest by Mori (1968).

3.5.1 Studied Sites

In total 13 study sites were chosen to analyse and characterise the distribution and composition of mainly the mixed natural forest at YURF (Figure 9). Three types of sites with natural mixed forest and evergreen plantation were considered. They are located in lower altitude areas of the forest: Riparian

forest sites, Terrace sites and Slope sites. Riparian sites are located along the Wasada river. These sites are characterised by flat areas; their orthomosaic borders captured the foot of the slopes. The characteristics of the riparian forests were captured in sites 1, 4, 6 and 7. The second forest type is characteristic for a riparian and mountainous tree species composition located in steep slopes of the mountain, represented by sites 11, 12 and 13. Slope sites are located along the slopes in lower altitude areas. The tree species composition differs from riparian forest, with their characteristic tree species composition more similar to beech forests. These sites are represented by sites 2, 3, 5, 8, 9 and 10. The following passage provides information about first Riparian sites, then Terrace sites and finally Slope sites.

Site 1 is characterised by a flat area covering 6 ha close to the river. In the northern part of grows mixed forest, in a small area surrounded by rivers on both sides that hereafter will be called “island”. During snowmelt and intensive rain events, the island becomes surrounded by the river. The island shows a characteristic tree species distribution of *Juglans ailantifolia* (Japanese walnut), *Pterocarya rhoifolia* (Japanese wingnut), *Phellodendron amurense* (Japanese wedding cake), *Salix* species (willow) and *Robinia pseudoacacia* (Black locust) trees. The southern part of site 1 is characterised by a dense patch of *Pterocarya rhoifolia* trees. The southernmost boundary and the eastern part of the orthomosaic imaged slope areas. The main species distributed in the slope is *Cryptomeria japonica*. All sites along the river (1, 4, 6 and 7) have a dense understory vegetation covering the forest floor from early summer until late autumn.

Site 4 is located 350 meters north of the first study site and is smaller, with only 3 ha. The main characteristic of the side is a patch of young willow trees in the southern part, while in the rest of the site grow mainly walnut trees. The northern part the orthomosaic of this site shows the bottom of a slope, where mainly cedar trees were planted. The river crosses site 4 from south to north and also from east to west. There is a high number of young trees, belonging to different species, in the middle of the site.

Site 6, covering 4.1 ha, is located at the entrance of YURF, 750 meters north of site 1, directly at the Wasada river, but in comparison to the other sites, where the elevation is around 1 meter higher than the river level. Site 6 is on the west side of the forest road, at the river level. Therefore, most times of the year the soil is usually water saturated and sometimes flooded by a couple of centimetres of water. In this area, mainly willow trees can be identified. In general, the site shows the characteristic tree species composition of riparian forests with walnuts and wingnuts. The eastern and western part of the orthomosaic captured the bottom of the slopes, with a change of tree species distribution.

Site 7 is located 200 meters north of site 6, around 1 meter above the river level and covers an area of 5.1 ha. The centre is dominated by riparian forest, with wingnuts, walnuts and willow trees. Exactly there a depression was found, where the soil is often saturated during the year. The western boundary of the orthomosaic imaged a slope and the eastern part mapped the transition to site 13, located on the slope. The site is crossed from the south to the north by the Wasada river.

Site 11 is situated on a slope, facing north and covering 3.5 ha. The site is characterised by a flat area in the northern part and the steep slope, both captured in the orthomosaic. The southern boundary of the site is the transition between the mixed forest and a cedar plantation. The site shows the characteristic tree species of the riparian forest (walnuts and wingnuts) but also a change to tree species like maples, chestnuts and magnolia trees. In comparison to the river sites the density of the understory vegetation is less. While the sites along the river are area-wide covered with scrub vegetation, the Slope sites show punctual high-density clusters of scrubs, while other parts contain only single plants.

Site 12, covering an area of 3 ha, is directly next to the northern boundary of site 11 and is characterised by a slope facing west. The area along the road is flat and starts to increase gently, while from the centre of the orthomosaic the slope becomes steeper to the east, partly having slope angles of almost 90 degrees. The site is characterised by the migration of riparian species composition to dense maple vegetation, limited by cedar trees in the eastern part. Between site 11 and 12 a small river appears in the melting season and the rain season in summer. The flat area, which can be seen in the orthomosaics of sites 11 and 12, is at the same time always water saturated.

Site 13 is characterised by a high density of walnut trees covering most parts of the site and orthomosaic. The site is located next to site 7, north of site 12 and covers an area of 4.8 ha. The slope in the site is facing mainly to the west; only in the southern part the slope is facing south. The eastern boundary is the transition to an uphill cedar plantation.

Sites 2 and 3 are located between the sites 1 and 4, while site 3 is at the east side of the river, located at the northern boundary of site 1; site 2 is on the western side of the river, approximately 100 meters apart from site 1. The sites 2 and 3 cover 8.1 and 5.5 ha, respectively and both sites have a characteristic mountain ridge and two valleys along it. The ridge in site 2 is pointing to the east, while the one of site 3 is pointing north. The western valley in site 3 is located directly next to the Wasada river and the eastern valley has a small river; both are filled with water in the snow melt and the rainy season, as the valleys of site 2. The main difference is that site 2 has a higher elevation than site 3 (approximately 350 m). The species composition is similar to the riparian forest in lower altitudes and a change to first maple and magnolia trees, then to oak, larch and beech trees with increasing elevation.

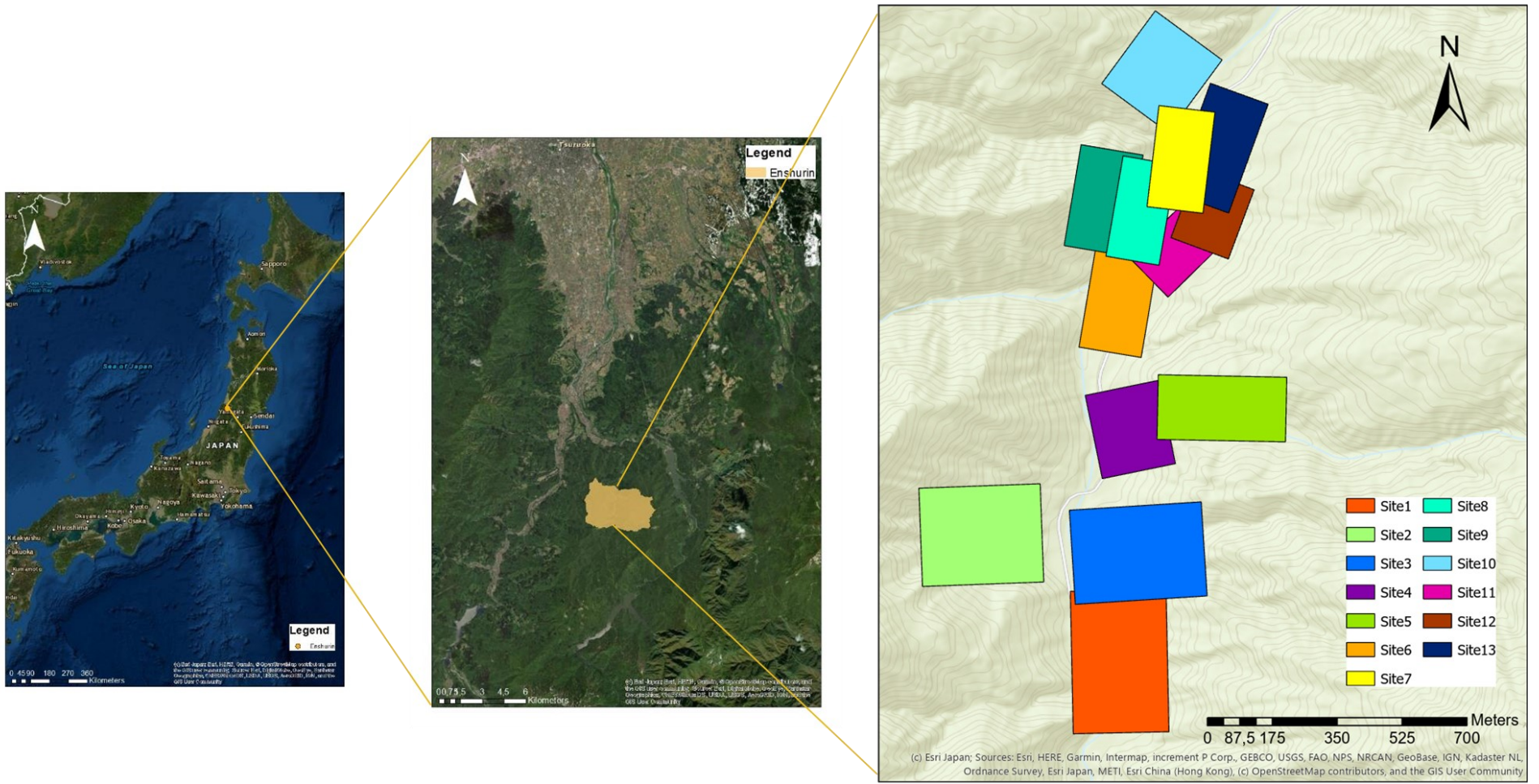


Figure 9 Location of study areas

Site 5 is located north of site 4 with a south facing slope. The site boundaries are the river in the south, and cedar trees in all other directions. In comparison to all other Slope sites, the species richness is small. The main trees occurring in the site are maple, oak and magnolia trees. The site is inaccessible as it is directly located at the river with a nearly 90-degree cliff.

Site 8 and 9 belong to one east facing slope, where site 8 is the lower part and site 9 the upper part of the slope. The sites are located on the western boundary of site 7 and cover 4.3 and 6.1 ha. In the northern and southern direction are also slopes, which end in a small valley formed by rivers. The forest is characterised by the steepness of the slope and a high mixture of tree species. The site is mainly composed of deciduous trees, and only in the southern part of the orthomosaic cedar trees occur.

The slope of site 10 faces east and the boundaries of the mixed forest patch are cedar trees and the Wasada river at the bottom of the slope. The site is north of the sites 8 and 9 and has a distance of approximately 1.3 km to site 1. The site covers 5.4 ha and has one of the steepest slopes of all sites. The mixture of trees is high compared to the Riparian sites.

3.5.2 YURF - Top sites

In addition to the 13 sites in lower altitude areas, four sites were chosen on approximately 600 m.a.s.l. in the eastern mountain. These sites represent beech forests mixed with tree species adapted to the lower temperatures. The sites are mainly composed of beech (*Fagus crenata*), larch (*Larix kaempferi*) and oak (*Quercus mongolica*). Three sites show dominance in each one of the tree species and the last site was the natural mixture of them. These four study sites were part of the master thesis of Mr. Luca Tomhave (M.Sc. student of LUH) and therefore only mentioned here, because the captured species were additionally used for the DL methodology.

3.6 Fieldwork

The purpose of the fieldwork was to identify tree species, to count trees and to generate manual maps for the study sites. Results of the fieldwork were used to evaluate the accuracy of image analysis and DL techniques.

Fieldwork was conducted in YURF in autumn 2019, spring 2020 and the beginning of summer 2020. Data for all Riparian sites (along the river and at the slope) were gathered, while four representative sites were chosen for fieldwork in the Slope sites. The chosen Slope sites (3, 8/9 and 10) were used since they provided the best environment to conduct fieldwork. The Slope sites were difficult to access

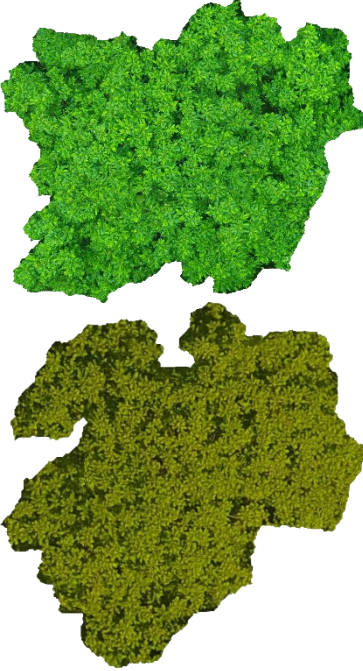


and the steepness of slopes decreased the possibility to gather accurate and precise information about tree stands. Therefore, the collected data is incomplete, the position and number of trees vary in comparison to the real conditions in the forest.




In total, 14 days were needed to gather the information of tree position and tree species. It has to be noted, that tree locations were plotted by the relations between trees, landmarks and with the help of the previously gathered orthomosaics. In general, no GPS coordinates for single trees were taken and no fixed plots were set up, as the studied area was large and small plots were found out to be not representative for the whole imaged area. Only for site 1 the island was geolocated with accurate measurements, which needed manpower of 10-15 people for five days. After an evaluation of the grid results, the data were identified as insufficient as they were not representative for the studied site. Therefore, the method of gathering data was changed and manual maps were drawn, indicating the position of the tree and the species name. Images of the bark and the leaves were taken to complete the dataset. Manual maps were digitalized with ArcGIS and the accuracy of the maps was increased by using winter images as a base map. Since the focus of the study was on deciduous trees, which are represented by the tree stem in winter images, accurate maps could be produced.







3.6.1 Tree species


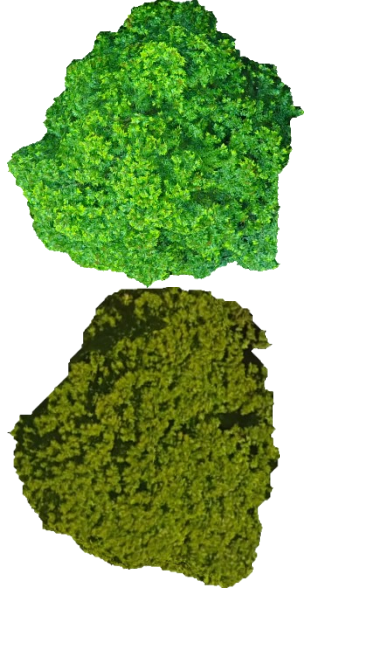


The following table gives an overview of the main tree species and shrubs identified in YURF. Table 2 provides the scientific name in the first column, the common name in the second column, a short description about every species, images of the aerial view, ground view and the leaves. The description contains general information about the species, their bark and leaves, height and further information. For the aerial view, UAV-acquired images are shown with different resolutions. The first image shows the tree with a resolution between 2.7 and 4.5 cm/pix, while the second image shows an image with the resolution between 1.3 to 1.7 cm/pix (depending on the flight height and imaged site).




Table 2 Tree species descriptions







Name	Common name	Description	Aerial view	Ground view	Leaf
<p><i>Juglans ailantifolia</i></p>	<p>Japanese walnut</p>	<p>Japanese walnut is a deciduous tree, native to Japan and Sakhalin. The tree usually reaches a height of 20 m. The tree forms a broad and half-round crown. The bark has a light grey colour with reticulate grooves in it. The leaves are imparipinnate, 40 – 60 cm long and has 11 to 17 leaf segments. The shape of the leaf is elongated to elliptical and 10 – 16 cm long. The leaf colour is dark green and turns yellow in autumn. The tree flowers in May and grow clusters of 20 fruits in autumn. The Japanese walnut is a clearstem tree and can form multi-stems.</p>		 <p>https://www.cirrusimage.com/tree_japanese_walnut/ (latest access 02. February 2021)</p>	






<p><i>Pterocarya rhoifolia</i> Siebold & Zucc.</p>	<p>Japanese wingnut</p>	<p>Japanese wingnut is a deciduous tree native in Japan. Its habitats are wet valley and mountain areas, where it dominates the canopy area. The tree grows up to 30 m. The bark shows a grey greenish colour with fissures, while the leaves are mid-green and turn yellow in autumn. The leaves imparipinnate are 20 – 40 cm with up to 25 leaflets, which are ovate to oblong formed and 4 x 12 cm in shape. The flower appears in June and the fruit in autumn.</p>		 <p>https://de.123rf.com/photo_68914359_japanische-fl%C3%BCgelnuss-pterocarya-rhoifolia-ist-eine-baumart-aus-der-familie-der-juglandaceae-die-in-feuch.html (latest access 02. February 2021)</p>	
--	-------------------------	---	--	--	---

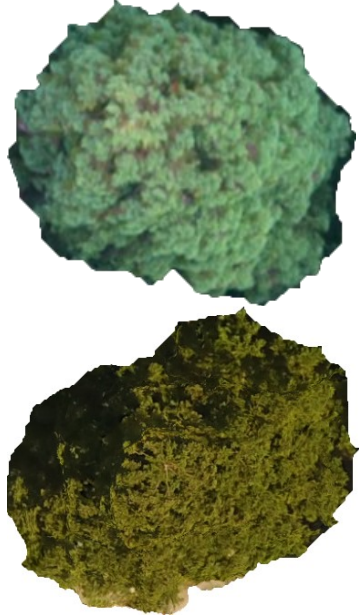


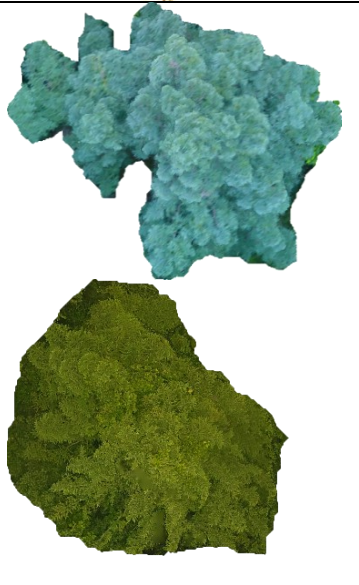


<p><i>Magnolia obovata</i></p>	<p>Japanese bigleaf magnolia</p>	<p>The deciduous tree grows up to 30 m, while the spread is usually wider than 8 m. It is native to Japan and occurs in broad-leaved forests. The bark of the tree is slate grey, while the leaves are large with up to 38 cm length and 20 cm width. The leaf colour is green with a silvery to grey pubescent. The tree flowers in early summer and they are characteristic because of their large cone shape size of 20 cm.</p>		 <p>https://commons.wikimedia.org/wiki/Magnolia_obovata (latest access 02. February 2021)</p>	
<p><i>Aesculus turbinata - Blume</i></p>	<p>Japanese Horse Chestnut</p>	<p>The deciduous tree is native to Japan and grows in mountainous areas, preferentially in moist slopes. The tree can reach a height of 20 m to 35 m and it is a vigorous, spreading tree. The bark is dark brown</p>			

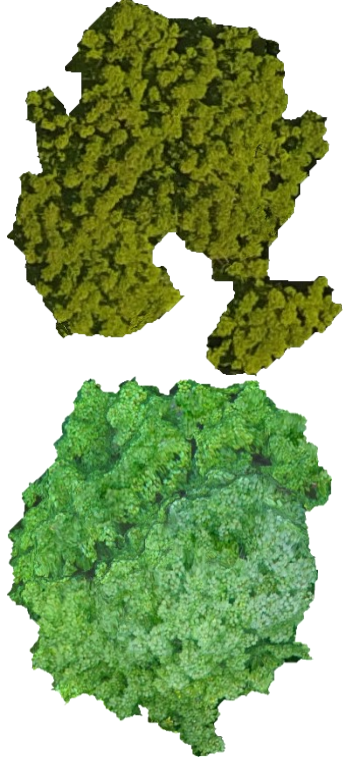


		and peeled off and waved. The palmate compound leaves with 5 to 9, 15 – 30 cm, leaves. The flower occurs in June and has a white colour. The fruits are formed in autumn.		https://www.cirrusimage.com/tree_japanese_horse_chestnut/ (latest access 02. February 2021)	
<i>Castanea crenata</i>	Japanese chestnut	The medium-sized (10 – 15 m) deciduous tree has a wide spread crown. The leaves are oblong-lanceolate dark green leaves with tooth. From the bottom the leaf is pubescent. In autumn leaves change their colour to yellow-bronzy. In late spring the flowers appear which show a characteristic upright catkin structure which are 7 – 20 cm long.		 https://tonysharks.com/Tree_of_life/Eukaryote/Plantae/Land_plants/Kuri/Kuri.html (latest access 02. February 2021)	





<p><i>Salix jessoensis</i> Seem.</p>	<p>Willow</p>	<p>The deciduous tree is a weeping willow tree reaching a height of 15 to 20 m. Preferentially the tree grows along rivers. The shape of the crown is round. The bark has a pale brown greyish colour and is furrowed. The toothed small leaves, which are powdery white from the bottom, are 10 cm long and have a dark green colour. In autumn the leaves turn brownish-yellow. The flower grows with the new leaves in early spring.</p>		 <p>https://www.botanic.jp/plants-sa/siyagi.htm (latest access 02. February 2021)</p>	
---	---------------	---	---	--	---








<p><i>Salix serissaefolia</i></p>	<p>Willow</p>	<p>This 10 to 20 m deciduous tree is native to Japan and occurs mainly in wet conditions, close to rivers. The bark is grey to brownish. The leaves are alternate organised, have a length of 3 to 7 cm with a sharp head.</p>		 <p>https://mikawanoyasou.org/data/kogomeyanagi.htm (latest access 02. February 2021)</p>	
<p><i>Fagus crenata</i></p>	<p>Japanese beech</p>	<p>Japanese beech is a deciduous tree growing in mountainous areas of Japan reaching a height of 35 m. The crown forms a round shape. The tree dominates deciduous forests, especially in higher altitudes. The bark has a light grey colour and a smooth shape. The leaves have an ovoid shape,</p>		 <p>https://en.wikipedia.org/wiki/Fagus_crenata (latest access 02. February 2021)</p>	

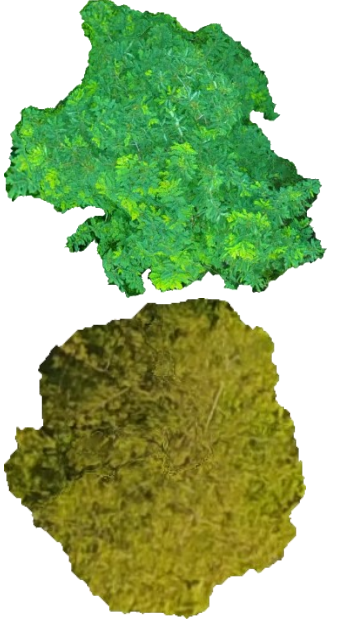





		the leaf margin in notched and the position of the leaf is alternate. The colour in summer is dark green and turns gold-brown in autumn.			
<i>Quercus mongolica</i>	Mongolian oak	The deciduous tree occurs in cooler regions of Japan. The tree grows up to 30 m and has an open crown spreading. The bark is dark grey and has deep ridges and furrows. The alternate position of the dark green, coarse toothed leaf with an ovoid shape turns red to dark red in autumn. The leaves built a dense cluster at the branch end and has a length of 7 – 19 cm and a width of 3 – 11 cm.	 	 https://landscapeplants.oregonstate.edu/plants/quercus-mongolica (latest access 02. February 2021)	






<p><i>Cryptomeria Japonica</i></p>	<p>Japanese cedar</p>	<p>The evergreen, coniferous tree grows up to 65 m. The shape of the crown is conical and it has characteristic straight, slender trunk with a reddish-brown colour. The bark is fibrous and it can be pilled of in strips. Th needle leaves are pale green and arranged in a spirally with a length of 0.5 to 1 cm.</p>		 <p>https://greenarborists.com/sugi-trees/ (latest access 02. February 2021)</p>	
<p><i>Larix kaempferi</i></p>	<p>Japanese larch</p>	<p>The deciduous conifer tree has a horizontally trunk and horizontally spreading branches. The crown is conical and dense, but can become more open with age. The bark is scaly and fissured with a greyish colour. The 2 to 3.5 cm needles are blue-green, spirally arranged and clustered in 20 to 35</p>		 <p>https://www.vdberk.com/trees/larix-kaempferi/ (latest access 02. February 2021)</p>	

		short shoots. In autumn the needles change their colour to yellow.			
<i>Acer mono maxim</i>	Maple	The deciduous maple tree grows in mountainous areas in Japan. The tree reaches a height of 15 m. The bark is grey with vertical furrows. The leaves grow five to seven lobes, which are 7 – 15 cm long. The leaf colour is green and turns yellowish red.		 <p>https://www.google.de/url?sa=i&url=http%3A%2F%2Fwww.bjrdhj.com%2Fpd.jsp%3Fid%3D211&psig=AOvVaw1YcZldm5sR2-d0yWLy3vPq&ust=1612332261565000&source=images&cd=vfe&ved=0CAkQjhxqFwoTCPDo6vDDyu4CFQAAAAAdAAAAABAD (latest access 02. February 2021)</p>	

<p><i>Acer sieboldium</i></p>	<p>Sieblod maple</p>	<p>This tree is a deciduous maple, which is often characterised as shrub or small tree of up to 10 m height. It grows often with multiple trunks. The leaves are palmately lobed with 9 to 11 lobes. The leaf is dark and turns red in autumn.</p>		 <p>https://plants.ces.ncsu.edu/plants/acer-sieboldianum/ (latest access 02. February 2021)</p>	
<p><i>Acer japonicum</i></p>	<p>Fullmoon maple</p>	<p>This maple is a deciduous tree growing up to 10 m. It grows in mountainous areas, preferentially under a bit shadowed condition. It often grows with multiple trunks, which have a grey colour. The leaves look roundish and have a green colour which turn yellow and red in autumn. The leaves have 9 – 13 separate lobes, which are around 7 cm long.</p>			

<p><i>Acer palmatum</i></p>	<p>Japanese maple</p>	<p>The Japanese deciduous maple tree or shrub, which grows up to 10 m. This tree can grow multiple trunks and often grows as understory vegetation. The leaves are up to 12 cm long and have usually 5 lobes, which are dark green and turn red in autumn.</p>		 <p>https://www.gardendesign.com/japanese-maple/ (latest access 02. February 2021)</p>	
<p><i>Cornus controversa</i></p>	<p>Wedding cake tree</p>	<p>The wedding cake tree is a 10 to 12 m high deciduous tree. The characteristic shape is generated by the horizontally layered branches. The leaf has an ovate shape, a dark green colour, which turn red-purple in autumn. The leaves are 8 - 15 cm long.</p>	 	 <p>https://caraghnurseries.ie/product/cornus-controversa-variegata-wedding-cake-tree/ (latest access 02. February 2021)</p>	

<p><i>Robinia pseudoacacia</i></p>	<p>Black locust</p>	<p>Is a fast-growing invasive deciduous tree. The crown of the tree is round shaped. The bark is furrowed with a dark brown colour. The leaves are coloured blue-green, which are paired by 5 – 11 leaves of oval leaflets. The leaves change their colour to yellow in autumn.</p>		 <p>https://landscapeplants.oregonstate.edu/plants/robinia-pseudoacacia-frisia (latest access 02. February 2021)</p>	
<p><i>Alnus fauriei</i></p>	<p>Miyama alder</p>	<p>This deciduous tree is a large shrub, which can reach heights of 7 m. The leaves are around 11 cm long have an obovate shape, look dark green-yellowish and have small teeth. They are often forming a dense understory vegetation.</p>		 <p>https://www.botanic.jp/plants-ma/mikaha.htm (latest access 02. February 2021)</p>	

<p><i>Morus australis</i></p>	<p>Korean mulberry</p>	<p>The deciduous shrub or tree is small with a height of maximum 7.5 m. The crown is rounded with a light green leaf colour. Leaves are varying in the size and have an ovate shape. The base is heart-shaped and the leaves are coarse toothed.</p>		 <p><small>markin</small> https://www.cirrusimage.com/tree_japanese_mulberry/ (latest access 02. February 2021)</p>	
<p><i>Hamamelis japonica</i></p>	<p>Japanese witch hazel</p>	<p>The up to 4 m high deciduous shrub or small tree is native to Japan. The grey bark and the oval leaves of 5 – 7 cm length are characteristic for the tree.</p>		 <p>https://shop.lve-baumschule.de/laubgehoeelze/914/hamamelis-japonica (latest access 02. February 2021)</p>	

3.7 Forest classification systems

One part of this study is to classify forests developing a methodology, which can be applied in other regions with a standardised basis, so that field data can be compared. There were several approaches presented in previous studies, which focussed on classifying Japanese forests.

The Braun-Blanquet approach, a commonly used methodology, is cited by several papers working with plant species classification, field surveys and forest compositions, especially in Japan (Sakio & Tamura, 2008). This approach uses the floristic composition to distinguish types of vegetation. The idea behind this technique is to understand the vegetation based on their structure, composition and community. Indicator or character species are identified to classify the vegetation and a differential species to define the syntax (Westhoff & Van der Maarel, 1978). Whittaker is another researcher, who influenced the vegetation classification strongly. His concept of population structure of vegetation analysis uses the dominance and diversity of species to indicate their importance for the ecosystem. Commonly used is also gradient analysis of vegetation by R.H. Whittaker, who introduced his concept to identify spatial patterns of vegetations to understand the structure and variation of vegetations in ecosystems (Whittaker, 1967). In modern studies, like Ohno (2008), dominant tree species were identified to classify forests based on the idea of Braun-Blanquet. A dominant species needs to comprise 30 % of the forest area (Makimoto, 2019).

The forest and forest vegetation can be further divided into different layers. Fukamachi et al. (2020) applied a vertical stratification and divided the forest into the layers: tree, subtree, shrub and herb. Sakio et al. (2002) recorded only three layers of the forest: canopy, subcanopy and understory vegetation.

Kikuchi (2008), who worked in riparian forests, classified different forest sites based on their stability, elevation and distance to the riverbed. He classified active sites with up to 1.5 m higher elevation and distances up to 10 m, while stable sites were areas above a height difference of 1.5 m and a distance greater than 10 m. Sites, which lay in between were considered as semi-active. Masaki et al. (2008) classified riparian forests based on their major topographic unit as riparian area, colluvial slope, denudation slope and upper terrace. The different sites showed specific conditions, like terraces with drier soils.

Bravo-Oviedo et al. (2014) specifically focussed on the definition and characterisation of mixed forest. The authors summarised different approaches used in recent years: compositional approach, structural approach developmental approach and functional approach. The compositional approach classified forests on depending on the occurrence of tree species, disregarding horizontal and vertical structures of the forest, as well as the spatial scale. The structural approach characterises forests based

on the form, type and grade of the mixture, which integrated horizontal tree patterns (form), vertical distributions in forest stands (type) and the number of trees (grade). The introduced development approach considers the development based on disturbances and natural gradients within the forest. A detailed classification can be found in [Smith et al. \(1997\)](#). The functional approach considers species and their functional importance for the ecosystem, instead of only considering the number of tree species. This approach is the most difficult one, as functions and their importance for the ecosystem are difficult to evaluate. In general [Bravo-Oviedo et al. \(2014\)](#) raised that there are missing harmonized definitions for mixed forests, leading to mainly three approaches: no definition of the forest, but a list with occurring tree species, definitions based on percentages of canopy covers, definitions based on other forests characteristics. The proposed definition for mixed forest were given by [Bravo-Oviedo et al. \(2014\)](#): *“A mixed forest is a forest unit, excluding linear formations, where at least two tree species coexist at any developmental stage, sharing common resources (light, water, and/or soil nutrients). The presence of each of the component species is normally quantified as a proportion of the number of stems or of basal area, although volume, biomass or canopy cover as well as proportions by occupied stand area may be used for specific objectives. A variety of structures and patterns of mixtures can occur, and the interactions between the component species and their relative proportions may change over time.”*

Furthermore, the authors ([Bravo-Oviedo et al., 2014](#)) raised that there are four aspects, which have to be provided:

- The dimension of the studied forest
- The development stage
- The occurrence and form of the mixture
- Drivers of species occurrence (facilitation, niche differentiation and competition)

The newest and most detailed approach was therefore presented by [Bravo-Oviedo et al. \(2014\)](#), who identified the most important aspects, which need to be considered when forests are classified. In the later chapters (**4 to 8**) this set of information is used to develop a new standardised methodology for forest classifications.

3.8 Diversity measures

Measuring the diversity in different ecosystems is an important aspect and commonly done. In this chapter several indices are introduced, which calculates the diversity, evenness and the effective number of species. In a community the number of species occurring and the evenness, which analysis if a species is rare or common, are important parameters to assess its diversity. There are several diversity indices available, which differ by the weight they put on species richness or evenness. The indices are highly dependent on the sampling strategy and discovered species in the community.

3.8.1 Species richness (*S*)

Species richness is a natural value, which describes the classified species in an ecosystem. It highly depends on the data base because it gives each species the same weight, which means dominant and rare species are treated equal.

3.8.2 Shannon index (*H*)

It is also called Shannon entropy and calculates the diversity, considering species richness and evenness. The index describes the uncertainty of a randomly selected species in the community, based on their occurring probability. The value will be zero in the case that only one species is in the community and it increases with the number of species in a community. The uncertainty is higher when all species occur evenly, while the value is lower when the species distribution is uneven. Therefore, the Shannon index is the highest for even and species rich communities, but the index is more abundant from the richness than evenness (Zeleny, 2021).

$$(1) H = \sum_{i=1}^S p_i * \ln(p_i)$$

With S = species richness, p_i = relative abundance of species i .

3.8.3 Simpson index (*D*)

This index also calculated the diversity by considering species richness and evenness, but compared to Shannon's index the Simpson index is strongly influenced by the species evenness. The probability, that two randomly selected trees are the same species, is calculated. With increasing species richness, the index D becomes smaller. Some studies prefer to use the Gini-Simpson index, which subtracts the Simpson index from the value 1, so that the index increases with increasing species richness (Zeleny, 2021).

$$(2) D = \sum_{i=1}^S p_i^2$$

$$(3) GS = 1 - D$$

With S = species richness, p_i = relative abundance of species i .

D ranges between 0 and 1, as it is a probability. It is known, that with more than 10 species the Simpson index is influenced by the evenness.

Figure 10 shows examples of species abundance distributions depending on the evenness of a community. Species richness alone cannot show differences in the three communities, in combination with Shannon entropy and the Gini-Simpson index it can provide more detailed information. The lower the Gini-Simpson index and the Shannon entropy, the more uneven is the community, which can be seen in Figure 11.

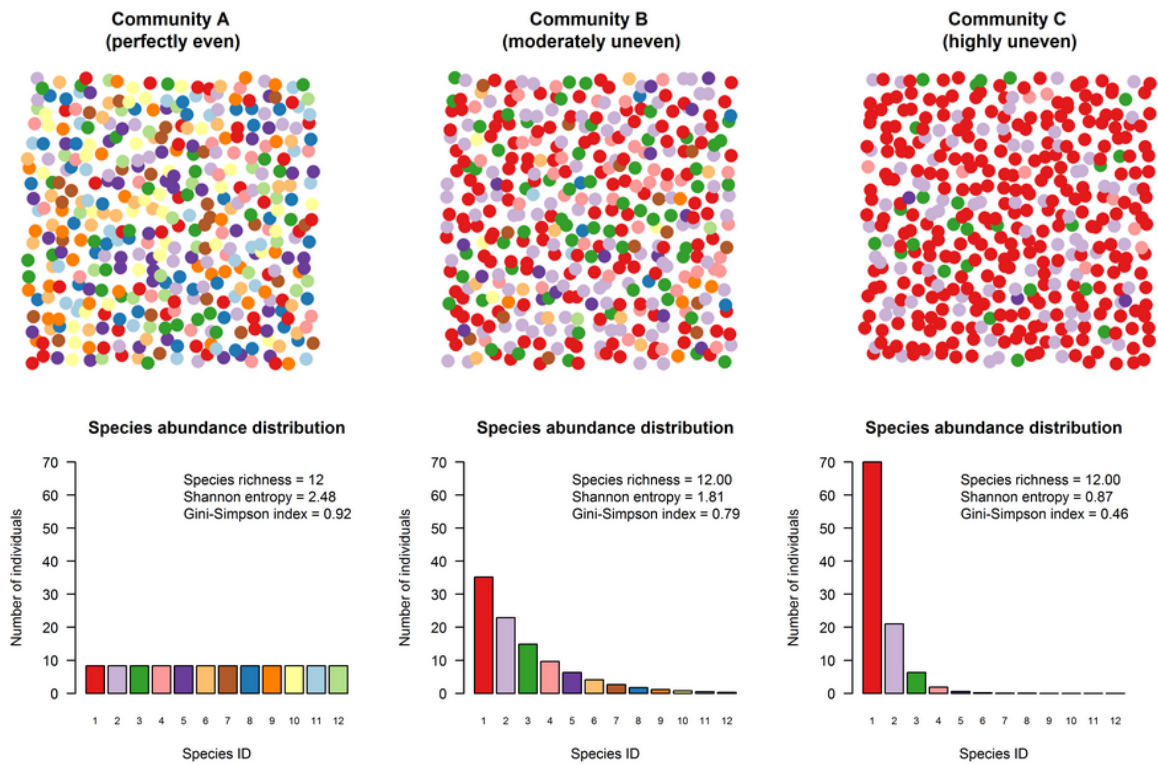


Figure 10 Three communities with different evenness at the top and diagrams of the species abundance corresponding to the three communities on the bottom. (<https://www.davidzeleny.net/anadat-r/doku.php/en:div-ind>, latest access 26. April 2021)

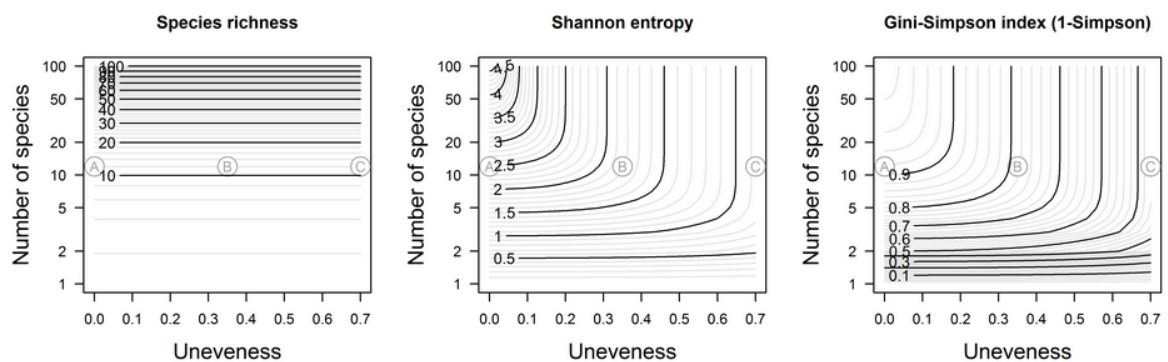


Figure 11 Example diagrams for the species richness, Shannon entropy and Gini-Simpson index based on the species number and unevenness (<https://www.davidzeleny.net/anadat-r/doku.php/en:div-ind>, latest access 26. April 2021)

3.8.4 Shannon Evenness

Is a measure, which describes relative species abundances in a community. The two main indices are Shannon's evenness and Simpson's evenness. Here, only the Shannon evenness is calculated by the ratio of the Shannon index divided by the maximum Shannon index. A value of 1 occur in case the species have the same relative abundance.

$$(4) J = \frac{H}{\log S}$$

3.8.5 Hill numbers

In the Hill numbers (or effective numbers of species) species richness, Shannon and Simpson's diversity are included. Hill numbers vary by the parameter q , which sets the weight of rare species, when the diversity is calculated, and therefore determine the sensitivity to estimate relative frequencies (Chao et al., 2014). For $q = 0$ the Hill number is the same like species richness, for $q = 1$ the Hill number is the Shannon entropy and for $q = 2$ it is the Simpson diversity. The parameter q puts a weight to rare or abundant species and calculates harmonic, geometric or arithmetic mean values for the diversity. 1D is the variable, which determines the proportion of the species frequency, while 2D increases the weight of abundance species and decreases the weight of rare species. Chao et al. (2014) pointed out that $q = 0$ is the diversity of the species, $q = 1$ is the number of typical species and $q = 2$ is the number of dominant species.

$$(5) {}^1D = e^H$$

$$(6) {}^2D = \frac{1}{D}$$

$$(7) {}^qD = (\sum_{i=1}^S p_i^q)^{\frac{1}{1-q}}$$

Figure 12 shows the effective numbers of species as a function of q , as species composition is highly uneven and q increases the strongest decline is observed.

3.8.6 Partitioning diversity

Another approach uses alpha, beta and gamma diversities. Alpha diversity is the diversity for individual locations, gamma diversity the consolidation of all locations and the difference between both is the beta diversity. These diversities can be calculated by using the Shannon entropy, as the single entropies of different locations can be summarised by adding them up. Beta diversity is used to measure similarities or overlaps between communities and their distribution. The use of alpha and beta

diversities allows to compare relative abundances in different samples on a local and regional basis (Jost, 2007).

$$(8) H_{\alpha} + H_{\beta} = H_{\gamma}$$

The comparison is performed using beta diversities. For a matrix, in each cell the beta diversity was calculated, by comparing the single sites with each other. High beta entropies stand for high differences between the sites, while low beta diversity stands for high similarities between them (Jost, 2006).

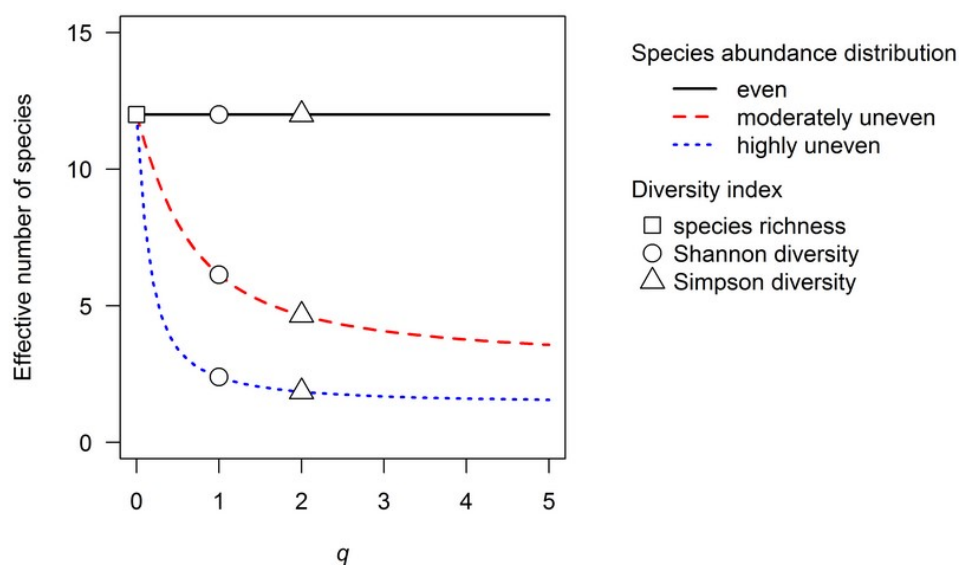


Figure 12 Diversity profiles for three communities (<https://www.davidzeleny.net/anadat-r/doku.php/en:div-ind>, latest access 26. April 2021)

3.9 Data gathering

Image collection was mainly done by a small quad copter drone called DJI Phantom 4. The Phantom 4 is a smart flying camera, able The Phantom 4 is equipped with four rotary propellers, an intelligent flight battery, a Micro SD card, a 3-axis Gimbal and an attached FC330 RGB camera (weight: 1.38 kg; max. speed: 20 m/s; flight height: up to 600 m; maximum flight duration 28 min). The camera can take images from different altitudes and track objects. The rotary propellers allow the drone to start and land vertically, which is useful for forest investigations, where space is limited. The camera specifications are 12 megapixels, 1/2.3" CMOS Sensor, a Focal length of 3.61 mm and a pixel size of 1.56 * 1.56 μm (DJI Manual, 2017). The phantom 4 is a light weighted, small and user-friendly model. Further studies showed that this pricy kind of drone has a high sensor quality, good functionality and portability in comparison to bigger and high-cost drones (Peppia et al., 2019).

In the end of 2020 and the beginning of 2021 another drone was used: the DJI Mavic 2 Pro, equipped with a fully stabilized 3-axis gimbal with a 1" CMOS sensor camera, shooting 20-megapixel images. In comparison to the Phantom 4, the Mavic 2 Pro is with 907 g lighter and with 214x91x84 mm smaller when folded, which makes the UAV easy to carry. The UAV can fly up to 72 km/h for 25 min when the UAV is flown normal (according to the [DJI Manual, 2017](#)). The maximal flight distance is 18 km under optimal conditions. Furthermore, the UAV is equipped with a vision system, which automatically detects obstacles and keeps the UAV in a safe distance.

There were two acquisition protocols, one for the usually performed automatic flights and another one for manual flights. The app DJI GS Pro was used for automatic flights, which allows inputting a flight area with specific flight settings, like flight altitude, image overlap and time-shot of the image capturing. In general, 250 to 500 images were taken per flight, depending on the area of each site. Flight altitude was 80 to 120 m for river sites, while flight altitudes of up to 250 m needed to be chosen because of the steep angle of some slopes. The image overlap was always more than 90 %. Detailed flight protocol descriptions were given in Appendix A. However, manual flights needed to be conducted to capture images from the canopies as close as possible. In those cases, no standardized protocol could be used, images were captured manually while flying slowly, assuring enough overlap of the images and safe distances to trees.

Data gathering in YURF started in summer 2018, when images of two sites (1 and 2) were captured. In autumn 2018, images were gathered for three sites (1 to 3), while for the winter seven flights were performed to gather images of the same sites, which were covered by snow at that time. Since spring 2019 images of all 13 sites were captured continuously every week until leaf-fall in autumn 2019. Pre-programmed flights were used to standardize the acquisition protocol. In winter 2020 further seven flights were conducted to capture the sites missing in the previous year. In 2020, additionally flights were performed to increase the data set. Two flights were performed in monocultures of *Castanea crenata* and *Salix* forests in YURF, which were minor tree species in the 13 sites. In total 295 flight missions were performed, resulting in a large forest data set.

3.9.1 Georeferencing

The dense structure of the forest, as well as the snow cover, hindered the use of manually installed Ground Control Points (GCP). The use of GCPs would have caused contortions in the later image processing steps. As only a DJI Phantom 4 and a Mavic 2 Pro drone were used for the study, the GPS localisations of these UAVs were used to localise the orthomosaic in ArcGIS. The location given by these drones was inaccurate, which caused that orthomosaics of the same site were placed in different

locations. In a post-processing step, the orthomosaics were manually georeferenced using marker points like power pole, buildings, streets or tree tops of evergreen trees. It has to be noted that this georeferencing method is not able to align the same pixels in two orthomosaics of the same site.

3.10 Data Processing

The collected data were pre- and post-processed with different kind of software. The first chapters focussed on images and their used formats to understand the different kind of data. The second part focussed on the software and tools, which were used to work with the data in order to process and understand them.

3.10.1 Images

An image stores visual information like drawings, graphs or pictures in a numeric representation. The numeric values are stored in each cell of an image, which is called a pixel. Every image has a specific number of pixels saved in rows and columns, which can be read by computers.

The entirety of those rows and columns of an image is called matrix or array. The number of pixels represents the resolution of an image. The more pixels an image contains the higher is the resolution, which means that usually more details are visible in the image.

Images can be binary, which means that the array of the image only contains only the values 0 or 1. The two colours, which are stored in those images, are black, represented by '0' and white, represented with the value '1'. Greyscale images represent an image by pixel values ranging from 0 to 255. Here, '0' represents black and '255' is the white colour. The numbers in between are shades from black to white, so different grey values. In colour images the information about the colour is stored in the three channels R for Red, G for green and B for blue. Every channel is stored in a pixel depending of the intensity of R, G and B. Therefore, every pixel contains three values.

Another kind of images are Digital elevation models. They store information as a greyscale image with an additional value, the z-value. The z-value is the information about the height.

3.10.1.1 Image formats

There are several image formats available, which represent standards to organise digital images and the way they are stored.

TIFF: Tagged Image File Format is the largest file format. TIFF files are not compressed, which means that they contain all the information as when the image was captured, and provide therefore the highest image quality. In the TIFF format geographic coordinates can be stored, which makes those files usable in geoprocessing software like ArcGIS. Since all information are stored in TIFFs, the size of the files is often big, which slows down computer programs using the images.

JPEG: Joint Photographic Experts Group is a compressed image format. The reduced size of the image results in a loss of information, even though the format is still capable to store a lot of pixel data. Therefore, the quality of the image is reduced and cannot be recovered. The benefit of this format is the small size and reduced storage needs. Furthermore, computer programs can handle these images easily.

PNG: Portable Network Graphics have a format between the quality of TIFFs and JPEGs. The complete colour information can be stored in PNGs, which increases the needed storage capacity in comparison to JPEGs. Still, the format is compressing the image, so the size is smaller than TIFF files. In comparison to TIFF, PNGs cannot store geolocation information.

In this study all three image formats were used. JPEG files are used for DL applications, since the computers needed to deal with a high number of images, causing a long processing time. TIFF files were used to geolocate the images in ArcGIS and provide the possibility to further use them for annotations in ArcGIS. PNG files are used to keep the high quality of the handmade annotations to input them into ArcGIS.

3.10.1.2 Digital Elevation Models

There are three ways to model the geospatial feature elevation: Digital Elevation Models (DEM), Digital Surface Models (DSM) and Digital Terrain Models (DTM) (Figure 13). Every model is different because of the methodologies they are using.

The DSM captures the natural and built features on the Earth surface, so it reflects the height of the ground, as well as the height of buildings or tree canopies e.g., which are contained in the area. Therefore, the DSM is showing the earth surface including objects on it.

The DTM shows the surface without any objects, it shows the bare-earth. Therefore, it contains information about the natural feature elevation of the terrain. It is a three-dimensional model of the terrain surface with the coordinates x, y and z.

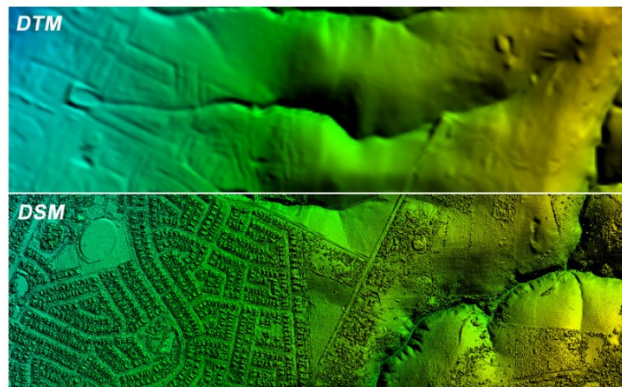
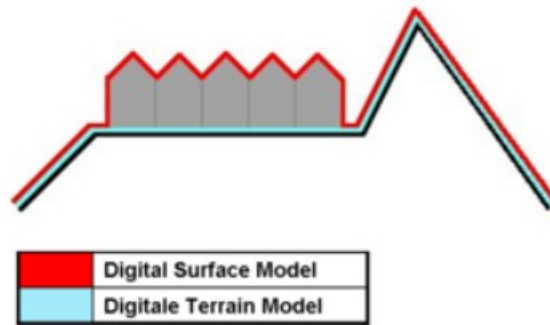


Figure 13 Example images of DSM and DTM. The upper image shows a sketch, where the red line shows the DSM and the blue line the DTM. The bottom image shows how the DTM and DSM of a real-world example (<https://www.gisresources.com/confused-dem-dtm-dsm/>, latest access 15. March 2021)

The DEM is the bare-earth raster grid produced especially for GIS applications. The DEM contains the elevation, the z-value for each cell in the raster corresponding to the terrain of a specific area. DEM is the hyponym, which includes DSMs and DTMs. The DEM can therefore contain objects in case they are imaged or the DEM can represent the terrain, in case no objects are on the imaged surface.

Those models are especially important in forestry, since they are used for Canopy Height Models (CHM). The difference between the DSM and the DTM can be seen as the CHM, as it calculates the height of trees above the ground level. This information can be used to derive individual tree canopies, their area and their boundaries.

3.10.3 Image Processing

Digital images are raw data which can be processed or used as they are. Pre-processing of an image is used to enhance the image quality for an application or a specific task.

Image processing can be explained as meaningful descriptions of objects which were generated automatically (Heipke et al., 2000). Objects in images can be identified, geometrically described and

radiometric information can be extracted. Images are interpreted using different strategies, by reducing the complexity contained in the images and by visualising information (Heipke et al., 2000).

Processing images and creating orthomosaics allow the faster analysis of larger amounts of data. DL techniques additionally automate classifications and localisations to generate maps, enabling the possibility to detect invasive species and enhance the chances for providing management tasks against them. There are several tools and software available to pre-process images, which will be introduced in the following sections.

3.10.3.1 Metashape

The raw images were processed using Metashape from Agisoft. This software is an advanced image-based modelling program. It uses the latest multi-view 3D reconstruction technology for aligning and reconstructing objects based on the input images. The aim of the processing is a 3D surface, orthomosaic and DEM (Metashape, 2018) (Figure 14). The basic steps are the alignment of the cameras, the single images, where the software search for common points and matches those. The results are a sparse point cloud and the position of the cameras. In further processing steps, the software generates a dense point cloud, based on the given information, a surface, which can be a mesh and/or a DEM and on that basis an orthomosaic will be generated.

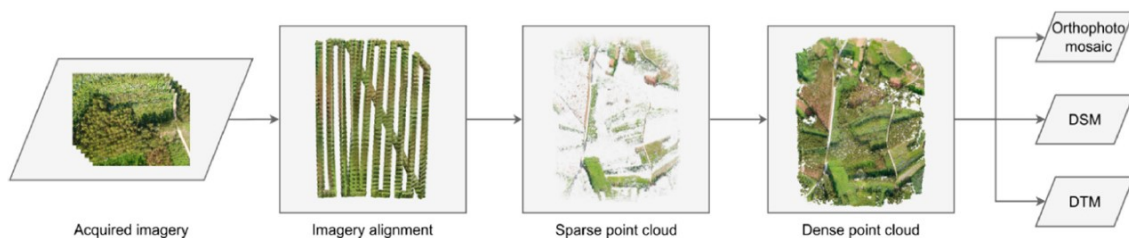


Figure 14 General workflow in Metashape, where first the acquired images are inputted, then aligned to create first a sparse, then a dense point cloud. The dense point cloud is the basis to generate the orthomosaic, DSM and the DTM (Guimarães et al., 2020)

The following important settings were used for generating each mosaic: The camera alignment was set to a high accuracy; Key point limit was 40,000 (and 200,000 for the manual flight acquisition) and the Tie point limit 0. All parameters were optimized. The dense map generation was done with medium quality and the filtering mode was chosen to be aggressive. The mesh was set on the surface type height field and the source data was the dense cloud. The DEM was produced with the coordinate system WGS 84 by the source of the dense cloud. Finally, the mosaic's surface was the mesh.

All parameters were set due to the recommendation of Agisoft and the effective processing, respectively to the time-demand and the usage. The settings were stored in a batch, which was uploaded into Metashape for each image-processing step.

3.10.3.2 GIMP

The GNU Image Manipulation Program (GIMP) is an open-source image editor. For this study the GIMP versions 2.7 to 2.10 were used. The image editor provides several tools to edit images in order to enhance the photo quality and perform retouching. The software supports all kind of image formats from JPEG to TIFF, which can be processed and exported in the desired format. In this study GIMP was mainly used to do image annotations. Furthermore, the software was compatible with a Wacom tablet, which decreased the time needed for annotations. In GIMP, the orthomosaics can be overlaid by several separate layers in which the annotation per species was done. For the annotations the scissor, bucket filling and pencil tools were mainly used.

3.11 Geographic information systems

Geographic information systems (GIS) are computer-based programs, which can display any kind of data with a georeferenced location. The system deals with attribute data and location data at the same time, which on the one hand helps to geolocate and display maps and features belonging to the data and on the other hand to record and analyse the characteristics of the dataset. For example, the dataset can contain the location of a forest and additional information about the number of trees in it, their species and height. The benefit of GIS is that it contains geodatabases, which can store every kind of information that can be correlated easily (Lillesand et al., 2008).

3.11.1 ArcGIS

ArcGIS is a commercial mapping and analytics platform, which provides contextual tools for mapping and spatial analysis of data to visualise and understand geographic data. The spatial analytic tool, which counts more than 1,000 tools available in ArcGIS, are used to visualise and interpret real world data for several applications. The software can be used with imagery and remote sensing data for every work environment and scale. The mapping options allow to visualise the gathered data within the real location in an eligible base map.

For this study ArcGIS Pro version 2.4 and 2.7 were used.

3.11.2 ArcGIS – Tools

Kernel density: This tool is used to calculate the magnitude-per-area from shapefiles (points and lines). A kernel function is used to calculate the density of features by considering their neighbourhood. In this study the tool was used to calculate the density of plants in their environment. The parameter area unit set the area units of the output density values, while the parameter method determines the path used (spheroid or planar).

$$Density = \frac{1}{(radius)^2} \sum_{i=1}^n \left[\frac{3}{\pi} \cdot pop_i \left(1 - \left(\frac{dist_i}{radius} \right)^2 \right)^2 \right]$$

For $dist_i < radius$

Figure 15 The equation used for calculating the kernel density of points

The kernel density does further determine a parameter search radius that can be chosen manually. Larger radius values generalise the density raster and smaller values provide more details in the analysis. At the centre, the location of a point is assigned the highest value, while the value is zero at the search radius distance from the point. Therefore, the value decreases from the point to the search radius distance with a smoothed curved surface. This kernel surface is applied to each point and for all raster cells the kernel surfaces are added to generate the population field value of each raster cell, in case there are overlaying kernel surfaces. The calculated density is multiplied with the number of points (or sum of the population field if provided) and outputted in a density map (Figure 15).

Integrate: This tool identifies features located in a specific radius and assumes that those features belong to the same area. Points are summed up and are represented by an assigned coordinate value based on their location before the use of the tool.

Collect events: This tool creates datasets based on weighted point data. It is usually applied after the tool *Integrate*, after the points were snapped together in feature points based on their location. *Collect events* assigns a new weight to the points considering the number of points integrated before. The number of points which are summed up in a location is stored in the ICount field of the output's attribute table (Figure 16). The output is usually used as input for the tool *Optimized Hot Spot Analysis*.

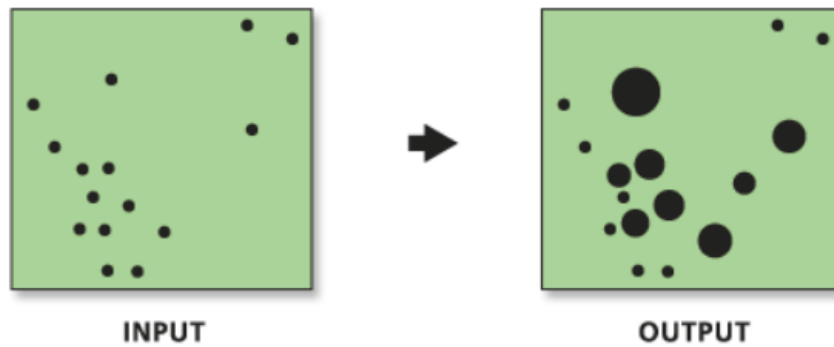


Figure 16 In- and output of the tool collect events, whereby the output shows the weighed points by having different radii (<https://pro.arcgis.com/en/pro-app/latest/tool-reference/spatial-statistics/collect-events.htm>, latest access 14. March 2021)

Optimized Hot Spot Analysis: This tool analyses the points or polygons in the input dataset, which are weighted features, and evaluates areas of significant hot and cold spots based on Getis-Ord Gi statistics. Therefore, the tool identifies statistically significant spatial clusters (Figure 17).

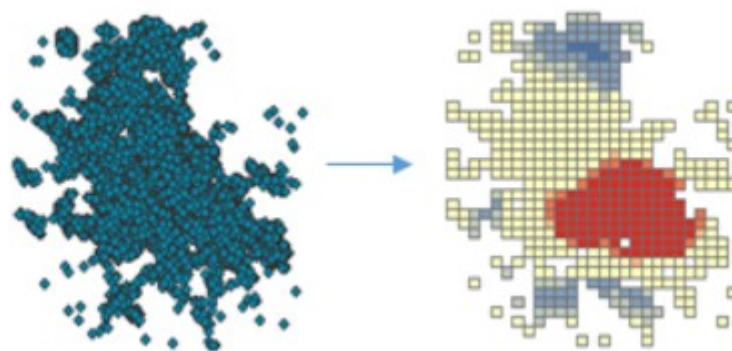


Figure 17 Example of a hot spot analysis of a point shapefile. Red are the significant hot spots; while blue are the significant cold spots, while darker colours represent a higher confidence interval (<https://pro.arcgis.com/en/pro-app/latest/tool-reference/spatial-statistics/optimized-hot-spot-analysis.htm>, latest access 14. March 2021)

In a first step, the tool combines the input feature class and the optional parameters analysis field, bounding polygons define where incidents are possible. A minimum of 30 features is required to execute the tool. *Optimized Hot Spot Analysis* further evaluates potential outlier values by using spatial statistics, like average nearest neighbour or median nearest neighbour, and defines an appropriate scale for the analysis. Therefore, the distance and distributions are calculated and evaluated for each point and characterised as outliers, when they have a distance higher than three standard deviations from the closest neighbour.

In another step, the data are aggregated using different incident data aggregation method, like counts incidents within a fishnet grid, a hexagon grid or aggregation polygons. In all methods, a basis shape is set in which the incidents will be counted that fall into the same shape. Considering invasive species

that spread over 1 km, the ideal scale of the analysis can be set to this match. The output is aggregated, weighted features in specific shapes assigned with the parameters and each feature has assigned a z-score, p-value and a Gi Bin result, as well as the numbers of considered neighbours. These three values indicate areas of significant hot and cold spots in a feature map (<https://pro.arcgis.com/en/pro-app/latest/tool-reference/spatial-statistics/h-how-hot-spot-analysis-getis-ord-gi-spatial-stati.htm>).

Filter: This tool *filter* is an image processing tool, which can smoothen or edge-enhance the values in a raster. It uses a low pass filter to smooth an image and a high pass filter to do the edge-enhancement. The tool is used to eliminate spurious elements in an image or enhance them so that they get visible in the image. *Filter* uses a 3x3 kernel which moves over the input image (Figure 18). Every pixel will be changed through the kernel using the pixel value, as well as the value of the eight direct neighbours to create an output value. The low pass filter, which is used in this study, increases the local variations and removes noises in the image. *Filter* calculates the average values for each pixel based on the kernel and the neighbour pixels. The outlier values will be discarded and average out.

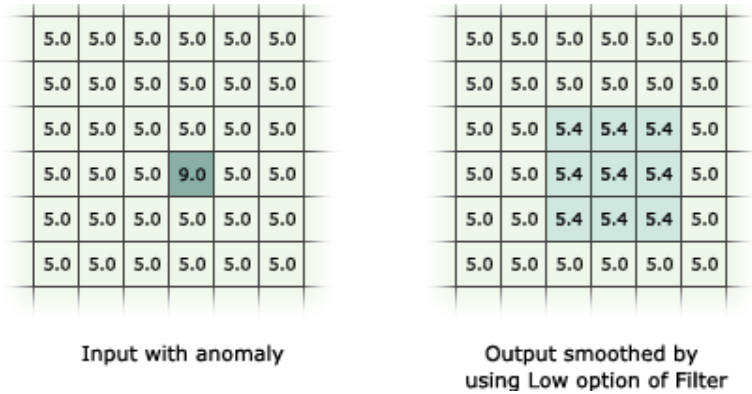


Figure 18 Example of Filter output using a low pass filter with a 3 x 3 kernel, <https://pro.arcgis.com/en/pro-app/latest/tool-reference/spatial-analyst/how-filter-works.htm>, latest access 03. February 2021

Focal Statistics: *Focal Statistics* calculates for every pixel a statistic value based on the neighbourhood. The tool uses a chosen neighbourhood to compute a new pixel value by using functions like maximum, average or minimum to include the neighbourhood into the output pixel value. The minimum was used, since it was the purpose to decrease the high outlier values. Therefore, the minimum value in the kernel matrix was chosen based on the neighbourhood. A window moves over the raster to identify the neighbourhood and performs the operation. The neighbourhood type can be chosen: Annulus, circle, rectangle wedge or irregular. In this work only the rectangle neighbourhood was used, providing a width and a height in cells, which are then considered as neighbourhood. The ArcGIS website provided the following two examples (Figure 19, Figure 20):

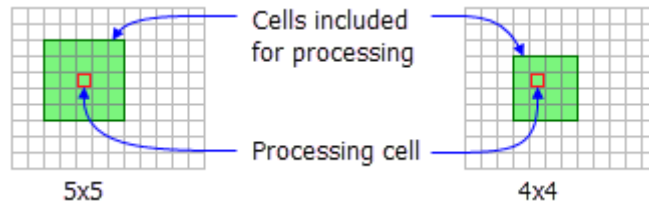


Figure 19 Example of two rectangle kernels and the included and processed cells. (<https://pro.arcgis.com/en/pro-app/latest/tool-reference/spatial-analyst/focal-statistics.htm>, latest access 03. February 2021)

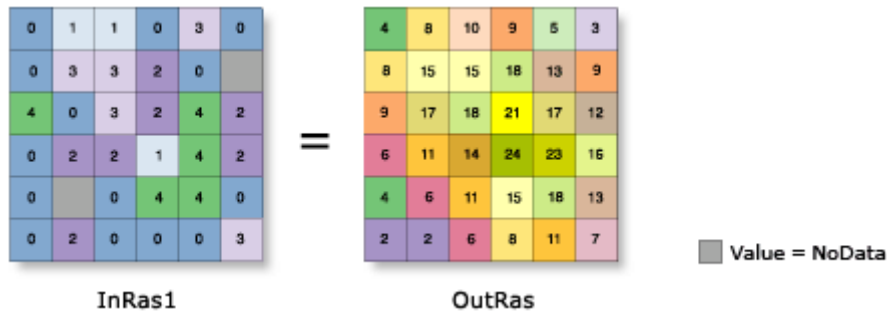


Figure 20 Example of the tool Focal Statistics and how it converts the input raster into an output raster. (<https://pro.arcgis.com/en/pro-app/latest/tool-reference/spatial-analyst/focal-statistics.htm>, latest access 03. February 2021)

Slope: Slope identifies the steepness of the raster based on the value stored in each pixel of the input image. A 3x3 kernel moves over the raster to process the data. The higher the slope value, the steeper is the corresponding terrain. The steepness of the slope was calculated in degrees for this study. The input dataset contains elevation data based on the DEMs, generated with Metashape. The tool reads the information of the DEM pixel values and outputs a slope raster, shading steeper slopes with a dark brown colour and a bright white colour, when there is no slope. The range of the output values is between 0 and 90 degree. The planar method was used to calculate the slope, where the maximum rate of change (maximum elevation over the distance) is calculated for every pixel and their neighbours, based on a projected flat plane using a 2D Cartesian coordinate system. The calculation is performed with a 3x3 matrix as a moving window over the DEM, as the following example shows (Figure 21):

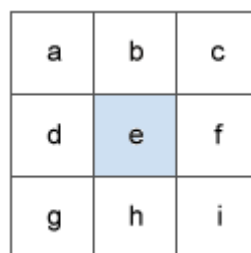


Figure 21 The image shows the surface scanning window as a 3 x 3 matrix. The calculation is performed for pixel e, while a to i are their considered neighbours (<https://pro.arcgis.com/en/pro-app/latest/tool-reference/3d-analyst/how-slope-works.htm>, latest access 09. February 2021)

Aspect: This tool calculates the down slope direction, which has the maximum rate of change. The output of the tool gives a representative value for each compass direction to the considered pixel value. The output values range from 0 to 360 in a 45-degree interval, where 0 and 360 represent the north direction, 90 the east direction, 180 the south direction and 270 the west direction (Figure 22). Flat areas were assigned a value of -1. Aspect is applied to DEMs and works similar to the tool *slope* using a 3x3 matrix to calculate the aspect of each value.

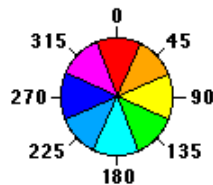


Figure 22 Aspect directions and their colour distribution used by ArcGIS (<https://desktop.arcgis.com/en/arcmap/10.3/tools/3d-analyst-toolbox/how-aspect-works.htm>, latest access 09. February 2021)

Near: *Near* calculates the distance between the input feature and another selected feature (Figure 23). Thereby the closest feature of the selected feature class will be used for the method. The proximity between all feature classes (point, line and polygon feature class) can be calculated, as well as between two different feature classes. The distance is calculated based on the input geographic coordinate system (in meters), when the parameter geodesic was used. Furthermore, the location of the nearest feature can be outputted as coordinate in x and y.

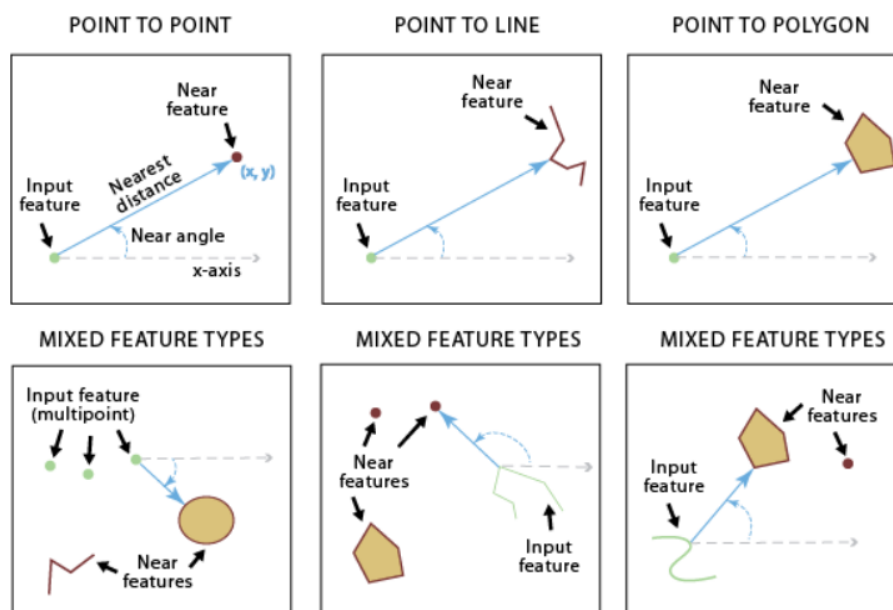


Figure 23 The function of the ArcGIS tool *Near* and how it works with different input feature classes (<https://pro.arcgis.com/en/pro-app/latest/tool-reference/analysis/near.htm>, latest access 14.03.2021)

Extract value to point: This tool extracts values into a new point feature dataset. The value is extracted from a single raster, in this work the DEM, based on the input point feature. Every point gets the height value of the DEM stored in a separate output feature class. A new field, added to the new feature class, stores the extracted value in the attribute table. Therefore, the input point feature datasets (location of trees) and in_raster were used, the DEM, from where the value gets extracted, was chosen. No interpolation was chosen; hence the value in the cell centre was used.

Raster to polygon: This tool *raster to polygon* converts a raster shapefile into a polygon, line or point shapefile. The tool converts areas with the same value into a corresponding polygon. The input file can be any raster file with any pixel size. Additionally, settings simplify the polygon, which means that the polygon will be smoothed into simpler shapes remaining close to the original input raster.

Contour function: This tool creates contours based on the DEM, where points of the same height get merged together and contour lines are generated. The tool provides contours over a large area fast, which enhances the visualisation of the elevation when added to maps or images. The contour intervals can be set manually; standard sizes are 1, 5 or 10. Furthermore smoothing of the contour lines can be applied. Also, the type of contours can be set up, where contour lines, contour fill and smoothed surface only can be chosen. For this study, the filled contour was applied, which fills the area between the contour lines with quantized values of each elevation.

Create Fishnet: This tool generates a fishnet with regular rectangle size cells and produces a polygon feature. *Create Fishnet* can use a fixed coordinate extension, which can be set manually. Additionally, there are two options to create the fishnet: adjusting the cell height and width or the number of rows and columns.

Summarize Within: *Summarize Within* exists in ArcGIS Pro in two variations: as analysis tool and as geoanalytics tool, which provide the same results in a different output file, just the settings can be chosen differently. Both tools overlay a polygon layer with another layer (point, line or polygon) and summarise the number of features, which fall within the polygon layer. Basically, the tool overlays the layers on top of each other and then counts the numbers of point features falling into each polygon. Furthermore, minority attributes, majority attributes and group percentages can be set as parameter and added to the attribute table, when the tool is executed. For the output the *geoanalytics* tool can

be used to keep only the raster cells with points inside, while the *analytics* tool keeps all cells of the polygon raster. A visualisation of the tool function is provided in Figure 24. Here, the tool was used to count points in a polygon (usually a fishnet grid).

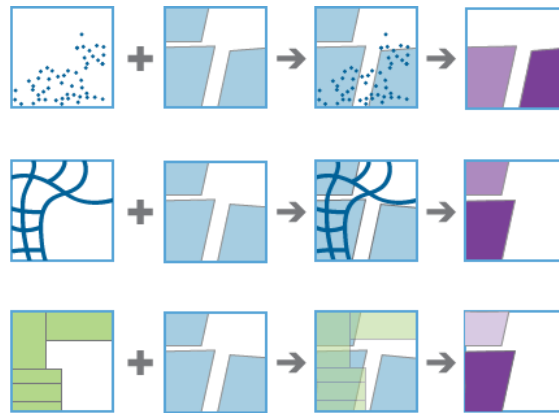


Figure 24 Example of summarizing features in polygons. First row: points in polygons; Second row: Lines in polygons; Third row: Polygons in polygons (<https://pro.arcgis.com/en/pro-app/latest/tool-reference/big-data-analytics/summarize-within.htm>, latest access 12.04.2021)

3.12 Machine learning

3.12.1 Artificial Intelligence

Talking about artificial intelligence means that the computer should be able to reach a similar level of the human intelligence by copying the human brain (Figure 25). Machine learning, especially DL, is the part of AI, which is used in this thesis. The computer shall learn to understand and to identify patterns in images and classify objects by mimicking the human intelligence.

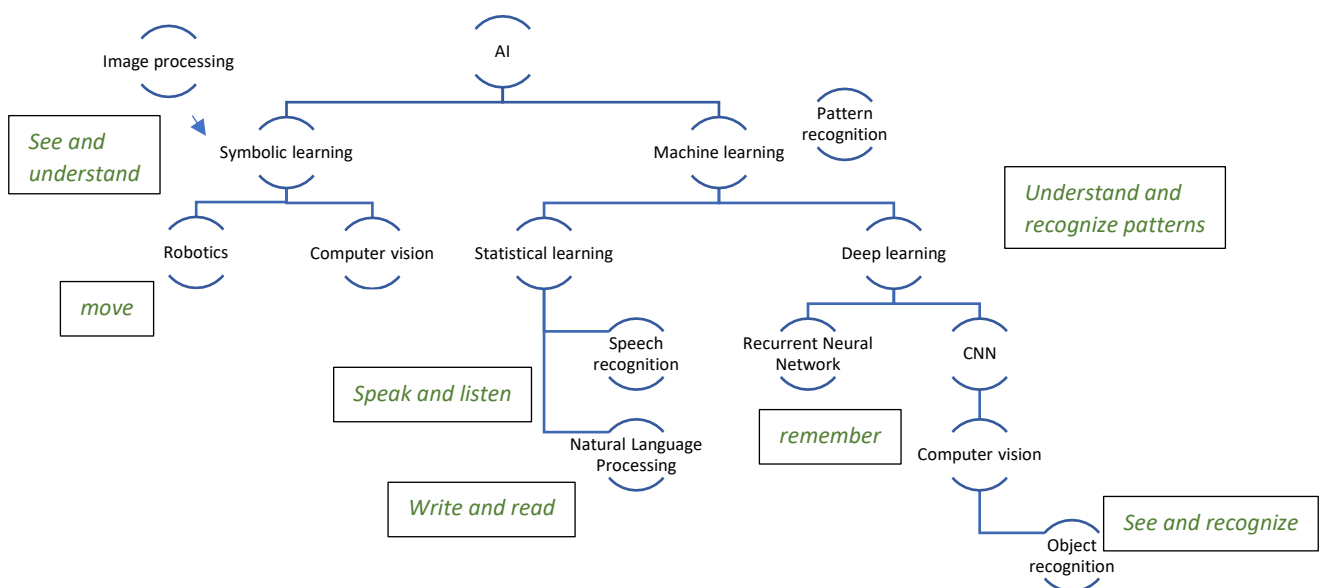


Figure 25 Diagram plotting the different fields of AI. The boxes with the green text are ways human intelligence is used and they are placed close to the part of how AI can copy human intelligence

3.12.2 Deep Learning

DL is a part of machine learning using artificial neural networks, which are inspired by the human brain. The performance of this technology in the fields of image classification, translation and game-playing is outperforming former techniques, which leads to a rise of this technology in different research fields, like forestry (Diez et al., 2021).

In DL the computer uses a network to identify features by themselves. For this task, they use neural networks, which are built up by several layers consisting of nodes/neurons. During the training of a DL network, specific nodes will be activated, which leads to a specific output. As described, DL networks allow the computer to mimic human brains. Even though this technique has limitations (which will be discussed later), DL is able to learn from visual inputs in order to recognize objects that are part of an image (Gupta, 2019). In this thesis, it will be examined if DL is a useful tool for tree species classification.

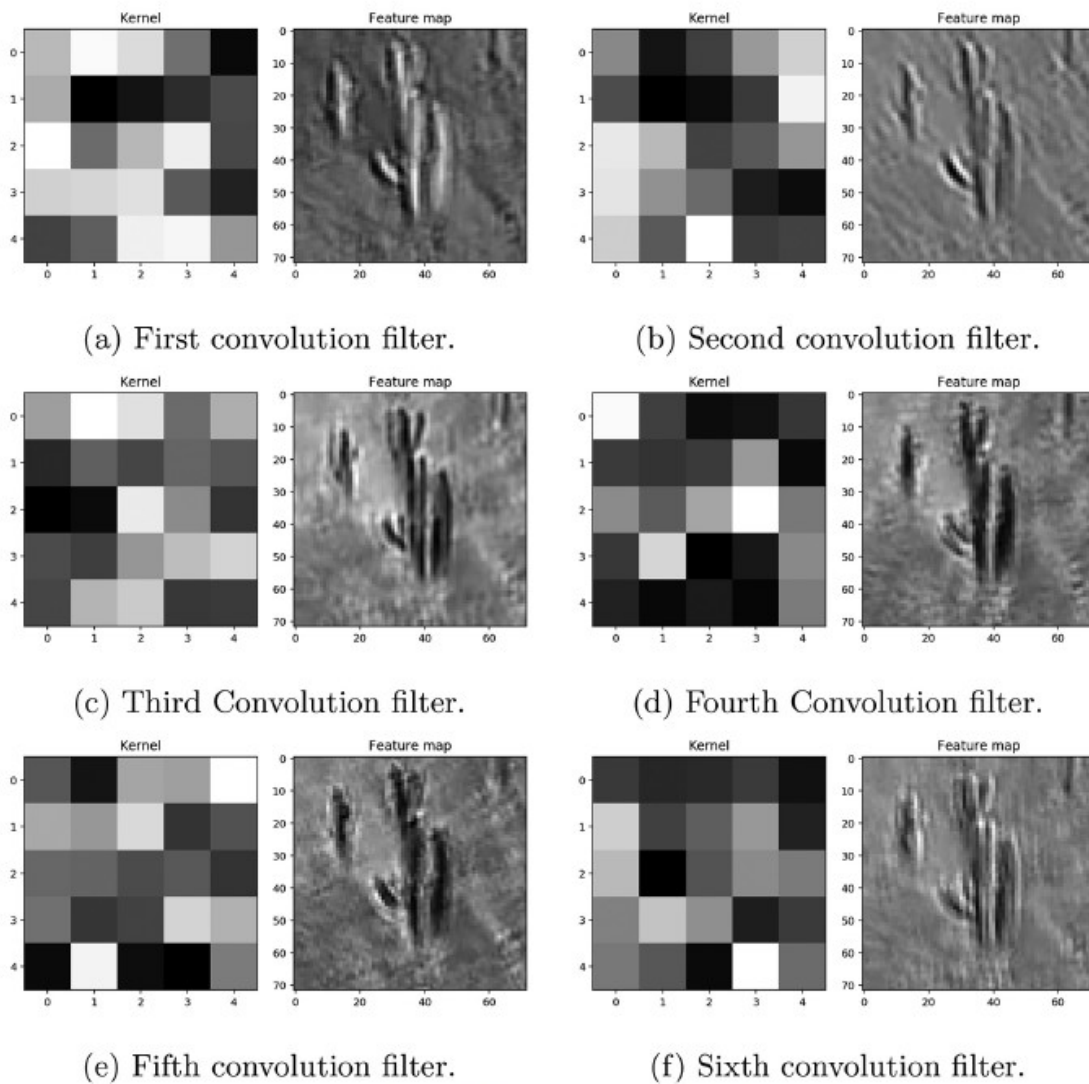


Fig. 14. Learned kernels and feature maps. The axes indicate pixel indices.

Figure 26 Examples of kernels, which identify different feature maps (López-Jiménez, 2019)

3.12.2.1 Convolutional Neural Networks

CNNs are a subcategory of Neural Networks (NNs) and one of the best performing methods for dealing with image classification, object detection and further image processing tasks (Diez et al, 2021). It is a powerful tool for detecting certain local features in an input image and for creating a hierarchical feature map (Kim et al., 2018). The strength of the network is its deep architecture, allowing the extraction of features at multiple levels by using an end-to-end learning. Feature extractions by hand or human experts are not required for this process (George et al., 2017). The architecture consists of three main layers: Convolutional, pooling and fully-connected layers (Guo et al., 2016). Convolutional layers create several feature maps by considering neighbouring pixels (Figure 26). Pooling layers reduce the dimension of the feature maps, as well as the parameters in the network. The fully-connected layers generate 1D feature vectors out of the feature map. These vectors are leading to different categories for image classification (Guo et al., 2016). Furthermore, the first layers of the network are initial layers, extracting generic features like edges, curves etc. which are applicable in most image classification tasks, while the last layers are able to recognize abstract features and data-specific features (George et al., 2017). Therefore, this network is combines low-level features with high-level features.

But this technique has also major problems. It needs a large amount of labelled data. However, high precision labelled data need a good expertise for the training of the network. The extensive computational and memory resources which are needed to work with this large amount of data need powerful computers to process the data. The final point is the problem of overfitting and convergence issues, which require repetitive adjustments in the network architecture (Tajbakhsh et al., 2016). The capacity of the model with its large number of parameters and layers is not able to weight the model in a correct way, when too small or too large numbers of datasets are giving to the network (Sharma & Mehra, 2018). This problem is called vanishing/exploding gradients and causes overfitting phenomenon (Kim et al., 2018). Therefore, the network is complicated and it needs to be adjusted to be able to deal with the problems of overfitting and convergence (Sharma & Mehra, 2018).

3.12.2.2 CNNs from an image point of view

The starting of the technology is a problem, which shall be solved with computers by defining an error and trying to reduce the error, so that the machine is able to compute the solution. Usually, the aim is to teach the computer to split a set of data. This happens using an error function, which is naturally discrete, but it can be changed into a continuous function using linear regressions and penalties for wrong classifications. A solution, which is far away from the correct solution is given a high penalty,

while the ones, which are close, receive a small penalty. By moving in the direction, which is stated to be the correct solution, the error will be reduced until a suitable solution is found.

One of the most important questions is how a computer sees or reads an image. Computers read pixel numbers, which means, that a computer classifies images by applying mathematical operations on the numbers each pixel contains. The benefit and advantage of computers (in contrast to humans) is that they are able to run fast many possibilities and process successfully mathematical operations. A successful operation can be found by starting first from random numbers, creating an error, which leads to a continuous change of numbers, following the gradient until a minimum of errors is reached. Usually, images are large and it is easier to break them down into smaller subcomponents in order to analyse those ones first and to put them together again afterwards. The breaking into smaller pieces is done with the convolutional layers and pooling layers within the network. Fully connected layers merge the pieces together and read them logically. On the small pieces, filters/kernels are applied, by overlaying the kernel over the image. The kernel values are multiplied with the pixel values and summed up. If the sum exceeds a threshold, a structure is identified. In this procedure, convolution layers apply the kernels by moving them over the image and the pooling layers identify if the value is over the threshold or not. The small pieces of the image will be then superimposed to generate the original image again, while the fully connected layer is logically identifying the object.

The training of a network is done in order to create specific kernels, which are able to identify specific objects in images. During the training the computer will produce several kernels (convolutional and pooling layers), which will lead to errors. When the training starts from random numbers and by following the gradient descent, the network will identify the kernels, which are able to identify the objects in images. When a kernel fits well, it outputs a high value during the testing and low value, when it does not. In any application, where images shall be classified, neural networks are used to break down images into small pieces, identify the simplest structures and by restoring the original image, objects can be identified

3.12.2.3 Image analysis with computer vision

Computer vision: Computers can get a high-level understanding of image contents which is examined by the interdisciplinary field of computer vision. Images can be collected by satellites, planes, UAVs, computers, tablets, smartphones, etc. Image analysis can be divided into three levels: 1: categorisation of objects in an image, also called classification; 2: object detection, determining the location of an object in the image; 3: segmentation, where parts of an image are identified by understanding the object and the location of the object. The understanding of objects in images can

be described as evolution by moving from recognizing to localization to detected and labelled object regions up to single objects (Garcia-Garcia et al., 2018).

Image segmentation: Image segmentation is one of the core tasks in computer vision being the initial step of image analysis (Caselles et al., 2005). The aim of this approach is to simplify image analysis by dividing the image into multiple regions. Pixels are classified into groups of segments by its similar texture features (Nadipally, 2019). In comparison to image classification there is no need-to-know what object is segmented in the first place. The focus is to output pixels belonging to the same class due to their contained information and often by adding information about contours and edges (Guo et al., 2018). Thereby, the focus was on the main object in the image (Harshall, 2019). Highly variable image features, missing edges and low contrasts between different regions can make image segmentation challenging (Merjulah and Chandra, 2019).

Object detection: It is important when an image contains multiple objects. The task is to classify and localize all objects by using bounding boxes to mark their position (Harshall, 2019).

Semantic segmentation: Semantic segmentation is a deeper step into the approach of object recognition. This approach is used for getting a better comprehension of the environment by associating visual information in the images to classes considering the spatial information (Ouaknine, 2018). Shortly, it helps to recognize what is where in an image. In comparison to object detection, semantic segmentation is not using bounding boxes for predicting the area where an object is located (Harshall, 2019). Semantic segmentation needs image classification, as well as object detection for localizing and classifying the pixels precisely. This kind of segmentation is also called dense prediction because the meaning of each pixel will be predicted by this method. The need of an efficient tool for doing accurate semantic segmentation with consistent labels for the pixel is high (Yu et al., 2018).

3.12.2.4 Deep learning techniques and settings

Data augmentation: This technique is used when a small number of trainings data are available, especially when a balance of the different classes is necessary to avoid overfitting. Data augmentation can therefore increase the size of the dataset by using transformations like rotation, scaling or flipping and can change colour properties like saturation or brightness of the trainings data (Dwivedi, 2019)

Overfitting and underfitting: These are two error types, which can occur, when data are classified. Underfitting is when the problem will be underestimated, while overfitting means that the problem will be overestimated.

Learning rate (LR): The learning rate is the speed in which a network learns and is therefore a hyperparameter, which needs to be set up and tuned for each network. During the training of a network, the loss between the actual output and the predicted output shall be as small as possible. The loss can be also called the error, which is output by the network. The loss becomes minimized in each step of the training because the weights and the bias are updated. The size of the steps can be considered as LR, as the steps are dependent on the learning rate. LR ranges between 0.0001 and 0.1. Is LR high, a big step will be taken to reduce the loss, which on the one hand reduces the training time but can cause on the other hand that the minimum can be overseen and usually weights are suboptimal. Otherwise, LR can be chosen to be small, which increases the training time, but the risk of passing the optimal loss is reduced (Brownlee, 2019c).

Epochs: In DL, an epoch is a full cycle of training, where the entire training set passes through the network, forward and backward. In each step of an epoch, the network first initializes the parameters, then propagates forward, computes the error and adjusts the parameters according to the output error. With increasing epochs, the weights of a network are better adjusted, which generalizes the network. However, if there are too many epochs it causes overfitting.

Freezing networks: Layers in DL networks can be frozen and unfrozen. Thereby, freezing means that the changes of the weights will be controlled. In a frozen model the weights cannot be changed, while they can change when they are unfrozen. Therefore, freezing some layers in a network can help to improve the training. Especially, when transfer learning is applied, the first layers in a network can be frozen, while the last layers are trained with the new dataset (Sagar, 2019). When a frozen model is re-trained, only the final layers of the model are re-trained. When an unfrozen model is re-trained, all of the layers are modified (Rother, 2018). However, changing weights can demand more computational power.

Transfer learning: Transfer learning is used to take advantage of a previously trained network to adapt it to another network. Usually, networks are trained for a single purpose for which data were collected. In case the data are changing, a network needs to be built up from the beginning. This is time-consuming, as training data need to be collected and processed again. Therefore, transferring the knowledge from a previously learned task to a new one can significantly decrease the needed data, solve new problems faster and increase the performance of the network. Figure 27 shows how transfer learning changes the performance of the network. There are three advantages: a higher start, slope and asymptote, compared with a network without transfer learning, that means, higher accuracies and higher speed in the end.

Several studies show the better performance of transfer learning in comparison to fully-trained networks (Sharma & Mehra, 2018; Kim et al., 2018; Tajbakhsh et al., 2016). At the beginning a network has randomly initialized weights, which are given on the basis of a normal distribution. Less data leads to wrong weights and to wrong results. Therefore, pre-trained weights are initially available before the training, instead of randomly initialized weights (Garcia-Garcia et al., 2018). This setting of weights is called Fine-tuning (Tajbakhsh et al., 2016). In CNNs changes can be done in the first layers and/or the last layers, it is therefore important to choose the changing layer carefully. Lower layers extract information of generic features while deeper layers are object-specific (Garcia-Garcia et al., 2018).

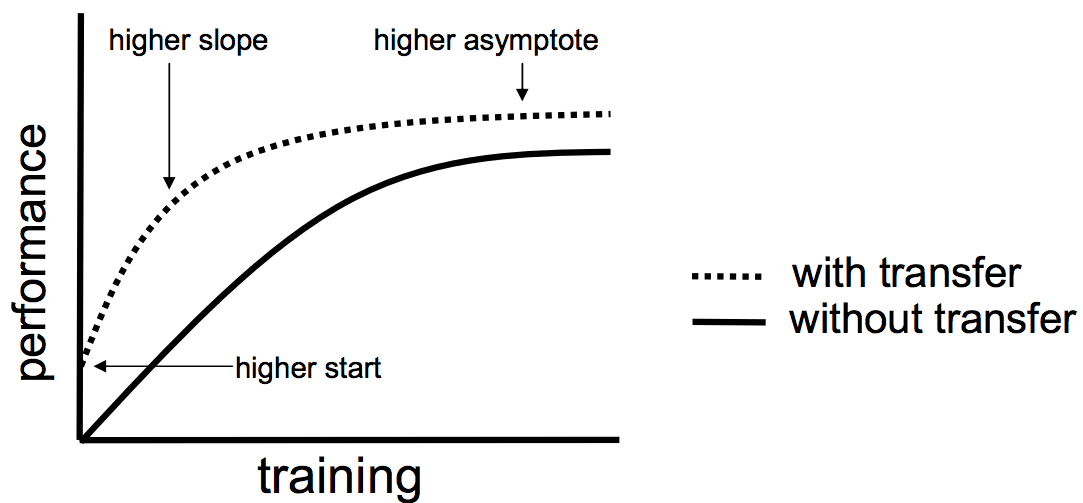


Figure 27 Influence of transfer learning on the performance of a network (Brownlee, 2017)

In the training for similar tasks a fine-tuning for the last layers is enough, while in distant tasks a deeper fine-tuning (a fine-tuning in early layers) is necessary (Tajbakhsh et al., 2016). Therefore, there need to be an understanding of the similarities and differences in the source and target task. In case of ImageNet, which is a general image database, the data can be used to initialize the first layers of a network. While a network, which is supposed to classify tree species, needs to be trained with tree data, to set the weights of the last layers.

3.12.3 Multi-label patch classification using ResNet

This study aimed at classifying tree species by using Convolutional Neural Networks (CNN). Previous studies show the efficiency of these networks for image classification issues (Natesan et al., 2019; Kamilaris and Prenafeta-Boldu, 2018). CNNs are able to reach high precision levels, higher than other image-processing techniques (Kamilaris and Prenafeta-Boldu, 2018). The matrix of a CNN is built up by convolutional layers which are working as filters; extracting deeper features from the input images (Natesan et al., 2019). They are therefore able to classify millions of images into different classes

(Krizhevsky et al., 2012). Therefore, this study is using one of those architectures to perform in forestry research. So far, only few studies were done in forestry using CNN (Natesan et al., 2019). One approach of this study was to use the CNN ResNet50 to show its good performance for forestry purposes.

ResNet50 is a network with 50 layers being able to classify images. It contains five stages with a convolutional and an identity block. Each of these blocks is built by three convolutional layers and has over 23 million trainable parameters (Dwivedi, 2019). The network uses identity shortcut connections to skip one or more layers whose input and output show the same dimension. Thereby, it overcomes problems occurring in CNNs, like the extensional computing time, the high amount of needed data or overfitting (Tajbakhsh et al., 2016). Furthermore, the network is using residuals instead of single features for the training (Sharma & Mehra, 2018).

ResNet-50 in combination with transfer learning was chosen and the basis for the developed multi-label patch algorithm. The multi-label patch algorithm consists of the following steps:

Pre-processing: The first step for using the multi-label patch classification was to build an orthomosaic of each site, which was analysed by the classifier in the third step. Annotations of the desired classes were manually prepared. The mosaic and the layer of the single annotations were the input data for training of the ResNet.

Patch-annotator: As mentioned before, orthomosaics generated out of the images were used. Due to the number of images and information contained in each image orthomosaic, the data needed a lot of memory and computational power to be processed. DL networks have problems dealing with such an amount of data. For that reason, the orthomosaic and the annotated layers were divided into patches using the developed image Patcher-Annotator algorithm. Patches were broken out of the orthomosaic during the process and .csv files was generated by using the annotated layers, containing the information of the patch number and the visible class on that patch. The image Patcher-Annotator ran with different patch sizes for a later comparison of the results with respect to the reached accuracies. Hence, the code produced patches with a specific size and with labels of the classes.

Classifier: The second part of the multi-label classification algorithm was the classifier. This code uses the previously generated patches and .csv files for the classification. The code was running several times with different settings. The important settings are the LR, the epochs, the used models and the frozen/unfrozen status of layers. The network becomes optimised due to the learning from the input and output during the training. Furthermore, the classifier can be trained with different databases for applying transfer learning.

Segmentation: In this work, manual segmentation was done for the orthomosaics by dividing objects into pre-defined classes using the visual information of the image. Automatic segmentations were

performed as well. The results of the multi-label algorithm were displayed and analysed on the basis of the output automatic segmentation. Furthermore, this segmentation was refined with watershed segmentation, which is described in the following chapter.

3.12.4 Segmentation refinement using watersheds

The multi-label algorithm generates a patch-based coarse segmentation. This segmentation adds bounding boxes around objects/object boundaries. Therefore, the segmentation contains the object, but also parts of other classes or the background. Thus, results need to be refined to obtain segmentations of the single object only. The approach is to refine this segmentation by using the watershed segmentation algorithm.

Previous studies revealed that the watershed transformation is a powerful tool for segmentation problems (Jiang et al., 2003; Hamarneh and Li, 2009; Huang and Chen, 2004; Tarabalka, 2010). The algorithm is working with binary images comparing pixel information for finding objects and their contours (Beucher and Meyer, 1993). Here, images were handled like geological landscapes with ridges and basins. Basins, also called seed regions, represent objects like evergreens, deciduous, rivers, man-made and uncovered. The ridges are the watershed lines, which separate different objects. Furthermore, the image is separated into the foreground, representing the objects and the background, representing the snow-covered soil. The initial state, before the watershed algorithm was run, was the identification of the sure background, the marking and labelling of the seed regions and unknown area.

The second step was to find the contact regions between the seed regions and the unknown area. The morphological tool *erosion* eroded the pixels until the plain foreground can be distinguished, where all the pixels belong to the same object class. Therefore, the next step was to grow the seed regions but only in the unknown area. The area grows fast, as long as the pixels in their neighbourhood have the same values. However, when the pixel values become different the growth is slowing down, until the pixel values are too different and the growth stops. This is the point where a seed region gets in contact with another seed region or the background. At this boundary a watershed line is generated. Retrospectively, the growth of the seed regions is comparable with basins filled up with water until water of different sources would merge. There, watershed lines are built on the ridges between the different basins, representing different classes (Kornilov, 2018). The watershed lines are representing the refined segmentation.

3.12.5 Image segmentation using UNet

Previous studies pointed out the efficiency of UNet for image segmentation applications, especially in the medical field (Chen et al, 2016; Guo et al., 2018; Siam et al., 2018; Funke et al, 2019). However, in comparison to ResNet, where images were classified, UNet is an efficient tool for image segmentation. In any case, there is a high number of architectures used for classification purposes. Furthermore, a comparison between different architectures provides useful information on which architectures fits different problems and data. Identifying the method providing the best results in the field of forestry is essential.

UNet provides semantic segmentations by classifying pixels in images using a vector-basis approach. The UNet architecture is composed of two paths: The encoder and the decoder path. Each path contains several layers, whereby the initial layers detect basic features of the image (like edges or colours) as well as spatial information. Deeper layers are able to identify complex features by losing the spatial information (Gupta, 2019).

The encoder path extracts features by passing its convolutional layers and it reduces the size of the image by passing the number of maximal pooling layers. Both layers use matrices to deal with the image and its content to combine them in a down sized feature map (Harshall, 2019). The output of the encoder path is object detailed information (Gupta, 2019). The decoder path is composed of transposed convolution layers. This path is restoring the size and the spatial information of the image by reducing the depth (Harshall, 2019). Feature maps from the encoder path are transferred to the decoder path by using skip connections. This avoids a loss of spatial or content information (Gupta, 2019). The results are visible information and the location of objects in an image are captured in a semantic segmentation map.

Further DL architectures were used in this study with detailed explanation for them in Appendix iv.

3.13 Evaluation Methods

Evaluation methods are needed to tell if a DL network is performing well or not. A DL network can in this case be compared with a student. Like a student is studying for an exam, a network is trained to classify objects. In the end, both need to be tested, whereby the student is writing an exam, while a network will be tested with a new set of data. Regarding the testing of a network, there is one important rule: Never use test data for training. The network can only be evaluated on their ability to classify object when the images are new to the network. Therefore, datasets are usually divided into training and testing data. A common applied technique is to use a K-fold cross validation, where the









dataset is split into four sets, while three are used for training and one for testing. In each training step, the test dataset can be exchanged with one training set.

When the performance of a model is evaluated, it is assumed that it needs to be checked if the network is classifying an object correctly or not. Checking the correct function of a network cannot provide accurate and useful information. For example, if there is a big dataset consisting of 10,000 coniferous trees and 10 deciduous trees, the network will always predict a conifer, it will be right in 99.9 % of the cases, which is a high accuracy, but the network will never identify a deciduous tree in the dataset. In case, the task is to find trees, the trained network will never be successful.

Therefore, confusion matrices were introduced in the field of DL (Table 3). Considering the same example, conifers and deciduous trees, where deciduous trees are the target tree, then there are four options:

- A tree is identified as deciduous, which is in reality a deciduous tree, then it is called a true positive (TP), as the target class was identified correctly.
- A tree is identified as conifer, which is in reality a coniferous tree, then it is called a true negative (TN), since the tree is classified correctly, but it is not the target class.
- A tree is identified as conifer, which is in reality a deciduous tree, then it is called a false negative (FN), as the target tree is misclassified.
- A tree is identified as deciduous, which is in reality a coniferous tree, then it is called a false positive (FP).

Table 3 Confusion matrix for a classification of deciduous vs coniferous trees. (Images modified after https://www.freepik.com/free-vector/tree-icons-pack_813723.htm, latest access 16. March 2021)

<u>Confusion Matrix</u>	Predicted deciduous	Predicted conifer
Actual deciduous	 TP 	 FN 
Actual conifer	 FP 	 TN 

With the confusion matrix several values can be calculated to evaluate the performance of the model.

- Accuracy: Out of all data, how many objects were classified correctly?

$$(11) ACC = \frac{TP+TN}{P+N} \quad (P = \text{positives}; N = \text{negatives})$$

- Precision: Out of the predicted positives (in the example: predicted deciduous), how many objects are classified correctly?

$$(12) Precision = \frac{TP}{TP+FP}$$

- Recall: Out of the actual positives (in the example: actual deciduous), how many objects are correctly classified?

$$(13) Recall = \frac{TP}{TP+FN}$$

The difference between the precision and the recall is the focus of the evaluation. If the task requires less FP, then the precision needs to be high. If the FN task requires finding the least FN, the network needs a high recall. Instead of having two values, the F-score can be calculated, which uses the harmonic mean of precision and recall. Furthermore, there are two important terms: Sensitivity and specificity. Sensitivity is also called recall or true positive rate (TPR), as mentioned it is used when the network is supposed to rarely misclassify. The specificity is also called the true negative rate (TNR) and measures the proportion of negatives that are correctly identified. The benefit of a high specificity is that a network with a high specificity rarely outputs actual positives as negatives.

$$(14) Specificity = \frac{TN}{TP+FP}$$

Classes can be chosen too complex or too simple. For example sorting the data into 'trees' and 'no trees' would be too simple, as the classes can be more precise like 'conifers' and 'broad-leaved' trees can be found. The network is further doing a mistake, which is called error due to bias. Classifying the data into the classes 'green-leaved deciduous trees' and 'not green-leaved deciduous trees', the network would still work well for the giving example, but if there is a deciduous tree imaged in autumn, with red leaves, the tree would be classified into the not green-leaved deciduous tree class. Therefore, the network would classify too specific and this error is also called error due to variance. In most applications, the problem of overfitting is more common, as it occurs usually when datasets are too small. In those cases, the network will learn to only identify the examples giving with the training set. Figure 28 shows the model complexity graphs, where training and validation errors are plotted. The shown training error should be as low as possible, so that the network classifies well. The validation

error shows the optimal results, which is when the curve reaches its minimum. When the training error is too low and the validation error increases, the network is overfitting.

For this study, cross validation was applied. Therefore, the dataset is split into training, validation and testing set. While the training set is to train the network, the validation set is used to decide when a network is trained well, and the testing set is used to evaluate the network.

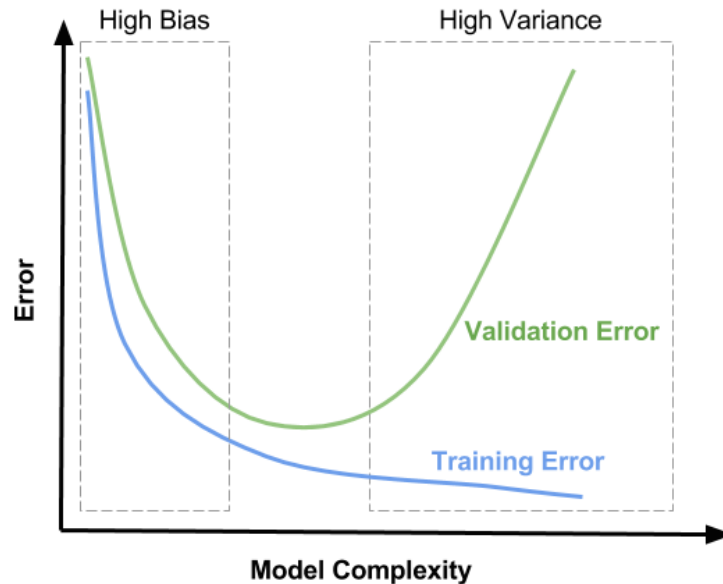


Figure 28 Model complexity plotted against the error (<https://zahidhasan.github.io/2020/10/13/bias-variance-trade-off-and-learning-curve.html>, latest access 19. March 2021)

Further evaluation metrics are used:

Full agreement - Full agreement with False positives - Partial agreement - No agreement

Full agreement means that the algorithm is classifying and labelling every object in the patches correctly. In the case of *Full agreement with False Positives*, the classifier correctly recognizes every patch and also labels objects which are not displayed in the patch. *Partial agreement* is that the classifier labels some of the visible objects correctly and *No agreement* is related to no correct identification of the objects.

Chapter 4 Tree species classification

This is the main chapter of the thesis, combining field inventories, image analysis and DL techniques, to detect and classify trees. Assessing the forest composition, distribution and structure is with the three different methodologies were the main goal (Figure 29).

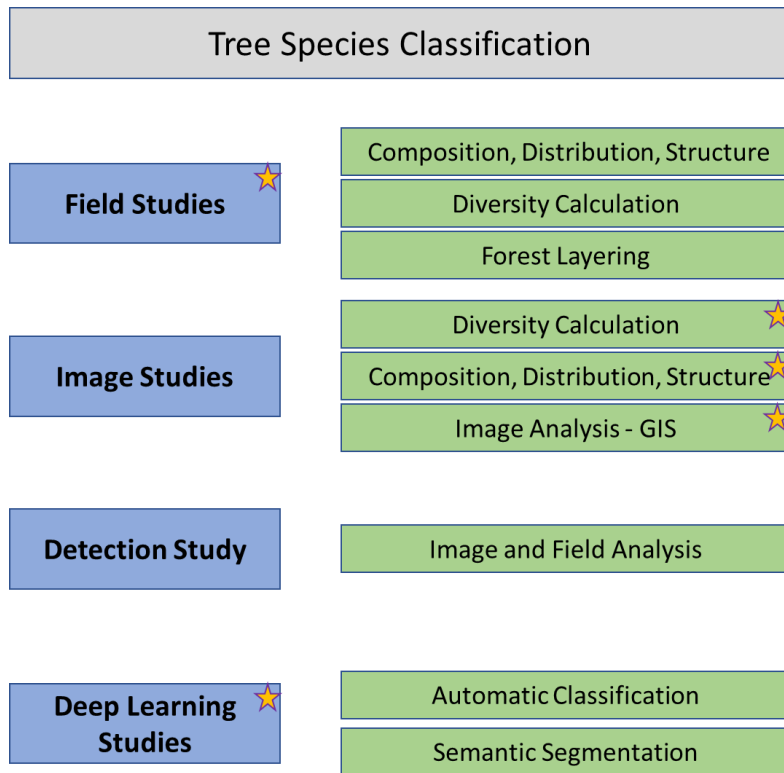


Figure 29 Structure of the tree species classification chapter. The stars indicate the different subchapters

The following chapters use different methodologies to assess the forest composition, distribution and structure. The first chapter focusses on assessing information only using fieldwork data. The data were evaluated to extract the information mainly about the tree species composition, dominances and forest layering. The second chapter focusses on information extracted from images, whereby only counting and composition were evaluated. Those information were used together with diversity calculations, which are commonly used when ecosystems and their diversity are studied. The results and discussions in this chapter focus therefore on numbers in order to understand and compare sites. The third chapter explains the use of image analysis tools, where pixel counting and manual annotations were used to assess the data in the images by classifying tree species. The information were used to use calculations for densities e.g., whereby the data were again presented as numbers for each tree species and site. The last chapter focusses on the visualisation and the further processing of the data. GIS applications were used to create maps and databases, which were processed by different tools to decrease the amount of data and to extract the important information.

Chapter 4.1 Assessing natural mixed forest composition, distribution and structure using field inventories

4.1.1 Problem definition

Field surveys are the state of the art, when it comes to evaluation of forest stand structures, compositions and diversities. Installing fixed plots like in the studies of Sakio (2002) or Fukumachi et al. (2020) can help to gather information about the plot and actual forest conditions over several years. In this study, field surveys had another important function, as they were the ground truth data for verifying the manual annotations and the automatic classification.

The methodology field survey is an accurate technique to map the location of trees and to classify plant species within the forest. The disadvantage is that the work requires man-power and much time. In this study, field surveys for all Riparian sites and Terrace sites were provided, including information about tree species identification, their census and location. For three of the Slope sites, where the access was difficult, only tree counting and species classification were done.

For this part of the study, the main objective was:

- i. Evaluate the composition, distribution and structure of mixed natural forests in Shonai area

This means, with the performed field surveys, information about tree species in the different study sites was gathered and their distribution in the field was determined. The composition and structure of the forests focus on the different forest layers and the representing tree species was provided, as well as the analysis of diversity and tree species dominance (Figure 30). At last, the forests were classified based on all gathered data.

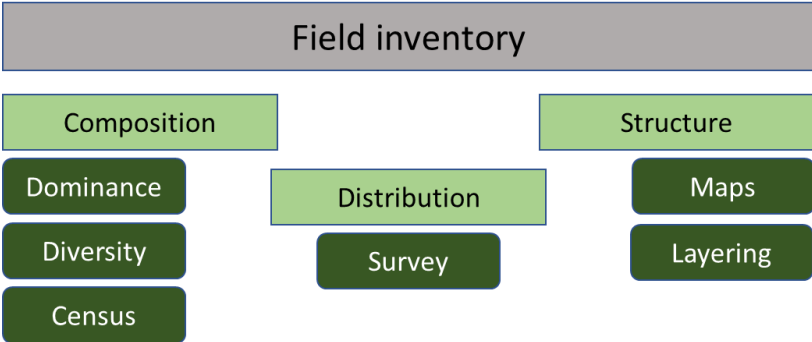


Figure 30 Structure of the chapter field inventories with the focus on forest composition, distribution and structure

4.1.2 Data collection

4.1.2.1 Field surveys

Fieldwork was conducted in autumn 2019, spring and summer 2020 in the Riparian sites 1, 4, 6 and 7, the Terrace sites 11, 12 and 13 and the Slope sites 3, 8, 9 and 10. The most accurate maps were provided for the Riparian sites, where the access was the easiest. Data were gathered for the whole imaged sites with areas between 3 ha and 6 ha. For the Terrace sites, data were gathered accurately, but challenging terrain in some areas limited the access; hence classification and counting from the distance was performed as well. The Terrace sites covered 3 ha up to 4.8 ha. The Slope sites had the most challenging environment with slopes angles generally ranging between 33 and 40°, even reaching 90° in some areas. The sites could not be accessed in all places; therefore, the counting and classification of the tree species were provided for patches along the slope. An overview of the occurring species and their number at different elevations were generated. In general, no fixed field plots were used because of the site's characteristics: dense understory vegetations, challenging slopes and the inaccessible areas. Surveys were done manually by assessing the species name, collecting leaves and images of leaves and bark, as well as localising the trees in the site, in relation to landmarks, surrounding tree species and the terrain. The manual data were digitalised with winter images. Summer images were used to accurately generate species maps of the sites 1, 4, 6, 7, 11, 12 and 13, while the trees were geolocated in Arc GIS. For the Slope sites only tree count surveys were evaluated.

4.1.3 Results

4.1.3.1 Species composition

The purpose of the fieldwork was first to get an overview of the occurring tree species, dominant species and their location. Second, this information were combined with data structuring, especially dividing tree species into forest layers and detection of species which belong to a niche in the forest. At last, the field data was used to validate the results of the image analysis.

70 species were identified, which belong to 31 families and 42 genera (Table 4). There were 11 species, which belong to the *Betulaceae*, of which five are *Alnus* and three *Betula* genus. Another 11 tree species belonged to the family *Sapindaceae* and six tree species to the *Rosaceae* family (three *Prunus* and three *Sorbus* species). Five species belong to the *Fagaceae* family, with two *Quercus* and two *Fagus* species. There were three tree species each from the *Juglandaceae* and the *Fabaceae* families. The families of *Salicaceae*, *Styracaceae*, *Pinaceae*, *Oleaceae*, *Makvaceae* and *Cornaceae* had each two tree species, while all other families had only one representing tree species.

In total 715 trees were counted for site 1, 427 for site 4, 450 for site 6, 470 for site 7, 511 for site 11, 458 for site 12, 374 for site 13, 635 for site 3, 639 for site 8/9 and 298 for site 10. In site 1, 27 different tree species were counted and one tree even could not be precisely identified. With 20 tree species, the number was lower than for sites 1 and 6, whereby also site 6 was inhabited by 27 species. Another additional eight trees were unknown. Site 7 had with 29 the highest number of tree species and eight unknown individuals. In the Terrace sites 11, 12 and 13, 29, 20 and 20 different tree species were identified. Unfortunately, there were in total 27 trees for the three sites, which could not be identified, as the sites were steep and partly inaccessible. The identification was therefore only performed on images from a camera and from the UAV. Depending on distance, blurring and light conditions, most of the time only one side of the leaf was imaged; hence there was no accurate identification performable. The same problem occurred in site 3, where 12 trees remained unidentified, but at least 26 tree species could be identified. Site 8/9 had 23 identified tree species and site 10 19, while three tree species stayed unidentified. In the Slope sites the main problem was the inaccessibility and the height of some trees. These trees could not be reached and had high branches; therefore, no leaves could be reached from the ground.

Table 4 Identified tree species in the field, with their Scientific names, family, genera and layer. The layers canopy (C), subcanopy (SC), understory (U) and shrub (S) were assigned to each species.

Number	Species	Family	Genus	Layer
1	<i>Salix jessoensis</i>	Salicaceae	Salix	C
2	<i>Salix serissaefolia</i>	Salicaceae	Salix	C
3	<i>Juglans ailantifolia</i>	Juglandaceae	Juglans	C
4	<i>Pterocarya rhoifolia</i>	Juglandaceae	Pterocarya	C
5	<i>Aesculus turbinata</i>	Hippocastanaceae	Aesculus	C
6	<i>Magnolia obovata</i>	Magnoliaceae	Magnolia	C
7	<i>Phellodendron amurense</i>	Rutaceae	Phellodendron	SC
8	<i>Robinia Pseudoacacia</i>	Fabaceae	Robinia	SC
9	<i>Quercus mongolica subsp. crispula</i>	Fagaceae	Quercus	C/U
10	<i>Fagus Crenata</i>	Fagaceae	Fagus	C/U
11	<i>Cornus Controversa</i>	Cornaceae	Cornus	SC
12	<i>Weigela hortensis</i>	Caprifoliaceae	Weigela	S
13	<i>Alnus fauriei</i>	Betulaceae	Alnus	S
14	<i>Ilex geniculata Maxim</i>	Aquifoliaceae	Ilex	S
15	<i>Carpinus cordata</i>	Betulaceae	Carpinus	C
16	<i>Sorbus sambucifolia</i>	Rosaceae	Sorbus	U
17	<i>Sorbus alnifolia</i>	Rosaceae	Sorbus	U
18	<i>Styrax obassia</i>	Styracaceae	Styrax	SC/U
19	<i>Lindera umbellata</i>	Lauraceae	Lindera	S
20	<i>Hamamelis japonica var. obtusata</i>	Hamamelidaceae	Hamamelis	SC/U
21	<i>Cercidiphyllum magnificum</i>	Cercidiphyllaceae	Cercidiphyllum	C
22	<i>Tilia maximowiczina</i>	Malvaceae	Tilia	SC
23	<i>Morus australis</i>	Moraceae	Morus	SC/U

24	<i>Alnus inokumae</i>	Betulaceae	Alnus	SC
25	<i>Castanea crenata</i>	Fagaceae	Castanea	SC
26	<i>Corylus sieboldiana</i>	Betulaceae	Corylus	C
27	<i>Prunus speciosa</i>	Rosaceae	Prunus	SC
28	<i>Prunus serrulata/grayana</i>	Rosaceae	Prunus	SC
29	<i>Prunus salicina Lindley</i>	Rosaceae	Prunus	SC
30	<i>Aralia elata Seemann</i>	Sapindaceae	Acer	U
31	<i>Acer palmatum</i>	Sapindaceae	Acer	U
32	<i>Acer sieboldianum</i>	Sapindaceae	Acer	U
33	<i>Acer japonicum</i>	Sapindaceae	Acer	U
34	<i>Acer mono Maxim.</i>	Sapindaceae	Acer	SC
35	<i>Alangium planifolium</i>	Cornaceae	Alangium	S
36	<i>Acer pictum subsp. mono</i>	Sapindaceae	Acer	SC
37	<i>Acer rufinerve Sieb. Et Zucc.</i>	Sapindaceae	Acer	SC
38	<i>Acer buergerianum</i>	Sapindaceae	Acer	SC
39	<i>Larix kampferi</i>	Pinaceae	Larix	C
40	<i>Ginkgo biloba</i>	Ginkgoaceae	Ginkgo	C
41	<i>Fraxinus lanuginosa</i>	Oleaceae	Fraxinus	SC
42	<i>Fraxinus platyoda</i>	Oleaceae	Fraxinus	C
43	<i>Celtis jessoensis</i>	Cannabaceae	Celtis	C/SC
44	<i>Betula schmidtii</i>	Betulaceae	Betula	SC
45	<i>Cryptomeria japonica</i>	Cupressaceae	Cryptomeria	C
46	<i>Betula maximowicziana</i>	Betulaceae	Betula	SC
47	<i>Betula corylifolia</i>	Betulaceae	Betula	SC
48	<i>Sorbus japonica</i>	Rosaceae	Sorbus	U
49	<i>Camellia japonica</i>	Theaceae	Camellia	U
50	<i>Acer disylum</i>	Sapindaceae	Acer	U
51	<i>Tilia japonica</i>	Malvaceae	Tilia	SC
52	<i>Alnus wirsata</i>	Betulaceae	Alnus	U
53	<i>Quercus detala</i>	Fagaceae	Quercus	C
54	<i>Wisteria floribunda</i>	Fabaceae	Wisteria	S
55	<i>Fagus Japonica</i>	Fagaceae	Fagus	C/SC
56	<i>Aleurites fordii/ Vernicia fordii</i>	Euphorbiaceae	Vernicia	U
57	<i>Platycarya strobilacea</i>	Juglandaceae	Platycarya	SC
58	<i>Abizia Julibrissin</i>	Fabaceae	Abizia	SC
59	<i>Alnus pendula</i>	Betulaceae	Alnus	U
60	<i>Symplocos chinensis</i>	Symplocaceae	Symplocos	S
61	<i>Acer amonesum</i>	Sapindaceae	Acer	SC
62	<i>Pterostyrax corymbosa</i>	Styracaceae	Pterostyrax	U
63	<i>Acer nippon</i>	Sapindaceae	Acer	SC
64	<i>Alnus japonica</i>	Betulaceae	Alnus	U
65	<i>Vaccinium oldhamii</i>	Ericaceae	Vaccinium	S
66	<i>Picea abies</i>	Pinaceae	Picea	C
67	<i>Euonymus sieboldianus</i>	Celastraceae	Euonymus	SC
68	<i>Clethra barvinervis</i>	Clethraceae	Clethra	U
69	<i>Kalopanax Septemlobus</i>	Araliaceae	Kalopanax	SC
70	<i>Hydrangea species</i>	Hydrangeaceae	Hydrangea	S

The distribution of the tree species is shown in Figure 32, where the sites were clustered to their forest type. In the Riparian sites the most species belong to the *Juglandaceae* family, mainly *Juglans ailantifolia*, followed by *Pterocarya rhoifolia*. The characteristic *Salix serissaefolia* was also identified in site 4, however the *Salix* species occurred generally less frequent. *Aesculus turbinata*, *Robinia pseudoacacia* and *Quercus mongolica* grew in all sites with around 20 trees per species and site. *Cornus controversa* was also more frequent in the sites 1 and 6, *Styrax obassia* in sites 1 and 4. Regarding the *Acer* species, *Acer palmatum* occurred more frequent in site 6, *Acer sieboldianum* in site 4 and *Acer japonicum* in site 7, while there was only a small number of *Acer mono maxim* trees. The invasive species occurred in all Riparian sites. In contrast, the Terrace sites contained more *Juglans ailantifolia* and *Aesculus turbinata* trees, less *Pterocarya rhoifolia*, *Alnus fauriei* and *Quercus mongolica*. In general, fewer trees grew in the Terrace sites. Additionally, in all sites *Cornus controversa*, *Magnolia obovata* and *Acer mono maxim* were identified. *Acer palmatum* and *japonicum* were distributed in sites 11 and 12, while *Acer sieboldianum* was more frequent in site 13. Still, there could be errors in the classification of the three previously mentioned *Acer* species, as the site had difficult access and some species needed to be identified from distance. While the overall distribution between the Riparian and Terrace sites had a similar shape, the Slope sites showed a different distribution of tree species. The most frequent species were *Acer* species: *Acer palmatum* in sites 8 and 10 and *Acer sieboldianum* in site 3. Additionally, *Acer mono maxim* had high numbers in site 10, while *Acer pictum* was more frequent in site 3. Tree species like *Juglans ailantifolia*, *Pterocarya rhoifolia*, *Aesculus turbinata* and *Salix* species were significant less, compared to the Riparian and Terrace sites. *Fagus crenata* and *Quercus mongolica* showed high tree occurrences, together with *Corylus sieboldiana*, *Larix kaempferi*, *Prunus* species, *Styrax obassia* and *Carpinus cordata*, with lower numbers than *Fagus* and *Quercus* but more frequent than in the Riparian sites. Figure 31 shows the region, where the field data were collected, which was the basis for the comparison of the field data with the image data. It can be seen that the fieldwork area of site 3 was larger than the areas of sites 8/9 and 10. Furthermore, the fieldwork mainly followed regions, where the forest was accessible, which resulted in the striped shape in site 8/9 and in a circle in site 10.



Figure 31 Investigated field survey area (approx.) for Slope sites

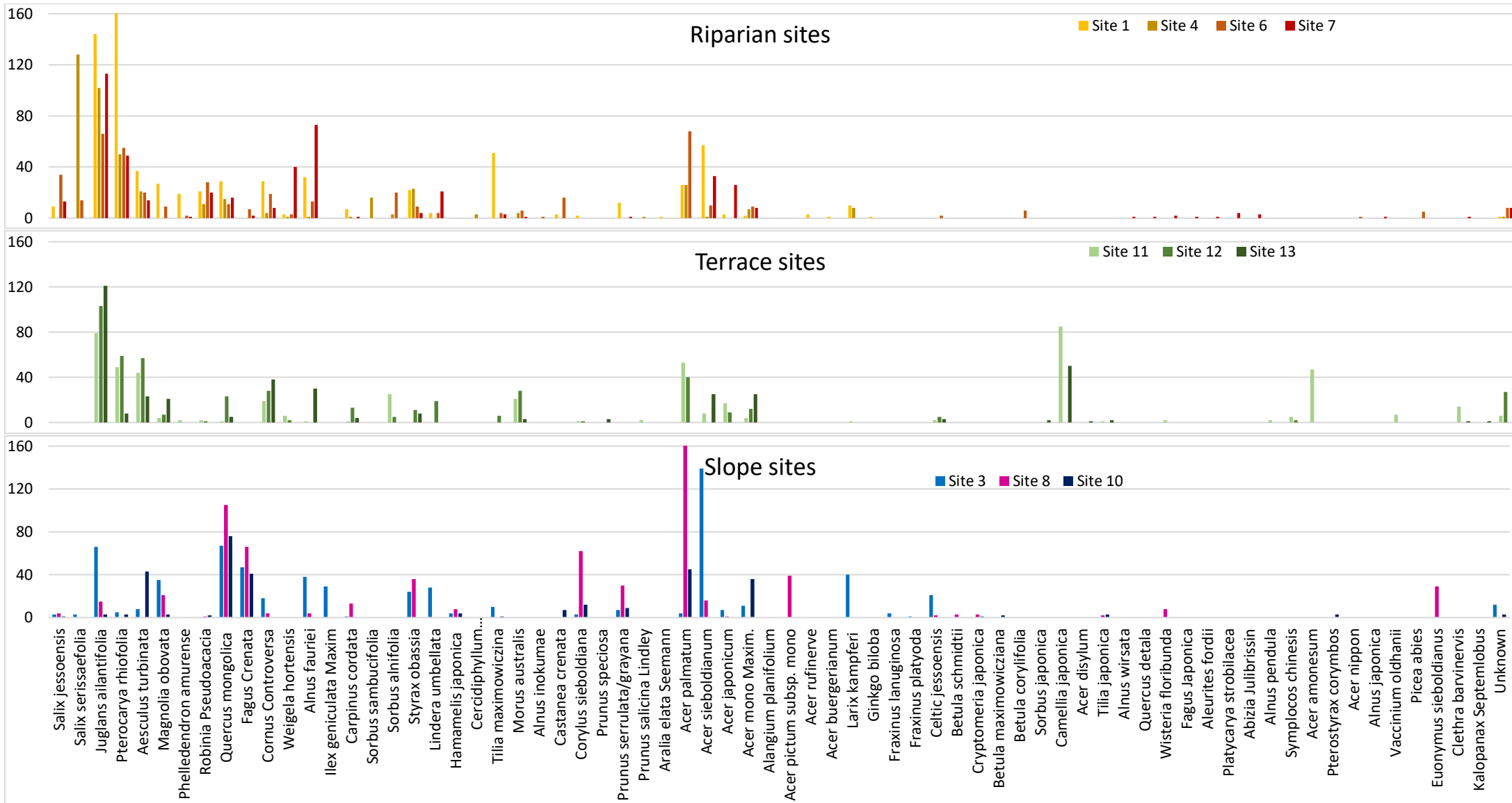


Figure 32 Species distribution in the three considered sites: Riparian (top), Terrace (middle), Slope (Bottom). The x-axis: the tree species; the y-axis: tree counts per species

4.1.3.2 Tree census

The conducted fieldwork followed the strategy to identify and locate trees manually for the whole imaged sites. No fixed plots were used, instead only a manual map and a later digitalisation were performed. For site 1 a fixed plot was set on the island, covering about 55 m², where the location of trees was measured and classified. The results are presented in Figure 33, while Table 5 contains the counts for the plot and the tree numbers, which were counted for the whole study site (4.29 ha). The table shows that the dominant species in site 1, according to the plot, was *Juglans ailantifolia*, followed by *Pterocarya rhoifolia* and *Phellodendron amurense*, both with 18 individual trees. These numbers suggested that the forest is composed of mainly *Juglans* trees and a mixture of subdominant species *Pterocarya* and *Phellodendron*. Considering the whole site 1, *Pterocarya* had a higher number of trees than *Juglans*. *Phellodendron amurense* had only one tree outside the plot on the island. *Cornus controversa* and *Aesculus turbinata* showed the opposite characteristic, as there was only one tree in the plot, but 28 and 36, respectively, in the rest of the site. These results approved the new selected fieldwork methodology, as the field data were important for the whole imaged area, but the plot did not provide representative results.

Table 5 Comparison field plot (site 1) with whole study site 1

Tree species	Plot 1 Tree numbers	Site 1 Tree numbers
<i>Juglans ailantifolia</i>	32	144
<i>Pterocarya rhoifolia</i>	18	173
<i>Phellodendron amurense</i>	18	19
<i>Salix jessoensis</i>	5	9
<i>Conus controversa</i>	1	29
<i>Robinia pseudoacacia</i>	11	21
<i>Aesculus turbinata</i>	1	37

In Figure 34 the important information orthomosaic of site 1 was marked with colours and symbols. In plot 1, the dominant tree species were *Juglans ailantifolia*, which were also located in the north and the south of the island. The blue circle shows the location of the *Phellodendron amurense* trees, which were clustered in the island area, like the *Juglans* trees. In the south of site 1 are two large areas (marked in red), where *Pterocarya rhoifolia*, *Aesculus turbinata* and *Cornus controversa* occurred in clusters, outside of the island. The clustering shows why the island is not representative for the whole studied site.

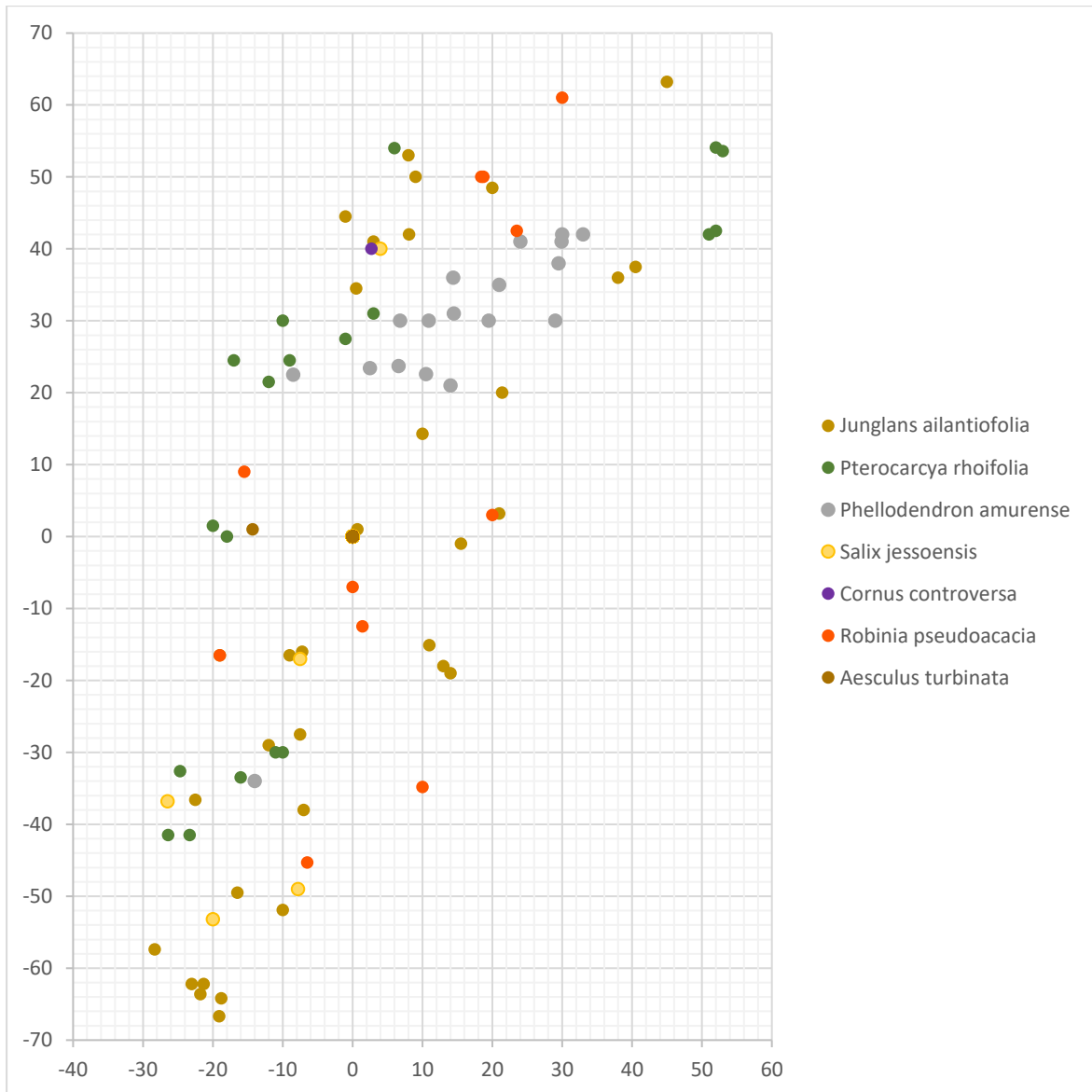


Figure 33 Location of the trees on island of site 1

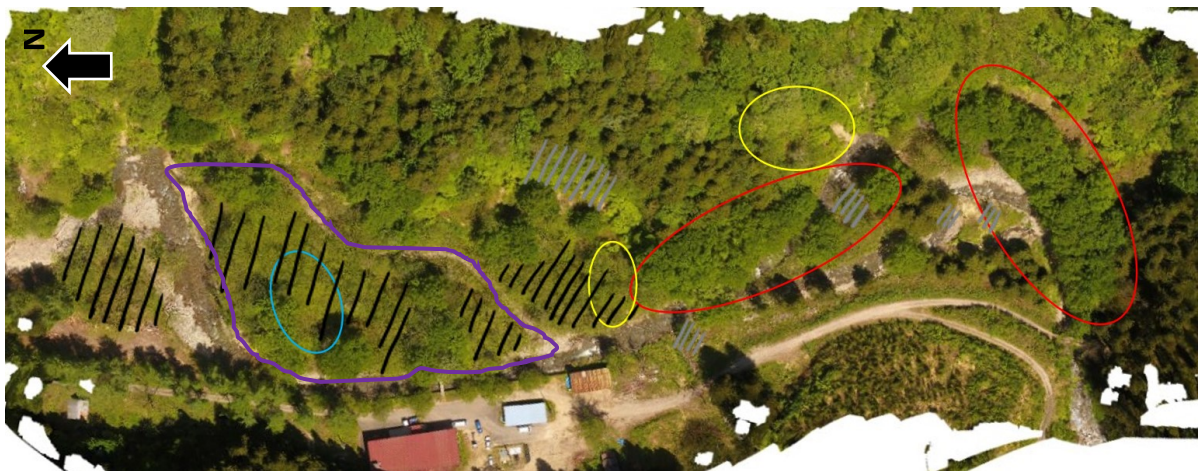


Figure 34 Orthomosaic of site 1, with the purple surrounded area of the sample plot 1. In black strips, the location of *Juglans ailantifolia* trees is marked, in grey strips the location of *Aesculus turbinata*, in the blue circle *Phellodendron amurense* tree, in red

4.1.3.3 Tree species dominance

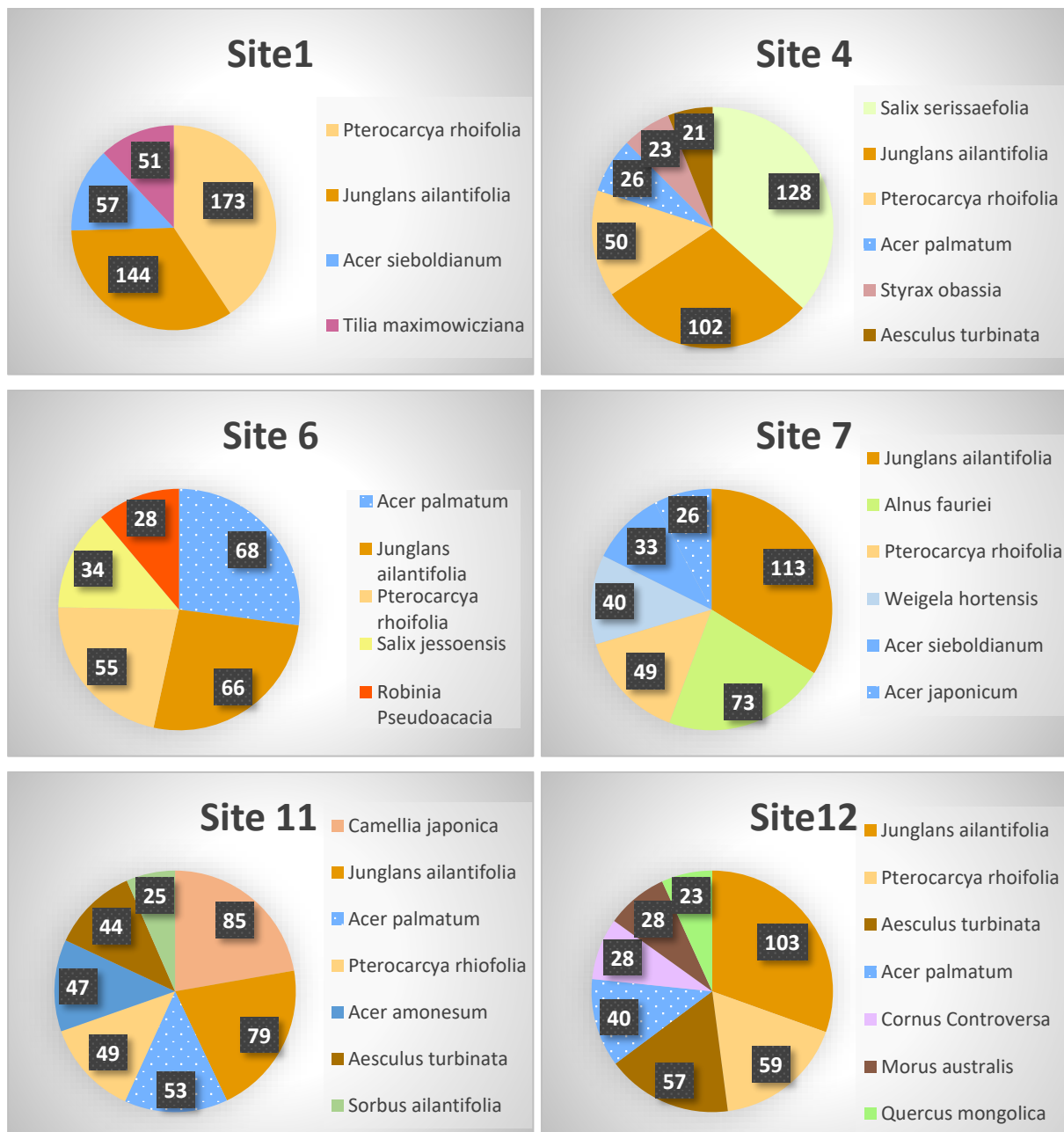
For evaluating the tree dominance relative densities were calculated, which are provided in Appendix L, as well as the tree species, which contributed 95 % of the trees (Figure 35). Using this approach, site 1 had a high number of *Pterocarya rhoifolia* and *Juglans ailantifolia* trees with 23.73 % and 19.75 %, followed by *Acer sieboldianum* and *Tilia maximowicziana* with 7.82 % and 7.00 %. Species like *Aesculus turbinata*, *Alnus fauriei*, *Quercus mongolica*, *Cornus controversa*, *Magnolia obovata*, *Acer palmatum* and *Styrax obassia* reached only between 5 % and 3 % and were not considered as dominant tree species of site 1. In comparison, the most frequent species in site 4 were *Salix serissaefolia* (29.98 %) and *Juglans ailantifolia* (23.98 %), while *Pterocarya rhoifolia* was less frequent with only 11.71 %. With 6.09 %, 5.39 % and 4.92 % *Acer palmatum*, *Styrax obassia* and *Aesculus turbinata* still belong to the dominant tree species in site 4. However, the total number of trees was lower than in site 1, therefore the relative density of the mentioned tree species was higher. With around 15 % relative density, *Acer palmatum*, *Juglans ailantifolia* and *Pterocarya rhoifolia* were the most frequent species. *Salix jessoensis* and *Robinia pseudoacacia* were subdominant with 7.56 % and 6.22 %. The tree species densities of site 7 were similar to site 4, with a high number of *Juglans ailantifolia* trees and a lower number of *Pterocarya rhoifolia*. However, in site 7 *Alnus fauriei* was dominant and *Salix jessoensis* had low densities with only 2.77 %. *Juglans ailantifolia* and *Pterocarya rhoifolia* were always dominant tree species in all Riparian sites, while *Acer* species, *Styrax obassia*, *Alnus fauriei* and *Weigela hortensis* were dominant shrub species. The Riparian sites had maximal six dominant tree species, while the Terrace sites showed a higher number with seven or eight dominant species.

In sites 11 and 12, *Juglans ailantifolia* (15.46 %, 22.49 %) and *Pterocarya rhoifolia* (9.59 %, 12.88 %) as well as *Aesculus turbinata* (8.61 %, 12.45 %) had the highest densities. Site 13 also contained a high number of *Juglans* trees (32.35 %), but only 2.14 % *Pterocarya rhoifolia* trees, while *Cornus controversa* (10.16 %), *Acer mono maxim* (6.68 %) and *Magnolia obovata* (5.61 %) had higher tree densities. In comparison, *Juglans ailantifolia* was the tree species with the highest relative density in sites 12 and 13, while the species distribution was more homogeneous for the species shown in Figure 35. Dominant shrubs were *Camellia japonica*, *Acer palmatum* and *sieboldianum*, *Sorbus ailantifolia*, *Morus australis* and *Alnus fauriei*.

The Slope sites had five to seven dominant tree species, two of them were found in all sites: *Quercus mongolica* (10.55 % site 3; 16.43 % site 8/9 and 25.50 % in site 10) and *Fagus crenata* (7.40 % site 3; 10.33 % site 8/9 and 13.76 % site 10). These species did neither occur with high densities in the Riparian nor in the Terrace sites. Together with *Acer sieboldianum* (AS) and *Acer palmatum* (APa), *Acer pictum* (APi) and *Acer mono maxim* (AM) occurred with higher densities, reaching values of 21.89 % (site 3, AS), 26.13 %, 15.10 % (site 8/9 and 10, APa), 6.1 % (site 8/9, APi) and 12,08 % (site 10, AM). Shrub

species, which were dominant in the Slope sites, were *Alnus fauriei* (site 3; 5.98 %) and *Styrax obassia* (site 8/9; 5.63 %). In site 3, *Larix kaempferi*, *Juglans ailantifolia* and *Magnolia obovata* were more frequent, while these species occurred in low numbers in sites 8/9 and 10, instead site 8/9 contained a higher number of *Corylus sieboldianum* and site 10 *Aesculus turbinata* trees.

All study sites showed different characteristics regarding growing tree species and their frequency. All sites further had a high number of tree species, whereby most of the species only had one or two trees per species. Also, there were a high number tree species, which occurred in only one site with also only one example tree.



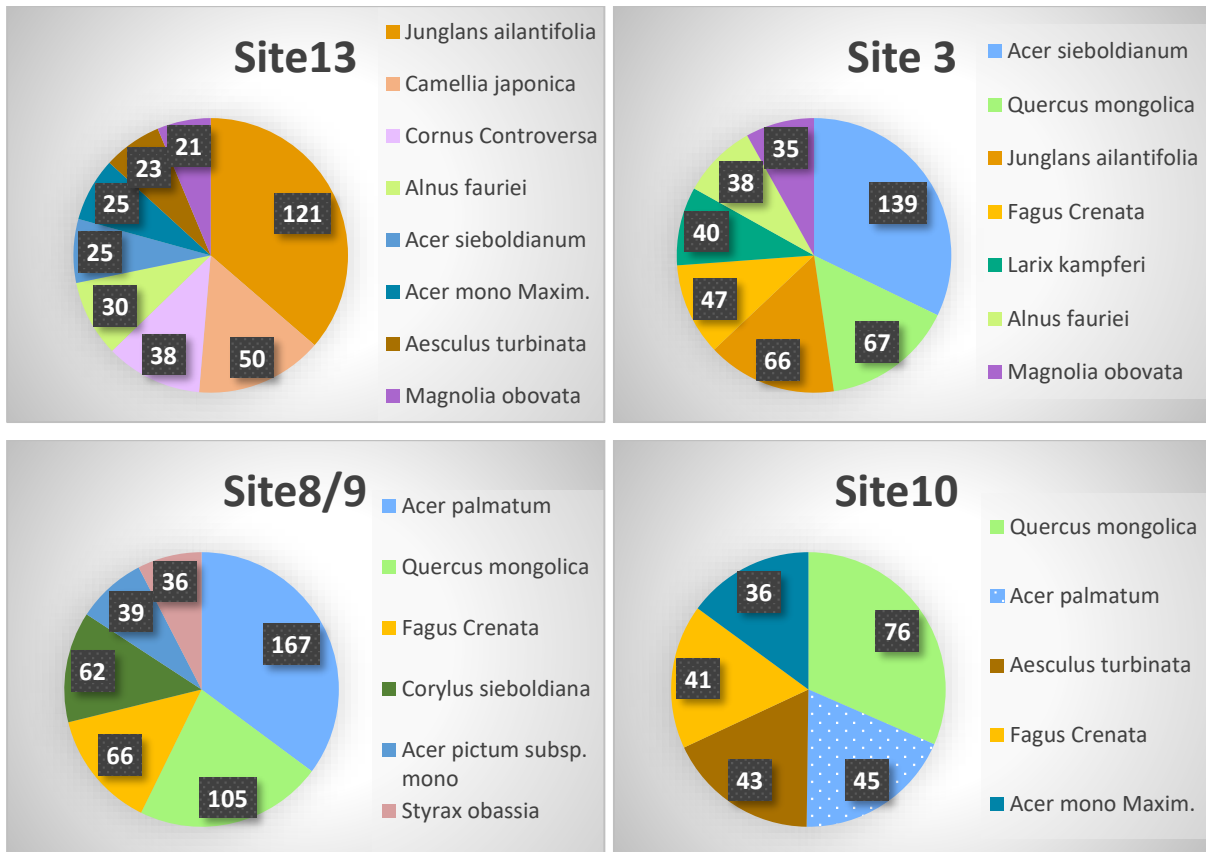


Figure 35 Tree species, which accounts 95 % of all trees

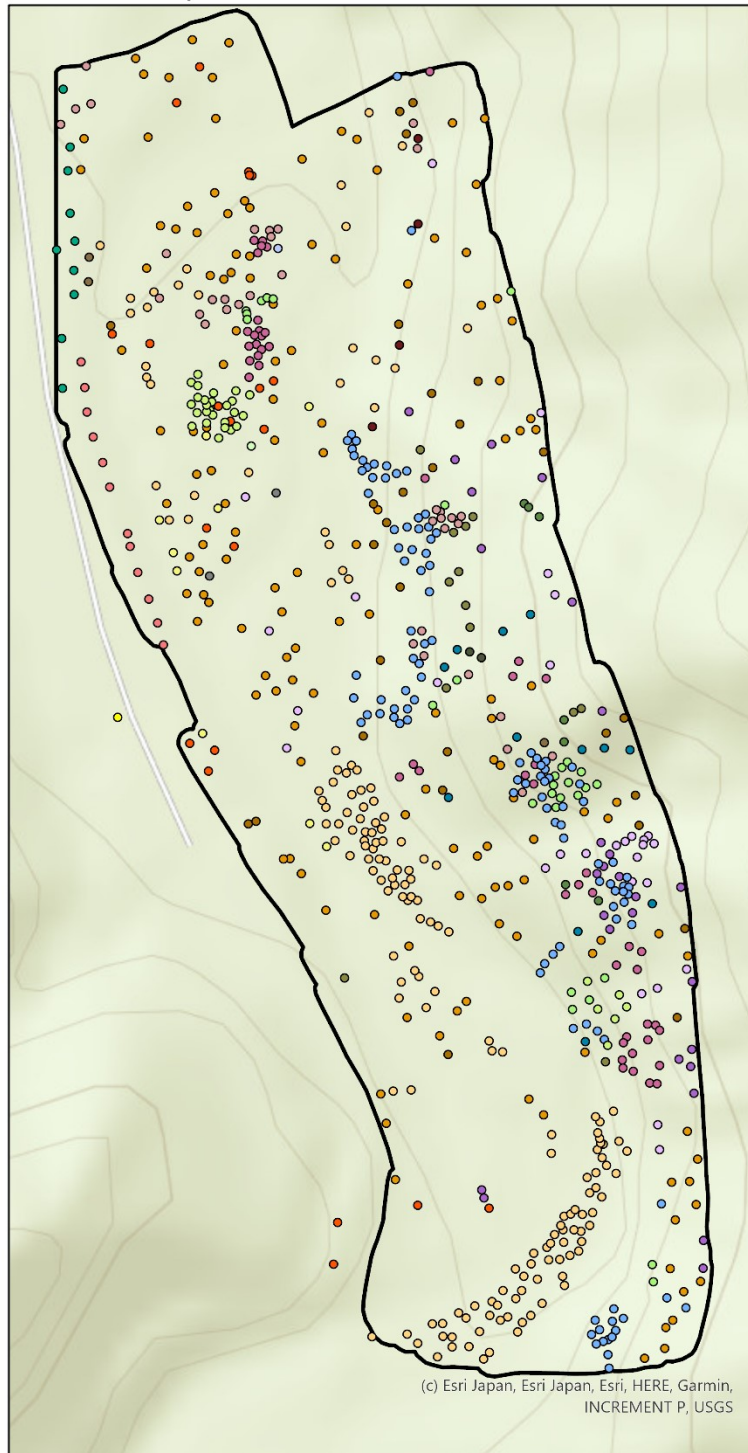
4.1.3.4 Field surveys and tree distributions

Field surveys were conducted for the Riparian sites, Terrace sites and for three Slope sites. The gathered data were used to geolocate tree stems and generate point maps in ArcGIS, on the basis of winter images. Those maps were not generated for the Slope sites, as the pathways of the field surveys could be only partially reconstructed, and the resulting map would have been inaccurate. All field survey maps are given in Appendix J, while in this chapter only two representative maps of sites 1 and 12 are presented (Figure 36, Figure 37). The maps contained the ROI boundaries for each site. Even some trees outside of the ROI were classified, because the fieldwork was done before the ROIs were selected.

In the map of site 1, 24 tree species were found, including one class with dead trees and another one containing trees, which could not be identified. *Juglans ailantifolia* trees spread homogeneously over the whole site, while trees like *Salix jessoensis*, *Robinia pseudoacacia* and *Phellodendron amurense* occurred mainly on the island of site 1. The point map (Figure 36) showed monoculture patches of *Pterocarya rhoifolia* in the south and in the centre of the map, where also no shrub or small tree species coexisted. On the island of site 1 a high number of *Tilia* species, *Quercus mongolica* and *Alnus fauriei* occurred. These trees were young and small, grew in the understory layer of the forest and created

Field survey site 1

by Sarah Kentsch



Legend

Species labels

Species_lat_name

- Acer
- Acer mono maxim
- Aesculus turbinata
- Alnus fauriei
- Aralia elata
- Carpinus cordata
- Castanea crenata
- Climbing plant 1
- Cornus controversa
- Corylus sieboldiana
- Ginkgo biloba
- Juglans ailantifolia
- Larix kaemferi
- Lindera umbellata
- Magnolia obovata
- Phellodendron amurense
- Prunus
- Pterocarya rhoifolia
- Quercus mongolica
- Robinia pseudoaccacia
- Salix jessoensis
- Styrax obassia
- Tilia
- dead
- unknown
- <all other values>

□ ROI

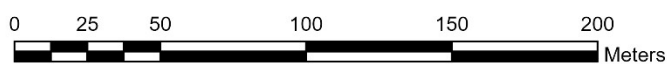
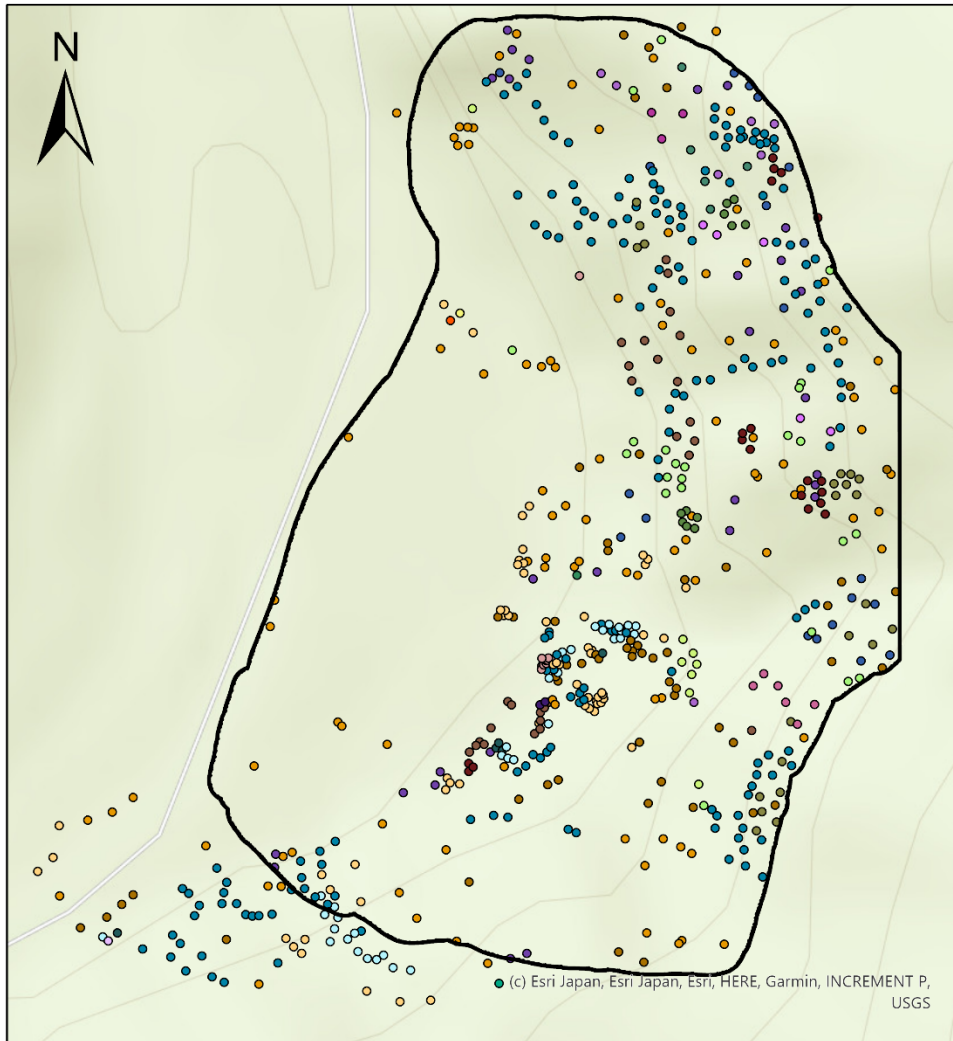


Figure 36 Field survey of site 1, digitalised in ArcGIS pro



Field survey site 12 (YURF)

by Sarah Kentsch



0 10 20 40 60 80 Meters

Legend

ROI

FieldData_Site12

Species_lat_name

- | | |
|------------------------|-------------------------|
| ● Climbing plant 1 | ○ Pterocarya rhoifolia |
| ● Climbing plant 2 | ○ Quercus monglica |
| ● Cornus controversa | ● Robinia pseudoaccacia |
| ○ Corylus sieboldiana | ○ Salix jessoensis |
| ● Juglans ailantifolia | ● Sorbus alnifolia |
| ● Kalopanax septemlobu | ○ Styrax obassia |
| ● Larix kaempferi | ● Synpolcas chinensis |
| ● Lindera umbellata | ○ Tilia |
| ● Magnolia obovata | ● Weigela hortensia |
| ● Morus australis | ○ <all other values> |

Figure 37 Field survey of site 12, digitalised in ArcGIS pro

dense vegetation with a small spread. Tree densities were higher towards the slope (the eastern part of the map), since tree points occurred in dense clusters, closer together. Small-leaved *Acer* species occurred frequently along the bottom of the slope in clusters; they had a wider spread than other small species. The higher slope parts, in the eastern side of the map, belonged to the *Cryptomeria japonica* patch, where tree species of the mixed forest occurred less frequent.

The species map of site 7 showed a similar tree distribution. Along the slopes in the eastern and western part of the map, many small-leaved *Acer* species, *Alnus fauriei*, *Lindera umbellata* and *Weigela japonica* grew; all of them occurred in clusters with a small spread across the site. The main part of site 7 contained only widely spread large trees like *Pterocarya rhoifolia*, *Juglans ailantifolia*, *Salix jessoensis* and *Robinia pseudoacacia*. Those trees were well separated from each other but young trees grew in small clusters. This separation between the tall trees was found in sites 4 and 6. In site 4 young *Salix serissaefolia* occurred in a cluster with more than 100 trees, young trees of *Robinia pseudoacacia*, *Sorbus alnifolia* and a *Fraxinus* species in the centre of site 4. The northern slope was mainly composed of *Cryptomeria japonica*, where only a couple of mixed forest species were identified in between. The only old-growth trees, which grew close, were coniferous trees, like *Cryptomeria japonica* and *Larix kaempferi*. The tree distribution in site 6 was different, as the trees grew closer together. Species like *Alnus fauriei*, *Lindera umbellata*, *Morus australis*, *Hydrangea* species and *Styrax obassia*, which were in the shrub layer, built clusters in most areas, while they did not spread over the whole site. Especially *Pterocarya rhoifolia* trees occurred often paired or in groups of three trees, usually one old-growth tree together with young trees. Young trees of *Robinia pseudoacacia*, *Juglans ailantifolia* and *Pterocarya rhoifolia* occurred frequent in site 6, especially along the river. Both *Salix* species grew in and around a depression, which was filled with water during the summer months. Additionally, the species occurred in clusters with several other species, which was not observed in other sites (except the young *Salix* trees in site 4). Furthermore, the occurring species varied for all sites, which made the species composition unique mosaics.

The Terrace sites all had different distributions and compositions of tree species. In site 11, the numbers of shrubs and understory vegetations were high, with nine different species of which most occurred in small clusters. Trees like *Juglans ailantifolia*, the most found species, *Magnolia obovata* or *Pterocarya rhoifolia* spread over the whole site. *Celtis jessoensis*, *Morus australis* and *Styrax obassia* grew as shrub species, reaching heights of about 2 m. In comparison, site 12 showed a dense vegetation structure, where only *Juglans ailantifolia* trees spread over the whole site (Figure 37). Most small tree species like *Lindera umbellata*, *Sorbus alnifolia* and *Styrax obassia* occurred in clusters. The densest clusters were found along the river, which crosses site 12. Small-leaved *Acer* spread over the whole site, while *Acer mono maxim* spread primarily in higher regions. Site 13 showed evenly

distributed tree species, except for the southern part, where *Acer* species were dominant, and for the northern part, where *Juglans ailantifolia* was distributed. In the lower part of the slope *Alnus fauriei* was increasingly found. In the map (Figure 37), the two kinds of climbing plants were marked; most of them grew on *Juglans ailantifolia* or *Cryptomeria japonica* trees.

Since no maps were created for the Slope sites, it should be mentioned that most species occurred in clusters. Small tree species grew usually in groups of three or more individuals, while species like *Quercus mongolica*, *Fagus crenata*, *Larix kaempferi* and *Hamamelis japonica* were found with five or more trees with wide gaps. Site 3 had some special characteristics. In the northern part, close to a small river, mainly *Juglans ailantifolia* trees occurred. The west facing slope of the ridge contained more species than the other side of the ridge, where mainly shrubs and small trees were found. On the top of the ridge grew large trees, like *Larix kaempferi* and *Quercus mongolica*. The whole site showed a high spread of small-leaved *Acer* species with more than 140 individuals. More small-leaved *Acer* trees were only counted in site 8/9, with more than 160 trees. In site 10 was also a change in the tree species composition recognisable with increasing elevation. While at the bottom of the slope *Juglans ailantifolia* and small-leaved *Acer* species were found, the top part was dominated by big-leaved *Acer* and *Fagus crenata*. Species, which were distributed over the whole slope, were *Corylus sieboldiana* and *Quercus mongolica*. *Magnolia obovata*, *Aesculus turbinata*, *Betula* and *Prunus* species occurred with single trees or in small groups along the slopes. In site 10, *Alnus fauriei* trees grew at higher elevations.

4.1.3.5 Forest diversity

Forest diversity measures were explained and calculated for all sites based on the image results. Two calculations were performed with the field data to compare them with the image data. The Shannon diversity and the evenness were calculated, once including the understory vegetation (for this section: UV) and once without.

The Shannon diversity was generally high for all sites, with values between 2.14 and 2.76, while evenness values ranged between 0.71 and 0.84. The diversity values varied for the Riparian sites, as site 4 had the lowest value and site 6 the highest; a similar range was observed for the Slope site values. The terrace values showed more constant values, ranging between 2.25 and 2.59 (Table 6). Sites 8/9 and 12 had lower Shannon diversities but a higher evenness than sites 11, 1 and 7.

When the understory vegetation was disregarded, the diversity and the evenness were usually lower. An exception was site 10, where the values with and without UV were similar. Site 10 was the site with the most difficult access and steepness of the slopes.

Therefore, the fieldwork in this forest patch focussed on tree species data, not on UV. Another exception was site 4, where the evenness without UV was slightly than with UV (0.72; 0.71). In general, the Shannon diversity values ranged between 1.75 and 2.45, and the evenness values without UV ranged between 0.57 and 0.78. These values showed that especially the evenness was insignificant, while the Shannon diversity values still showed a moderate distribution.

The highest differences between the Shannon diversities were observed in site 7 and 11, while they were the lowest for site 4 and site 10. It was, however, almost the same for sites 1, 12 and 8/9, with a value of 0.23. While the order of the sites was the same, when differences between the evenness values were observed, the only difference was that the evenness of site 8/9 was higher (0.04) than site 12 (0.02) or site 1 (0.01). The highest difference was 0.17 in site 7.

Table 6 Diversity and evenness values calculated on the basis of the field counts

Site	Shannon diversity	Shannon evenness	Shannon diversity without UV	Shannon evenness without UV
1	2.54	0.77	2.31	0.76
4	2.14	0.71	1.95	0.72
6	2.76	0.84	2.45	0.78
7	2.48	0.74	1.80	0.57
3	2.64	0.81	2.19	0.70
8/9	2.41	0.77	2.18	0.73
10	2.18	0.74	2.18	0.74
11	2.59	0.77	1.93	0.63
12	2.35	0.79	2.12	0.77
13	2.25	0.75	1.75	0.62

4.1.3.6 Layering of mixed forests

A forest usually grows in different layers, depending on their heights, divided as dominant, co-dominant, suppressed and understory trees, also called the canopy, subcanopy, understory and shrub layer (Table 4). They contain therefore different tree species. As the dominant canopy layer consists of the tallest trees with the largest canopy area, trees receive enough light, while the understory vegetation is usually composed of young or small trees and has to be adapted to shadow conditions. In this chapter, the species were assigned to the different forest layers.

The layers in the forest were divided according to the maximal recorded height of the tree. Trees, higher than 20 m, were considered as canopy layer, 15 m – 20 m were subcanopy layer, 5 m – 15 m

were part of the understory layer and all trees lower than 5 m were classified as shrub layer (Figure 38). In a second step, a re-evaluation was performed based on the occurrence and heights of the trees in the field (in case trees were smaller in some sites). Tree heights were not continuously measured but the layer was chosen based on field observations classified.



Figure 38 Layering of the forest

In total, there were 15 tree species assigned to the canopy layer, 24 to the subcanopy layer, 15 to the understory layer and 8 to the shrub layer. *Salix* species, *Juglans ailantifolia* and *Pterocarya rhoifolia* were the dominant species of the canopy layer in the Riparian sites. Species like *Phellodendron amurense*, *Robinia pseudoacacia*, *Castanea crenata* and *Cornus controversa* were typical examples for tree species in the subcanopy layer of Riparian mixed forests studied. The coniferous tree species *Larix kaempferi* and *Picea abies* belonged to the species growing the highest in mixed forests and were therefore characterised as canopy layer species. *Cryptomeria japonica* was also assigned to the canopy layer, but since it was a planted tree, it was not further considered.

Quercus mongolica and *Fagus crenata* belong to the canopy layer, but in the Riparian and Terrace sites *Quercus mongolica* often occurred as young tree between the dominant tree species. Hence, they were assigned to the understory layer in riparian forests and to the subcanopy layer in the Terrace sites. *Fagus crenata* was only found in sites 6 and 7, where the trees were still young and hence belonged to the understory layer.

The subcanopy layer in slope areas was dominated by big-leaved *Acer* species, like *Acer mono maxim* and *Acer pictum*, but also by *Tilia maximowicziana*, *Prunus* species, *Alnus inokumae* and *Platycarya strobilacea*. Together with the subcanopy layer species of the Riparian sites, the species formed a canopy layer that was lower than the ones of the canopy species, which means that these trees would usually be covered by canopy layer species. They were only visible from above on the borders of the

canopies of bigger trees or when the subcanopy species grew in clusters. *Betula* species grew usually up to 20 m, which was the limit for the subcanopy layer. *Hamamelis japonica* was another example for a small tree, which sometimes occurred as a shrub species, while it was assigned to the subcanopy and understory layer in this study, because the tree was usually growing high in Slope sites. Smaller trees occurred especially in clusters. *Styrax obassia* was a further species assigned to both, subcanopy and understory layer, as the tree grew as bushes in the riparian areas, but higher in slope areas, most probably because of the light conditions.

The tree species in the understory vegetation layer were mainly *Acer* species like *Acer palmatum*, *Acer sieboldianum* and *Aralia elata*, but also species of the family *Betulaceae*, with examples like *Alnus wirsata* and *Alnus japonica*. These species were characterised as the understory layer, as they can grow as small trees or shrubs in the forest. In the Riparian sites, all of these tree species mainly grew as shrubs, while they were small trees in the Terrace sites. In Slope sites they grew as shrubs or small trees, depending on the density of the forest and the canopy cover. Species like *Sorbus japonica* and *Sorbus sambucifolia*, which usually grew high, were found in the YURF sites to be mainly small and therefore assigned to the understory layer. There were furthermore several *Pterocarya rhoifolia* trees and some *Juglans ailantifolia* trees, which were still young, so that they had to be considered in the understory layer (however the table had the focus on adult trees).

Typical examples of the shrub layer were *Weigela hortensis*, *Ilex geniculata*, *Alnus fauriei*, *Sorbus alnifolia*, *Wisteria floribunda* and *Vaccinium oldhamii*. The species grew as bushes in different sizes, especially in lower slope areas in sites 1, 7, 11, 12 or 13. The species might also occur in higher slope areas, but as the access in site 8/9 and 10 was difficult, they were not specifically determined. Shrubs occurred in high numbers in one area, where they covered the whole ground and created a dense forest floor.

Three species were classified as canopy as well as understory tree species, another three as subcanopy/understory layer tree and one into canopy and subcanopy. The main reason, why the trees could not be assigned to only one layer, was that they showed different growing behaviours in the forests. Out of the 15 tree species, which belong to the canopy layer, ten grew in site 10, nine in site 1 and only five in site 13. All other sites contained six to seven tree species from the canopy layer. The subcanopy layer, with 24 species, had a maximum eight different species in one site, while there were two sites (4 and 12), where only four different species grew. Four sites had only three different understory vegetation species, site 7 had six different species and site 11, with 7 different species, was the richest site. Site 11 further contained the most different shrub species (five different ones).

Table 7 shows the number of trees per layer with 73.47 % of the total number of trees, most trees in site 4 belong to the canopy layer, while it was around 62 % in site 10 and 12 and 56.32 % in site 1. The canopy layer had fewer trees in sites 7 and 8/9, was around 45 %, only 36.18 % had been classified as canopy layer in site 11. The high number of shrub individuals in site 7, was 29.44 %, and the high number of understory tree species in site 11, was 44.73 %. The individuals belonging to the subcanopy layer ranged between 10 % and 30 %, except for site 4, where it was only 5.34 % (the shrub layer had only 0.47 %). In most areas the subcanopy layer was missing. The understory vegetation layer was relatively high with 16 % (site 10), up to 44 % (site 11), whereby most sites had around 20 % of their trees in this layer. Significant differences were observed when shrubs were considered, as the number of trees ranged between 0 % (site 10) and 29 % (site 7).

Table 7 The calculated sum for the layers: canopy, subcanopy, understory and shrub are presented for each site

Layer	Site 1	Site 4	Site 6	Site 7	Site 3	Site 8/9	Site 10	Site 11	Site 12	Site 13
Sum C	410	313	223	210	300	291	183	182	268	185
Sum SC	141	23	86	48	78	152	64	75	47	69
Sum U	138	88	113	68	150	184	48	225	93	90
Sum S	39	2	20	136	95	12	0	21	23	30

4.1.4 Discussion

4.1.4.1 Challenges during the field work

During the field work all trees and shrubs were identified, and for the Riparian sites also geolocated. In Slope sites a geolocation was not possible because of the steep slopes and the dense vegetation. In the Riparian sites the shrub vegetation started to grow already, when there was still snow cover, and therefore reached a high density in summer, covering the whole sites and being 1 - 2 m high. Additionally, dangerous animals and the weather conditions with heavy rain events or storms further limited the time window for conducting field surveys.

In contrast, the Slope sites were only partly covered with dense vegetation, which, however, could barely be cut, because of the steepness of the slopes. Setting field plots was impossible for the same reasons. Partly, steep areas needed to be climbed, where no data could be collected without risking injuries. Hence, information about the tree species and tree location needed to be gathered before and after the climbing. Usually, it was not possible to climb up straight, pathways needed to be found, which resulted in wrong positioning and mapping of trees. Marker points like open spaces or high trees were usually not found in the dense forest. Since most of the field works needed to be conducted over several days to cover major parts of each site, marker points were essential to accurately produce

maps. Also, large tools to cut leaves could rarely be used, mainly because of the steepness. Therefore, leaves from trees with high branches could not be sampled. High resolution cameras were helpful to make images of the leaves, but still for some leaves, the resolution was too low due to image taking from distance.

Another challenge was to map the field data on the winter orthomosaics in the Terrace sites, where steep slopes were, too. In sites 11 and 13 (also part of site 7 along the road) field work was once performed from the bottom of the slope and once from the top to avoid steep passages. Therefore, double counting and missed trees occurred, which happened definitely in site 13, where 109 shrubs could be detected in the winter image, while the field data did not contain the data for that species.

The short time, in which the forests were easily accessible, was in late spring to early summer, before the vegetation reached high densities. After evaluating the plot of site 1, which was not representative for the whole imaged site, the methodology was modified to conduct the field survey for the whole rest of site 1. Gathering data for all other sites were done with the same style. The proposed methodology for conducting field surveys included a point map, which was generated, without intensive and detailed tree location measurements. That allowed gathering more information about tree species, necessary for high precision image analysis. The combination of the field maps with orthomosaics in GIS applications, especially winter orthomosaics, was relatively fast and produced accurate maps of the forest with geolocated trees. This combination increased the precision to digitalise field data.

4.1.4.2 Tree species distribution

In this chapter the distribution of some of the occurring tree species will be discussed, as a discussion of all tree species would be out of the scope for this study.

A dominant tree species of the riparian forests is *Pterocarya rhoifolia*. The species was distributed in all the studied Riparian sites and even occurred close to the river in sites 3, 5, 8, 11 and 12. The species is known for their distribution in cool temperate riparian forest of Japan. [Sakio et al. \(2002\)](#) explained that the species occupies a broad ecological niche and can grow up to 30 m. In site 1, the species occurred as a monoculture, which happens often according to [\(Ohno, 2008\)](#), as they prefer to grow in even-aged forests. The species were mainly found along the river, where most disturbances affect growth, but the well-adapted reproduction mechanisms of the tree allowed quick recovery after changes ([Sakio et al., 2002](#)). Additionally, *Pterocarya* trees have high physically and eco-physiologically tolerances when rocks and stone are accumulated as disturbances take place ([Suzuki, 2002](#)).

Riparian sites two kind of *Salix* species were identified in YURF, *Salix jessoensis* and *Salix serissaefolia*. (Niiyama, 1990) pointed out that these species often co-exist with several other *Salix* species. *Salix* exclusively grew in areas close to the river, in areas where the soil was water saturated, but always in mixed conditions (Niiyama, 1990) or in open floodplains. Their reproduction mechanism is well-adapted to floodplain areas, because they spread their seedlings with water and can grow well under moist conditions. Azami (2004) explained that *Salix* are pioneer species after snow melt, since seeds spread that way. On the other hand, growing tall is more difficult for them; an effective growth of *Salix* can be provided when they grow on sandbars with high soil moisture contents.

Also, the deciduous tree *Juglans ailantifolia* prefers forest areas with high water content. *Juglans ailantifolia* trees often dominate riparian areas, because their seeds can be spread fast by animals like squirrels and rodents. Animals can carry the seeds or nuts of walnut trees with a high density in up to 25 m distance (Goto and Hayashida, 2008). Furthermore, they can carry the seeds in all directions, along the river or up the slopes. *Juglans* preferentially grow in floodplains, however, in too moist conditions, *Juglans ailantifolia* trees do not grow well. This can be seen in site 6 for example, where there are no trees found in the moist depression. In YURF they were also distributed on the Terrace sites and even in dryer Slope sites showed their potential to adapt to different kinds of environments. There was a dominance of *Juglans ailantifolia* trees observed in the Riparian sites, even more in the Terrace site, as well as a gradual decrease with increasing elevation. Nuts were usually buried before heavy rain falls and snow melt, disturbing riparian areas (Goto and Hayashida, 2008). Therefore, the seeds are resistant to these kinds of disturbances. It was found out that *Juglans ailantifolia* distributions are less affected by elevation, however Riparian and Terrace sites seemed to be the preferable sites. *Juglans* is more affected by competition and soil conditions (Goto and Hayashida, 2008).

Aesculus turbinata is a tree species, which was found as small trees between *Juglans ailantifolia* and *Pterocarya rhoifolia*, but also as tall grown trees, preferentially in lower slope areas. The species is an example of a tree that can ideally survive in gaps, whereby light conditions are the driving factor for the survival of seedlings (Hoshisaki et al., 1999). The species prefers low-density forest areas and moist soil conditions. The distribution of the seeds is similar to *Juglans ailantifolia* trees, as nuts are carried by animals along rivers, but also up the mountains, up to 114 m, found in Hoshisaki et al. (1999). The tree species is characteristic for riparian areas, but in YURF the tree was found in higher areas, mainly Terrace sites, while it occurred less frequent in riparian areas. A reason might be that the competition in riparian areas is too high, better adapted tree species like *Salix*, *Pterocarya rhoifolia* and especially *Juglans ailantifolia* dominated most of the Riparian sites.

Acer mono maxim is a tree species that was found in slope areas, even though the species was characterised as riparian forest species (Masaki et al., 2005). They pointed out that the species needs a good water supply and high litter-fall to survive during the juvenile stage. *Acer mono maxim* is strongly depended on pollinators to produce enough seeds for the spreading of the species, which is supported when the species occur in dense stands. When the species grew in mixed and dense forest areas, the seeds usually grew smaller, because of increased competition (Shibata et al., 2009). The growth and survival of the trees is higher in riparian forests than on Terrace sites, according to Masaki et al. (2005). The observed pattern of the species distribution in YURF is in Slope sites preferentially closer to water areas, and most of the time in denser clusters of several trees. It did not grow in Riparian sites, which might be due to the competition with *Juglans ailantifolia* and *Pterocarya rhoifolia*, which occupied the largest area. Small leaved *Acer* occur in the same regions, distributed under closed canopies because of their high shade-tolerance and their strong seedlings growing in small canopy gaps. Their main occurrence along the bottom of the slopes can be explained by their dominance in intensively disturbed areas, as erosion occurs debris flow disturb these areas frequently (Suzuki, 2002).

Another tree species is *Magnolia obovata*, which occurs usually in low numbers and densities in forests mainly composed of one dominant tree species, like *Fagus crenata*. As observed in this study, Isagi et al. (2000) stated that *Magnolia obovata* occurs mixed with *Cornus controversa*, *Aesculus turbinata* and *Pterocarya rhoifolia*. Also, the authors stated that the species occur in low densities, but are important for the structure and diversity as they dominate areas of the forest, as they grow in clusters. The clustering occurs because pollen grains have a limited distribution around the source, so they usually grow close to their adult tree. The tree species prefers moist and organic rich soils, with high intolerances for poor soils, in sun or partially shaded forest areas (weblink: Missouri Botanical Garden). The tree is a species, which can occur in riparian forests, but the most probably poor soil conditions and the dominance of *Juglans ailantifolia* trees in areas with good soil conditions are the main reasons for the occurrence of the species in slope areas. Suzuki (2002) characterised the soil in riparian areas as unstable with stony sediment structures and shallow organic layer, which is non-preferential for *Magnolia* trees.

Quercus mongolica is one of the dominant tree species in cold temperate forests. The species needs large areas to regenerate, which means that dense areas with a lot of understory vegetation and bamboo harm growth (Suh and Lee, 1998). For a good spread the trees need to produce many acorns, so that animals can spread them (Fujita and Sano, 2000). When the species is established, it grows fast and usually taller than all other trees. Dolezal et al. (2007) concluded that *Quercus mongolica* is significantly influenced by their neighbours and reduces its growth when competition increases, it is also affected soil water deficiencies (Masaki et al. 2005). The benefit of the tree is that they fruit from

an age of 26, while *Fagus crenata* e.g., fruits from an age of 40. This allows *Quercus mongolica* trees to spread faster after disturbances and establish a dense forest, before competition becomes strong (Fujita and Sano, 2000). The species is also known for their competitiveness with *Fagus crenata*, but there is less competition with other species because of the high shade and snow tolerances of both species (Suzuki, 2002). The distribution of *Quercus mongolica* is mainly in slope areas, where they grow as single trees or in groups. In YURF, the number of individuals was high, but heterogeneously distributed in the different Slope sites. It could be observed that they preferentially occurred in areas with lower forest density and seemed to be less frequent in dense areas. In comparison to species like *Magnolia obovata*, the species was less dominant and occupied smaller basal areas.

Fagus crenata is like *Acer mono maxim* a shade-tolerant species and prefers areas with high litter fall, but grow preferentially in slope areas with cooler climate conditions (Masaki et al., 2005). *Fagus crenata* trees are almost uninfluenced by topography and seem to be less affected by water deficiencies or light conditions, according to Masaki et al. (2005), because they produce long roots. Precipitation in winter, warmth index and the temperature of the coldest month contribute the most to the distribution of the species, while topography and summer precipitation can be influential on a regional scale (Matsui et al., 2004). Another benefit for the species is that their stems grow straight, even with deep snow covers, increasing the chance to survive in winter. *Fagus crenata* was found in the Slope sites, whereby most of the trees were small, most probably because the elevation of the mountain was still low. The tree adapted well to colder climate regions and must compete intensively with better adapted trees in the lower mountain regions.

All species information in combination with species distribution maps, density maps and count maps of several regions allowed an evaluation of stand conditions and species behaviours in different kinds of forest ecosystems. With the small amount of gathered data, it can be explained that a high number of *Fagus crenata* trees occurred, due to their characteristic shade-tolerance, but they were rarely visible in the orthomosaics because they only grew small. The dominance of *Juglans ailantifolia* trees was based on their high seed spread and climatic tolerances. The species occurred in all sites, while it only gradually disappeared in higher altitudes. This dominance, together with *Pterocarya rhoifolia* (both species grew fast and built large canopies) might be the reason, why *Aesculus turbinata* was rare in Riparian sites and mainly occurred in lower elevation slope areas, as there seemed to be more open spaces and good soil conditions.

Extensive analyses could be performed, when, additionally to tree distribution, soil samples or water measurements would be performed in areas. Therefore, image analysis or even automatic classification can be the basis for focussed and precise forest investigations, which would help to understand the forest and its species on a single tree, stand, regional or even global level.

4.1.4.3 Forest structure

The forest layer structure of all sites was found to be different. There were no trends observed when Riparian, Terrace and Slope sites were compared. There was a smaller number of shrubs identified in the Slope sites, which was most probably the result of the difficult access to the sites. Field work in site 3 was comparably easy, as there were several flat areas or slopes with lower degrees; hence many shrubs were identified. Only the bottom parts of the slope in site 8/9 were considered to classify shrubs, resulting in only 1.8 %. Site 10 had already steep slopes at the bottom of the site, so that only trees of the understory, subcanopy and canopy layer were identified. This was acceptable in the study, as the main purpose of the field work was to gather ground truth data. The images, taken from above, usually could not image shrubs or understory vegetations, as they were covered by the trees of the canopy and subcanopy layer.

While the canopy layer was usually composed of several tree species, the number of understory layer trees and shrubs was small. The reason might be that shrub grew in large clusters consisting of several individuals, which was similar to the understory trees, whereby usually one *Acer* species and one *Sorbus* species were dominant per site. The exposition of the slopes, soil conditions and the distribution of canopy layer trees had a significant influence, too. Especially tall trees produced large shadow areas, which decreased the available light for subcanopy trees and shrubs.

The high number of shrubs in site 7 was most probably a consequence of the forest road. Understory and shrub vegetation were mainly identified along the bottom of the slope towards site 13, which was mainly open and under full light conditions. The slope was steep and mainly shrubs like *Alnus fauriei* and small trees like *Acer palmatum* grew under these conditions. In contrast, the centre of site 7 did not contain these shrubs and small trees. Instead, young trees of *Pterocarya rhoifolia* and *Juglans ailantifolia* trees grew there. Another different example was site 11, with a high number of understory tree species. The site contained a high number of *Sorbus alnifolia*, *Acer palmatum* and *Camellia japonica*, which were distributed along the bottom and the steeper parts of the slope, where tall trees were rare. Also here, shrubs were dominant when the area was open and steep slopes benefit the light condition in the site. Furthermore, it could be observed that shrubs and understory vegetations occurred only in open or partly canopy-covered grounds. Consequently, when the canopy was dense, few or no shrubs grew. While the understory vegetation had a similar ratio along the sites, with around 20 %, shrub vegetations were rare in Riparian sites. One reason was that those sites were located near the river, having high soil moisture. There were different bamboos and grasses, which covered most of the area and therefore decreased the area for identified shrub species. Especially sites 1, 6 and 7 were affected, while in some areas of site 1 and site 4 those plants did not grow. These areas were in higher elevations; the soil moisture must have been lower, so that the bamboo and grasses could not

grow. Areas, which were still close to water sources and locations in lower altitude areas seemed to be the best places for shrubs and understory layer trees.

Furthermore, with increasing elevation, only *Acer* species occurred in slopes, while all other tree and shrub species disappeared. Especially, the small-leaved *Acer* species seemed to be better adapted to shady conditions, as already pointed out by [Lei and Lechowicz \(1990\)](#). *Acer* trees were usually smaller when they were located in shady areas, while they grew tall, when there was more light available. This was discussed in the study of [Kneeshaw et al. \(2006\)](#). [Hedwall et al. \(2018\)](#) already pointed out, that the occurrence of shade-tolerant species is often a result of life-form-specific responses, species use to enter niches in forests. The study of [Woods and Turner \(1971\)](#) explained that stomatal responses of species like *Acer* or *Quercus* are good for shaded conditions. This could explain the growth of several *Acer* species and also *Quercus mongolica* in Riparian sites. In comparison, *Sorbus* species were some of the species that disappeared towards the Slope sites. A study of [Pyttel et al. \(2013\)](#) indicated that the studied *Sorbus* species had significantly reduced height and growth under shaded conditions, but the main factor for species thinning might be the increasing competition and stresses in slopes. At the same time the number of tree species belonging to the canopy layer increases ([Giertych et al. 2013](#)).

Young trees, which are part of the understory vegetation, were mainly found in Riparian sites, next to water channels, as well as at the bottom of slopes. These areas suffer from disturbances, like erosion, debris flows and flooding. When those events happened, niches were created in the forest and seedlings had enough space, light and less competition to grow. Disturbances mainly benefit *Pterocarya rhoifolia*, *Juglans ailantifolia* and *Robinia pseudoacacia* trees, as these species had young trees in sites 1, 6 and 7. Additionally, in site 1 were two patches with monocultures of *Pterocarya rhoifolia*, where shrubs and understory vegetations were rare. A similar structure was observed in monocultures of *Cryptomeria japonica* plantations. Hence, monocultures must have a significant influence on soil conditions, available nutrients and light availability, so that shrubs do not grow well. In the study of [Spanner et al. \(2007\)](#), where they analysed reflectance of the forests and found in open stands broad-leaved plants, shrubs and grasses, while closed canopy areas only signals of forest litter were found. [Hedwall et al. \(2018\)](#) pointed out that monocultures have a significant effect on light conditions, soil nutrients and available water. As *Pterocarya rhoifolia* grows large canopies, shadowing the whole forest floor and reducing light, this might be the main reason why no understory and shrub vegetations grew in these patches.

The percentages showed that more trees in the canopy layer resulted in general in fewer trees in the subcanopy layer, which was observed in the Riparian sites. In the Slope sites the percentage of trees belonging to the subcanopy layer was high, while the percentage for trees of the canopy layer was low. The slope angle might cause that small growing trees could be located at the same height or even

higher because of the elevation of the slope. This benefits species like *Betula*, which are light demanding, but usually smaller than *Quercus mongolica* or *Fagus crenata* (Giertych et al., 2013). The varying tree numbers, belonging to canopy and subcanopy layers in the different sites, were also described in the study of Gomes da Silva et al. (2008). The authors concluded that structures in canopy and subcanopy individuals were influenced by light and moist conditions, but also from mainly edge effects and topographical gradients, as also pointed out by Svenning et al. (2004).

The structure of forests can be regarded as a combination of disturbances, competition and stand conditions, which influences the occurrence of tree species, their location and distribution. First, disturbances can open niches, spaces for sunlight and nutrients to increase plant growth. Second, depending on which factors influences the site conditions the most, tree species can survive in the environment. And third, depending on the competition between tree species, some survive and some grow even tall. The interactions between physical and physiological properties of forest environments and tree species need to be studied further on a large scale to explain forest ecosystems.

4.1.4.4 Forest classification

In the chapter 3.2 Japanese forests, it was already mentioned that forest inventories, conducted in Japan, provided detailed information about forest plantations, but missed to provide forest classifications of mixed broad-leaved forests (Makimoto, 2019). When forests were classified, usually only *Fagus crenata* and *Quercus ssp.* were mentioned (Makimoto, 2019). Other studies like Fukamachi et al. (2020) studied cold-temperate forests and identified dominant species, but they did not classify riparian forests more specifically. The results of the current study analysed the relative density of tree species and proceeded to classify those forests. The relative densities were calculated based on tree counting, done in the field. Additionally, species of the shrub layer were not considered for the classification of mixed forests. Their contributions to the functions of the ecosystem are definitely interesting, but they do not affect forests that much that they need to be part of the classification.

The Riparian sites showed different tree species densities and dominances. In site 1 *Pterocarya rhoifolia* and *Juglans ailantifolia* were the dominant species, followed by *Acer sieboldianum* and *Tilia maximovicziana*, which were considered as subspecies. Therefore, the riparian forest was called 'Japanese walnut and wingnut mixed forest', with the subspecies Japanese lime and Siebold maple. Site 4 was a 'willow and walnut forest', with the subspecies *Pterocarya rhoifolia* and *Aesculus turbinata*. The understory vegetation was dominated by *Acer palmatum* and *Styrax obassia*. The dominant tree species in site 6 was *Acer palmatum*, which was mainly distributed along the slopes and dominated the understory layer. Therefore, the forest was classified as 'Japanese walnut and wingnut forest', with

the subspecies *Salix jessonensis* and *Robinia pseudoacacia*. Site 7 was a 'Japanese walnut forest', with the subspecies *Pterocarya rhoifolia*. The understory vegetation was dominated by *Acer japonicum* and *sieboldianum*.

The Terrace sites showed a colourful mosaic of tree species dominating the sites. *Juglans ailantifolia* was the dominant canopy species in all sites; hence they were all named as Japanese walnut mixed forests with changing subspecies. In site 11 the subspecies were *Pterocarya* and *Aesculus turbinata*, with *Acer amoenum* and *palmatum* dominating the understory vegetation. Site 12 was similar, except that *Quercus mongolica* occurred additionally as subspecies, while *Acer amoenum* was replaced by *Morus australis*. In site 13 the subspecies were *Cornus controversa*, *Acer mono maxim*, *Aesculus turbinata* and *Magnolia obovata*. *Acer sieboldianum* dominated the understory vegetation.

In comparison to the Terrace and Riparian sites, *Acer* species grew taller and were even dominant in large parts of the Slope sites. As the species were found frequently distributed over the whole sites, they were named after them. Therefore site 3 and 8/9 were 'maple forests', mixed with Japanese walnut and oak in site 3, and only with oak in site 8/9. The subspecies in site 3 were *Fagus crenata*, *Larix kaempferi* and *Magnolia obovata*. The subspecies in site 8/9 were *Fagus crenata*, *Corylus sieboldiana*, *Acer mono maxim* and *Styrax obassia* (as the species occurred here as subcanopy trees). The forest in site 10 was classified as 'Oak forest' mixed with *Aesculus turbinata*, *Fagus crenata* and *Acer mono maxim*. *Acer palmatum* or *sieboldianum* dominated the understory vegetation in all sites.

With greater distance to the river vegetation changed from trees, well-adapted to riparian forest sites, over a tree mixture of riparian and slope species in the Terrace sites, *Quercus mongolica* and *Fagus crenata*, dominating the Slope sites. Therefore, the Slope sites were already representative for *Quercus* forests in Japan, as described by Okitsu (2003) or Sasaki (1970). The general species composition in YURFs Slope sites with *Fagus crenata*, *Acer mono maxim*, *Acer sieboldianum*, *Tilia japonica*, *Quercus mongolica*, *Kalopanax septemlobus*, *Acer rufinerve*, *Magnolia obovata* and *Sorbus alnifolia* would be also characteristic for a Japanese *Fagus* forest, according to Sasaki (1970).

4.1.4.5 Comparison of different riparian and mountain forests in Japan

There were a couple of studies performed in riparian forests in Japan, which were discussed in this chapter in order to understand the structure, composition and distribution of the Riparian sites in YURF.

Fukamachi et al. (2020) studied a cold-temperate forest, like YURF, at the upper Watarase river basin in Midori City (Gunma Prefecture). The precipitation is lower than in YURF with only 1807 mm per year (300 mm snow precipitation). The dominant species, which they found in valley bottom areas are *Fraxinus platypoda* and *Styrax obassia* and with *Quercus mongolica* and *Castanea crenata* on Slope

sites. [Fukamachi et al. \(2020\)](#) monitored 600 individual trees from 2006 to 2017 in a 1 ha plot, which belonged to 85 deciduous species. In YURF sites, the numbers of individuals were lower, as a 3-ha plot had only around 400 trees. Furthermore, only 70 different species were identified in all sites, Riparian, Terrace and Slope. Another study was conducted by [Sakio et al. \(2002\)](#) in cold temperate riparian forest in Ooyamazawa in the Chichibu Mountains. They investigated a 4.71 ha study site, finding 46 tree species and a total number of 2144 trees, from which 492 trees belonged to the canopy layer. The number of trees in Ooyamazawa was higher than the highest number found in YURF, site 1 with 729 trees, whereby 410 trees corresponded to the canopy layer. [Masaki et al. \(2008\)](#) used census methods to evaluate their studied plots in riparian area and Terrace sites. In the Riparian plot they identified *Cercidiphyllum japonicum* (26 %), *Aesculus turbinata* (19 %), *Fagus crenata* (15 %), *Quercus crispula* (13 %), *Pterocarya rhoifolia* (9 %), and *Acer mono maxim* (8 %) based on the total basal area at breast height. The study of [Sakio et al. \(2002\)](#) found that 61.6 % of their studied forest trees were *Fraxinus platypoda*, 16.2 % *Pterocarya rhoifolia* and 10.0 % *Cercidiphyllum japonicum* with *Acer species* being the dominant subcanopy species. The presented counting and species showed that riparian areas in Japan have completely different characteristics. [Ohno \(2008\)](#) characterised valley-bottom forests on the Japan Sea side of northern Honshu and compared them with *Salix* riparian groves and *Alnus* swamp forests. The valley-bottom forests were located in the area of Mt. Gassan in Yamagata Prefecture. The dominant species were *Pterocarya rhoifolia*, *Aesculus turbinata* and sparsely *Cercidiphyllum japonicum*. *Fraxinus platypoda* and *Pterocarya rhoifolia* seemed to be species which occurred frequently in forests, *Pterocarya rhoifolia* grew also in the YURF study sites, together with *Juglans ailantifolia*. *Juglans ailantifolia* trees were not found or studied in other regions, while it was the dominant tree species in the YURF study sites. Furthermore, in the studies of ([Masaki et al., 2008](#); [Fukamachi et al., 2020](#); [Sakio et al., 2002](#)) a high dominance of *Quercus crispula/mongolica* was found. As the species also occurred in Slope sites in YURF, it was characterised as dominant species. Another similarity was the occurrences of *Acer species*, which were also dominant in ([Sakio et al., 2002](#)). It was pointed out by [Ohno \(2008\)](#) that all forests were significantly different in their conditions and therefore their structure, which was also concluded for the sites in YURF.

[Sakio et al. \(2002\)](#) discussed that the coexistence of tree species in riparian forests depends on niche- and chance-determined causes, due to varying disturbances, which fits well to the findings of the sites in YURF. Tree species growing in such areas are generally well-adapted to the varying conditions in riparian forests. [Naiman et al. \(1998\)](#) explained that plant colonisation and the initial stage of tree growth starts in new open spaces caused by disturbances. After the free space is occupied only trees survive, which have a competitive advantage. In a next stage trees fertilise the soil and enable the growth of understory vegetations to develop finally a complex forest structure. Due to past flooding

events and other disturbances in YURF explained this study well the characteristics of the researched riparian forests.

Masaki et al. (2008) explained the species distribution based on different soil preferences during the juvenile stage of the trees. Additionally, under stable microtopographic conditions, species richness was the highest, while only adapted trees grew well under unstable conditions. The trees which seemed to grow the best under unstable conditions were *Pterocarya rhoifolia* and *Robinia pseudoacacia*. Both trees grew in areas with the most unstable conditions, affected by regular flooding and poor soil conditions. Even juvenile trees of these species grew well over the observed time, other species did not reproduce.

Sakio et al. (2002) further pointed out that the coexistence, reproduction strategies and the relation to the disturbances is not sufficiently investigated, especially riparian forests, as the mentioned studies showed clearly, can have many different structures and compositions. The aim should be to compare more riparian areas to understand those ecosystems better. To study tree species compositions and species diversity, discussions with a dependency on spatial scales, stand-levels and landscape-levels, need to be started (Masaki et al., 2008), for which larger study areas need to be considered, together with a fast and efficient surveying methodology.

4.1.5 Conclusion

Forest inventories are an efficient tool to assess forest composition, distribution and structure and allow analyses of dominances, diversity and layering. 70 tree and shrub species were identified and their characteristic distribution in the sites was analysed. The layering in the forest was assessed and presented, representing the vertical structure of the forest. Field surveys were generated and based on the calculated dominances mixed forests were classified. The forests were named after the main species with adding the subspecies to further characterise the sites, as it was found out that even though sites were classified into Riparian, Terrace or Slope sites, the sites had all different compositions. Also, the presented forest sites were classified as different to other riparian and mountainous forests in Japan.

Chapter 4.2 Tree species diversity in different kind of cold-temperate forests calculated on image-based analysis

4.2.1 Problem definition

Differences in biodiversity further affect ecosystem functioning, because they influence biomass production, nutrient cycling and health conditions (Baeten et al., 2013). The functioning of forest ecosystems is important for their several ecosystem services, including the human well-being. Keeping forests stable in changing climatic conditions is a challenging topic nowadays.

Species numbers differ not only on a global scale, because of climatic conditions, but also on a local scale, because of microclimate, disturbances, competition and local interactions between tree species (Ricklef & He, 2016). Species richness is an indicator for the biodiversity and therefore for the health and natural status of forests. It reflects characteristics of the location and the potential climate or anthropogenic disturbances. Species production, extinction and dispersal are influenced by physical conditions of the environment, which can vary significantly, as in this study riparian and slope forests were studied. Further adaptation to the environment and reproduction strategies are critical aspects in species settlements. In high diverse systems, positive interactions between species results in an efficient use of resources, like light, nutrients or water (Jacob et al., 2009). The numbers of biotic and abiotic factors, which influence species compositions, are huge and need to be considered when forest ecosystems are studied. Ricklef and He (2016) pointed out that there are many diversity studies conducted on local communities with extents over a broad range of global climate conditions. At the same time, local communities are often undercounted, since ancient records were used. This problem affects the analysis of local environments significantly. Baeten et al. (2013) raised the limitation of diversity studies as they were conducted in small plot sizes, simplified age-structures and stand-structures, since the works had always limitations in time and man-power.

The analysis of forest stands in YURF introduced the comparison of four Riparian sites, three Terrace sites and six Slope sites under the same climatic conditions, but with different expositions and slope angles. Species richness could be analysed in a stable physical environment, with less varying influence factors. The results could be then analysed more specifically, regarding small-scale influences, species interaction and competition aspects. This study helped to better understand the composition of tree species in the different stands. Therefore, the objective for this study was to evaluate forest diversities with tree species composition information extracted from images:

- ii. Analyses of standard forest diversity measures using image classifications
- iii. Assessing the comparability of diversity indices for different sites

4.2.2 Methodology

4.2.2.1 Data collection

In this study images were collected for 13 different sites in four seasons from summer 2018 until winter 2021, in total 295 times. Out of this large data base images from summer 2019 were chosen for the first set of tree species annotations, for each site one flight. For sites 1 and 3 the flights on the 20th of June 2019 were chosen, for sites 9 and 10 the 10th of July and for site 8 the 26th of July. For all other site's images taken on the 14th of June were used. Data collection was performed with a DJI phantom 4 flying in altitudes between 80 m and 205 m.

4.2.2.2 Data processing

The gathered images were first processed with Metashape, where all images per site were aligned. The aligned orthomosaics and DEMs, which represent the 3D surface in a 2D map, contained height information of the imaged area. Then, GIMP was used to do manual annotations. The orthomosaics were opened with the software and layers were added on top of it, one per tree species. The canopy each tree species was coloured black in its layer, while the rest was coloured white, therefore binary layers were generated. Additionally, tree tops were annotated by marking the tree tops with a black dot. All layers and the orthomosaic were afterwards exported as JPEG files.

Another aim of the study was to compare different locations. Therefore, the sites were divided into Riparian and Slope sites. Sites 1, 4, 6, 11, 12 and 13 were grouped as Riparian sites based on the occurring tree species, while sites 2, 3, 5, 8, 9 and 10 were considered as Slope sites. Note that only in this chapter sites 11, 12 and 13 were grouped into the Riparian sites.

4.2.2.3 Image analysis

4.2.2.3.1 Census code

The Census code is a developed code of the research team, which used the exported binary files from GIMP, the orthomosaic and file containing the path to the data, the name of the data files and the count of the files. On that basis, the code scanned tree tops and checked to which layer the tree tops belong. The output contained the name of the species, the counted tree tops, the percentage of the tree tops belonging to this species and the total number of counted tree tops.

4.2.2.4 Species diversity

Species diversity is an important measure for biodiversity of different ecosystems. Species abundances and richness are considered to quantify diversity, which is reflected in the Shannon index. Furthermore, the Simpson index is considered in this thesis, as it can be used as a measure for species dominance, while the Shannon evenness considers the evenness of species spreads. Another measure is the Gini – Simpson index, which is supposed to show dominances clearer than the Simpson index according to Ifo et al. (2016). These values were calculated for each site and species identified on the images.

The first step was to calculate p_i for all species. Therefore, the numbers of tree counts were divided by the total numbers of tree counts per site. In a second step the Shannon entropy for each species and site was calculated with the following formula:

$$\text{Shannon diversity } H = -1 * \sum_{i=1}^n (\ln(p_i) * p_i)$$

The mean values for each site were calculated for all sites but also separately for all Riparian sites and Slope sites. The total alpha diversity was calculated by summarizing the Shannon diversity or Shannon entropy per site. From the sum of the alpha diversity the Hill numbers were calculated with the following equation:

$$\text{Hill } ^1D = e^H$$

The Simpson index was calculated by:

$$\text{Simpson } D = \sum_{i=1}^n p_i^2$$

Furthermore, the Gini – Simpson index, the Shannon evenness and the 2D Hill numbers were calculated:

$$\text{Gini Simpson} = 1 - D$$

$$\text{Evenness} = H/\ln(S)$$

$$\text{Hill } ^2D = \sum_{i=1}^n (p_i^2)^{\frac{1}{1-2}}$$

With S being the species richness, the occurring species per site and n the number of species.

Furthermore, the similarity was calculated with p_i previously calculated. A site-per-site comparison was performed, sites 1 and 4, sites 1 and 6, sites 1 and 7 etc. The sites were separated in Riparian and Slope sites and separately compared. The following two calculations were performed for each cell in the comparison table:

$$X = \frac{p_i(\text{site } a) * \text{weight factor of site } a + p_i(\text{site } b) * \text{weight factor of site } b}{\text{weight factor of site } a + \text{weight factor of site } b}$$

$$Y = -\ln(X) * X$$

The weight factor was 100 divided by the number of sites, which was 14.2857 for the Riparian sites and 16,66667 for the Slope sites. In the last calculations the alpha, beta and gamma diversities were calculated.

$$H_{\alpha} = \frac{H(\text{site } a) * \text{weight factor site } a + H(\text{site } b) * \text{weight factor site } b}{\text{weight factor site } a + \text{weight factor site } b}$$

$$H_{\gamma} = \sum_{i=1}^n Y$$

$$H_{\beta} = H_{\gamma} - H_{\alpha}$$

$$Horn = \frac{\ln(2) - H_{\beta}}{\ln(2)}$$

The Horn value is a measure for the similarity and was presented by Goebel (2012a).

4.2.3 Results – Diversity

The most important terms in the concept of diversity are richness, abundance and evenness. Richness is the number of species in an ecosystem. Species abundance is the number of trees, which belong to the same species, while relative abundance means the distribution of trees in the community. The relative abundance is also called evenness. The combination of richness and evenness gives the true diversity (Hill numbers), which is needed to evaluate the diversity of an ecosystem, as forest ecosystems have usually heterogeneous distributions. In this study, several indices were calculated by checking the tree species richness, abundance and evenness, in order to provide an overview of the diversity.

Image-based counting of tree species were performed (Table 8) and diversity calculated (Table 9). The species richness corresponds to the different tree species in each site. The highest number of tree species had site 3 with 24 different tree species, while site 11 had the lowest, with 12 tree species. The mean of all sites was 17.2 tree species per site. Shannon entropy, Simpson and Gini – Simpson indices gave an idea about the evenness and diversity of the sites. In case of the Simpson index, a value of 1 means that all individuals belong to the same species (no diversity) and a value of 0 means that the diversity is high. The mean value for the Riparian sites, and also for the mountainous sites, is 0.21.

Table 8 Image-based tree counting

Tree species	Species label	Site1	Site4	Site6	Site7	Site11	Site12	Site13	Site2	Site3	Site5	Site8	Site9	Site10
Juglans ailantifolia	S01	107	58	47	72	54	91	106	23	53	47	32	7	14
Aesculus turbinata	S02	24		4	3	26	31	10	35	3	18	8	30	29
Cryptomeria japonica	S03	201	129	156	55	125	73	229	195	122	51	7	53	74
Pterocarya rhoifolia	S04	125	9	25	22	31	29	2	3	3	14	1		
Quercus mongolica	S05	9	7	3	13		12	2	45	66	53	42	51	51
Larix kaempferi	S06	19	7			1	1			27				
Fagus crenata	S07									27	4	1	53	10
Magnolia obovata	S08	19	6	5	1	6	7	17	63	32	42	7	22	35
Acer japonicum, Acer sieboldianum, Acer palmatum	S09	145	12	10	67	36	144	60	351	605	176	241	140	167
Prunus salicina Lindley, Prunus serrulata/grayana, Prunus speciosa	S10	13								3				4
Acer mono maxim, Acer pictum subsp. Mono, Acer nipponicum	S11	15	1	5	16	16	38	21	63	75	52	38	169	88
Salix serissaefolia	S12		78	8						1				
Salix jessoensis	S13	8	1	16	14					2	3	1		
Castanea Crenata	S14	4		10						4	1	2		1
Robinia pseudoacacia	S15	14		7	14									
Cornus controversa	S16	23	2	5		9	21	22	7	17	13	14	24	16
Phellodendron amurense	S17	9												
Betula corylifolia	S18			6					2			13	45	13
Alnus inokumae, Alnus hirsuta	S19			1										
Picea abies	S20			4										
Cercidiphyllum japonicum var. Magnificum	S21		2											
Albizia julibrissin	S22				2									

Japanese Hydrangea, Schizophragma hydrangeoides and Smilax	S23	13	12	9	1	5	17	26	2	14	17	15	8	5
Morus australis	S24		1				14	2	6	7		14	6	8
Clethra barvinervis	S25				1									
Tilia japonica, Tilia maximowicziana	S26	28				2	9	1	4	7		3	7	19
Japanese honeysuckle/Lonicera japonica	S27						4	15		2	12	2	4	1
Kalopanax septemlobu	S28						3	3		1	4			13
Celtis jessoensis	S30			2		3	5							
Alnus fauriei	S31				20		4	8		19				
Betula corylifolia	S32		1											
Zanthoxylum piperitum	S34			5										
Fraxinus lanugiosa	S35									3				
Fraxinus mandshurica var. japonica	S36				1									
Styrax obassia	S39						1	1	6	4				3
Hamamelis japonica	S40							3	10		4	33	30	30
Acer japonica (red)	S41									1				11
Corylus sieboldiana	S42	5									6	18	1	4
Carpinus Cordata	S43	2								14		16	14	
	mix								2				53	
	Sum	783	326	328	302	314	504	528	831	1098	515	508	717	596

When the location of the mountain sites and the Simpson indices were compared, it was evident that in lower elevation areas the Simpson index was higher (site 2, 3 and 8) than in areas located higher in the slopes (site 5, 9 and 10). There was no trend visible for the Riparian sites. Therefore, the diversity seems to be the highest in sites 9 and 10, with 0.13 and 0.14 respectively, and the lowest in site 3 with 0.33. However, (except site 9) the species richness was in these sites higher than in all other sites. The Simpson index alone cannot explain the diversity of the sites well.

A high diversity is also equal to a high value for the Shannon index. The Shannon index for the studied sites was high with a value > 2 . The index was usually higher for the mountain sites than the Riparian sites. The same behaviour was observed for the Gini – Simpson index. The values of the Gini – Simpson index were around 84 % for site 1, 7 and 12 (Riparian sites) and values between 83.3 % and 87.5 % for the mountain sites (5, 9 and 10). Generally, the Shannon entropy and the Gini – Simpson index values showed the same range. Only site 3 was different, having the lowest Gini Simpson value and the second lowest Shannon entropy (GS = 67.01 % and $H = 1.74$), while site 4 had a higher Gini – Simpson index with the lowest Shannon index ($H = 1.73$ and GS = 74.97 %).

The evenness value for site 3 was the lowest, while it was also low for sites 2, 4, 6, 8 and 13. Comparing all indices revealed that site 9 had a high diversity with an even distribution of tree species, followed by 5 and 7, then 1, 10 and 12. Sites 2, 4, and 11 had a lower diversity with an uneven distribution of species. Sites 6, 8 and 13 had a high diversity but an uneven distribution, while site 3 had the highest number of species and was highly uneven.

At last, the Hill numbers were calculated, which characterised the distribution of species when they were randomly picked. The values supported the previously mentioned distributions. The Hill numbers are a measure for the effective classes, which means that a randomly picked sample belongs to a certain number of different classes. For Hill 1D , the highest class numbers were found for sites 1, 12, 5, 9 and 10. For site 1 it means that out of the 19 species, 10 species are minor, since a randomly picked species belongs to a high probability to 9.43 classes. Therefore, the Hill numbers are another measure for the evenness. Compared with a species richness of 18, site 9 had the highest value with 10.71 and was considered as well distributed. A similar behaviour was found in site 7, with a species richness of 15 and a Hill number of 9.22. Sites 3 and 4 had the lowest Hill numbers compared with a species richness of 24 and 15, respectively.

The Hill numbers can be interpreted as representation of typical species ($q = 1$) and dominant species ($q = 2$). Based on this relation, half of the species were typical for sites 1, 5, 7, 9, 10, 11 and 12, while for all other sites the numbers were lower. For Hill $q = 2$, the dominant species, ranged for the

mentioned sites from 6 to 7 species, which was more than one-third of the occurring species. For all other sites, the number of dominant species ranged between 3 and 4 species.

Table 9 Calculated diversity indices for all sites

Site	Shannon entropy	Evenness	Simpson	Gini Simpson	Hill 1D	Hill 2D	Species richness
1	2.24	76.21	0.15	84.97	9.43	6.65	19.00
4	1.73	63.90	0.25	74.97	5.64	3.99	15.00
6	1.99	67.48	0.26	73.97	7.29	3.84	19.00
7	2.09	77.07	0.16	84.19	8.06	6.33	15.00
11	1.84	74.15	0.22	77.80	6.31	4.50	12.00
12	2.22	76.87	0.15	84.70	9.22	6.54	18.00
13	1.84	64.84	0.25	75.04	6.28	4.01	17.00
2	1.81	64.25	0.25	74.89	6.10	3.84	17.00
3	1.74	55.34	0.33	67.05	5.71	3.04	24.00
5	2.20	77.64	0.17	83.31	9.02	5.99	17.00
8	2.02	64.18	0.25	74.83	7.56	3.49	20.00
9	2.38	82.08	0.13	87.46	10.81	6.85	18.00
10	2.39	76.66	0.14	86.44	10.91	7.28	21.00

Table 10 presents the similarities calculated with the Horn values, presented by [Goebel \(2012a\)](#). The similarity values ranged between 90.11 % and 64.51 % for the Riparian sites and between 94.17 % and 68.23 % for the Slope sites. In case of the Riparian sites, site 11 had the highest similarity values, followed by sites 1, 12 and 13. The lowest similarity values had site 4, then sites 7, 1 and 11. Sites 1, 11, 12 and 13 had more similarities, which can be related to the site's characteristics, as these sites are distributed partly on the slope. Sites 4, 6 and 7 are flat sites along the river and had more similarities among each other than the Slope sites had. Site 1 has both characteristics, as it is located along the river but also partly on the slopes. When the similarity values were compared with the species composition, it was observed that the composition of sites 1, 11, 12 and 13 were more similar than others. All sites contain *Aesculus turbinata*, a high number of *Acer* trees and *Cornus controversa*. Site 4 has a high number of *Salix* trees, which do not grow that frequent in other sites. Site 6 has a high number of *Robinia pseudoacacia*, *Salix* and *Castanea crenata*, which was a unique combination for all sites, and in site 7 the open spaces between the trees allowed to detect *Alnus fauriei* shrubs, which grow usually beneath the canopy layer. All Riparian sites along the river have unique tree compositions, which decreased their similarity values. Still, the main composition was similar, as all sites have *Juglans ailantifolia* and *Pterocarya rhoifolia*, the two dominant species, together with *Cryptomeria japonica*.

Regarding the Slope sites, site 5 had the highest similarity values, followed by sites 10, 9, 8 and 2. The lowest similarity values occurred between sites 8, 9 10 and sites 2 and 3. Sites 2 and 3 are located close to the river and at the bottom of the mountain, while sites 5, 9 and 10 are located in higher elevations. As all sites were mixed, it can be said that they had some similarities and some differences. The similarity numbers compared with the distribution of the sites showed, that sites 2 and 3 share similar

distributions when *Juglans ailantifolia* trees, *Quercus mongolica* and *Acer* species were considered. Species like *Fagus crenata*, *Corylus sieboldiana*, *Hamamelis japonica* and *Carpinus cordata* occurred rarely. In sites 8, 9 and 10 the distribution of *Juglans ailantifolia* was less frequent, while *Fagus crenata*, *Corylus sieboldiana* and *Hamamelis japonica* occurred more frequent. All sites shared the occurrence of *Cornus controversa*, *Magnolia obovata* and climbing plants. Also, all sites had a high variety of *Acer* species, which were more frequent in sites 2 and 3, but less frequent in the other Slope sites. Even though *Cryptomeria japonica* is a planted tree, which usually frames mixed forests, they were still part of the orthomosaics. In sites 2 and 3, there were many *Cryptomeria japonica* trees, while there were fewer in sites 5 to site 10.

Table 10 Calculated similarities between all sites, divided into Riparian and Slope sites (Horn index)

Riparian sites			Slope sites		
Site a	Site b	Similarity in %	Site a	Site b	Similarity in %
1	11	90.11	5	10	94.17
11	13	89.49	9	10	91.02
11	12	87.82	5	8	90.83
1	12	86.22	2	5	89.61
6	11	84.89	8	10	88.63
12	13	84.81	3	5	85.89
7	12	83.12	2	3	85.02
1	7	82.60	5	9	81.92
4	6	81.31	3	10	81.58
6	13	81.27	2	8	80.59
1	6	80.87	8	9	80.08
1	13	80.07	3	8	77.75
7	11	78.97	2	9	77.37
4	13	77.02	2	10	69.41
7	13	76.76	3	9	68.23
6	7	75.02			
4	11	74.93			
1	4	70.57			
6	12	68.58			
4	7	64.51			

Table 11 to Table 14 show the alpha and beta diversities for the Riparian and Slope sites. Alpha diversities describe the diversity in one site, while beta diversity describes the differences in the diversity between the sites and gives insights into the relative abundance between the sites (Goepel, 2012b). The alpha diversity of the Riparian sites shows differences for all sites, it reflected the tree species composition, but in general all diversity values were high (above 1.7). There are no patterns or structures visible in this table, which allowed a deeper analysis. The values showed that sites 4, 11 and 13 had the lowest diversity, which influenced the comparison between the sites the most.

Table 11 Calculated alpha diversity for the Riparian sites

	Site 1	Site 4	Site 6	Site 7	Site 11	Site 12	Site 13
Site 1	2.24	1.99	2.12	2.17	2.04	2.23	2.04
Site 4	1.99	1.73	1.86	1.91	1.79	1.98	1.78
Site 6	2.12	1.86	1.99	2.04	1.91	2.10	1.91
Site 7	2.17	1.91	2.04	2.09	1.96	2.15	1.96
Site 11	2.04	1.79	1.91	1.96	1.84	2.03	1.84
Site 12	2.23	1.98	2.10	2.15	2.03	2.22	2.03
Site 13	2.04	1.78	1.91	1.96	1.84	2.03	1.84

In comparison to the Riparian sites, the diversity values for the Slope sites were also high, but there was a structure visible (Table 12). The diversity values of all Riparian sites were lower than the ones for sites 9 and 10. Performed field and GIS analyses showed that, with increasing site numbers, the steepness of the slope and the distance to potential water sources increased. The alpha diversity must have a strong influence on the evenness, which was higher in sites 9 and 10 than in sites 2 and 3.

Table 12 Calculated alpha diversity for the Slope sites

	Site 2	Site 3	Site 5	Site 8	Site 9	Site 10
Site 2	1.81	1.78	2.00	1.92	2.09	2.10
Site 3	1.78	1.74	1.97	1.88	2.06	2.07
Site 5	2.00	1.97	2.20	2.11	2.29	2.29
Site 8	1.92	1.88	2.11	2.02	2.20	2.21
Site 9	2.09	2.06	2.29	2.20	2.38	2.39
Site 10	2.10	2.07	2.29	2.21	2.39	2.39

The beta diversity matrices elucidated the differences or similarities between sites, considering alpha and gamma diversities, which was the pooled entropy of all considered sites. The minimum beta

diversity, with a value of 0, was unity, which means that the sites were completely equal (Jost, 2006). The higher the beta diversity value, the higher the differences between the sites. In both tables (Table 13 and Table 14) areas with the highest similarities in darker green colours or marked with a purple square. There were high similarities between the Riparian sites 11, 12 and 13, and for the Slope sites between sites 5 and 8 as well as between 9 and 10. The similarities, which were evaluated with the Horn index, can be also observed in Table 10. Comparing alpha and beta diversities can further help to understand the differences and similarities between sites. Site 10 had low beta values compared to sites 5, 8 and 9 (0.04, 0.08, 0.06), similar differences were found between site 5 and 2 (0.04), 8 and 10 (0.08) (Table 12). For sites 5, 8, 9 and 10 low beta values occurred together with high alpha diversities, while site 2 had the second lowest alpha diversity with 1.81, but high beta diversities with values between 0.13 and 0.22. Site 4 showed in comparison to site 1, 7 and 12 that high differences between alpha diversities (1.73 and 2.24, 2.09, 2.22) caused also high beta diversities values of around 0.25. Low differences in alpha diversities, comparing sites 4, 11 and 13, showed high beta diversities (0.16 and 0.17). Another example is site 6, where the beta value was 0.13 when compared to sites 1 or 4, whereby the alpha diversity of site 1 was 2.24 and 1.73 for site 4. Therefore, the calculated gamma diversities had an influence on the beta diversity. The gamma diversity calculated the sum of all species for the considered sites, which means that the number of occurring species influenced the beta diversity.

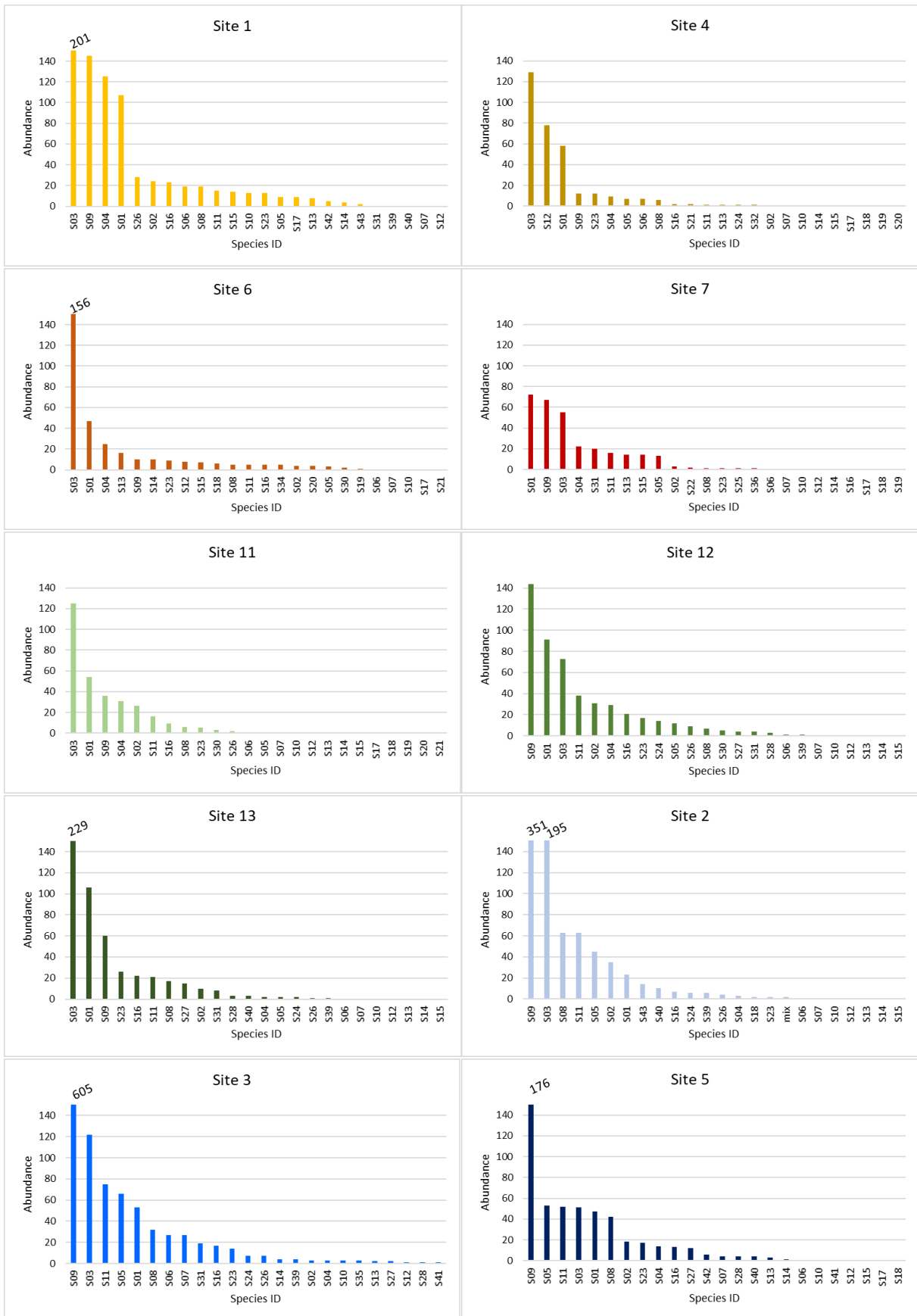
Table 13 Calculated beta diversity for the Riparian sites

	Site 1	Site 4	Site 6	Site 7	Site 11	Site 12	Site 13
Site 1	0.00	0.20	0.13	0.12	0.07	0.10	0.14
Site 4	0.20	0.00	0.13	0.25	0.17	0.25	0.16
Site 6	0.13	0.13	0.00	0.17	0.10	0.22	0.13
Site 7	0.12	0.25	0.17	0.00	0.15	0.12	0.16
Site 11	0.07	0.17	0.10	0.15	0.00	0.08	0.07
Site 12	0.10	0.25	0.22	0.12	0.08	0.00	0.11
Site 13	0.14	0.16	0.13	0.16	0.07	0.11	0.00

Table 14 Calculated beta diversity for the Slope sites

	Site 2	Site 3	Site 5	Site 8	Site 9	Site 10
Site 2	0.00	0.10	0.07	0.13	0.16	0.21
Site 3	0.10	0.00	0.10	0.15	0.22	0.13
Site 5	0.07	0.10	0.00	0.06	0.13	0.04
Site 8	0.13	0.15	0.06	0.00	0.14	0.08
Site 9	0.16	0.22	0.13	0.14	0.00	0.06
Site 10	0.21	0.13	0.04	0.08	0.06	0.00

Figure 39 presents the species abundance distribution. There were usually three or four species in the Riparian sites (1, 4, 6 and 7), which were the most frequent ones, while all other species occurred with only a couple of individuals. The most frequent species were *Cryptomeria japonica*, *Juglans ailantifolia*, *Pterocarya*, *Salix* and *Acer* species. In comparison to sites 1 and 4, sites 6 and 7 had a more homogeneous distribution, reflected by the high evenness value for site 7, but not for site 6. Site 13 showed a distribution similar to sites 1 and 4, with a high number of *Cryptomeria* and *Juglans* trees. Species abundances in sites 11 and 12 decreased exponential towards the minor species. Sites 3 and 10 showed the same characteristics as 11 and 12, but with a higher number of species. The distribution of sites 5, 8 and 9 was similar, as it could be separated into three parts with a high number of *Acer* species (S09 and S11), a high number of four to five dominant species and a several minor species. Site 3 had a distribution pattern between the Riparian sites and the sites 5, 8 and 9. It should be noted that the numbers of individuals per species varied among all sites.



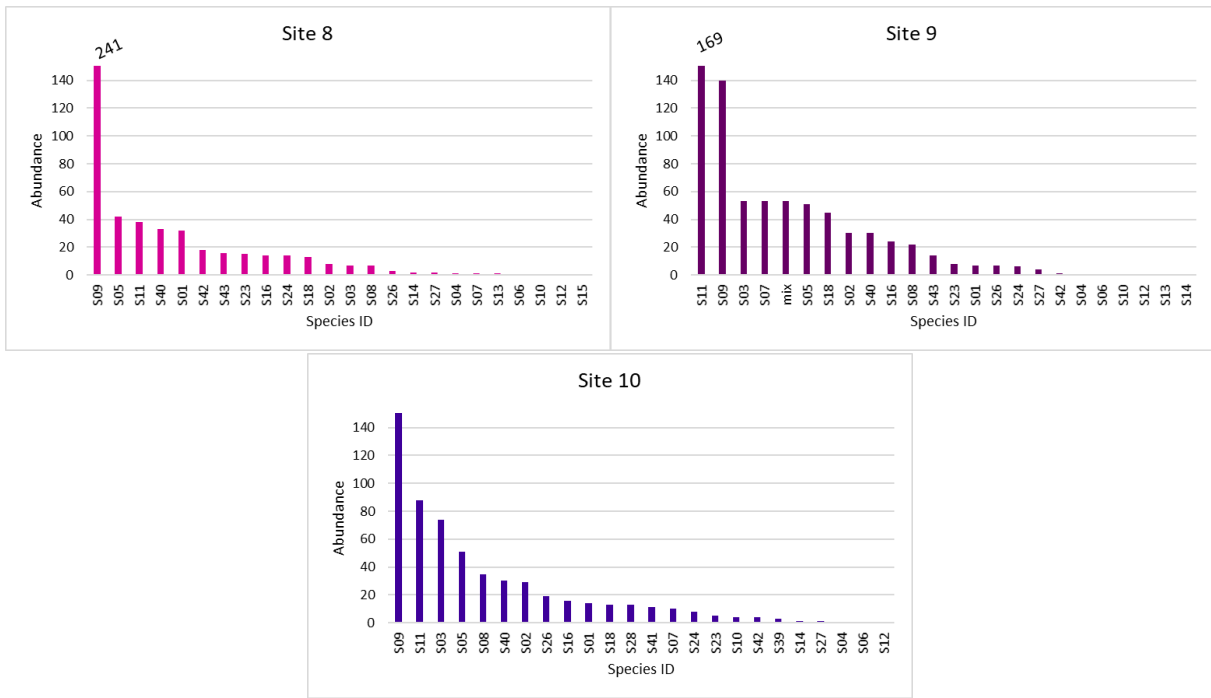


Figure 39 Species abundance for all 13 sites

Furthermore, the relation between the site areas and the species richness was evaluated. Figure 40 showed a relation with $r^2 = 0.1288$, which means that there was no significant relationship between the area and the species richness. The varying area had no influence on the number of species, as most sites had a similar size of around 2 ha, while the richness varied between 12 and 20 species.

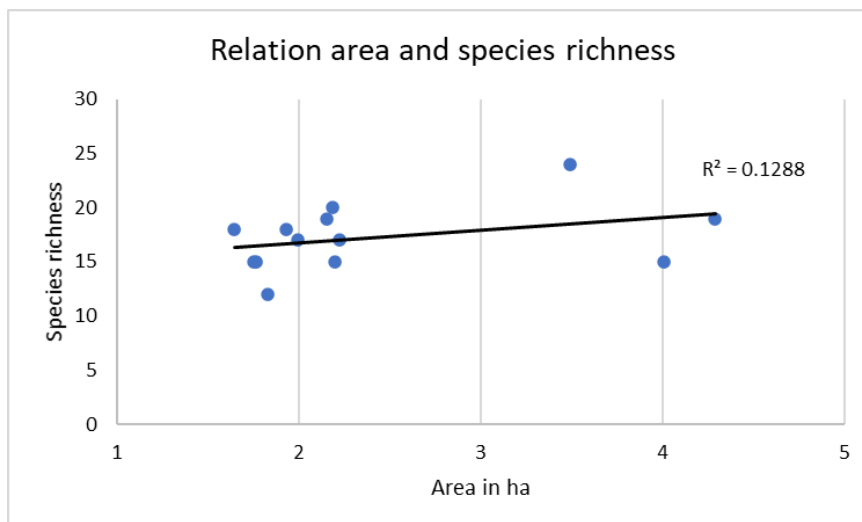


Figure 40 Relationship between the species richness and the area in hectare

4.2.4 Discussion

Assessing the biodiversity with species compositions and species richness is a common methodology and needed for management practices (Tenzin and Hasenauer, 2016). The calculated indices indicated that the considered forests are diverse ecosystems, which will be evaluated in the following discussion.

4.2.4.1 Species distribution and abundances

Riparian forests are known for their high biodiversity, as several disturbances open niches and offer space for new species or the distribution of well adapted species. Generally, the sites were composed of a couple of dominant species, which were well adapted to the challenging environment of riparian forests. These species are *Juglans ailantifolia*, *Pterocarya rhoifolia* and the planted tree *Cryptomeria japonica*.

Even though riparian forests are known for their species diversity, slope forests contained as many tree species as the Riparian sites, or even more. High ground forests in Japan are usually beech forests, while forests located in lower elevations are oak forests. The species in the Slope sites were characteristic for oak forests but they still contained a high number of riparian species. The mixture of riparian and oak forest species is the reason for the high species diversity in the Slope sites. They can be regarded as a transition zone between riparian and oak forests. This can also be seen in the species abundance diagrams, where sites 11 and 12 showed an exponential decrease of abundance towards minor species. Dominant species of the riparian forest still occurred, but with a smaller number of species, while species like *Quercus mongolica*, *Acer mono maxim* and *Magnolia obovata* occur became more frequent. Hence, it was the distribution of a transition zone between riparian and oak forests.

The distribution diagrams did not show any structure in similar mixed forests, but it showed that the distribution and structure of each forest site varied. The occurrence of different kinds of species with their number of individuals showed that there must be an underlying characteristic which allows distributions of specific species in specific areas.

In site 1 one part of the image was located on the slope, where a high number of *Acer*, *Cornus controversa*, *Aesculus turbinata*, *Magnolia obovata* and *Quercus mongolica* trees were found. Site 4 contained an area where young *Salix serissaefolia* trees are growing, which increased the number of this species significantly. In general, site 4 contained a high number of *Juglans ailantifolia* trees and a high number of young trees, which could not be identified from the orthomosaic.

Site 6 was one of the sites with a high species richness, but comparably low evenness. The species abundance distribution showed that there were three dominant species (*Cryptomeria japonica*,

Juglans ailantifolia and *Pterocarya rhoifolia*) together with a high number of minor species. Suzuki et al. (2002) explained that infrequent species occur in low densities because of the unstable environmental conditions and the strong competition within riparian forests. The results, which Suzuki et al. (2002) gathered, were the same that were observed in this study. Site 6, but also sites 4 and 7 contained a couple of species with only one individual tree. In sites 4 and 7 the canopy density of *Pterocarya rhoifolia* and *Juglans ailantifolia* was high, hence rarely infrequent species occurred close to these trees. Sites 6 and 7 contained many species, low abundance and also a high number of young trees, which means that there were many disturbances, like gaps in which other species grew. Also, those sites contained a high number of *Robinia pseudoacacia* trees, which is an invasive species in the natural mixed forest. The tree species can adapt well to the environment but needs open spaces to grow.

The sites had all a similar species composition with regards to the main species, but in general all sites had a specific species composition. This means that mixed forests seem to have a similar basis of tree species, depending on site characteristics like slope angle, aspect or distance to the water. Suzuki et al. (2002) pointed out that site conditions, especially topographic variations and occurring disturbances, have the strongest influence on tree species composition. In this study it was discussed that tree species develop a specific guild structure based on the various types of forests and forest conditions, like a varying physical environment. In riparian forests, flooding and channel migration, changing properties of the forest with high groundwater, unstable soil textures and shallow organic soils characterise the species composition the most (Suzuki et al. 2002).

4.2.4.2 Diversity indices

Diversity indices are useful tools, which are already used for decades. Measuring similarities with alpha and beta diversities to quantify differences in species compositions was discussed and approved as useful tool as well (Jost, 2007). In this study, several diversity indices were used to evaluate the different sites and especially their composition. Each index provided useful information about the sites; all indices together can complete the overview of the sites and allows interpretations of the differences. A good example provided site 3, which had the highest species richness with 24 species, which indicated a high diversity of the site, but when the Shannon index was considered, the diversity was the second lowest of all sites. Since the evenness was the lowest in site 3, the species, which occurred, had completely different numbers of individuals and the highest number of *Acer* species (605) of all sites. If only one index would have been considered, the site would have been misinterpreted. Similar indices and abundance distributions showed site 10. Median evenness and high

species richness, but high Shannon index for site 3 and 10, but beta diversity values were comparably low. The individuals of the species differed between the sites. The three dominant species were *Acer*, *Cryptomeria japonica* and *Acer mono maxim*, in different orders.

Site 9 had a low number of species occurring in the site, while the diversity and the evenness values were one of the highest among all sites. The shape of the species abundance distribution was identified to be similar with sites 5 and 8. Furthermore, the beta diversity index of site 5 was closer to site 9 than to site 8. When the order of the species in the abundance diagram for site 5 was analysed, *Acer* species, *Quercus mongolica*, *Acer mono maxim*, *Cryptomeria japonica* and *Juglans ailantifolia* were the most occurring species, which was exactly the same for site 8, except that *Hamamelis japonica* grew instead of *Cryptomeria japonica*. The species had a different abundance order.

Site 4 had the lowest diversity indices, for evenness, Shannon entropy and species richness. Furthermore, the site seemed to have several differences with the other sites. A deeper analysis of the species composition explained these results. *Salix* trees and *Juglans ailantifolia* trees made about 70 % of the species (without *Cryptomeria japonica*). No other site had such a dominant species composition. However, species abundance distribution of site 13 was alike, as well as the Shannon index (1.84), the evenness (64.84 %) and the species richness (17). On the other hand, the similarity between the sites was low with 77.02 % and a high beta diversity of 0.16. The order of species abundance was different for both sites with *Cryptomeria japonica*, *Salix*, *Juglans ailantifolia* and *Acer* species in site 4 and *Cryptomeria japonica*, *Juglans ailantifolia*, *Acer* species and climbing plants in site 13.

When all the previously mentioned values were compared, Gini – Simpson indices and Shannon entropy values were the highest for site 1 and 10, with the highest species richness and the lowest Simpson values, which means that these sites had the highest diversity with a more even species abundance distribution. Sites 2, 4 and 11 had the lowest values for Shannon entropy, Gini – Simpson index and species richness, together with higher Simpson indices, which means that these sites had a lower diversity and a moderate uneven species abundance distribution. The high species richness in site 3, but also in sites 6 and 8, seems to indicate a high diversity, but together with a higher Simpson index as well as lower values for Shannon entropy and Gini – Simpson, the evenness in those sites had a strong influence on the indices. In those cases, the species abundance distribution tended to be highly uneven in comparison to all other sites. Therefore, the evenness was calculated and analysed, as it is a measure for the distribution of the individuals in the population. Also, there was a relation between low and high alpha diversities; both resulted in high beta diversities, especially between sites 2 and 3 or 8, 9 and 10. In the Riparian sites, the beta diversity was higher than in the Slope sites. There was no clear relationship between the alpha diversity and the beta diversity in the Riparian sites.

The different diversity indices helped to analyse the species composition, abundance and diversity. The comparison of the indices showed that they cannot be used as a standalone tool to give accurate information about the sites. Still, diversity indices can give a simple value for different sites and allow a discussion about differences and similarities. Jost (2007) discussed that the use of diversity indices only considers species frequencies and the weights of each species is considered as equal. *Robinia pseudoacacia*, which is invasive, should not be treated equal to other native species in a natural mixed forest and it can be discussed to adjust the weight for the diversity measurements.

4.2.5 Conclusion

Diversity indices are an effective measure to characterise forests. In this chapter, automatic counting of manual annotated tree tops in images were used to calculate the diversity indices for all sites. Fast tree counting was possible through image analyses and the possibility to perform counting for all sites enabled the fast comparison between sites with simple calculations. The reduced numbers of tree species, which were visible from above, enhanced the handling of the data for diversity measurements. The combination of species richness, Shannon entropy and Evenness, as well as Hill numbers and Horn index allowed a comparison of site characteristics and similarities. Diversity calculations provided values for the species composition with high values, when the species number was high and evenly distributed. The benefit of the calculated values was that site diversities, similarities and differences were assigned a value, which was easy to compare. But the value did not provide detailed information about how tree species were calculated or where and why the sites were similar or different. In the end, the value is a simple measurement which needs further details for providing essential information about forests. High diversities did not necessarily correspond to high diversities, but the number per species and evenness influenced diversities, which were highest for the Slope sites 9 and 10. Riparian sites had lower diversities and were also less even.

Chapter 4.3 Assessment of Forest composition and distribution with image analysis

4.3.1 Problem definition

Forests are influenced by climate, topography and hydrology, which significantly affect structure, composition and plant distribution. Structures refer to patterns and relationships in forest ecosystems (Gadow et al., 2012), which determine their properties, like biomass production, biodiversity or several ecosystem services. Quantifying spatial stand structures is one of the important aspects to identify horizontal and vertical forest structures, their heterogeneity and changes along with different type of forests. Zoning in forests is prominent from low to high elevations and from the river to the slopes or the layering of the forest from shrubs to the canopy layer. Pommerening (2002) explained the forest structure as a combination of spatial distribution, species diversity and variation in three dimensions. Smith (2002) included measurements of the species composition, diversity, stem height, basal area, tree density and spatial distribution. Analysing forest structures is challenging, as it is dynamic. Therefore, spatial distributions of trees as well as their attributes are important aspects. The main part is the distribution of trees in the ecosystem, which is a process of seed distribution, seedling establishment and survival in the competition between tree species; all influence population dynamics (Gadow et al., 2012). Disturbances, resource competition, tree growth and mortality intensively influence forest structures. These complex ecosystems, which vary in temporal and spatial dimensions, as well as the many interactions between plants and human influences, have to be analysed to properly understand forest ecosystems and their function.

The first step in analysing forest structure was to measure tree species compositions and distributions, which are the results of long-term developments under varying environmental factors. Soil texture, soil moisture and nutrient availability determine the composition of tree species, while characteristics of the species and the competition with neighbouring species further influence the distribution. The information on tree species occurrences and their distribution are usually content of field inventories, where tree species are determined and trees are counted in field plots.

In this study, orthomosaics were used to provide information about canopy areas and tree counting based on manual annotations. The objective for this part of the thesis was:

- iv. Evaluate the composition and distribution of mixed natural forests in Shonai area based on image analysis.

Density, frequency, dominance and abundance measurements were used on the basis of the calculated tree species areas and performed counts. In a first step, the sites were characterised to provide an overview of the considered forest areas (Riparian, Terrace and Slope). In the next steps,

forest areas, compositions and distributions were analysed to finally classify the forests and their structure.

4.3.2 Methodology

In order to identify tree species several methods were applied to provide an overview of the composition, distribution and structure of the study area. The first part of the methodology focussed on the gathered field data, the second part on the image analysis with GIS systems and the last part on the automatic segmentation and classification of tree species.

4.3.2.1 Image surveys and data preparation

The data basis for this chapter is the same as for chapter 4.2, therefore only a short description is presented here (for more details see chapter 4.2). Images were collected in the summer season 2019 for all 13 sites. For these 13 sites, GIMP was used to do tree tops and tree species annotations, which were then run with the Census code (see chapter 4.2 for details). The code output the counts per tree species, which are presented in Table 8.

In another step, those layers were uploaded in ArcGIS Pro and georeferenced. The JPEG files were then converted from a raster into a polygon shapefile using the tool raster to polygon.

4.3.2.2 Pixel counting code

The pixel counting code used all annotated layers and counted the total number of pixels, the number of white pixels and then calculated the number of black pixels in the image (Note: python does not have a function to directly count black pixels).

4.3.2.3 GIS analysis

The images gathered from the forest can be used for different image analysis. ArcGIS provides a good base to perform several image analyses and the possibility to visualise the results in the real environment. The following analysis were performed to access the site characteristics stored in the images.

The DEM generated as geoTIFF by Metashape, can be directly processed by ArcGIS. In this work, winter DEMs were used to calculate the slope and aspect of the studied sites. The DEM file was first pre-

processed by applying the tools *Filter* and *Focal Statistics* to smoothen the surface. Winter images still contain the deciduous trees, which are represented by the stem and the branches, as well as the evergreen trees, influencing the structure and values in the DEM. The applied tools help to focus the analysis on the earth surface. In a second step the tools slope and aspect were applied on the output of the *Focal Statistics* tool.

4.3.2.4 Data analysis

There are several species, which occurred infrequent, with one or two individuals per site. Those tree species contribute to the diversity and the structure of the forest, but they also hamper the analyses of main species, which contribute the most to the conditions in the forest. Therefore, infrequent species were identified and some analyses were only performed for the most frequent ones (as all analyses would be out of the scope of this thesis), and to reduce the influence of extremely rare tree species. The analyses for canopy areas, tree counts and density measurements were performed for all species, while frequencies, abundances, dominances and the important value index were only calculated for the most frequent species. As frequent species the following were identified: *Juglans ailantifolia*, *Magnolia obovata*, *Pterocarya rhoifolia*, *Robinia pseudoacacia*, *Salix* species, *Tilia* species, *Acer mono maxim*, small-leaved *Acer* species, *Aesculus turbinata*, *Cornus controversa*, *Quercus mongolica* and *Larix kaempferi*.

The canopy area was obtained by the manual annotations. The annotated layers and the orthomosaics had the same pixel size; therefore, pixels could be transformed into square meters. Furthermore, the area was calculated in the same way and the canopy area for each species could be presented in percent. Tree counting was performed together with the manual colouring of the trees, whereby each identified tree was marked with a black dot. Those dots were counted with the Census code.

For the important tree species, frequencies, abundances, dominances and important values were calculated. The species counts performed per site were summarised in one point layer using ArcGIS; in a second step the single species were extracted from the point layer and stored in a species-specific point layer. The sites in the north (sites 6, 7, 8, 9, 10, 11, 12 and 13) and south (sites 1, 2, 3, 4 and 5) were combined, based on their geographic location, and a fishnet grid was overlaid. The tool *summarise within* was used to count first all trees in each cell of the fishnet, then for the single tree species separately. The result showed only fishnet cells in which the analysed tree species were contained, therefore the total number of cells could be checked in the attribute table. The cells represented the quadrants in which the species occurred. As two layers were considered, one containing all trees and one per tree species, the number of total quadrants and the ones in which the

species occurred could be read out of the attribute tables. With these numbers the following equations could be solved.

The density is a measure of total individuals in all sampled plots divided by the total number of sample plots and is calculated as follows:

$$\text{Density} = \frac{\text{Total No. of individuals in all sampled plots}}{\text{Total No. of sample plots}}$$

The relative density gives the total number of individuals divided by the total number of all species and can be calculated as follows:

$$\text{rel. Density} = \frac{\text{No. of individuals of species} * 100}{\text{Total No. of all species}}$$

As mentioned before, for the frequent species, considering all sites, frequency, relative frequency, relative dominance (also for all sites and species calculated) and species abundance were calculated:

$$\text{Frequency} = \frac{\text{No. of quadrants in which species occur} * 100}{\text{Total of quadrants studied}}$$

$$\text{rel. Frequency} = \frac{\text{Frequency of occurrence of species} * 100}{\text{Total frequency of occurrence}}$$

$$\text{rel. Dominance} = \frac{\text{Total canopy area of species} * 100}{\text{Total canopy area of all species}}$$

$$\text{Abundance} = \frac{\text{Total No. of individuals in all plots}}{\text{Total No. of plots in which species occur}}$$

Species contributions to their community can be calculated with the importance value index (IVI), whereby the relative canopy area, relative density and the relative frequency are the metrics, which account for the importance of species. The calculation is performed as follows:

$$\text{Important value index} = \text{rel. Dominance} + \text{rel. Frequency} + \text{rel. Density}$$

4.3.2 Results

4.3.2.1 Site characteristics

This chapter describes the site characteristics, based on the gathered information from the images. DEMs and orthomosaics were used and analysed with ArcGIS to provide the following information. The DEMs, slope and aspect maps are included in Appendix H for all sites, while examples of site 2 were provided, here (Figure 41 to Figure 43).

The Riparian forests are mainly flat, while the slopes are usually east/southeast and west/northwest facing, which is the result of the mountains which are left and right of the river and captured in the images. The Terrace sites were all located on the western side of the river and had therefore similar aspects. Site 11 included a slope which faced to the north, as site does 12, but a second slope faced to the west/southwest, while the slopes in site 13 faced southwest, west and northwest.

The Slope sites were located close to the Wasada river, on the western and eastern sides. The south facing slope of site 5 was in contrast to the aspects of slopes for the sites 8, 9 and 10, which were east/southeast facing. Sites 2 and 3 were characteristic as the sites were divided by a ridge, which caused north and east/southeast facing slopes in site 2 and north, south and southwest facing slopes.

The sites, where mainly *Cryptomeria japonica* grew in the slopes, were mainly the Riparian sites. There, the *Cryptomeria japonica* trees distorted the values calculated for the slope angles. For site 1 the slope angles ranged between 30 and 45°, the slope map provided fewer details of the surface structure, as the canopy in the winter DEMs was too dense and disturbed the slope generation. The ROI of site 4 included slope angles of mainly less than 10°, like in sites 6 and 7. A characteristic depression can be found in the south of the imaged site 4, also in site 6, where a characteristic depression was close to the road, which lies almost on the river level. Also, in the slope map of site 7 a riverlike structure in a depression was visible.

For the sites 2 and 3 the slope angles were 20 to 30°, whereby the slope maps provided a detailed structure of the slope and river systems, which flow through the sites. Site 5 had the steepest slopes, which ranged between 31 and 45°, having no visible river structures, depressions or hills. Sites 8, 9 and 10 had slopes, which ranged between 20 and 30°, rarely 45°. The slope maps of these sites provided insights in the location of the periodically watered river systems. As the area is known for the intensive rain events in summer and the snowmelt in early spring, all slopes have channels, which are dry most of the time of the year.

The slope maps provided useful insights into the structure of the areas, which can help to interpret species distributions and forest structures. Also slope directions have an influence on species compositions and needed to be analysed.

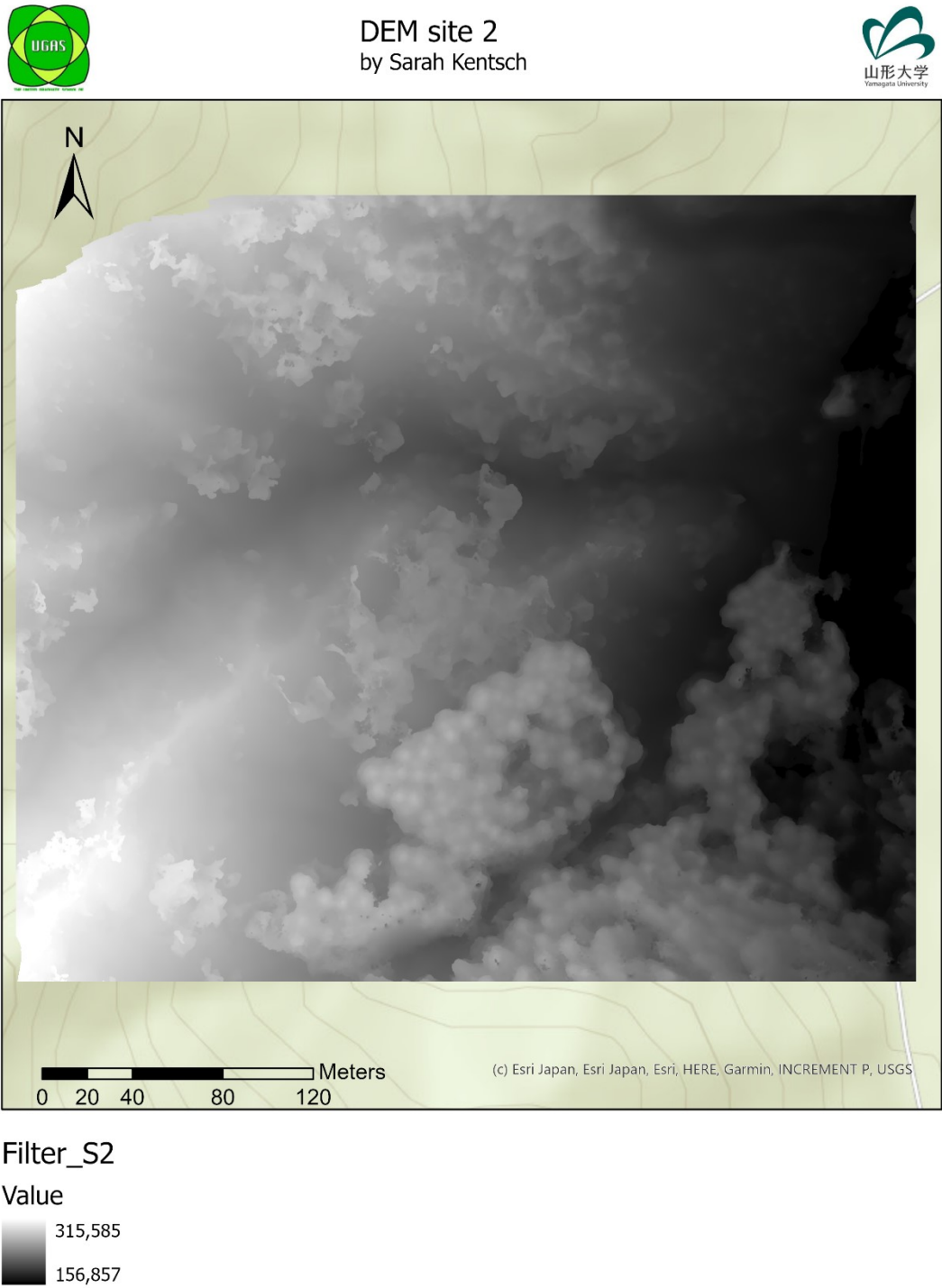


Figure 41 Filtered DEM of site 2, which was processed in ArcGIS Pro



Aspect site 2 by Sarah Kentsch

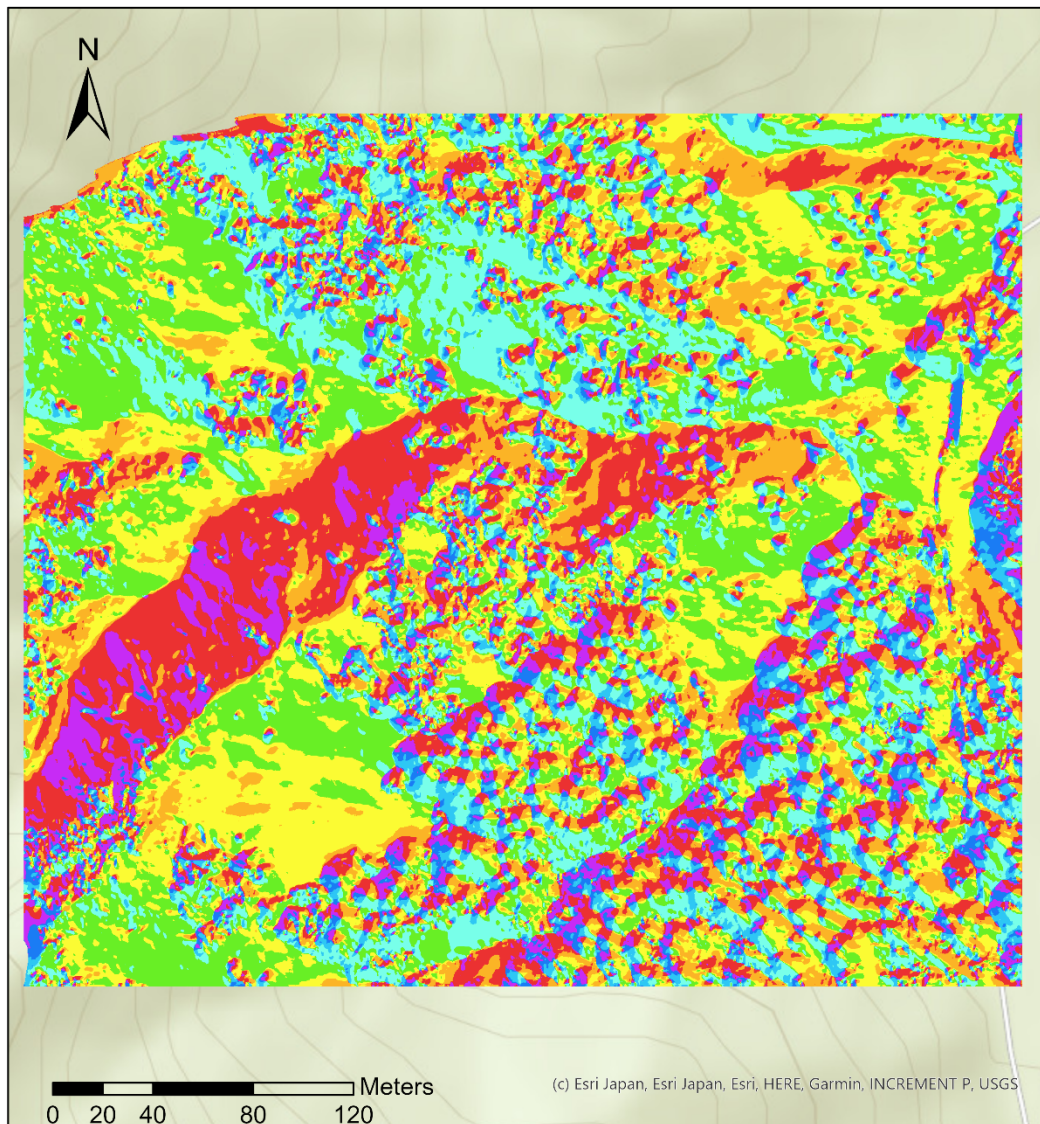


Figure 42 Aspect of site 2 generated with ArcGIS pro based on the DEM, which was filtered and smoothed before

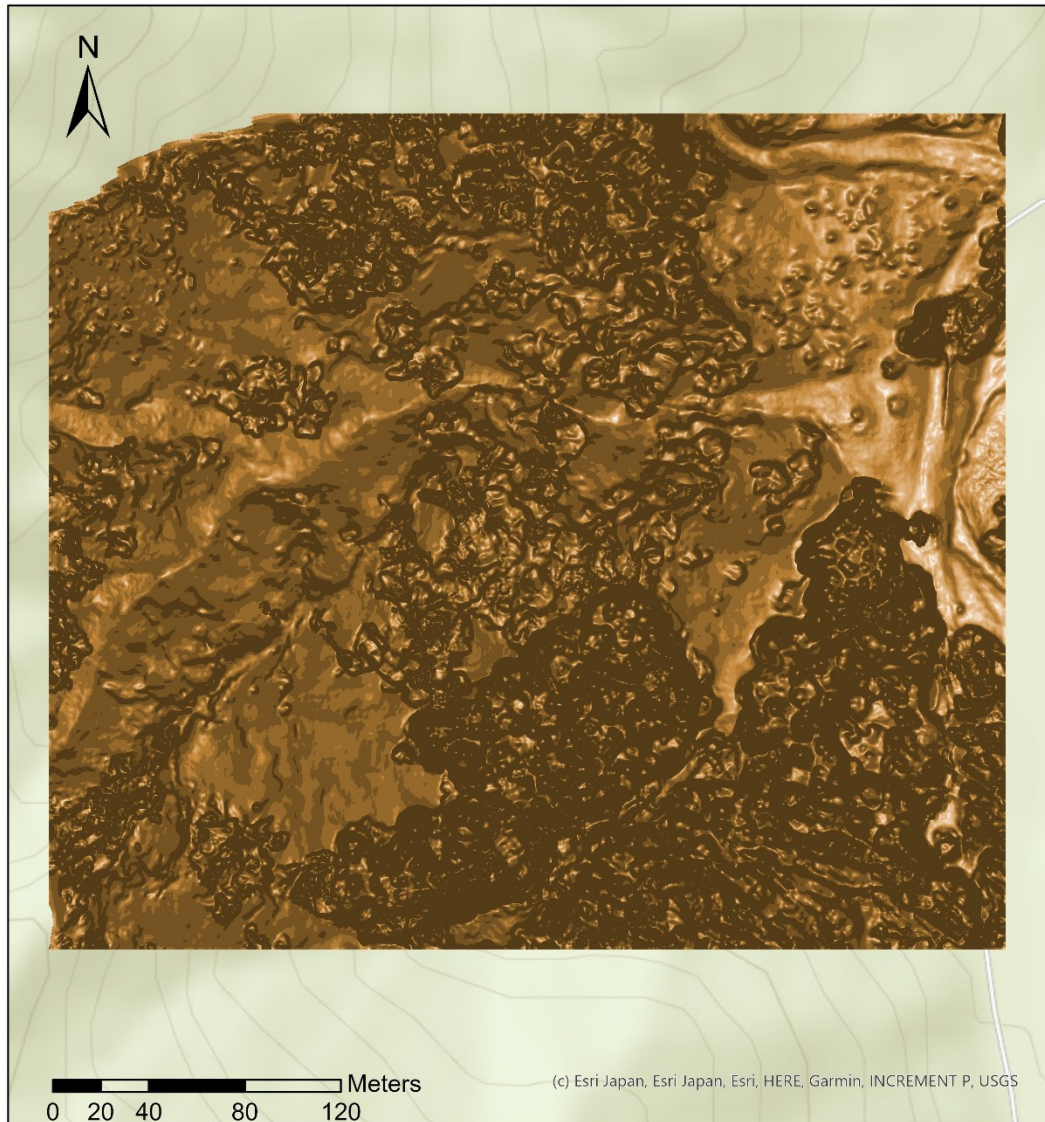


Figure 43 Slope map of site 2 generated by ArcGIS pro on the basis of the filtered and smoothed DEM

Forests are located along the rivers and along the slopes, which influenced their tree species compositions and distributions. The identification of site characteristics regarding relief, slope and aspect properties is a first step to indicate differences, which may influence forests.

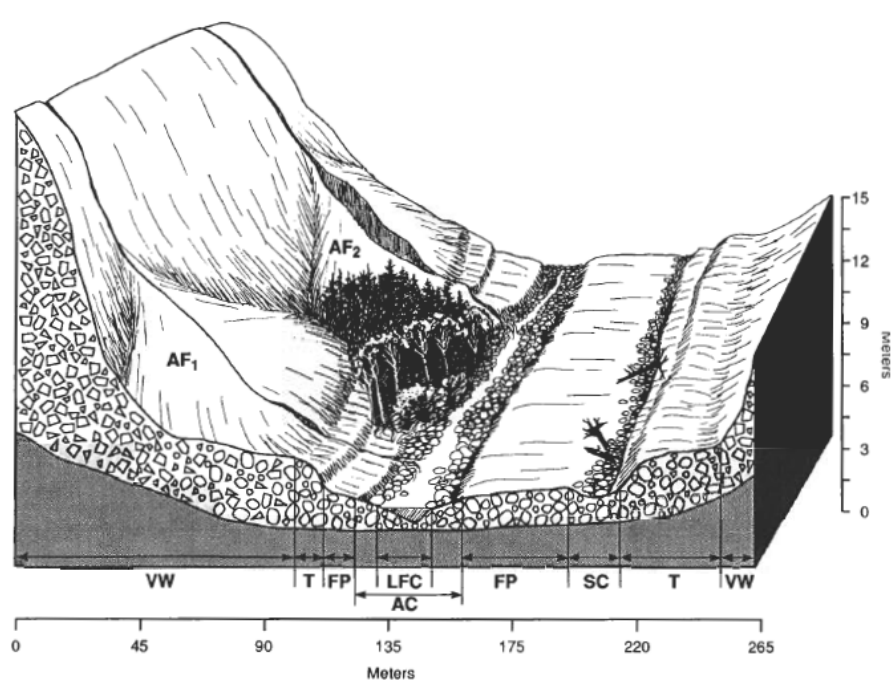


Fig. 4. Schematic diagram of valley floor surface types. Abbreviations used: LFC = low-flow channel; AC = active channel; FP = floodplain; SC = secondary channel; T = terrace; AF₁ = unincised, active alluvial fan; AF₂ = incised, inactive fan; VF = valley wall.

Figure 44 Sketch of the surface types in riparian areas. The abbreviations used are: LFC = low-flow channel, AC = active channel, FP = floodplain, SC = secondary channel, T = terrace, VW = valley wall and AF = active/inactive alluvial fan (Grant et al.)

Riparian forests in valleys are composed of active channels, flood plains, terraces and valley walls (Figure 44). The riparian forests of sites 1, 4, 6 and 7 were located along the river, on active channels and terraces. The sites 11, 12 and 13 were considered as upper Terrace sites and the Slope sites (2, 3, 5, 8, 9 and 10) were located on the valley walls. Active channels were 0.5 m above the river level and characterised by regularly occurring flooding. The soil was usually composed of coarse gravel and high water contents (Grant et al., 1995). Typical vegetation patterns were willows and alders. Floodplains were located up to 3 m above the river level, with a finer soil texture. The terrace areas were located from 3 m, up to 10 m above the river level, with soils composed of alluvial deposits (Grant et al., 1995).

4.3.2.2 Forest area distribution

The 13 sites were selected by tree species composition and their specific location in the forests. All sites together should provide enough information to characterise the forests and to apply DL for species classification. Therefore, the sites had different sizes, ranging between 3 ha and 8.1 ha. The site conditions, like the location on the slopes or the study area surrounded by Japanese cedar trees, determined the region of interest (ROI), which was usually smaller than the imaged area. Especially the orthomosaics of sites located in slopes had blurred borders, where species classifications were barely possible; those areas were excluded from the analysis. ROIs were also selected in order to

minimise overlaps, only between site 11 and 12 the ROIs had small overlaps. The largest considered areas were in sites 1, 2 and 3, with 4.29, 4.01 and 3.49 ha. The smallest ROI areas had sites 7, 8 and 9, with 1.65 to 1.76 ha. It needs to be considered that the areas were calculated with ArcGIS, based on the orthomosaics, which was a 2D plane area, while the area in the slopes is larger, when the slope angle would have been considered.

Figure 45 gives an example for the area distribution, based on image classifications for sites 4 and 11. The diagrams for all other sites can be found in Appendix G. Only site 1 is missing, as there were no annotations performed for river, ground and riverbed, and therefore no information on the understory vegetation could be provided. In both sites a ROI of 38 % was selected, of which 52 % of the area in site 4 belonged to trees and 58 % in site 11. While the ROI of site 11 did not contain river, but 1 % riverbed and 3 % ground, site 4 contained 1 % river, 4 % riverbed and 8 % ground. For all Riparian sites the ROI area ranged around 40 % (with maximum 51 % for site 1), while it was varying for the Terrace sites, with values between 33 % and 46 %. It varied strongly for the Slope sites, whereby site 2 had, with 74 %, the most pixels contained in the ROI and site 9 the lowest, with 17 %. The strong variations in the Slope sites occurred, because of the steep slope angle. Also, the ROI of the Slope sites did not contain river or riverbed areas. Ground areas were not separately annotated for the Slope sites, as the sites did only contain a small number of pixels belonging to this category. The goal of the area distribution was to gain some insights into the different site structures, whereby small numbers of pixels, which are categorised wrongly, did change the overall result, but it had to be mentioned and noted. The Riparian sites had around 35 % understory vegetation and 45 to 73 % trees. While sites 4, 6 and 7 contained 45 to 54 % tree pixels, site 1 had 73 %, which can be related to the imaged slope, where the tree density was higher than along the river. The same distribution can be observed in the Terrace sites (11, 12, 13), where the tree canopy area corresponded to 58 to 79 %, whereby site 11 had the lowest pixel number, as some flat areas along the river and road were imaged. Except site 13, where only 21 % understory vegetation were visible, 35 % and 38 % of the pixels belonged to the understory vegetation. In the Slope sites 63 % to 83 % of the pixels belonged to trees, which resulted in high tree densities, regarding the canopy area.

The canopy area per site was calculated and is presented in Table 15. The highest canopy areas were observed in sites 9 and 10, with 8291.9 m²/ha and 8034.82 m²/ha, respectively. The smallest canopy area was found in site 7, with 4519.27 m²/ha. Similar canopy areas were found in sites 1, 3 and 13 (7400 to 7900 m²/ha). Sites 8, 12, 6 and 2, with values between 6300 m²/ha and 6600 m²/ha, and the sites 11, 5 and 4, ranging between 5200 m²/ha and 5800 m²/ha, represented the average tree canopy area.

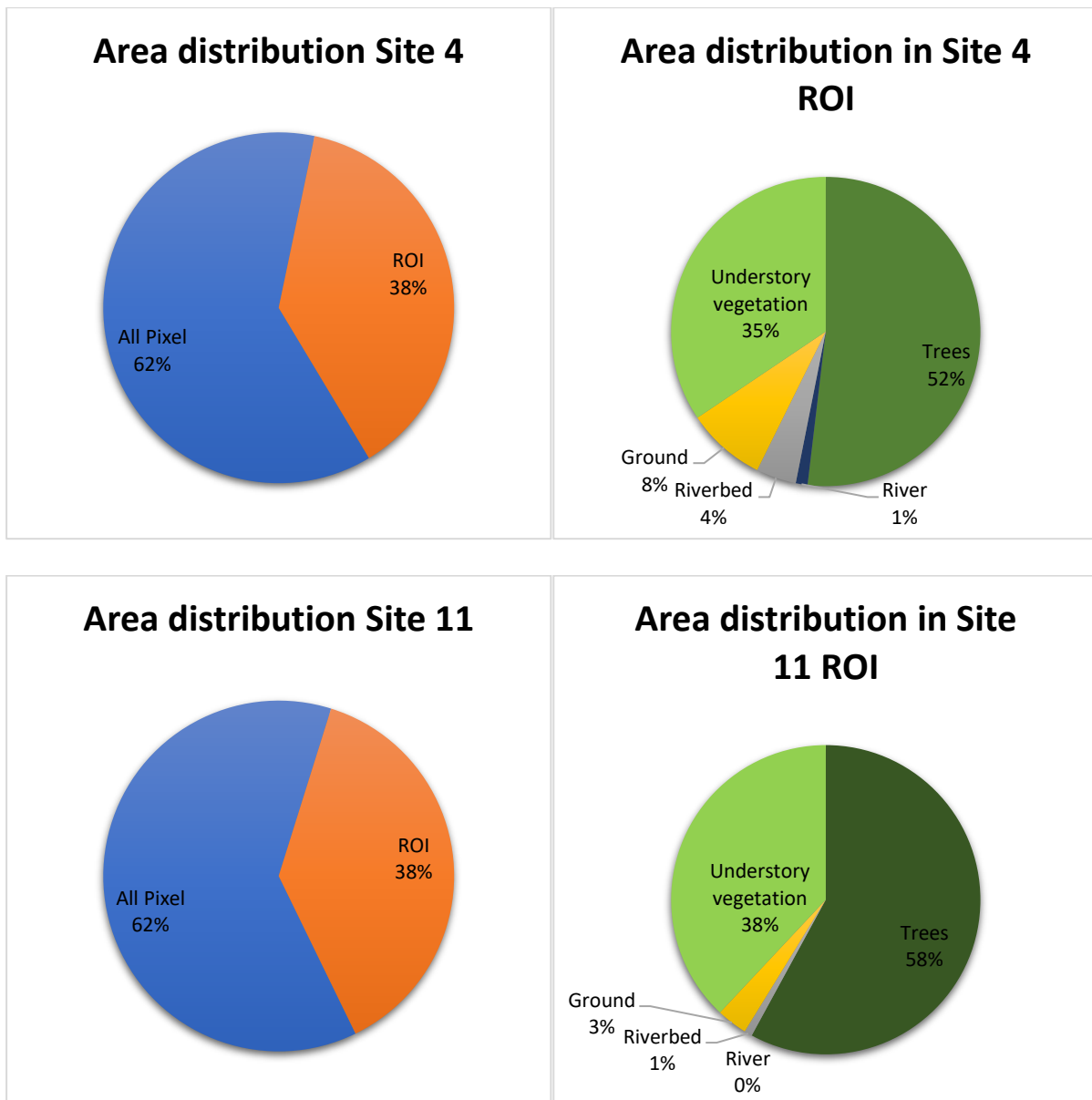


Figure 45 Area distributions for all counted pixel (without the ROI) and the ones belonging to the ROI in the left figures and the distributions of trees, understory vegetation, ground, river and riverbed within the ROI shown in the right figures

There seemed to be a relation between a greater canopy area and increasing species richness, as lower canopy areas had usually 12 to 15 different species and higher canopy areas about 20 different tree species.

Tree stem densities in the different areas varied between 87.18 and 446.94, whereby site 5 had the highest and site 7 the lowest density. In general, the sites located along the river had lower densities, with values between 100 and 150 trees/ha, than the Slope sites, with around 250 trees/ha. The species, which occurred, seemed to have no direct connection to the considered area, as site 3 had the highest species richness, with 24 different species but only the third highest ROI area, while site 2, which had a greater ROI, only contained 15 different species.

Table 15 Site characteristics with area calculations, stem densities and species richness for the study sites

	Tree counts	Area orthomosaic	Area ROI in ha	Canopy area/ha	Tree stem density	Species richness
Site1	590	6	4.29	7386.18	137.59	19
Site2	609	8.1	4.01	6298.35	151.84	15
Site3	903	5.1	3.49	7553.39	258.67	24
Site4	261	3	1.76	5208.42	147.94	15
Site5	893	3.4	2.00	5550.03	446.94	17
Site6	234	4.1	2.16	6435.75	108.45	19
Site7	192	5.1	2.20	4519.27	87.18	15
Site8	372	4.3	1.65	6625.69	226.06	18
Site9	428	6.1	1.75	8034.82	243.91	15
Site10	626	5.4	2.18	8291.90	286.58	20
Site11	353	3.5	1.83	5795.59	193.02	12
Site12	434	3	1.93	6506.09	224.83	18
Site13	546	4.8	2.23	7856.55	245.18	17

4.3.2.3 Forest composition and distribution

In total, 41 species classes were identified from the images, presented in detail in Table 16. Two classes contained climbing plants (S23 and S27), combining different species based on their leaf colours and structures. S23 contained climbing plants like Japanese Hydrangea/*Schizophragma hydrangeoides* and *Smilax*, which usually showed a light green colour and climbed up trees like Japanese walnuts, wingnuts and cedars. For S27 species like Japanese honeysuckle and *Lonicera japonica* were identified. All other classes mainly contained only one tree species, except the groups S09, S10, S11, S19 and S26. S09 and S11 contained different kind of maples, with S09 being maples with smaller leaves: *Acer japonicum*, *sieboldianum* and *palmatum*, and S11 with bigger leaves: *Acer mono maxim*, *pictum subsp. Mono* and *nipponicum*. S10 included several identified cherries: *Prunus salicina Lindley*, *Prunus serrulata/grayana* and *Prunus speciosa*. S19 and S26 contained two species each, *Alnus inokumae* and *Alnus hirsuta*, and *Tilia japonica* mixed with *Tilia maximowicziana*. In total, 52 species were identified, which belonged to 22 families and 33 genera (there were no families and genera provided for the climbing plants).

Table 16 Identified tree species, families and genera

Short	Common name	Scientific name	Family	Genus
S01	Japanese Walnut	<i>Juglans ailantifolia</i>	Juglandaceae	Juglans
S02	Japanese horse-chestnut	<i>Aesculus turbinata</i>	Hippocastanaceae	Aesculus
S03	Japanese Cedar	<i>Cryptomeria japonica</i>	Cupressaceae	Cryptomeria
S04	Japanese Wingnut	<i>Pterocarya rhoifolia</i>	Juglandaceae	Pterocarya
S05	Mongolian Oak	<i>Quercus mongolica</i>	Fagaceae	Quercus

S06	Japanese Larch	<i>Larix kaempferi</i>	Pinaceae	Larix
S07	Japanese Beech	<i>Fagus crenata</i>	Fagaceae	Fagus
S08	Japanese bigleaf magnolia	<i>Magnolia obovata</i>	Magnoliaceae	Magnolia
S09	Maple species	<i>Acer japonicum, sieboldianum, palmatum</i>	Sapindaceae	Acer
S10	Cherry	<i>Prunus salicina Lindley, Prunus serrulata/grayana, Prunus speciosa</i>	Rosaceae	Prunus
S11	Painted maple	<i>Acer mono maxim, Acer pictum subsp. Mono, Acer nipponicum</i>	Sapindaceae	Acer
S12	Kimura	<i>Salix serissaefolia</i>	Salicaceae	Salix
S13	Willow1	<i>Salix jessoensis</i>	Salicaceae	Salix
S14	Japanese chestnut	<i>Castanea Crenata</i>	Fagaceae	Castanea
S15	Black locust	<i>Robinia pseudoacacia</i>	Fabaceae	Robinia
S16	Wedding cake tree	<i>Cornus controversa</i>	Cornaceae	Cornus
S17	Amur cork tree	<i>Phellodendron amurense</i>	Rutaceae	Phellodendron
S18	Hazel-leaved birch	<i>Betula corylifolia</i>	Betulaceae	Betula
S19	Alder species	<i>Alnus inokumae / Alnus hirsuta</i>	Betulaceae	Alnus
S20	European spruce	<i>Picea abies</i>	Pinaceae	Picea
S21	Caramel tree	<i>Cercidiphyllum japonicum</i>	Cercidiphyllaceae	Cercidiphyllum
S22	Persian silk tree	<i>Albizia julibrissin</i>	Fabaceae	Albizia
S23	Climbing plant	<i>Japanese Hydrangea, Schizophragma hydrangeoides and Smilax</i>	/	/
S24	Korean berry	<i>Morus australis</i>	Moraceae	Morus
S25	Japanese clethra	<i>Clethra barvinervis Sieb. et Zucc.</i>	Clethraceae	Clethra
S26	Japanese lime, Japanese linden	<i>Tilia japonica, Tilia maximowicziana</i>	Malvaceae	Tilia
S27	Climbing plant 2	<i>Japanese honeysuckle/Lonicera japonica</i>	/	/
S28	Castor aralia	<i>Kalopanax septemlobu</i>	Araliaceae	Kalopanax
S29	Nippon maple	<i>Acer nipponicum</i>	Sapindaceae	Acer
S30	Japanese hackberry	<i>Celtis jessoensis</i>	Cannabaceae	Celtis
S31	Miyama alder	<i>Alnus fauriei</i>	Betulaceae	Alnus
S33	Japanese angelica tree	<i>Aralia elata</i>	Araliaceae	Aralia
S34	Japanese pepper	<i>Zanthoxylum piperitum,</i>	Rutaceae	Zanthoxylum
S35	Japanese ash	<i>Fraxinus lanuginosa</i>	Oleaceae	Fraxinus
S36	Manchurian ash	<i>Fraxinus mandshurica</i>	Oleaceae	Fraxinus
S38	Ginkgo	<i>Ginkgo biloba</i>	Ginkgoaceae	Ginkgo
S39	Fragrant Snowbell	<i>Styrax obassia</i>	Styracaceae	Styrax
S40	Japanese witch-hazel	<i>Hamamelis japonica</i>	Hamamelidaceae	Hamamelis
S41	Full moon maple	<i>Acer japonicum</i>	Sapindaceae	Acer
S42	Japanese Hazel	<i>Corylus sieboldiana</i>	Betulaceae	Corylus
S43	Bigleaf Hornbeam	<i>Carpinus Cordata</i>	Betulaceae	Carpinus

4.3.2.4 Tree counts and distribution

The Census code gave a first number of trees belonging to each species, by counting manual annotated tree tops. This analysis provided a first overview of the number of species occurring in the sites and which were the frequent and less frequent species.

In total, 7431 trees were manually annotated in the 13 orthomosaics. The Riparian and Terrace sites counted 3085 trees and the Slope sites 4346. In the Slope sites as well as in the Riparian sites 27 different species were identified from the images, while 18 different species were found in the Terrace sites. Figure 46 shows the distribution of trees in the four forest parts: Top, Slope, Terrace and Riparian. Most of the dominant species differed for the considered parts of this study. While the top part was mainly composed of *Quercus*, *Larix* and *Fagus* (S05-S07), the Slope sites were dominated by different *Acer* species, *Quercus* and *Magnolia* trees (S09, S11, S05 and S08), the Terrace sites by *Juglans ailantifolia* and *Acer* species (S01, S09) and the Riparian sites by *Juglans* and *Pterocarya rhoifolia* trees (S01 and S04). *Cryptomeria japonica* (S03) was found in all sites, but not further considered, since the tree was a planted species. Furthermore, there were several minor species which occurred in the different sites.

Figure 47 provides a detailed overview of the different sites. It further illustrates that the Riparian site was mainly composed of *Juglans* and *Pterocarya* trees. Sites 1 and 7 had a high number of *Acer* species, while site 4 had a high number of *Salix* trees, which occurred in a small area as monoculture of young trees. Furthermore, 19 different species occurred in site 1, of which *Tilia japonica*, *Corylus sieboldiana*, *Magnolia* and *Carpinus cordata* usually occurred in higher elevated regions. The species distribution varied between the different sites, especially when the minor species were considered. In comparison to the Riparian sites, the Terrace sites contained less tree species. *Acer*, especially the *Acer mono maxim*, as well as *Aesculus turbinata*, *Cornus controversa* and *Morus australis*, occurred more frequent. Furthermore, those sites had a higher number of *Juglans* trees. The Slope sites showed a different distribution. The main species were *Acer*, whereby the numbers of *Acer mono maxim* were higher than in the Terrace sites. *Quercus*, *Fagus* and *Magnolia* trees were found frequently. Additionally, the *Betula corylifolia*, *Morus australis*, *Tilia japonica* and the *Hamamelis japonica* occurred more frequent.

4.3.2.5 Canopy area, densities and relative dominance of tree species

The total canopy area of all trees in the 13 sites accounted 211,167.39 m² (Table 18). Note that *Acer nipponicum*, *Aralia elata* and *Ginkgo biloba* had no area, as these trees were identified in the orthomosaics, but were located outside of the ROI. The largest canopy area had *Juglans* trees, which were distributed in all sites, followed by *Cryptomeria japonica*, occurred along the borders of the

orthomosaics. *Pterocarya rhoifolia*, *Magnolia obovata* and the both *Acer* species classes had canopy areas of 7 to 9 %. While *Quercus mongolica* and *Aesculus turbinata* made about 5 % of the canopy area, all other species occurred with 2 % or less in the sites. Interesting were the tree counts compared with the canopy area and the density. The density was calculated based on the stem occurrences and the canopy area. The highest tree counts were for small-leaved *Acer* species, followed by *Cryptomeria japonica* and *Juglans ailantifolia*. The relative densities mirrored this observation when (TC) and (BA) were compared. With a comparably low TC relative density of 8.56 % and the BA relative density of 26.14 % for *Juglans ailantifolia*, the values varied strongly. The BA density of the *Acer* species was lower, with 8.78 %, while the TC density showed values of 33.54 %. *Magnolia obovata*, *Aesculus turbinata* and *Pterocarya rhoifolia* had lower TC density values and higher BA density values. *Quercus mongolica*, *Larix kaempferi*, *Prunus* species, *Cornus controversa*, *Morus australis* and *Tilia japonica* showed all similar relative density values.

Figure 48, which contains the tree densities, shows how the tree species were distributed in the different sites. The figure clearly states that *Juglans ailantifolia*, *Pterocarya rhoifolia* and *Salix* species were dominant in the Riparian sites and also in the Terrace sites (except for the *Salix* trees). From site 11 to site 13 the amount of *Pterocarya rhoifolia* trees decreased, while the number of *Cornus controversa* and *Magnolia obovata* increased. All sites, which had a slope imaged in the orthomosaic, showed a higher number of *Acer* species, Slope sites had a high number of big-leaved *Acer* species (mainly *Acer mono maxim*). The figure furthermore shows that there were only a couple of *Larix kaempferi* trees found, mainly in sites 3, 5, 8, 9 and 10, which were Slope sites. Further it was observed that there were several species, which occurred in all sites, but with different densities: *Acer mono maxim*, small-leaved *Acer* species, *Cornus controversa*, *Juglans ailantifolia*, *Aesculus turbinata* and *Quercus mongolica*. Forests, which were located in the slopes contained species like *Hamamelis japonica*, *Morus australis* *Carpinus cordata* and *Corylus sieboldiana*.

The relative dominance was calculated for each site and species, provided in Table 17 and Appendix D. For the Riparian sites, the relative dominance was the highest for *Juglans ailantifolia* with 36.53 %, *Cryptomeria japonica* with 21.47 % and *Pterocarya rhoifolia* with 16.67 %. Species like *Magnolia*, small leaved *Acer* species, *Aesculus turbinata* and *Salix* species made up between 2 % and 3 % of the species dominance, all other species had values below 2 %. There were differences between the four Riparian sites, which should be addressed. Relative dominance values ranged between 23.92 % and 54.95 % for *Juglans ailantifolia*, while sites 4 and 7 had higher values. In comparison, site 4 had the lowest values for *Pterocarya rhoifolia* with 5.15 % but high values for willow trees (S12), with 8.49 %.

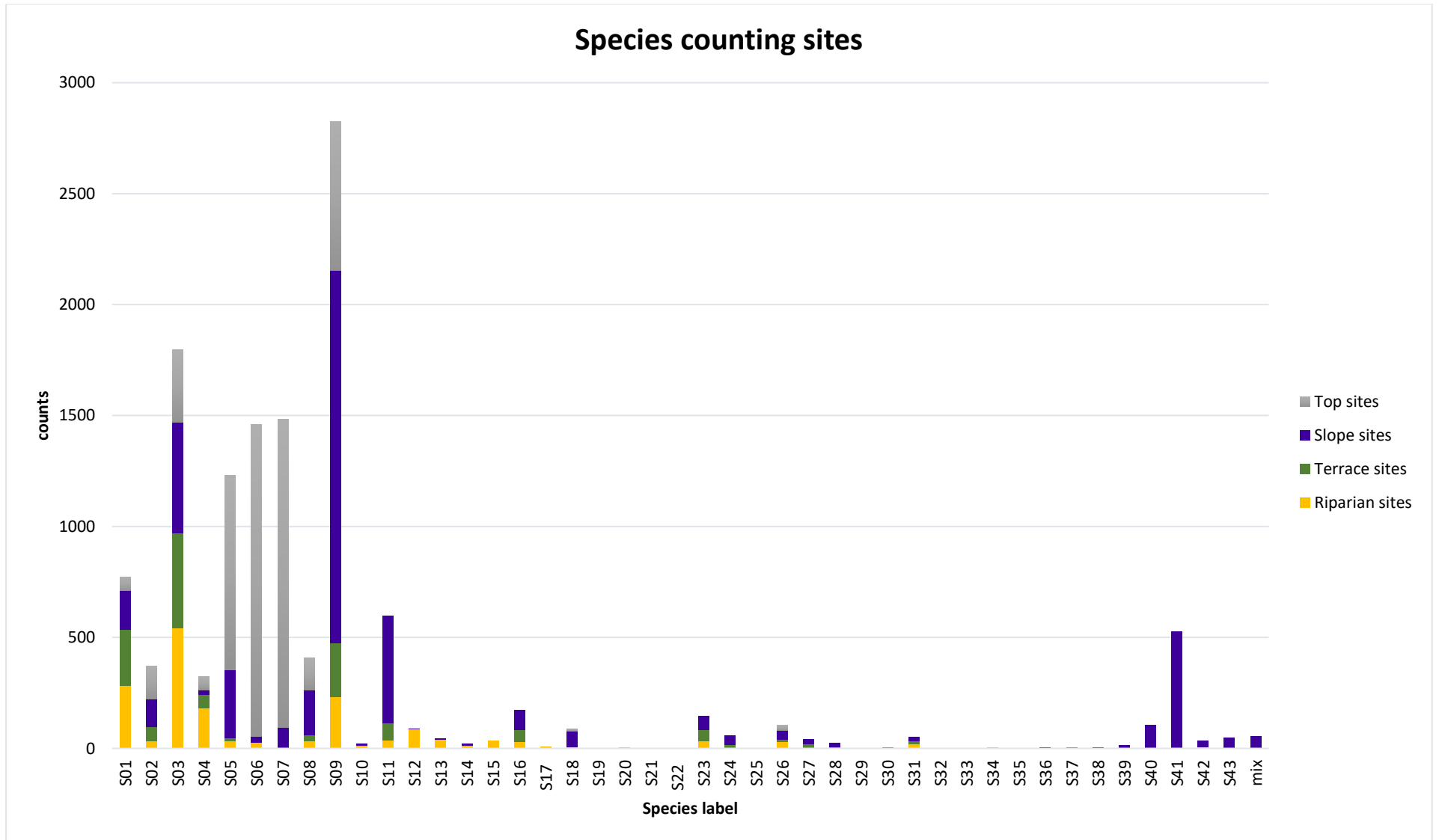
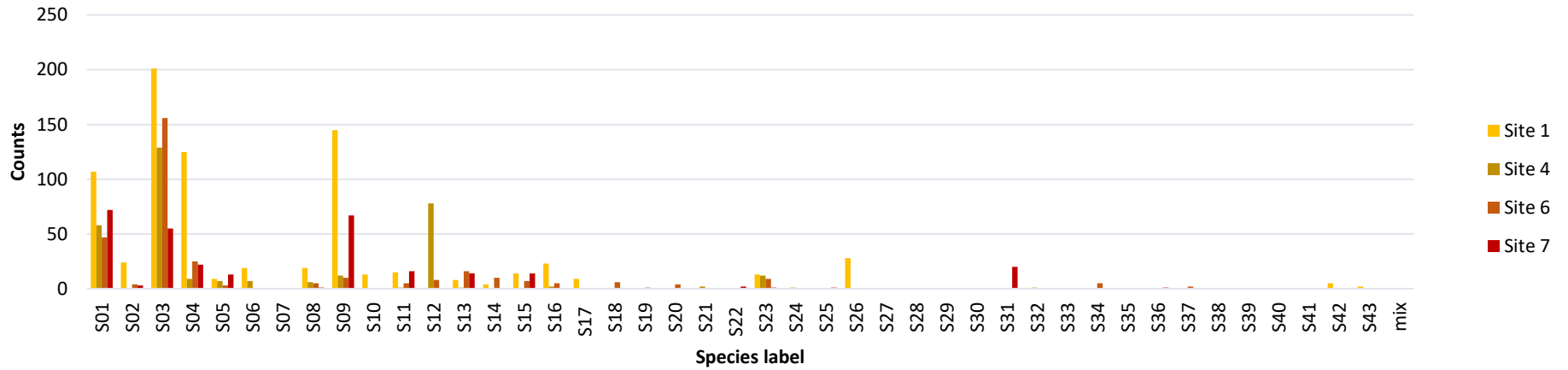
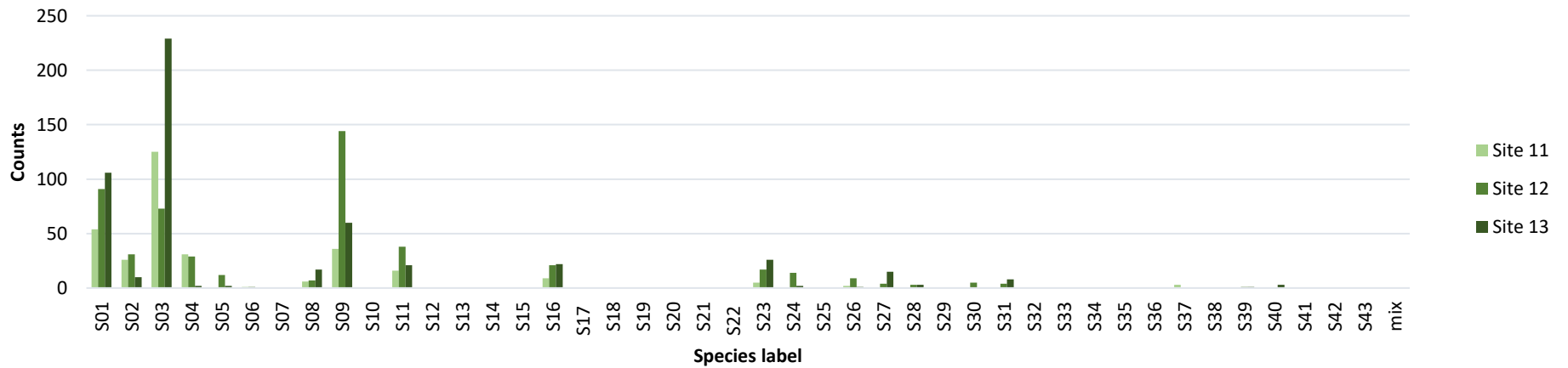


Figure 46 Counts per species for the different sites, which are considered: Top, Slope, Terrace and Riparian sites

Species counting Riparian sites



Species counting Terrace sites



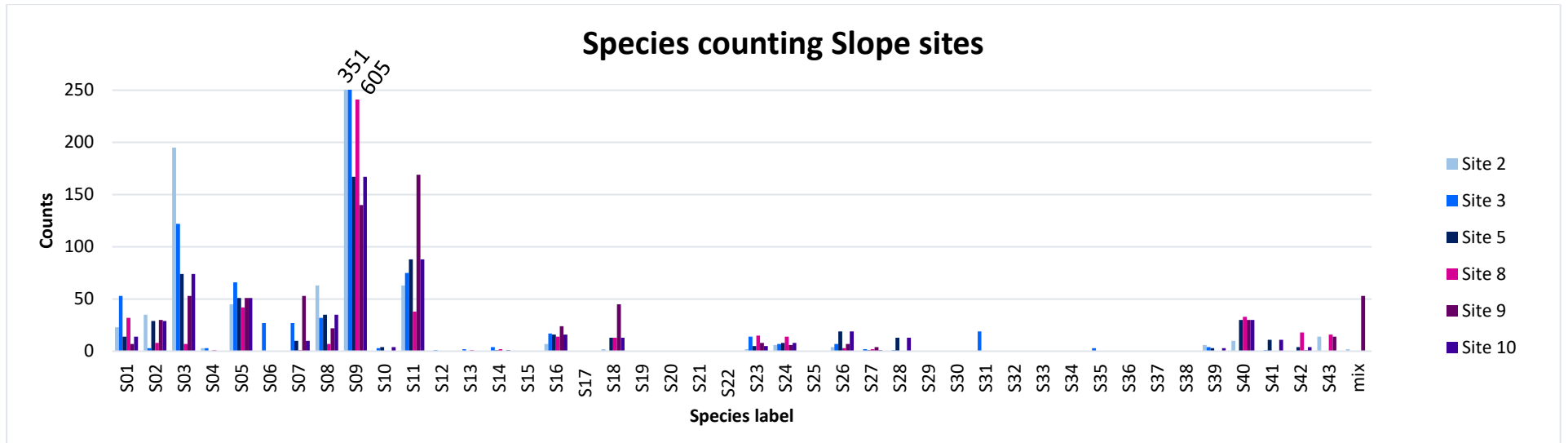


Figure 47 Detailed counts for the considered sites separated: Riparian, Terrace and Slope sites. In each diagram, the counts per site are shown

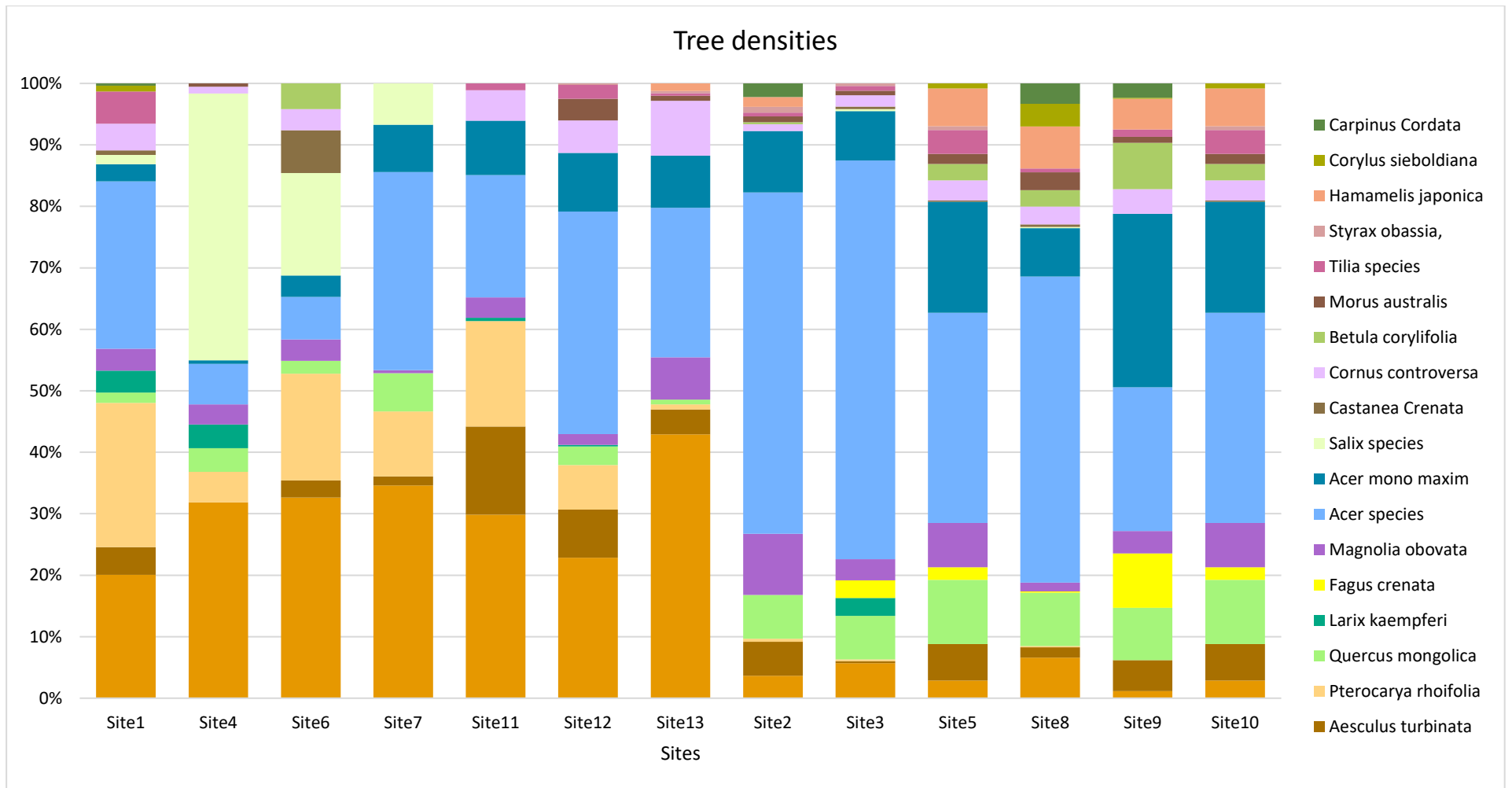


Figure 48 Information about the tree densities 18 tree species classes. Note that the two occurring *Salix* species were grouped together in this graphic, as well as the small-leaved *Acer* species

Table 17 Relative dominance for the Riparian, Terrace and Slope sites, as well as the total in %

rel. Dominance in %	S01	S02	S03	S04	S05	S06	S07	S08	S09	S10	S11	S12
Riparian sites	36.53	2.24	21.47	16.67	1.57	1.29	0.00	2.32	2.34	0.92	1.35	1.68
Terrace sites	44.43	6.26	19.60	8.45	0.75	0.08	0.00	2.96	4.76	0.00	4.23	0.00
Slope sites	13.37	4.85	12.41	1.05	9.03	1.15	3.03	12.96	13.95	0.29	12.69	0.02
Total	26.14	4.36	16.45	7.05	5.25	0.99	1.56	7.91	8.78	0.42	7.73	0.50
rel. Dominance in %	S13	S14	S15	S16	S17	S18	S19	S20	S21	S22	S23	S24
Riparian sites	2.76	0.82	1.10	1.15	0.83	0.00	0.14	0.48	0.18	0.07	1.13	0.04
Terrace sites	0.00	0.00	0.00	2.66	0.00	0.00	0.00	0.00	0.00	0.00	1.93	0.94
Slope sites	0.45	0.26	0.00	2.37	0.00	1.66	0.00	0.00	0.00	0.00	1.37	1.04
Total	1.04	0.37	0.32	2.07	0.24	0.85	0.04	0.14	0.05	0.02	1.41	0.73
rel. Dominance in %	S25	S26	S27	S28	S29	S30	S31	S32	S33	S34	S35	S36
Riparian sites	0.07	1.76	0.00	0.00	0.00	0.00	0.27	0.14	0.00	0.07	0.00	0.13
Terrace sites	0.00	0.77	0.83	0.25	0.00	0.18	0.44	0.00	0.00	0.00	0.00	0.00
Slope sites	0.00	1.61	0.44	0.28	0.00	0.00	0.15	0.00	0.00	0.00	0.16	0.00
Total	0.02	1.49	0.39	0.19	0.00	0.04	0.24	0.04	0.00	0.02	0.08	0.04
rel. Dominance in %	S37	S38	S39	S40	S41	S42	S43	mix				
Riparian sites	0.09	0.00	0.07	0.00	0.00	0.26	0.05	0.00				
Terrace sites	0.21	0.00	0.12	0.12	0.00	0.00	0.00	0.00				
Slope sites	0.00	0.00	0.38	2.67	0.08	0.74	1.15	0.40				
Total	0.07	0.00	0.24	1.40	0.04	0.46	0.60	0.21				

The highest percentage of *Pterocarya rhoifolia* and *Aesculus* trees occurred in site 1, with 22.88 % and 3.90 %, respectively. The highest relative dominance of small-leaved *Acer* was found in sites 1 and 7, with around 3 %. With relative dominance values of 3.44 % *Tilia japonica* occurred only in site 1 and 2.95 % *Picea abies* only in site 6.

The Terrace sites showed a slightly different distribution, as the relative dominance of *Juglans ailantifolia* increased to 44.43 % and the amount of *Pterocarya rhoifolia* trees decreased to a value of 8.45 %. The order of the three dominant species was still the same with *Juglans ailantifolia*, *Cryptomeria japonica* and *Pterocarya rhoifolia*. Significant were the differences between the sites regarding the occurrence of *Pterocarya rhoifolia* trees. With 17.68 % relative dominance in site 11, the number was higher than in most of the Riparian sites, while site 13 had reached values of only 0.24 %. The occurrence of *Aesculus turbinata*, big-leaved and small-leaved *Acer* species and *Cornus controversa* increased to values of (6.26 %, 4.76 %, 4.24 % and 2.66 %). The relative dominance of *Magnolia obovata* increased slightly to 2.96 %. Generally, the species distribution shifted a bit towards *Acer* species and *Aesculus turbinata*, also the dominance of *Juglans ailantifolia* trees increased, compared to the other two main species. The highest number of *Acer* species can be found with relative dominance values of 6.52 % and 5.43 % in site 12, together with around 2 % relative dominance of *Quercus mongolica*, *Morus australis* and *Tilia japonica*.

The Slope sites had less dominated species occurrences, as the relative dominance was split among five species, accounting more than 10 % each. The highest relative dominance values belonged to small-leaved *Acer* species, *Juglans ailantifolia*, *Magnolia obovata* and *Cryptomeria japonica*. With 9.03 % the relative dominance of *Quercus mongolica* was also high, followed by *Aesculus turbinata* (4.85 %), *Fagus crenata* (3.03 %) and *Hamamelis japonica* (2.67 %). When all Slope sites are considered, the strongly varying dominance becomes distinct. *Juglans ailantifolia* accounted 22.05 % to 24.44 % in sites 3, 5 and 8, while the lowest dominance was found in site 9 (1.71 %). A similar behaviour was observed for *Magnolia obovata*, with high dominances in sites 2 and 5 (19.60 % and 23.18 %), small-leaved *Acer* species for sites 2, 3 and 8 (19.60 %, 17.92 % and 17.70 %), *Cryptomeria japonica* for sites 2, 10 and 3 (23.47 %, 12.37 %, and 11.97 %) and big-leaved *Acer* species for sites 9, 10 and 5 (28.39 %, 15.72 % and 12.28 %). *Carpinus cordata* had in sites 2, 8 and 9 relative dominance values of 2.40 %, 3.33 % and 1.90%, and *Tilia japonica* was more frequent in sites 3, 8, 9 and 10 (1.81 %, 1.19 %, 2.02 % and 3.99 %). The three dominant species for the different sites are provided in Table 19. It was observed that the occurrence order of the five main species was in all sites different.

Table 18 Species identified from images with the following parameters: Canopy area (CA), tree counts (TC), relative Density, Density and Density per ha

Species	Canopy area in m ²	Canopy area in %	Tree counts	relative Density (TC)	relative Density (CA)	Stem density pro ha
S01	55208.69	26.14	453	8.56	26.14	14.39
S02	9198.51	4.36	124	2.34	4.36	3.94
S03	34738.63	16.45	990	18.72	16.45	31.45
S04	14890.64	7.05	202	3.82	7.05	6.42
S05	11087.50	5.25	289	5.46	5.25	9.18
S06	2088.29	0.99	53	1.00	0.99	1.68
S07	3288.59	1.56	42	0.79	1.56	1.33
S08	16711.67	7.91	210	3.97	7.91	6.67
S09	18534.28	8.78	1774	33.54	8.78	56.35
S10	883.08	0.42	20	0.38	0.42	0.64
S11	16330.68	7.73	353	6.67	7.73	11.21
S12	1059.26	0.50	87	1.64	0.50	2.76
S13	2192.87	1.04	45	0.85	1.04	1.43
S14	782.92	0.37	22	0.42	0.37	0.70
S15	682.12	0.32	35	0.66	0.32	1.11
S16	4364.24	2.07	97	1.83	2.07	3.08
S17	512.97	0.24	9	0.17	0.24	0.29
S18	1805.13	0.85	34	0.64	0.85	1.08
S19	88.16	0.04	1	0.02	0.04	0.03
S20	294.20	0.14	4	0.08	0.14	0.13
S21	112.77	0.05	2	0.04	0.05	0.06
S22	44.04	0.02	2	0.04	0.02	0.06
S23	2974.49	1.41	88	1.66	1.41	2.80
S24	1540.99	0.73	36	0.68	0.73	1.14
S25	43.57	0.02	1	0.02	0.02	0.03
S26	3149.99	1.49	61	1.15	1.49	1.94
S27	821.90	0.39	17	0.32	0.39	0.54
S28	407.04	0.19	18	0.34	0.19	0.57
S29	0.00	0.00	0	0.00	0.00	0.00
S30	74.50	0.04	0	0.00	0.04	0.00
S31	510.78	0.24	39	0.74	0.24	1.24
S32	85.24	0.04	1	0.02	0.04	0.03
S33	0.00	0.00	0	0.00	0.00	0.00
S34	43.42	0.02	5	0.09	0.02	0.16

S35	168.80	0.08	3	0.06	0.08	0.10
S36	82.38	0.04	1	0.02	0.04	0.03
S37	144.48	0.07	2	0.04	0.07	0.06
S38	0.00	0.00	0	0.00	0.00	0.00
S39	505.67	0.24	13	0.25	0.24	0.41
S40	2952.27	1.40	77	1.46	1.40	2.45
S41	92.10	0.04	12	0.23	0.04	0.38
S42	963.61	0.46	33	0.62	0.46	1.05
S43	1271.55	0.60	32	0.61	0.60	1.02
mix	435.41	0.21	2	0.04	0.21	0.06
Sum	211167.39		5289	100.00	100.00	

Table 19 Dominant species for the Slope sites, whereby the first row contains the most frequent ones, the second frequent ones in the second row and the third frequent in the third row. When the values of the relative dominance were less than 1% different between two species, they were both counted

Site 2	Site 3	Site 5	Site 8	Site 9	Site 10
<i>Cryptomeria japonica</i>	<i>Juglans ailantifolia</i>	<i>Juglans ailantifolia</i>	<i>Juglans ailantifolia</i>	Big-leaved <i>Acer</i>	Big-leaved <i>Acer</i>
Small-leaved <i>Acer</i>	Small-leaved <i>Acer</i>	<i>Magnolia obovata</i>	Small-leaved <i>Acer</i>	<i>Cryptomeria japonica</i>	<i>Magnolia obovata</i> / <i>Cryptomeria japonica</i>
<i>Magnolia obovata</i>	<i>Cryptomeria japonica</i> / <i>Quercus mongolica</i>	Big-leaved <i>Acer</i>	<i>Quercus mongolica</i>	<i>Quercus mongolica</i> / <i>Magnolia obovata</i>	<i>Quercus mongolica</i> / <i>Aesculus turbinata</i>

4.3.2.6 Tree species frequencies and abundances

The presented analyses used the tree counts of the orthomosaics for the most frequent species. As a study with 41 identified species was complex, the reduction to the above-mentioned species was necessary.

Figure 49 presents the frequency of the considered tree species. The highest frequency had *Juglans ailantifolia* trees, with a value of 40.89, when all 13 sites were taken into account. Small-leaved *Acer* species had a frequency of 37.50. *Acer mono maxim*, *Magnolia obovata*, *Quercus mongolica*, *Aesculus turbinata* and *Cornus controversa* occurred also frequent. All other species were less frequent, even though they still belonged to the main species.

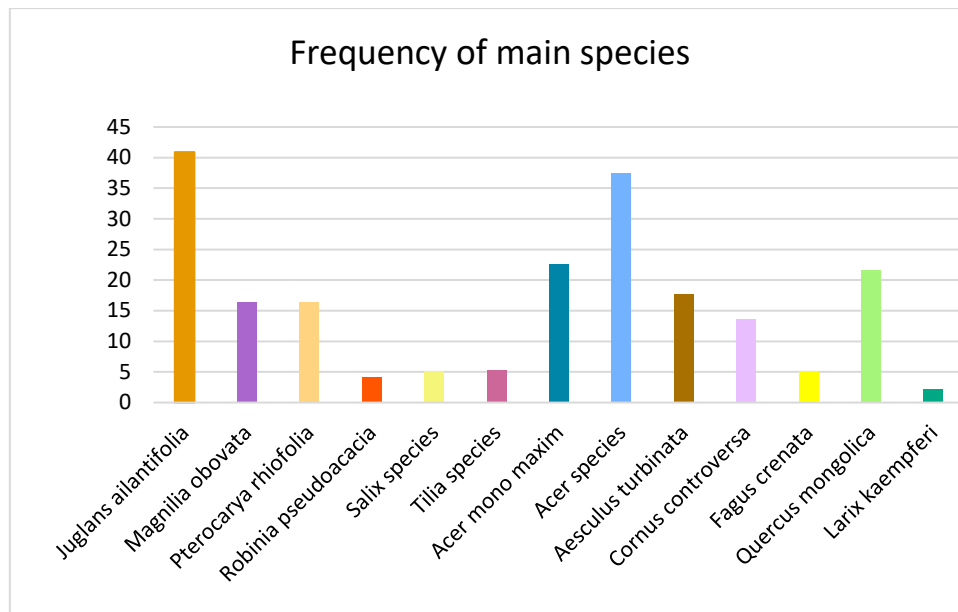


Figure 49 Frequency of main species of all sites

Juglans ailantifolia trees had the highest relative frequency with 19.6 (Table 20), followed by the small-leaved and big-leaved *Acer* species (17.97 and 10.82), and *Quercus mongolica* with 10.4. The order slightly changed, when the relative density, relative dominance and important value index were considered, but the top four tree species were still the same. Only the relative dominance of *Magnolia obovata* became higher (10.92) than its relative frequency and important value index. It was further observed that the important value index for *Juglans ailantifolia* and small-leaved *Acer* species was the highest (67.51 and 76.46), while the abundance for both species was low (1.09 and 4.95). Generally, the abundances of *Salix species*, *Larix kaempferi* and *Fagus crenata* were high, while their other values were usually low. The relative dominance values showed that the tree species, which occurred in most sites, still had completely different distributions and influences on the calculated values. The relative dominance of *Juglans ailantifolia* trees was three times higher than the value of small-leaved *Acer* species, and significantly higher than *Robinia pseudoacacia*. *Quercus mongolica* had an average relative dominance of 7.24, but the importance value of 25.20 was high.

Table 20 Main species with the following parameter: Frequency, density, abundance, dominance and importance value

Tree species	Relative frequency	Abundance	Relative density	Relative dominance	Important value index
Juglans ailantifolia	19.60	1.09	11.84	36.06	67.51
Magnolia obovata	7.85	1.37	5.49	10.92	24.26
Pterocarya rhoifolia	7.90	1.19	5.28	6.01	19.19
Robinia pseudoacacia	2.00	0.81	0.92	0.45	3.36
Salix species	2.46	2.49	3.45	2.12	8.04
Tilia species	2.55	1.24	1.59	2.06	6.21
Big-leaved Acer species	10.82	2.24	9.23	10.67	30.72
Small-leaved Acer species	17.97	4.95	46.38	12.11	76.46
Aesculus turbinata	8.45	0.85	3.24	6.01	17.70
Cornus controversa	6.50	0.86	2.54	2.85	11.89
Fagus crenata	2.46	1.79	1.10	2.15	5.71
Quercus mongolica	10.40	1.52	7.56	7.24	25.20
Larix kaempferi	1.02	2.41	1.39	1.36	3.77

4.3.2.7 Forest main tree species areas

For the 13 sites, the 5 % interval was calculated, as total areas for tree species below the 5 % interval were considered as minor tree species, and the ones above 5 % as dominant species. The 5 % border was calculated based on the total area of all tree species with the following result:

Riparian sites: site 1: 1584.33 m²; site 4: 458.34 m², site 6: 555.00 m²; site 7: 497.11 m²

Terrace sites: site 11: 530.30 m²; site 12: 627.84 m²; site 13: 879.01 m²

Slope sites: site 2: 1262.82 m²; site 3: 1318.07m²; site 5: 695.06 m²; site 8: 546.62 m²;
site 9: 703.05 m²; site 10: 903.82 m²

All species with canopy areas lower than these values were not considered for the respective site. The values for the canopy area are provided in Appendix E (part2). The Riparian sites had the following dominant species, which were between three and four different ones: site 1: *Juglans ailantifolia*,

Pterocarya rhoifolia and *Cryptomeria japonica*; site 4: *Juglans ailantifolia*, *Cryptomeria japonica*, *Salix serissaefolia* and *Pterocarya rhoifolia*; site 6: *Cryptomeria japonica*, *Juglans ailantifolia*, *Pterocarya rhoifolia* and *Salix jessoensis*; site 7: *Juglans ailantifolia*, *Pterocarya rhoifolia*, *Cryptomeria japonica* and *Salix jessoensis*.

The Terrace sites had the following dominant tree species: site 11: *Juglans ailantifolia*, *Cryptomeria japonica*, *Pterocarya rhoifolia* and *Aesculus turbinata*; site 12: *Juglans ailantifolia*, *Pterocarya rhoifolia*, *Cryptomeria japonica*, *Aesculus turbinata*, small-leaved *Acer* species and big-leaved *Acer* species; site 13: *Juglans ailantifolia* and *Cryptomeria japonica*. While site 13 had basically only one natural tree species, site 12 had five.

The Slope sites had more species, which passed the border of 5 % of the total canopy area. This indicates that the trees were distributed more equally among the species. The dominant species were: site 2: *Cryptomeria japonica*, small-leaved *Acer* species, *Magnolia obovata*, big-leaved *Acer* species, *Quercus mongolica* and *Aesculus turbinata*; site 3: *Juglans ailantifolia*, small-leaved *Acer* species, *Cryptomeria japonica*, *Quercus mongolica*, *Magnolia obovata* and big-leaved *Acer* species; site 5: *Juglans ailantifolia*, *Magnolia obovata*, big-leaved *Acer* species, *Quercus mongolica*, small-leaved *Acer* species; site 8: *Juglans ailantifolia*, small-leaved *Acer* species, *Quercus mongolica*, big-leaved *Acer* species, *Hamamelis japonica*; site 9: Big-leaved *Acer* species, *Cryptomeria japonica*, *Quercus mongolica*, *Magnolia obovata*, small-leaved *Acer* species, *Fagus crenata*, *Betula corylifolia*, *Hamamelis japonica* and *Aesculus turbinata*; site 10: Big-leaved *Acer* species, *Magnolia obovata*, *Cryptomeria japonica*, *Quercus mongolica*, *Aesculus turbinata*, small-leaved *Acer* species and *Juglans ailantifolia*.

4.3.2.8 Area per tree

'Area per tree' calculations were performed to evaluate the accuracy of tree detection in images based on the annotated canopy area. The values were supposed to provide an overview of different tree species canopy areas. For the analyses only tree species were evaluated in Figure 50, which were found in most of the sites, to be able to compare the values. The values for all sites are provided in Appendix F (part 3).

The two figures show some of the characteristic tree species of Riparian and Terrace forests in A) and Terrace and Slope species in B). As already presented before, the tree species distributed in nearly all sites and changes between the sites can be observed. *Juglans ailantifolia* trees had large canopy areas in most of the sites, ranging between 54.19 m² and 111.31 m², with a mean value of 73.73 m². The highest values were found for sites 1, 3 and 10, while the lowest were in sites 2 and 6. There seemed to be no significant differences between Riparian, Terrace and Slope sites. *Salix jessoensis* showed a

similar trend of the canopy area as *Juglans ailantifolia*, except for site 1, where the value was significantly lower (46.45 m²). With 64.53 m², the mean canopy area was around 10 m² smaller than the one of *Juglans ailantifolia*. *Pterocarya rhoifolia* did not occur in sites 9 and 10, had values between 20.64 m² (site 13) and 118.41 m² (site 8) and a mean value of 58.08 m². The canopy areas for the Riparian sites were similar, with values around 55 m², but the values for the Terrace and Slope sites varied strongly. *Aesculus turbinata* did not occur in site 4, *Salix jessoensis* not in sites 2, 9, 11, 12 and 13 and *Cornus controversa* not in site 7. Similar variations were found for the canopy areas of *Aesculus turbinata* and *Cornus controversa*, the latter having lower values than *Aesculus turbinata*. Large canopy areas of *Cornus controversa* occurred only in sites 2 and 3 (48.25 m² and 38.1 m²). Both species did not show significant differences between the considered sites.

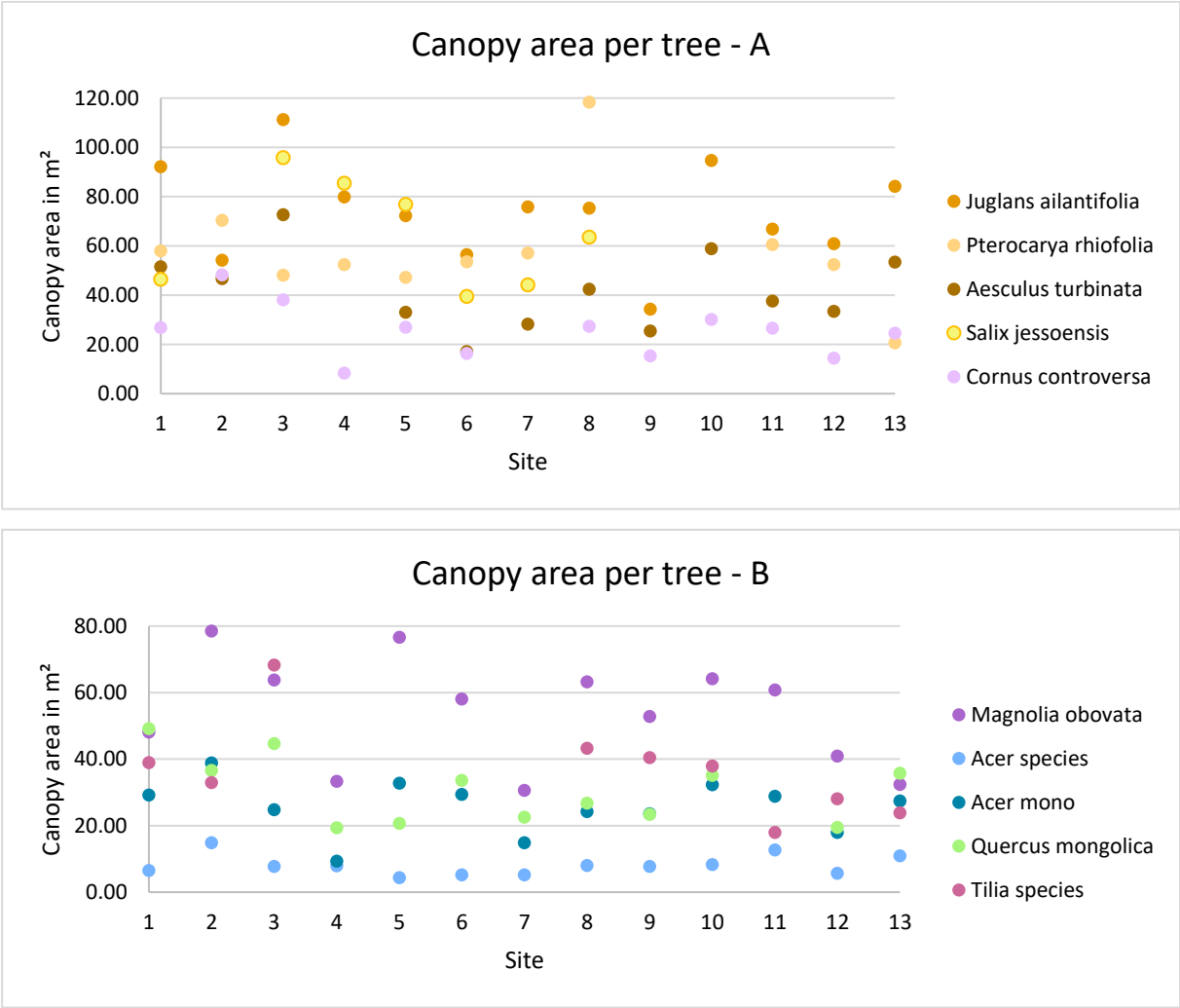


Figure 50 Canopy area per tree for all sites, divided into species which mainly occur in Riparian and Terrace sites (A) and species that mainly occur in Terrace and Slope sites (B)

The canopy areas of *Cornus controversa* and *Acer mono maxim* showed a similar trend along the different sites, with mean canopy areas of 25.69 m² and 25.26 m². The small-leaved *Acer*, *Acer mono maxim*, *Tilia* and *Quercus mongolica* had smaller canopy areas, with maximum values of 49.20 m² for

Quercus mongolica, 38.92 m² for *Acer mono maxim* and 14.93 m² for small-leaved *Acer*. Only *Tilia* had large canopy areas in site 3, with 68.35 m². Highest mean canopy area had *Tilia* (36.9 m²), followed by *Quercus mongolica* (30.63 m²) and *Acer mono maxim* (25.69 m²). Small-leaved *Acer* species had the lowest canopy areas (8.12 m²), with little variations between the sites. An exception was *Magnolia obovata*, which had a higher mean canopy area (54.16 m²), with smallest areas in sites 4 and 13 (33.33 m² and 32.42 m²). The largest canopy areas for *Magnolia* were identified in the Slope sites (more than 60 m²) and the lowest in the Riparian sites (around 40 m²). *Tilia* species had also large canopy areas in the Slope sites, but the lowest in the Terrace sites.

The smallest mean canopy areas of all trees belong to shrub species, like *Alnus fauriei*, *Zanthoxylum piperitum*, with 9.34 m² and 4.34 m². *Robinia pseudoacacia*, one of the larger tree species, had the smallest canopy area of all trees from the subcanopy layer (14.41 m²). The coniferous tree species *Larix kaempferi* and *Cryptomeria japonica* had also comparably small canopy areas of 23.73 m² and 23.34 m², while *Picea abies* had a large mean canopy area (73.73 m²). Tree species, like *Styrax obassia*, *Corylus sieboldianum*, *Carpinus cordata*, or *Hamamelis japonica*, which were located in the slope, had canopy areas between 12.13 m² and 22.23 m². The largest measured mean canopy area was found for *Alnus* species, with a value of 88.16 m².

4.3.3 Discussion

4.3.3.1 Species composition

The analyses of tree densities, dominances and frequencies revealed some clear characteristics of the considered forests. Overall, the forest sites were all composed of more than ten different tree species. Those different species showed different frequencies, when all sites were considered together, but also the comparison of the single sites revealed significant differences, when tree densities were analysed. Riparian sites consist of *Pterocarya rhoifolia*, *Juglans ailantifolia* and *Salix* species, which are representative for this kind of forest. While *Juglans ailantifolia* trees occurred basically everywhere, *Pterocarya rhoifolia* and *Salix* trees grew mainly close to the river. *Pterocarya* seemed to be the better adapted species, compared with the *Salix* trees, as they dominated the forest parts close to the river or in water saturated depressions (site 6, e.g.). Other species grew rarely in between. In areas, further away from the river or in higher elevations, neither *Pterocarya rhoifolia* nor *Salix* species occurred. Only in site 3 a small number of *Salix* trees grew near the river. *Pterocarya rhoifolia* trees were also found in sites 11, 12, 13, 2 and 3, which were further away from the river, but still at low elevations. *Juglans ailantifolia* trees occurred in all sites, but it preferred the lower elevated regions, as the higher tree numbers for the Riparian and Terrace sites confirmed. *Aesculus turbinata*, *Magnolia obovata* and

Cornus controversa had similar frequencies and tree numbers in the different sites. The species did not occur directly in the riparian areas, but were located along the borders of the ROI, often at the bottom of the slopes. The species occurred especially in sites 11, 12 and 13, while *Magnolia obovata* trees grew additionally more frequent in sites 2, 4 and 10. Those species seemed to occur mainly in transition zones between river and mountains, and showed that their physiology adapts well to different environmental conditions. Their lower frequency indicated that their adaptability to different environments worked well (allrounders), but that they could not compete with species, which were specialists to characteristic niches, like *Pterocarya rhoifolia* or *Salix* species, which dominated the wet areas.

In sites 1 and 7 a high number of *Acer* species occurred, which were mainly distributed along the bottom of slopes. The numbers of individuals were less in flat areas and also decreased towards the mountain ridges. Small-leaved *Acer* species are known for their shade-tolerance, which allows the species to grow in more challenging environments. Individuals grew under huge canopies of *Juglans ailantifolia*, *Aesculus turbinata* or *Magnolia obovata* trees e.g. In comparison, *Acer mono maxim* (or in general big-leaved *Acer* species) occurred less frequent in lower sites, but more frequent in higher altitude areas of Slope sites, which indicated their tolerance to lower temperatures and their survival abilities with low soil moisture.

In comparison, species like *Larix kaempferi* or *Fagus crenata* occurred only in small numbers in the Riparian sites. While *Larix kaempferi* was planted in sites 1 and 4, *Fagus crenata* only grew in sites with higher elevations. This indicated that the climate in the bottom sites might be too warm for these species. Tree species like *Carpinus cordata*, *Corylus sieboldiana* and *Hamamelis japonica* seemed to have similar characteristics.

Each site was unique in their species composition and also in the observed distribution. The relative frequencies and densities indicated that there were characteristic species for each forest type: the Riparian forest with *Pterocarya rhoifolia*, *Juglans ailantifolia* and *Salix* species; Terrace sites with *Juglans ailantifolia* and *Acer* species; the Slope sites with *Acer* species (big and small-leaved), *Quercus mongolica* and *Magnolia obovata*. There were several species, which occurred in all sites, but with different densities, which has to be related to the stand conditions (soil conditions, water availability) and competition with other tree species. Those factors made the forests unique. The analysed species compositions showed that mixed forests are a mosaic of various species, characterised by a couple dominant, a couple minor and infrequent ones. A mixed forest should therefore be classified more precisely, based on the occurrence of tree species, the dominance of tree species and the degree of mixture.

4.3.3.2 Species distribution

The observed values elucidated the dominance, importance and density of *Juglans ailantifolia* and small-leaved *Acer* species for all sites, while tree species like *Magnolia obovata*, *Aesculus turbinata* and *Pterocarya rhoifolia* were relatively rare in a direct comparison. Most of the identified species occurred with less than 50 individuals in all sites, resulting in low stem densities. A direct comparison between the canopy area and the counted tree steps showed that there was a wide range of canopy structures. Small-leaved *Acer* with a large number of stems, had low canopy areas, which also means that even though the trees grew dense, the total area of small-leaved *Acer* species was small. Opposite, *Juglans* trees cover large parts of the forest floor when they grow dense.

The combination of results of the canopy area, tree counts, the differences of occurring tree species and their dominance illustrated significant differences for the different sites. *Juglans ailantifolia* and *Pterocarya rhoifolia* trees occurred in Riparian and Terrace sites, while *Salix* species only occurred in Riparian sites. Therefore, conditions between the Riparian and Terrace sites change, but are still comparable. The distribution of *Juglans* trees also in the Slope sites indicated that they must have suitable conditions there. The dominance of trees like *Quercus mongolica*, *Magnolia obovata* and *Acer* species indicated that the site conditions of the Riparian and Terrace sites were different. Tree distributions therefore indicate changes along the sites and allow comparisons.

Analyses of single tree species and their occurrence can improve the understanding of their distribution. While frequencies and relative densities take all quadrants and all species into account, which are based on tree counting, the dominance is calculated from the canopy areas. The observed patterns with stem densities and canopy areas were therefore presented in these data, as well. Trees like *Magnolia obovata* and *Pterocarya rhoifolia*, which occurred in different sites, showed the same relative frequency and density, while the relative dominance elucidated that *Magnolia obovata* dominated more parts of the forest. Similar relative dominances had *Acer mono maxim*, while both relative frequency and density were higher than the ones of *Magnolia obovata*. *Acer mono maxim* had therefore more tree stems, while the abundance with 2.24 indicated that the tree stems grew close together as they did not occur in many plots. Again, compared the abundance of *Acer mono maxim* with the one of *Magnolia obovata*, *Magnolia obovata* trees were distributed further. The important value index then summarised the data, considering all single calculated values.

The dominance and importance values would be higher for *Pterocarya rhoifolia*, when only Riparian sites would have been considered. It would be similar for *Quercus mongolica*, *Aesculus turbinata*, big-leaved *Acer* species and *Magnolia obovata*, when only higher elevated sites would have been considered. But also, for single sites significant differences would be found, like in sites 1, 6 and 7 of

the Riparian sites for *Robinia pseudoacacia*. The invasive species had only 35 trees, but they were all distributed in sites 1, 6 and 7, varying significantly in relative tree canopy area.

All calculated values allowed therefore the interpretation of the composition and distribution in the forest, by comparing the values and using the knowledge from tree stem densities and area calculations.

4.3.3.3 Tree canopy areas

Canopy areas can be used as a measure for forest densities, stand volumes, growth and biomass estimations, which are needed to provide essential management services. With image analyses, where the forest is observed from above, it is relatively easy to first annotate, then to measure or calculate the canopy area.

The data provided an overview of the canopy structures of the different tree species. It was expected to find significant differences, because the canopies were stronger overlapping in slopes than in riparian areas, because of the slope. However, there were almost no significant differences between Riparian, Terrace and Slope sites. *Cornus controversa* is a tree species, which was often partially covered by taller neighbouring trees, as in orthomosaics the canopy was visible at the borders of larger trees in a half-moon shape. In the case of *Juglans ailantifolia* and *Pterocarya* trees, the canopy areas seemed to be large in sites 1, 3, 8 and 10 with values around 100 m². Especially in higher elevated areas the possibility of miscounting trees was given due to the high density of the forest. However, patches with high densities of trees were also found in riparian forest sites, increasing the risk of miscounting and hence influencing the canopy area per tree. Trees like *Aesculus turbinata* and *Quercus mongolica* grow usually large, but the values calculated for this study were low, especially compared to e.g., *Juglans* trees. Both species had small as well as old-growth trees. The calculated value was a mean value and did therefore not represent the spectrum of trees and their ages. Especially the canopy areas for *Quercus mongolica* were small, but in lower elevated areas it could be observed that these trees were often partially covered by *Magnolia* or *Juglans* trees. Furthermore, the canopy areas of *Acer mono maxim* seemed to be quite large, since *Acer* trees usually have smaller canopy areas, confirmed by values of the small-leaved *Acer*. *Acer* belongs to the species, which can have multi-stems, forming a dense canopy, where it is hard to differentiate single tree canopies.

Generally, the calculated canopy areas revealed differences between species and helped to evaluate the dominance of trees in the forest. Large canopy areas must belong to a species, which dominates the forest. Species, belonging to canopy layer, were, according to the calculated canopy areas: *Juglans ailantifolia*, *Pterocarya rhoifolia*, *Picea abies*, *Salix jessoensis*, *Phellodendron amurense*, *Magnolia*

obovata, and *Fagus crenata*. Species with canopy areas between 20 m² and 45 m² were mainly considered as subcanopy species. Still, further comparisons with field data would help to increase the accuracy of the data, as the sites had different characteristics, like slope angles, which influence the canopy structure. In a future analysis it would be helpful to annotate single trees, to get a distribution of canopy areas of the same species to provide a better overview of the tree species.

A main point, which was identified, was that canopy areas can be annotated fast and areas can be calculated accurately. In comparison, tree counting was difficult in images, as tree canopy areas can be dense and influence annotations of tree tops. As already mentioned, small-leaved *Acer* species have multi-stems characteristics, the tree stems can be overestimated and hence canopies can be miscounted. In dense *Juglans* or *Pterocarya* areas, which have flat canopies, the number of trees can be easily underestimated, especially when the tree stems are located close to each other. Therefore, the use of canopy areas is a better measure, for densities, dominances, abundances and frequencies of tree species, as they provide more accurate results than counting.

4.3.3.4 Forest classification on image-based analysis

When the forest is observed from above, the main information about tree species is the canopy surface. Usually, for forest classifications tree numbers and densities were chosen, manual surveys were performed (Fukumachi et al., 2020; Suzuki et al. 2002). With the obtained results of this study, tree counting based on UAV images cannot be recommended for forest classifications in YURF. Especially in mixed deciduous forests, even manual tree counting on images was inaccurate, and counting with automatic systems failed. However, the canopy area was clearly detectable on images and automatic classifications worked well for several tree species already. Therefore, it is recommended to use canopy areas to classify forests.

Cryptomeria japonica trees were excluded from the naming of the forests. They were part of most of the sites; however, they were planted around the study sites and did therefore not occur naturally in the sites. Since the research focussed on the naturally grown forests, *Cryptomeria japonica* patches were not surveyed and therefore also not included in the naming. The naming was performed using the main species and the subspecies.

All riparian forests were *Juglans ailantifolia* forests mixed with *Pterocarya rhoifolia* and *Salix* species. As in site 1 *Juglans ailantifolia* and *Pterocarya rhoifolia* trees had a similar percentage, the site was called a 'Mixed Japanese walnut and wingnut forest'. Sites 4, 6 and 7 were 'Japanese walnut forests with the subspecies Japanese wingnut and willows'. As the species *Pterocarya rhoifolia* was less than half of the *Juglans ailantifolia* canopy area, it was only considered as subspecies.

The Terrace sites were also classified as *Juglans ailantifolia* forests, as the species had the largest canopy area of all considered sites. In site 13 it was the major species by far, the site was therefore named a 'Japanese walnut mixed forest'. Site 11 is a 'Japanese walnut mixed forest with the subspecies Japanese wingnut and horse-chestnut'. While site 12 had five different species, it was classified as 'Japanese walnut forest with the subspecies Japanese wingnut and horse-chestnut and a subdominant layer of Maple species'.

The Slope sites contained more species, whereby a dominance of a single species, like in the Riparian and Terrace sites, was usually not found. In site 2, small- and big-leaved *Acer* were frequent, together with *Magnolia obovata*. Therefore, the forest was called 'Maple-Magnolia mixed forest with the subspecies Oak and Japanese horst-chestnuts'. Site 3 had a clear dominance of *Acer* species and *Juglans ailantifolia* trees, therefore the forest was called 'Japanese walnut and Maple mixed forest with Oak and Japanese horse-chestnuts'. Site 5 was a 'Japanese walnut – Magnolia mixed forest with the subspecies Maple and Oak'. Site 8 was named as 'Japanese walnut – Maple mixed forest with Oak and Japanese witch-hazels as subspecies'. Site 9 is a 'Painted maple forest with the subspecies Oak, Magnolia, Beech, Hazel-leaved birch, Japanese witch-hazels and horst-chestnuts'. Site 10 had again two main species, *Acer mono maxim* (mainly) and *Magnolia obovata*. It was therefore called 'Maple – Magnolia forest with the subspecies Oak, Japanese horse-chestnuts and walnuts'.

For an easier understanding use this study suggests the use of common names for tree species, while Latin tree species names should be provided for the analyses. In general, a naming of the forests of the main/dominant species should already help to classify mixed forests better, improving the system provided by [Makimoto \(2019\)](#), where mixed forests were only specified when they were composed of beech or oak trees. As it can be seen for the riparian and Terrace sites, which were all 'Japanese walnut mixed forests', a further classification of the subdominant species seems to be necessary, in order to specify those forests.

4.3.4 Conclusion

The performed manual annotations together with simple pixel counting and Census codes allowed a fast and effective assessment of important forest parameters: Density, frequency, rel. dominance and abundance. With these calculations and measurements, area distribution was analysed and characteristics of the area were provided. The benefit of image annotations was that both, counts and canopy areas, could be evaluated. Therefore, forest sites were analysed in detail using only information contained in the image.

The several applied analyses helped to understand forest composition and distributions. Riparian, Terrace and Slope sites were classified based on their tree composition. It was pointed out that Riparian areas were mainly composed of *Juglans ailantifolia*, *Pterocarya rhoifolia*, *Salix* species and small-leaved *Acer*. Terrace sites mainly contain *Juglans ailantifolia* and small-leaved *Acer*, while small- and big-leaved *Acer* were the dominant species in Slope sites. Furthermore, with increasing height, the composition of tree species changed to greater numbers of *Quercus mongolica*, *Fagus crenata* and *Larix kaempferi*.

Significant differences between tree counting and tree canopy areas enhanced the use of canopy areas for forest classifications. Therefore, forests were classified based on the dominant species, while subcanopy species needed to be added, in order to accurately name forests. Especially, because the sites all showed different characteristics.

At last, tree compositions could be accurately provided with several calculations, and diversities between the sites could be compared, while excessive analyses of the tree species distribution within one site could not be evaluated. Also, the overall forest structure could not be characterised in detailed.

Chapter 4.4: Analysis of Forest composition, diversity and structure with GIS applications

4.4.1 Problem definition

The new technologies opened the field of forestry for the collection of high-resolution data in short time. The availability of data increased the need of appropriate tools to analyse them. Image analysis and GIS software are able to deal with large datasets, can process and visualise them. Transformation of the data into diverse and multivariate forms turn the data into usable states (Wulder and Franklin, 2003).

Nowadays, field inventories can be replaced by remote sensing measurements, specifically image analyses, as they are well developed and able to deliver information, like counting or classifying trees. Plot based approaches struggle, when large-scale information are required, which can be provided by remote sensing applications. Also, there are characteristics of the forest, which are difficult to assess from field inventories, like measuring the canopy area. Hall (2003) indicated that image analysis can be a precise measure for species compositions, tree height, stand volumes or densities with the result of a detailed mapped area. Therefore, canopy structures can be still presented as discrete points, but also as two-dimensional thematic map (Fournier et al., 2003). Wulder and Franklin (2003) and Culvenor (2003) pointed out that forest management regimes became more flexible and the integration of new tools to develop forest management is increasing. The need of detailed and high-resolution data comes together with advancing technologies, enabling the gathering of the needed data. The understanding of forest increases with the analyses on different scales of forests and allows acquiring new insights into the forest environment. Fournier et al. (2003) further supported image analysis approaches, as he pointed out that structural variables (densities, frequencies, etc.) can be collected at each scale and horizontal and vertical structures of the forest could be assessed.

Image analyses are mainly performed to simplify the gathered data, analyse them in a concrete context and visualise them in a way that the necessary information can be accessed easily. Forests can be characterised on small or large scales, while they are not necessarily homogenous patches (Fournier et al., 2003). The gathering of large-scale data allows to see competition, dispersion and aggregation of tree species on a different level. Furthermore, temporal features can be easily applied in image processing software like ArcGIS or QGIS, and forest developments can be assessed and analysed. Benefits of environmental GIS data are their ability to show geomorphological or hydrological characteristics of the forest area, which can help to interpret data (Fourier et al., 2003).

Image analysis and GIS were mainly used to perform vegetation indices calculations (Asner et al., 2003; Franklin et al. 2010; Möttus and Takala, 2014). The benefits of large-scale vegetation reflectance are

adumbrated by intensive sensor calibration and atmospheric corrections. The influence of atmospheric conditions, solar geometry and changes in time affect vegetation indices significantly, which makes them less usable for fast and efficient image analysis (Asner et al., 2003). However, the analyses of RGB images have a good potential, since they have already been used by Wijaya et al. (2009) for mapping and modelling of forest biomass with GIS. Still, the potential of GIS applications for image analysis is not fully evaluated for forestry. Therefore, this study evaluated image analysis with the use of ArcGIS for forestry inventories, as they are classified as powerful, low cost and fast helpers for foresters (Culvenor, 2003). The assessment of forests characteristics on different scales was analysed and evaluated to check how such a comparison provides deeper insights into the forest.

The objectives, which were dealt with, were:

- v. Evaluation of the composition, distribution and structure of mixed forests and main tree species.
- vi. Characterization of the mixed forest with the state of art GIS techniques by using low cost and low time demanding methodologies.

In order to characterise the mixed forest, several GIS tools were applied on UAV-gathered data, which were manually annotated. The analysis focussed on the forest composition, distribution and structure, using different scales (Figure 51).

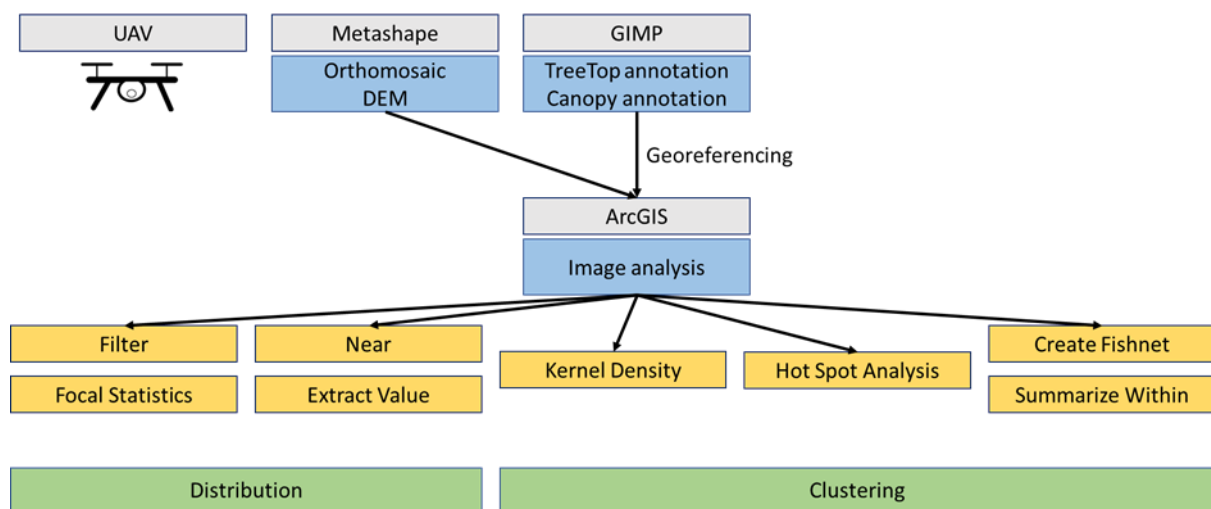


Figure 51 Overview of study

4.4.2 Methodology

Previous chapters focussed on assessing images by using counting techniques, like pixel counting for area measurements or tree top counting for composition and distribution measurements. In this chapter the idea was to provide maps supported by image analyses, which include spatial aspects of compositions, distributions and structures of the forests. ArcGIS was an efficient software for this application and was used in for the analysis of this chapter.

4.4.2.1 Data collection and processing

Images were collected with a DJI phantom 4 UAV, which is a small and user-friendly quadcopter, to perform automatic and standardised flight protocols for all sites. The flight altitude ranged between 80 and 205 m, depending on the imaged site, with the UAV flying a speed of maximal 3.7 m/s. Front and side overlaps between 90 and 97 % were chosen.

For this analysis images from summer 2019 were chosen and tree species were annotated, for each site one flight. For site 1 and 3 the flights from the 20th of June 2019 were chosen, for site 9 and 10 the 10th of July and for site 8 the 26th of July. For all other sites images taken on the 14th of June were used. The total imaged area was 61.9 ha, with 31.48 ha located in the analysed ROI. Images from the manual flights in the summer 2020 were additionally used, which were closer to the canopy (approximately 15 m above the canopy) to gather super high-resolution images. These images were used as validation of the manual annotations, as the resolution with around 1.3 cm/pixel was higher than the resolution of 2.73 cm/pixel for the automatic flights. The images from 2020 were not used for annotation because the UAV had a problem with the camera white-balance, so that the colours were incorrect. Another problem was that the alignment of the manual flights did not always work well, as the overlap of the images was not uniform.

Images from the winter season 2018, 2019 and 2020 were used to generate winter orthomosaics and DEMs. Site 1 was imaged on the 16th of April and site 4 and 6 on the 9th of April. Site 7, 11, 12 and 13 were imaged on the 19th and 20th of February 2019 and site 5, 8, 9 and 10 on March 8.

All data were processed with Metashape ([Agisoft](#)) to create orthomosaics and DEMs, which were exported with the fixed image resolution (2.73 cm/pixel) for the flight of 2019 and without a fixed resolution for the images of 2020.

4.4.2.2 Manual annotations

The first annotations were done using the GIMP software, creating layers for each tree species and the tree tops per site. The layers were exported as JPEG files for further processing.

The initially faced problem was that manual annotations were time consuming and to perform them for the same sites several times was not effective. Therefore, the initial annotations were uploaded in ArcGIS. As the annotation layers were JPEG files, they did not contain geocoordinates. The files needed to be georeferenced as a first step. For the georeferencing the original TIFF file orthomosaic of each site was used and uploaded into ArcGIS. Then, the JPEG file of the orthomosaic was uploaded and georeferenced using the coordinates stored for each site. Four control points were set, one for each corner of the orthomosaic. These four points were saved and imported for the next images of each site, and then the georeferencing automatically applied and saved. As a next step, every layer was converted with the tool *raster to polygon*. The generated shapefiles contained several polygons, based on the pixel values of the raster file. In the attribute table the single polygons were saved with their gridcode. The gridcode reflects the original pixel value. Usually, values between 0 and 255 were found in the gridcode column, because the exported layer contained some fragments of grey pixels. As the pixel value of interest was 0, which represented the black pixels in annotations, all other values were erased. In the end, all annotation layers were stored as separate polygon shapefiles. In a post-processing step, holes in the polygons were closed. Furthermore, a treetop point shapefile and the ROI were added into the ArcGIS project for each site.

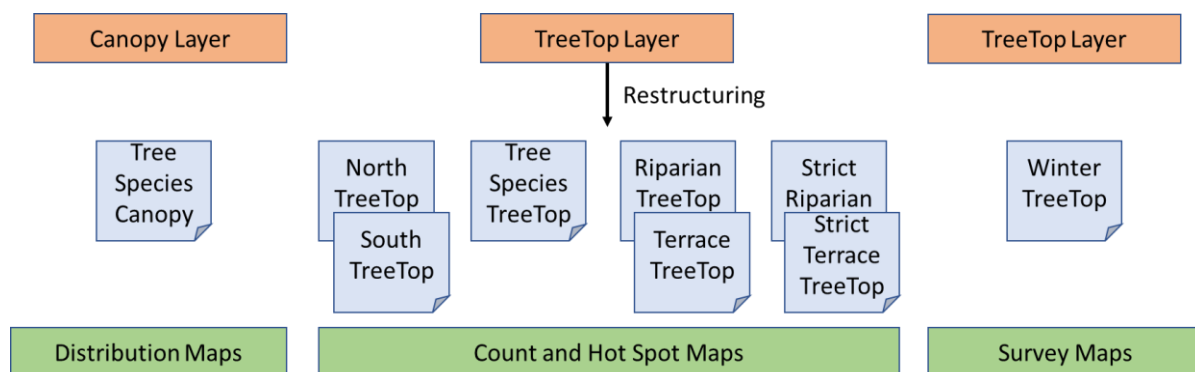


Figure 52 Generated point shapefiles and maps, an overview

4.4.2.3 Point shapefiles

The tree top layers were used for the Slope sites (treetops), while for all other sites tree top layers were corrected with the winter images, so that all tree tops were annotated for the further processes (hereafter called winter tree tops). Another set of tree top layers was annotated for the Slope sites,

only using winter images. Here, assigning labels to the stems could not be performed with a high accuracy; hence these maps were only used for further image analysis, not for survey maps. Note that no shrubs were annotated as they were not visible in winter images (Figure 52).

Every layer contained an attribute table, where the species name was assigned to each tree top. With the raster calculator the tree tops with the same name could be selected. The selected points were copied into a separate point shape file containing only the points of the same species. Tree species of sites 1, 2, 3, 4 and 5 were summarised together in the shapefile 'South point' for each tree species, and the other sites (6 to 13) in a shapefile named 'North point'. For the south a grid raster of 18 x 24 m per cell with a total of 1600 cells were used and for the north a 15 x 17 m raster with a total of 5000 cells.

A last layer set was generated, where several tree species were combined. These tree species were selected based on the information provided by [Suzuki et al. \(2002\)](#), who evaluated tree species distributions in riparian, terrace, colluvial slope and denuded slope and assigned indicator species for the mentioned kind of areas. In the riparian point shapefile, the following species were added: *Pterocarya rhoifolia*, *Salix* species, *Morus australis*, *Aesculus turbinata*, *Cercidiphyllum japonicum*, *Alnus fauriei*, *Cornus controversa* and *Juglans ailantifolia*. The terrace point shapefile contained *Quercus mongolica*, *Hamamelis japonica*, *Acer* species, *Prunus* species and *Fagus crenata* species. Another two layers were created, which contained species which only occur in Riparian sites (hereafter strict riparian): *Pterocarya rhoifolia* and *Salix* species; only in the Terrace sites (hereafter strict terrace): *Hamamelis japonica*, *Quercus mongolica* and *Fagus crenata*. The purpose here was to find the border between Riparian and Terrace sites and to see if the assumed border is the beginning of the slope.

Generated maps are called hereafter: distribution maps for maps with tree canopy areas annotated, survey maps for tree top annotations (both corrected and not corrected), count maps for winter tree top annotated maps (Figure 52).

4.4.2.4 Application of ArcGIS tools

The images gathered from the forest can be used for various image analyses. ArcGIS provides a good base to perform several image analyses and the possibility to visualise the results in the real environment. The following analyses were performed to access the site characteristics caught in the images:

The DEMs, generated as geoTIFF by Metashape, can be directly processed by ArcGIS. In this work, winter DEMs were used to calculate the slope and aspect of the studied sites. Each DEM file was first

pre-processed by applying the tools *Filter* and *Focal Statistics* to smoothen the surface. Winter images still contained the stem and the branches of deciduous trees, as well as the evergreen trees, influencing the structure and values in the DEM. The applied tools helped to focus the analysis on the earth surface. In a second step the tools *slope* and *aspect* were applied on the output of the *Focal Statistics* tool.

To evaluate the distribution of tree species and structure of the forest, the tools *Near* and *Extract value to points* were used. The goal was to assign a distance value from the river to every tree stem and a height difference value to every tree, identified in the field or in the images. At first, a river line shapefile was generated, whereby the middle of the river was annotated. In a second step, the nearest distance was calculated between the river line shapefile and the point shapefiles of the tree locations. Therefore, each tree got a distance value assigned. In a third step, the smoothened winter DEM was used to extract for each tree point a height value, which was stored in the attribute table. Both tables, containing the distance and height values, were exported from the attribute table into separate excel files.

Analysis of the density and clustering of the data were performed with the tool *Kernel density, Hot spot analysis, Summarize within*. The winter tree top layers were used for this application. In a first step, the tool *Kernel density* was run with the settings geodesic, a radius of once 8 m and once 16 m to find spatial clusters in the data. In another step grids were generated for each site. At first a rectangle polygon shapefile was generated for each site, covering all parts of the orthomosaic (ROI of the orthomosaic). With the tool *Create Fishnet* a grid was generated with a raster size of around 8 x 8 m. The tool *Summarize within* was used next, where the winter points and the grid raster (per site) were input. The tool counted the points, which fell into each raster. The geoanalytics version of the tool was used, so that only the raster cells were kept that contained a value greater than zero. Hot spot analyses were performed to identify randomness in the data. Each polygon was compared to its neighbours and it was checked if the information were significantly different to the study area. High values were marked as hot spots and low values as cold spots, while insignificant raster cells were white and marked as not significant. The parameter distance was first identified with the optimized hot spot analysis and then applied with the tool *hot spot analysis*. The analysis was performed on the winter tree top layer to identify hot and cold spots in the sites. The same tool combinations were used on the riparian/terrace point shape files and the species layer.

4.4.3 Results

In this chapter only image analysis results are presented, that have been performed with ArcGIS using manual annotations of the data. In these parts tree species usually means the tree species classes selected for the image analysis.

4.4.3.1 Tree species composition

Species compositions mean the number and the kind of species that occur in and contribute to an ecosystem or, more specific, to the studied sites. In forest inventories species compositions are represented by the number of tree stems, the DBH, the basal area and the volume of the different tree species. For tree composition survey maps were analysed, the results for all sites can be found in Appendix J and K.

At first the tree top annotations and binary layers were digitalized in ArcGIS. During this step, species names were assigned to the tree tops in the attribute table and coloured by species names to generate maps, like presented in Figure 53, which is the tree survey map of site 1. The points mark the position of the trees based on image analyses and corrected with winter images in the ROI, which is visualised with a black boundary. The survey maps further provide information about the number of species classes per site, which was in the Riparian sites 20 for site 1 and 6, 14 for site 4 and 7. ArcGIS further directly provides the function to generate histograms with data in the attribute table; two examples are provided in Figure 54 for site 1 and 6. This information is needed to assess the different site compositions. The three trees, which had the highest frequencies, were *Pterocarya rhoifolia*, *Juglans ailantifolia* and *Salix jessoensis* in site 1, while site 6 had a higher frequency of *Juglans* trees and small-leaved *Acer* species as third most frequent species. *Pterocarya* trees occurred with a slightly higher number than *Juglans* trees in site 1, but were already 100 trees more than small-leaved *Acer* species. In site 6 *Pterocarya rhoifolia* was only half the number of trees than *Juglans ailantifolia*, while in site 4 and 7 the number of *Pterocarya* was less than one quarter. Site 4 was the only site where the majority of trees belonged to *Salix serissaefolia*. In site 1, 11 species had between 10 and 40 trees per species, while site 6 had less than 10. Site 4 had a low number of trees other than *Salix* and *Juglans*, with maximum 14 trees belonging to one species, including five species with less than five trees. In site 6, 16 of the 20 tree species had less than 11 trees and in site 7, five species had less than five trees per species and a gradually increase in tree numbers from *Quercus mongolica* to *Pterocarya rhoifolia*.

The Terrace sites had 12, 18 and 17 different species classes, respectively, and a high number of trees, which could be identified on the images, but not assigned to a class label, with 149, 94 and 211 (in site 11, 12 and 13). The main two species, which were found in these sites, were small-leaved *Acer* and

Juglans ailantifolia. In site 11 and 12 *Aesculus turbinata* and *Pterocarya rhoifolia* were the next two dominant species, and climbing plant of type 1 and *Cornus controversa* in site 13. All other species in site 11 had 10 or less trees, site 13 had seven species classes with less than five trees and site 12 had an exponential increase in trees per species from *Styrax obassia* to *Aesculus turbinata*.

The numbers of tree species classes in the Slope sites were: 17 (site 2 and 5), 25 (site 3), 20 (site 8 and 9) and 21 (site 10). The dominant tree species were small-leaved *Acer*, *Cryptomeria japonica*, *Acer mono maxim* and *Quercus mongolica* for the sites 2, 3 and 5. In site 8 *Juglans ailantifolia* trees were dominant with *Quercus mongolica* and small-leaved *Acer*, while site 9 had *Acer mono maxim* as tree species with the most trees. In site 3, 15 out of the 25 tree species had less than ten trees per species, while it was eight in sites 2 and 9, seven in sites 9 and 10, and only five in site 5. Site 5 had between 40 and 55 trees of *Quercus mongolica*, *Cryptomeria japonica*, *Acer mono maxim*, *Juglans ailantifolia* and *Magnolia obovata*, which was similar to site 9, but for the species *Betula corylifolia*, *Cryptomeria japonica*, *Fagus crenata* and *Quercus mongolica*. Site 8 had a lot species with 10 to 20 trees per species. An increasing trend in trees per species was prominent in site 10.

The histograms provided a fast overview of the existing species and their number of individuals. Also, the distribution of trees per species can be read out easily. Furthermore, the data were automatically summed up and plotted in the histograms after the attribute table was generated. Still, the histograms do not provide spatial information, but the survey maps and distribution maps do.

4.4.3.2 Tree species distribution

Tree species distributions are the shape of tree species composition in a forest, the area in which a tree species lives. There are several drivers for tree species distribution, whereby climate is the most important one, and all other environmental factors, biotic and abiotic, which influence the tree species survival and reproduction. Assessing tree distribution is more challenging compared to counting of trees and a visual support allows often a better understanding of the distribution.

As already mentioned, Figure 53 contains the survey map of site 1 and a map including the canopy areas annotated in polygon shapefiles for each tree species. For all other sites the maps are shown in the Appendix I and J. The distribution maps of the Riparian sites demonstrate clearly the dominance of *Juglans ailantifolia* and *Pterocarya rhoifolia*. In site 1, *Juglans ailantifolia* was more dominant in the northern part of the image, while *Pterocarya rhoifolia* dominated the southern part. The tree survey map shows that there were a high number trees, which belonged to the *Pterocarya*, while the number of *Juglans ailantifolia* trees was lower. Also, it was observed that the composition of tree species was more homogeneous in the flat western part of the image than the eastern part (slope area), where a

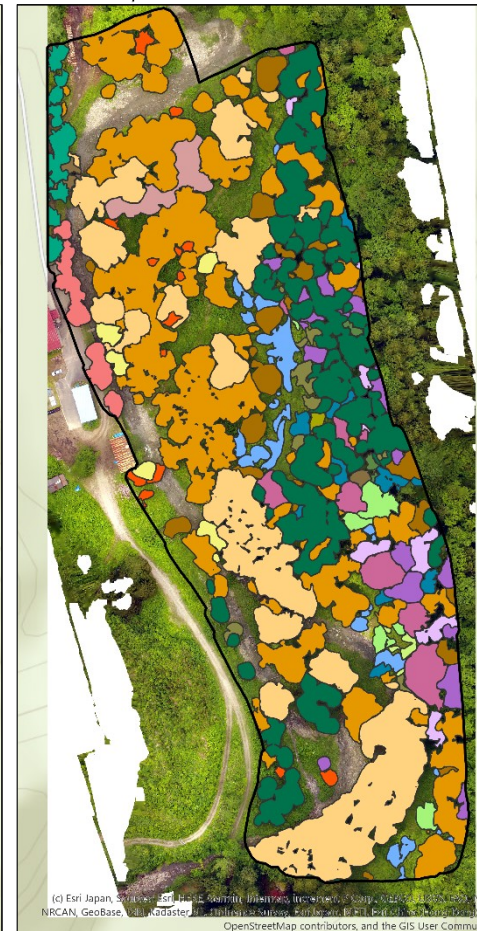
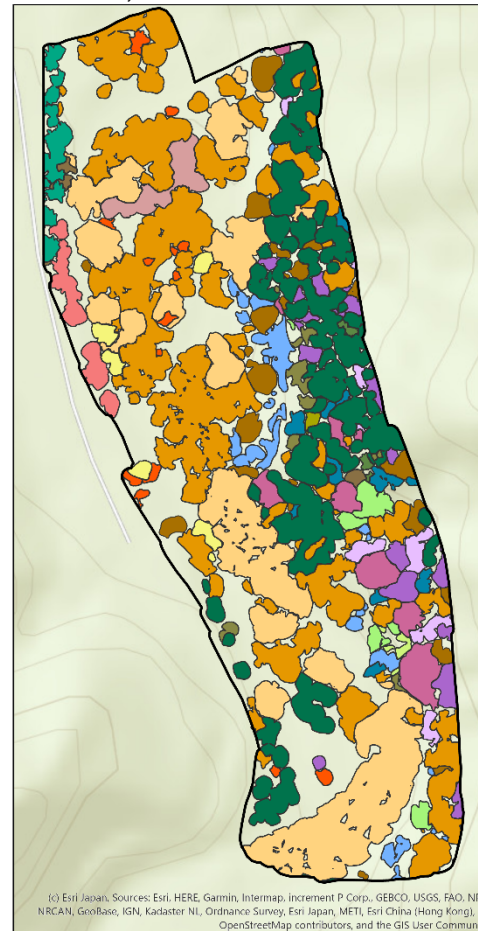
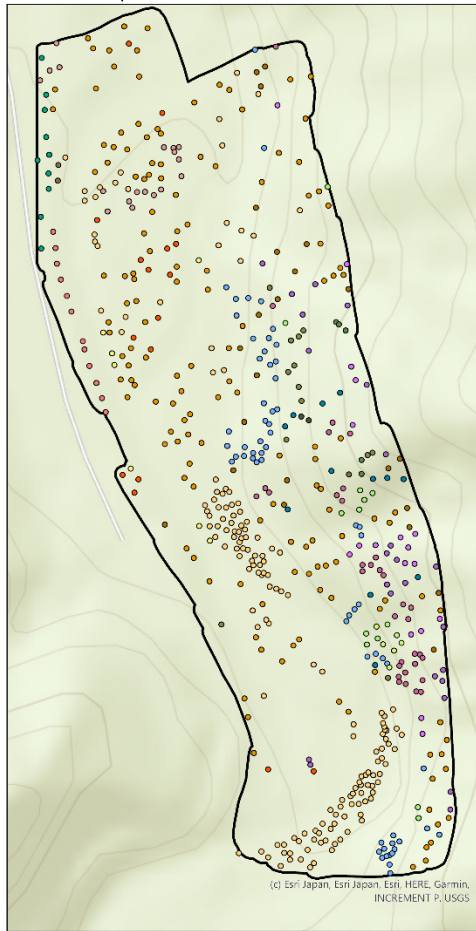
higher number of different tree species occurred. Also, minor species like *Robinia pseudoacacia* were visible, with a relatively small area compared to *Juglans ailantifolia*. Site 7 showed similar characteristics, whereby *Pterocarya rhoifolia* trees were distributed along the river, and *Juglans ailantifolia* dominated the rest of the site. Sites 4 and 6 seemed to be less dense than 1 and 7, concerning the canopy area of all trees. Site 6 showed a high diversity with the high number of tree species, while site 4 was composed of *Juglans* and a large *Salix* patch in the south. The tree survey map of site 4 showed that there was a high number of tree stems below the annotated *Salix* polygon.

All Terrace sites showed different distribution characteristics. Site 11 and 12 were similar to the Riparian sites, with a large area covered by *Juglans ailantifolia* and *Pterocarya rhoifolia*. Site 13 contained mainly *Juglans ailantifolia*, which covered, together with *Cryptomeria japonica*, most of the site. There were smaller areas covered with small-leaved *Acer* species and *Magnolia obovata*, *Cornus controversa* or *Tilia Japonica*, which distributed along higher altitude areas in all sites, except *Acer mono maxim*, which was distributed only in site 12 and 13. The point maps of all Terrace sites showed that the detected but unidentified trees were mostly distributed in areas, where the canopy area of the *Juglans* trees was less dense. They grew also along the street in site 13 and in low altitude areas in site 11 and 12. For tree species like *Tilia japonica*, *Acer* species and *Morus australis* there were higher numbers of tree tops than expected, as when only the canopy area would be considered.

The tree distribution in the Slope sites was more heterogeneous compared to the Riparian and Terrace sites. Trees grew less dense in sites 2, 3 and 8, while site 10 had the highest tree densities. In each site one species seemed to be dominant. In sites 2, 5 and 10 *Magnolia obovata* trees had a large canopy area in the higher elevated areas of the sites, and in site 9 *Acer mono maxim* dominated. Site 8 had a high degree of mixture of different tree species, with larger areas occupied by small-leaved *Acer* and *Juglans ailantifolia*. Along the ridge in site 3 *Quercus mongolica* trees were dominant; the slope areas were a mix of mainly small-leaved *Acer* and *Magnolia obovata*, and on the western slopes *Juglans ailantifolia* grew. In site 2, *Magnolia* trees grew along the ridge and small-leaved *Acer* in all directions of the slope around the *Magnolia* trees. In site 5 *Magnolia obovata* and *Quercus mongolica* distributed mainly in higher elevation areas (Figure 55). *Acer mono maxim* is a species which seemed to occur in all altitudes and *Juglans* trees at the bottom of the slope in most of the sites. In site 2 and 3 small areas of small-leaved *Acer* occur together with a high number of trees. *Juglans* and *Magnolia* tree tops seemed to be less compared to the area. Furthermore, all other tree species have an even distribution of trees in the site

Species map site 1 (YURF)

by Sarah Kentsch



Legend

Species labels

- ROI
- Juglans ailantifolia
- Aesculus turbinata
- Cryptomeria japonica
- Pterocarya rhoifolia
- Quercus mongolica
- Larix kaempferi
- Magnolia obovata
- Acer
- Prunus
- Acer mono maxim
- Salix jessoensis
- Castanea crenata
- Robinia pseudoaccacia
- Cornus controversa
- Climbing plant 1
- Tilia
- Alnus fauriei
- Phlledendron amurense
- Corylus sieboldiana
- Carpinus cordata

S1.jpg

- RGB
- Red: Band_1
 - Green: Band_2
 - Blue: Band_3

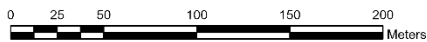


Figure 53 Count map (left), species map without orthomosaic (middle) and with orthomosaic (right) of site 1

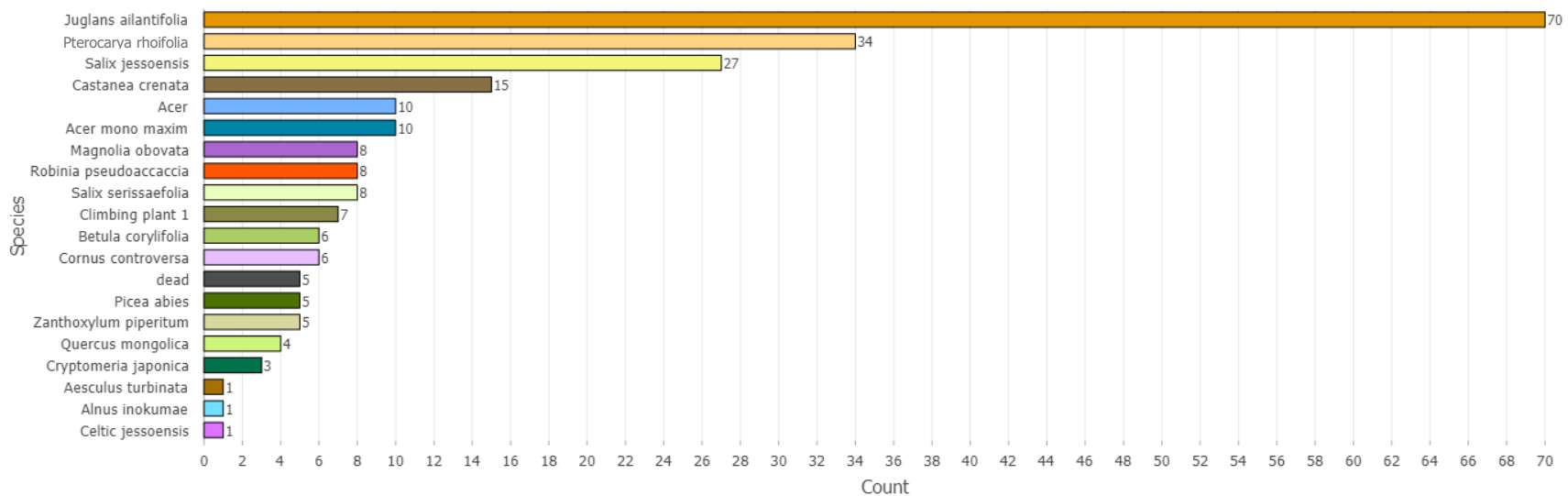
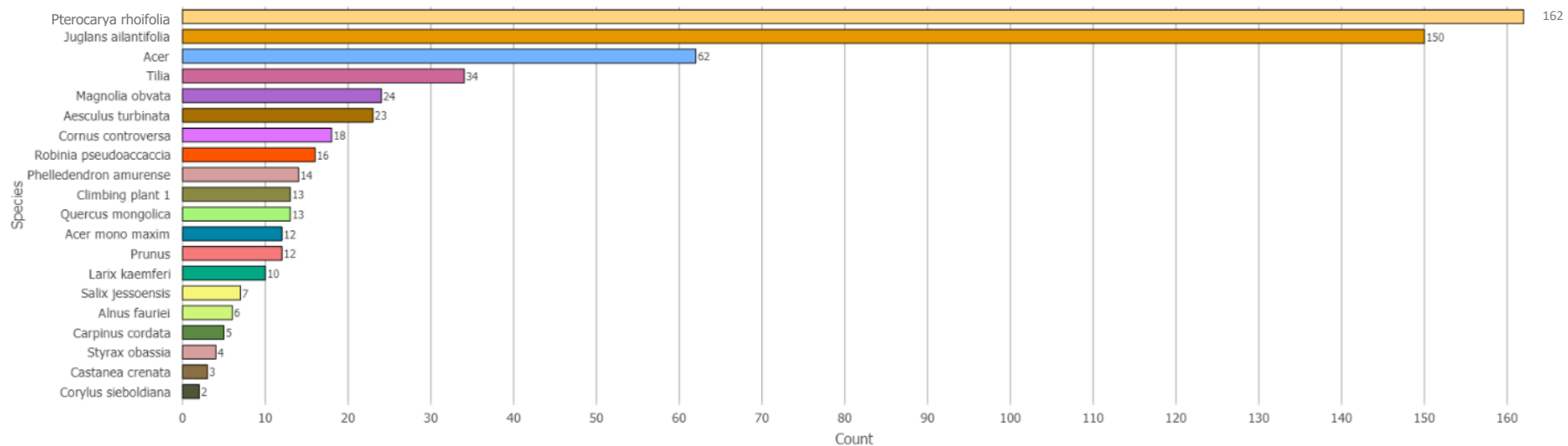
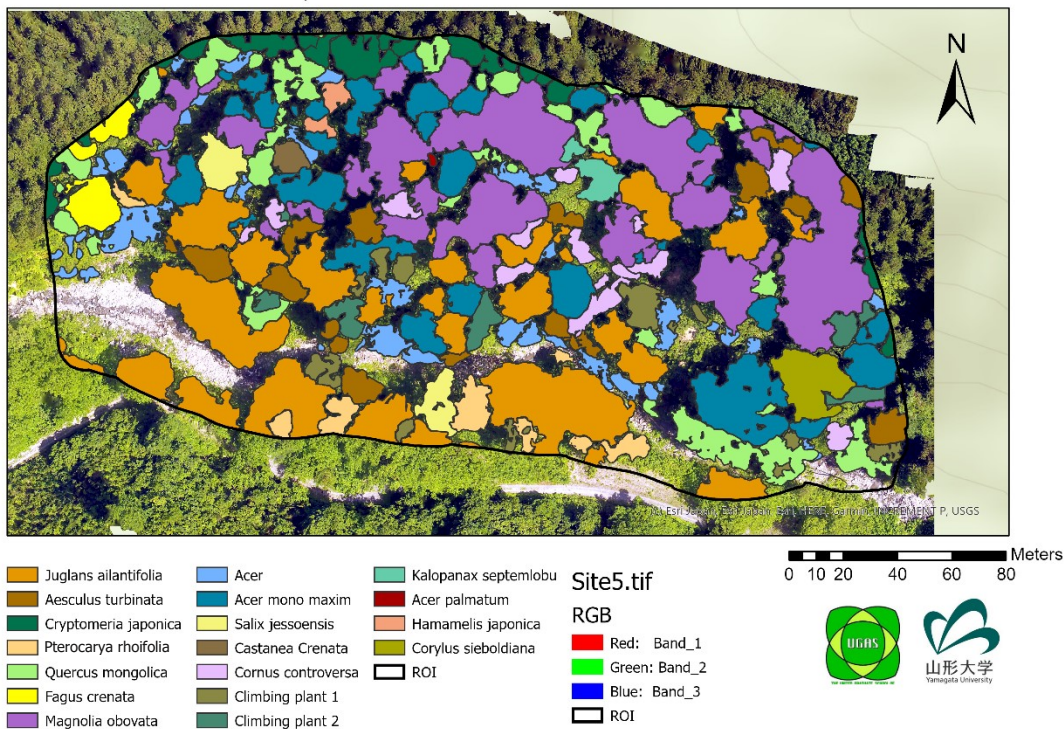


Figure 54 Species counts for site 1 and site 6, automatically generated by ArcGIS

Tree species map site 5 (YURF) by Sarah Kentsch



Tree species survey site 5 (YURF) by Sarah Kentsch

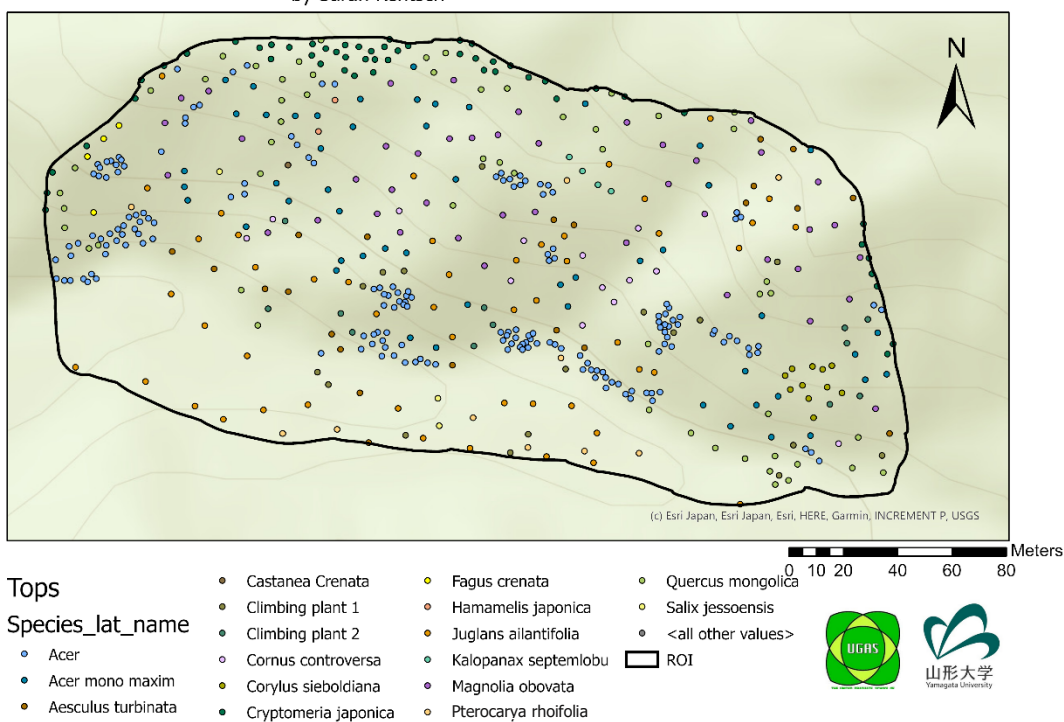


Figure 55 Site 5 tree species map and tree species survey map

There are several tree species, which seemed to distribute only along the river and disappear with increasing elevation. To validate the observation, tree distributions were further analysed by their distance from the river and their location on the slope.

Figure 56 provides six examples for the trees distributing in YURF, while the results of other species are provided in Appendix.

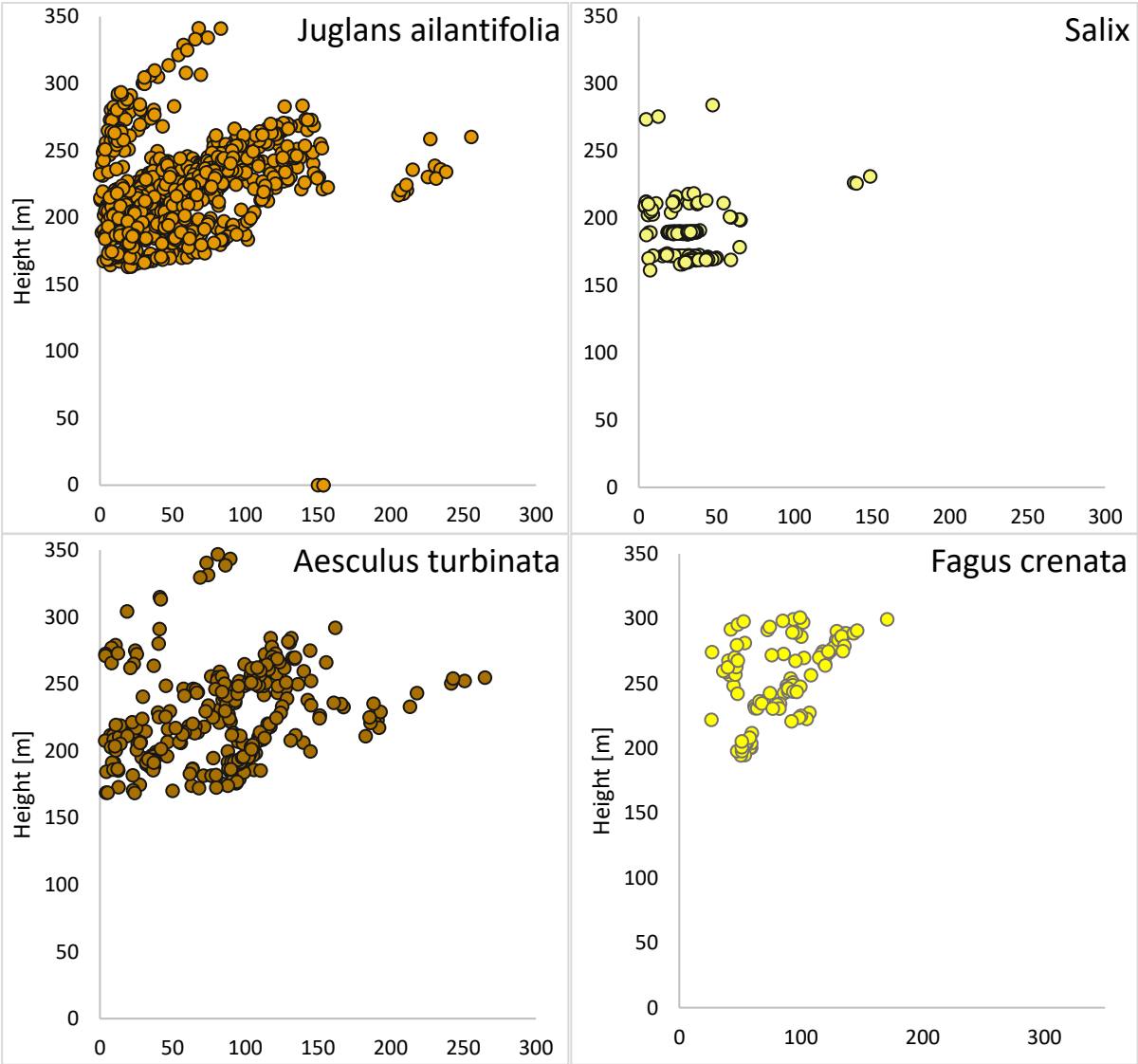
Tree species like *Salix*, *Robinia pseudoacacia* and most *Castanea crenata* trees distributed along the same elevation, with distances of less than 100 m. *Salix* and *Castanea* had a couple of species, which occurred in a higher elevated regions and further away, these can be treated like outlier. *Pterocarya rhoifolia* also showed a distribution along similar elevations, with some more individuals distributing in higher regions. The distance to the river was found to be between 0 and 120 m. *Juglans ailantifolia* occurred mainly until a distance of 150 m to the river and grew mainly below 300 m elevation, which was also observed for *Cornus controversa*. The most trees occurred in lower elevated regions and closer to the river. *Hamamelis japonica*, *Betula corylifolia*, *Tilia* and *Prunus* species occurred between the same values than *Juglans ailantifolia*, but most of their trees followed a linear trend. *Aesculus turbinata*, *Magnolia obovata*, *Acer mono maxim* and *Quercus mongolica* occurred between height values of 160 to 350 m and in up to 300 m distance from the river. *Carpinus cordata*, *Fagus crenata* and *Corylus sieboldiana* were the only species, which did not grow next to the river, but further than approximately 25 m away.

4.4.3.3 Image analysis – spatial tree species distribution

The survey and species maps were used in a first step to evaluate the species composition and distribution on a visual basis, but ArcGIS offers several tools, which allowed deeper analysis. While the survey and species maps contained a high load of information, which were evaluated with a high level of subjectivity, the goal of the following analyses was to decrease the amount of information and specify them into objective information.

Density measures, based on tree stems, analysed where a high and where a low number of trees occurred in the sites, also provided by counting and summarizing trees in a fishnet. The difference between the density measures and the counting were the considered neighbourhood. With the density measures, a radius was set: once 8 m, once 16 m. Then areas with high densities were coloured in red, areas with low densities in green. Counting was performed in a fixed fishnet grid and only trees inside the grid cells were considered. Therefore, density measures illustrated fluent/smooth changes in the distribution without a fixed value, where even small-scale changes were identified. The difference

between the chosen radiuses was interesting, when small scale changes or a generalized trend in the site were found.



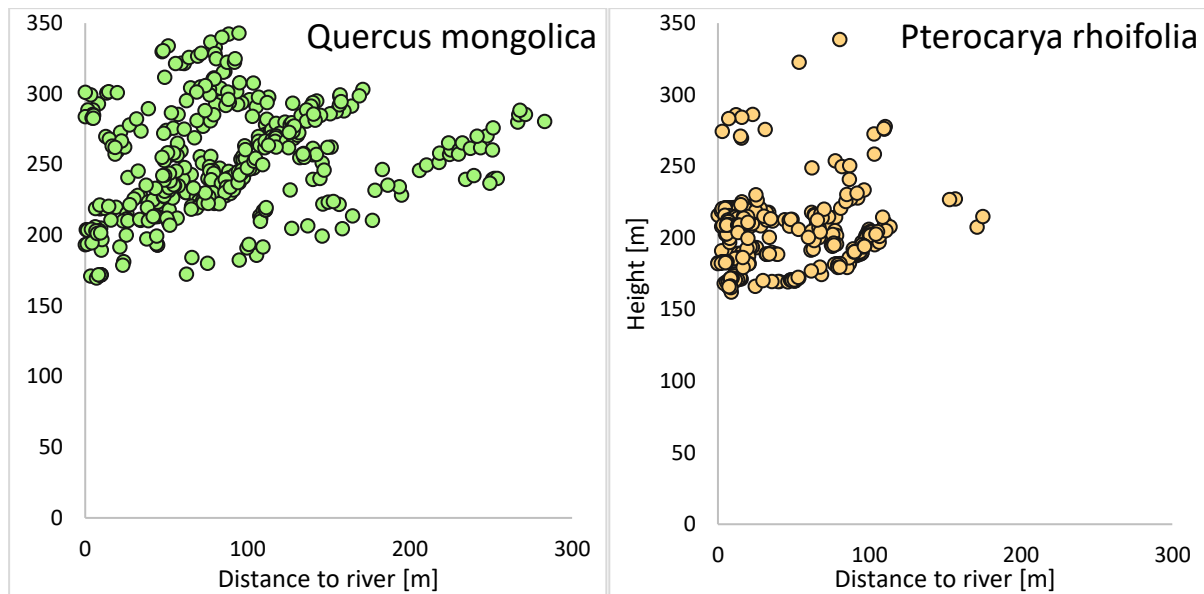


Figure 56 Tree species distributions dependent on the distance to the river and the height

Changes between cells with a fixed and visible value were counted (low numbers with brighter colours and darker colours for high numbers of individuals). Both analyses were performed and shown in Figure 57 and Appendix M. Hot spot analyses checked randomness in data (here tree distributions). The output provided information about areas that were significantly different compared with the study site. Here, areas with high tree numbers were considered as hot spots and areas with unusual low tree numbers were classified as cold spots. The results of all analysis provided similar results, as they pointed out high and low tree densities, with different considered details, the results were summarised and the maps (Appendix M) all provided for further details.

The first observation was that in site 4, with a radius of 16 m, only a dense cluster was found in the *Salix* monoculture in the southern part of the site, which was also observed for site 1, where *Pterocarya rhoifolia* grew as monoculture. In site 6 most of the areas were marked in yellow, having four areas with high density. With lower radius for the density measure, the overview of the whole site created, but single hot spots were clearer visible, with high densities in the centre of the map and in the southern part. Site 7 also showed a more even distribution, like site 6, but with lower intensities. When this information was compared with the counts, high density areas in site 1 had between four and eight trees per cell and in site 4 four to 20 trees. In sites 6 and 7 only one or two cells had high densities, with four to five trees in a cell. The difference between site 6 and 7 was the higher number of cells with 2 trees in site 6. The hot spot areas were for all sites located in the region of high densities. Significant cold spots were found in all sites, located in the north of sites 1 and 7, but having only a couple of cells in sites 4 and 6.

The Terrace sites 11 and 12 had higher densities in the middle of the site, only decreasing to the borders of the orthomosaic, while site 13 only had one high density area. The count maps provided that number of trees per cell was rarely one, instead there many cells included three individuals or more (especially in site 12). In site 13 the numbers of trees per cell were usually low with one to four trees. The hot spot analysis also indicated regions of higher densities as hot spots, while areas at some of the borders were cold spots. Density measures already indicated low tree numbers in those regions.

The Slope sites 2 and 3 showed large area with points, but no indication for high density, while other parts, especially along the ridge showed high densities. Differences were observed, as in site 3 the highest densities occurred in higher elevated areas, and in site 2 in lower elevation areas. In sites 8, 9 and 10 the densities of trees were high, where trees grew, however there were large areas, especially in sites 8 and 9 where no trees were growing (in site 10 the empty areas mainly contained *Cryptomeria japonica* trees, which were not annotated in winter images). Site 5 was the only Slope site with a regular density, with only two density spots, similar to site 7.

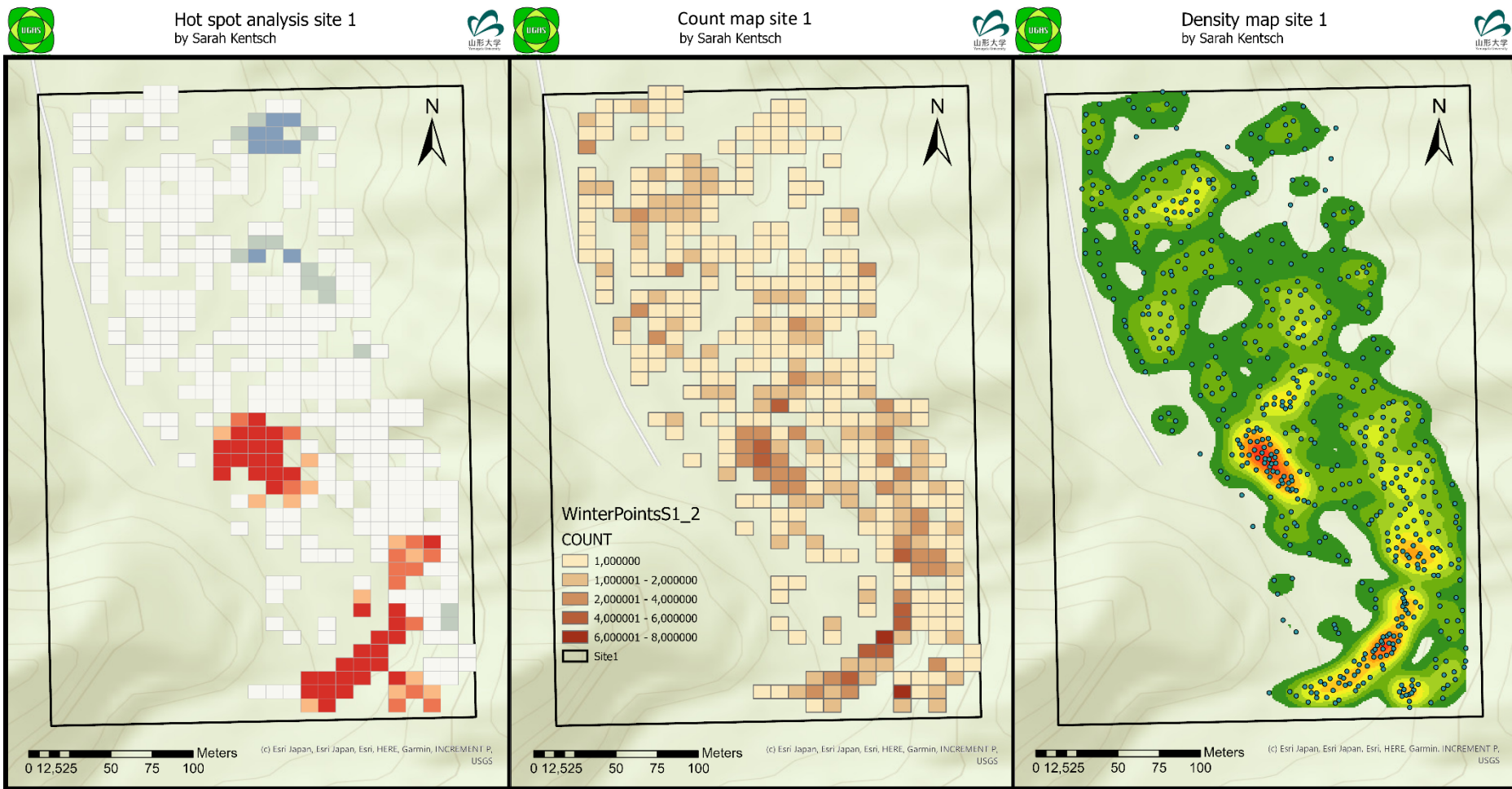


Figure 57 Three maps of site 1, the results of: hot spot analysis, counting in a fishnet grid and density measures (16 m)

The count map of site 5 showed that the trees were evenly distributed with two to four clusters and some with up to six trees. The count maps of sites 2 and 3 were compared with the density maps slightly different, as site 3 had many clusters with one or two trees, and site 2 had many clusters with 2 or 3 trees per cell. Areas identified as cold spots were in site 2 the highest elevated regions, in site 3 the lower slope regions and in site 5 the eastern part of the site. Sites 8, 9 and 10 had the highest tree numbers per cell ranging from six to nine trees. Site 10 had a south-west to north-east gradient, with decreasing trees per cell to the north-east, shown in the hot spot maps. The count maps of sites 8 and 9 showed mixed tree numbers per cell without significant structure, while the hot spot analysis found two regions, one in each site along the west-east line. Even though site 9 was above site 8, there was no connection between the hot spot areas, but cold spots were located partly in the northern and southern parts of both sites.

The image analysis significantly reduces the amount of information in the images and increase the visibility of areas of high and low densities. Therefore, tree distributions along the sites can be identified and analysed.

4.4.3.4 Large scale image analysis

Plots of 1 ha are large with regards to field investigations, but are small, when it is compared with image analyses, considering 3 to 8 ha forest area. The same data were collected: tree location and tree classification. The data were mainly collected in two regions of the YURF, one located in the North and one in the South. For the following analyses, the sites belonging to the North and South were summarised and single tree species data were extracted. The analysis for counts and hot spots were performed based on the summarised North and South data. These analyses helped to illustrate trees of the same species and in which areas they occur.

The Figure 58 to Figure 60 provide examples of the distribution maps and the hot spot analysis maps. For all other species, the maps are given in Appendix N. The first sets of data were generated to provide information about the location of the species from a broader perspective. To support visual information of the maps, filtered and smoothed winter DEMs were used to show regions of high and low elevations (high red to white colours, low green colours).

Tree species, like *Juglans ailantifolia*, *Pterocarya rhoifolia*, *Robinia pseudoacacia* and *Salix* were mainly located in flat areas, in the North and the South of YURF. *Salix* and *Robinia pseudoacacia* trees grew exclusively along the river, while *Pterocarya rhoifolia* was also located along the rivers, but single trees grew at higher elevations (sites 2 and 5). A high number of *Pterocarya rhoifolia* trees occurred in the slopes of sites 6, 11 and 12, where even up to nine trees were found in a raster cell. Another

representative species in the sites was *Juglans ailantifolia* trees, which dominated the flat riparian areas, as well as slopes that faced west, like in sites 3, 11, 12 and 13, but also in the slope of site 5, facing south. The highest numbers of trees were still found in riparian areas, with a decrease towards higher elevations. In site 4, *Juglans ailantifolia* had one hot spot with a 99 % confidence, being significantly different, while only *Pterocarya rhoifolia* had another hot spot with 99 %, in the south of site 1. All other trees of the mentioned two species, but also *Salix* and *Robinia pseudoacacia* distributions were identified as random, except the cluster of *Salix* trees in site 4, which had a confidence of 95 % to be significantly different to the neighbourhood. In the North, a *Salix* hot spot was found in site 6, a *Juglans* hot spot in site 13 and a *Pterocarya* hot spot in site 12.

Cornus controversa, *Tilia* species and *Aesculus turbinata* were trees, which were distributed in the south, mainly along the slopes, with a couple of trees in flat riparian areas. *Tilia* grew mainly as single tree, distributed all over the sites; their distribution was random, except for site 1, where several trees were found. Even though in site 1 had many *Tilia* trees, the area was not identified as hot spot. Also, for *Cornus controversa* and *Aesculus turbinata*, only a couple of cells were identified as hot spots in sites 1, 4 and 13. *Cornus controversa* and *Aesculus turbinata* showed similar distribution patterns, as they grew in different places and elevations, with only one or two trees in some raster cells and in others with a high number of trees. However, the two species did not grow together in one cell.

The distribution patterns of *Quercus mongolica*, *Acer mono maxim*, small-leaved *Acer* and *Magnolia obovata* were similar in the southern sites, rarely growing close to the river and with high occurrences in higher elevations. In the southern sites, *Magnolia* trees occurred in lower slope sites more frequent than at higher elevations, while the distribution in the northern sites was less least less dense. The number of *Quercus* trees increased with elevation, which is also reflected by the distribution of *Acer mono maxim* trees. Generally, differences between the northern and southern sites were reflected by the small-leaved *Acer* distribution. While the number of trees in high elevation areas of site 2 and 3 was high, they occurred in the sites 8, 9, 10, 11 and 13 mainly at the bottom of the slopes. *Larix* trees mainly grew along the river in the southern sites, while *Fagus crenata* only occurred in high elevation areas. Hot spots in the south were only identified for the small-leaved *Acer* (site 3) and *Magnolia obovata* (site 2). In the North, significantly different areas were identified in the distribution of *Acer mono maxim*, small-leaved *Acer* and *Quercus mongolica*, all located in sites 8 and 9.

In the study of [Suzuki et al. \(2002\)](#) forests were classified as riparian, colluvial slope, denuded slope and terrace sites. They identified species in each site and evaluated their probability of occurrence in one of the sites. In the end they assigned riparian type species and terrace species among others. The study sites considered here were Riparian, Terrace and Slope sites, based on the tree species occurrence and relief.

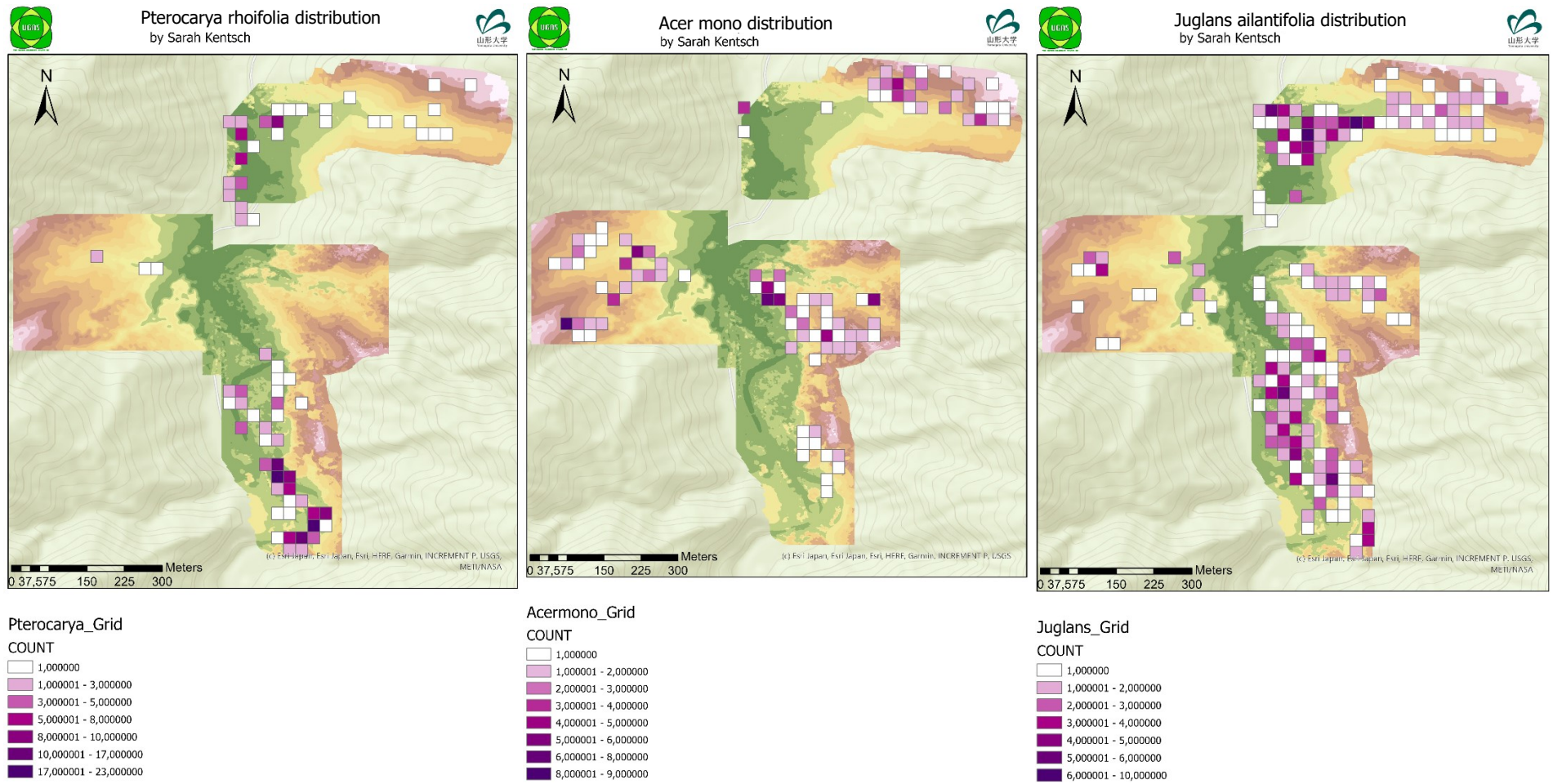


Figure 58 Distribution of *Pterocarya rhoifolia*, *Acer mono maxim* and *Juglans ailantifolia* in the southern sites of YURF

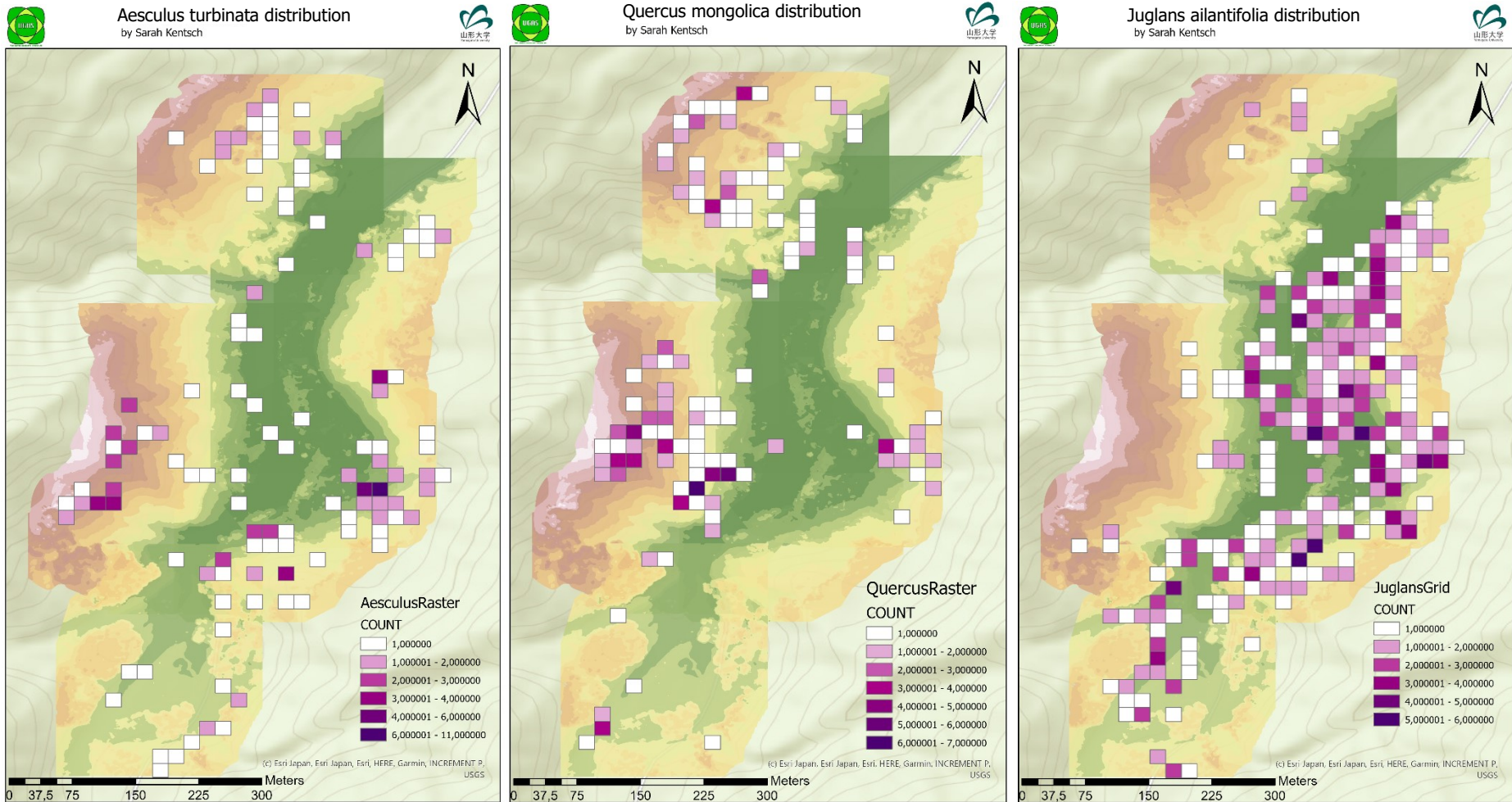


Figure 59 Distribution of *Aesculus turbinata*, *Quercus mongolica* and *Juglans ailantifolia* in the northern sites of YURF



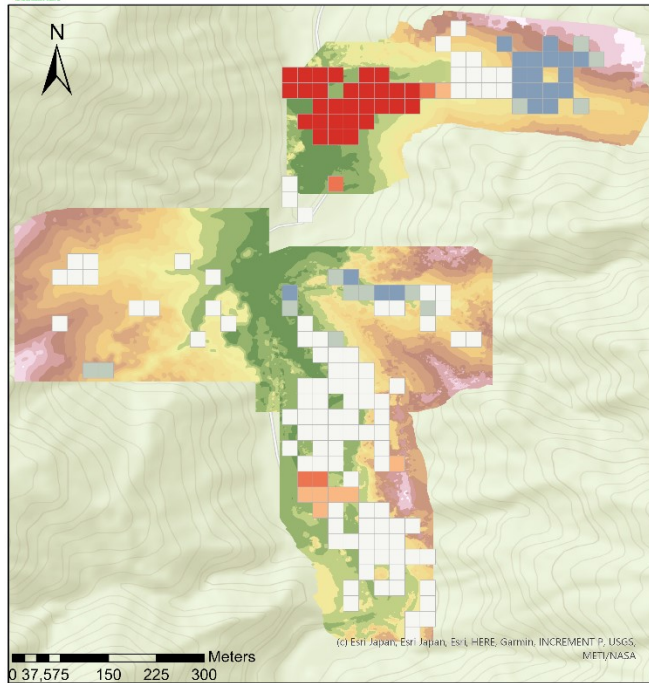
Juglans ailantifolia Hot spot analysis
by Sarah Kentsch



Hot spot analysis Acer mono maxim
by Sarah Kentsch



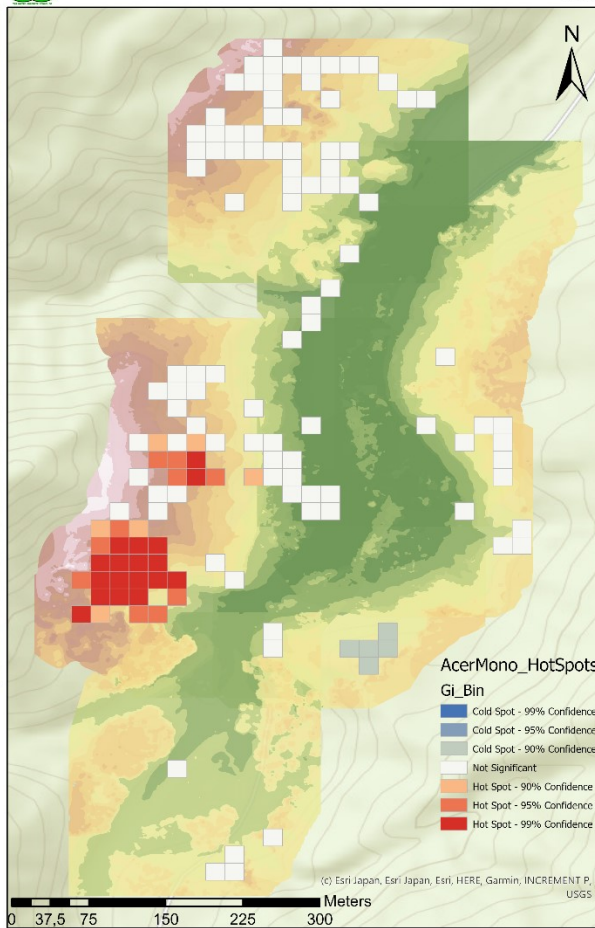
Hot spot analysis Riparian - Terrasse
by Sarah Kentsch



Juglans_HotSpots

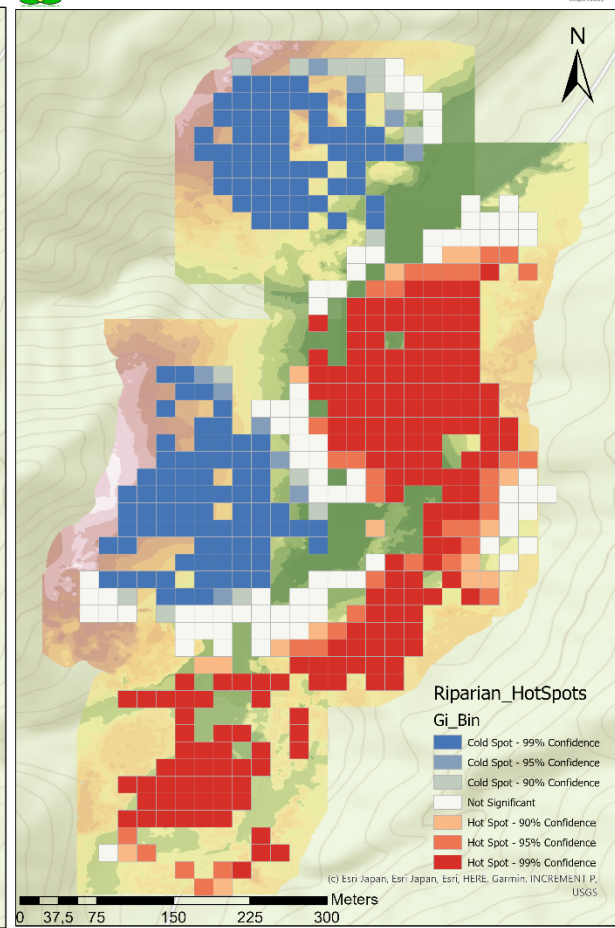
Gi_Bin

- Cold Spot - 99% Confidence
- Cold Spot - 95% Confidence
- Cold Spot - 90% Confidence
- Not Significant
- Hot Spot - 90% Confidence
- Hot Spot - 95% Confidence
- Hot Spot - 99% Confidence



AcerMono_HotSpots

- Cold Spot - 99% Confidence
- Cold Spot - 95% Confidence
- Cold Spot - 90% Confidence
- Not Significant
- Hot Spot - 90% Confidence
- Hot Spot - 95% Confidence
- Hot Spot - 99% Confidence



Riparian_HotSpots

- Cold Spot - 99% Confidence
- Cold Spot - 95% Confidence
- Cold Spot - 90% Confidence
- Not Significant
- Hot Spot - 90% Confidence
- Hot Spot - 95% Confidence
- Hot Spot - 99% Confidence

Figure 60 Hot spot analysis maps for three examples, Juglans ailantifolia in the southern sites, Acer mono maxim in the northern sites and the riparian – terrace hot spot map

Terrace sites were site 11, 12 and 13, which contained slopes, but showed characteristic tree species compositions of Riparian sites. With the information gathered by [Suzuki et al. \(2002\)](#) and the identified species in the YURF sites a re-evaluation of the Terrace sites was performed, also to identify the borders between the sites. For this approach the data set was prepared as described in the methodology section, and then a new field was added in the attribute table, where the ratio between riparian species and terrace species was calculated. This field was used as input for the hot spot analysis.

The result maps show that hot spot areas belonged to areas identified as riparian areas with a high confidence level, and cold spots were identified as terrace areas. The maps with all riparian species provided a more detailed map, as there were more clusters in which the species occurred. The strict riparian species did not occur in high numbers, so that the clusters showed areas without raster cells. For all riparian species the border of the riparian area ended higher on the slope, than when only the strict riparian species were considered. This means that strict riparian species, concentrated the riparian area more on the flat river areas. In the northern part of the study area, the incorporation of *Juglans ailantifolia* trees resulted in large parts of site 11, 12 and 13 classified as riparian area. Both sets of results did not vary significantly and marked a border between the Riparian and Terrace sites. The white cells in the map show insignificant areas, which had similar numbers of trees belonging to the riparian and terrace species. The areas belonging to sites 8, 9 and 10 are with a 99 % confidence interval Terrace sites.

The results of the large-scale analysis provided maps for the northern and southern region of YURF, which were analysed in this study. The coloured DEMs in the background of the map informed the reader about the relief of the terrain and each map provided information about tree species distributions, densities and hot spot analysis results.

4.4.4 Discussion

4.4.4.1 Surveying with GIS methods

After the orthomosaics were annotated, the data were visualised as histogram, survey maps and distribution maps. Histogram data mainly provided tree species and the numbers of individuals per site. This kind of data allowed getting a fast overview about the total number of species and the exact number of trees in order to evaluate the forest composition. The survey maps still contained all the previously mentioned information, but added a location to every tree. In comparison to the histogram, tree numbers cannot be read out easily, but the distribution of the trees can be seen. Single dots increased the detection of dense patches and mixes of different species. The distribution maps

captured the canopy areas of major tree species. Here, no point information was provided, but polygons, which increased the visual understanding of the canopy distribution. Compared with the points, dense tree areas and the proportion of each species can be evaluated. As example, small-leaved *Acer* species had high numbers of trees, which were indicated in the histograms, a high density is shown by the point map, but only the distribution maps visualised that the area they covered was small. On the other side, *Magnolia obovata* had fewer trees counted in the histograms and shown in the point maps, while their canopy area was especially large in sites 2, 5 and 10. Furthermore, the high point density in most sites decreased the possibility to get an overview of species distributions in the sites, and single trees with a large canopy area might be overseen. The distribution maps increased the visibility of trees and the dominance of tree canopies in the forest. But at the same time, the dominance of canopies decreased the visibility of smaller trees, whose canopies was below larger trees. An aspect, which cannot be provided by histograms and point maps, is the forest structure. The canopy areas provided with their colours in the orthomosaic the basis to distinguish between species, and areas with higher and lower densities could be extracted easier from the images. The structure of the canopies, represented by polygons, was easier to analyse than with raw images. From the shape of the canopy, conclusions on the level of the forest can be drawn. An example was *Cornus controversa*, which usually showed a long or stretched shape always along with canopy areas of *Magnolia obovata*, *Acer mono maxim* and *Juglans ailantifolia*, which indicated that the *Cornus* trees were smaller and must belong to the subcanopy layer. The canopy size of *Quercus mongolica* trees in sites 2 or 5 e.g., was small and they were often surrounded by trees like *Magnolia obovata* or *Cryptomeria japonica*. Hence, the species belongs in these sites to the subcanopy layer. In most studies *Quercus mongolica* was described as a dominant tree species in forest areas, but in the studied sites the species seemed to be less dominant than expected.

Even more interpretations followed when point maps and area distribution maps were combined, as it integrated the vertical perspective on the sites. When the maps were overlaid, points and polygons of the same colour showed how many trees were identified in a tree canopy area. Points and polygons with unlike colours indicated that the pointed tree belonged most probably to the subcanopy or understory layer. Note here: shrubs usually could not be identified from images and belonged to the ground level of the forest, so it was most likely that the points did not belong to this layer.

Already without performing intensive image analyses, there were several forest characteristics, which could be extracted from the data and helped to analyse the forest, its species composition, distribution and the structure. The information was further used to classify mixed forests.

4.4.4.2 Forest structure

Information about numbers and tree species areas were provided with the tree maps, distribution maps and histograms. More important was the information regarding the location of tree species, their expansion and the number of trees in the different areas. The numbers and colours of tree species in maps were therefore combined with essential spatial information about sites and species.

Tree species like small-leaved *Acer* had the highest tree counts in the Slope sites and small numbers in the Riparian sites or Terrace sites. The species started to grow upslope, starting almost at the bottom of slopes, where they occurred in dense clusters. Compared with the high number of stems, the canopy area is small, which is a result of the multi-stem characteristic of the species and the conditions of the sites. The trees occurred along with *Juglans*, *Aesculus*, *Quercus* and *Fagus* trees and distributed below and around their canopy area, which can be explained by their shade tolerance and their occurrence in disturbed areas at the bottom of slopes (Suzuki, 2002).

Pterocarya rhoifolia and *Salix* species occurred only along rivers and in low depression areas. Both species usually did not occur next to each other. In site 6 *Salix* species were found in a depression, while *Pterocarya* trees grew along the river and in site 7 *Salix* trees occurred mixed with *Juglans* trees, also in a depression. In Terrace sites only *Pterocarya rhoifolia* trees grew, where some of them were even located in the slope. In site 12, most of the trees were again located next to the river, as the species distributed mainly because water spreads their seeds. Also, the river area might be flood areas in the melting and rainy season, which means that the disturbances there benefits their distribution, as disturbances open spaces.

Robinia pseudoacacia, which occurred in sites 1, 6 and 7, had small areas and was distributed irregularly over the sites, it only occurred in Riparian sites, which can be interpreted as a result of more frequent disturbances increased the distribution in those areas. Furthermore, the species is invasive and known for its well adaption to environments and survival under strong competition, which can be seen in site 1, where it grew between the dense canopies of *Juglans ailantifolia* trees.

Juglans ailantifolia trees were mainly distributed in Riparian and Terrace sites, while their number decreased with increasing elevation; there were a large number trees in sites 1, 13 and 8 and less in sites 9 and 10. In slopes exposed to the west in site 3 had a large number trees, while the higher areas and the east facing slope did not contain the species. There were no significant differences between the Riparian and Terrace sites observed; only the strong dominance in site 13 was different to all other sites. In sites 2 and 10, only a couple of *Juglans* trees occurred. In comparison to all other Slope sites, where riparian forests grew close, sites 2 and 10 had no direct connection, therefore other *Juglans* trees were in greater distance so that the seed spreading was less effective. The species usually

occurred in clusters and built large canopy areas, as *Magnolia obovata* and *Pterocarya rhoifolia* does. *Magnolia obovata* distributed opposed to *Juglans* trees, as it occurred more frequent at higher elevations than at lower ones. Therefore, the species barely occurred in Riparian sites, with low numbers in Terrace sites and with highest in Slope sites.

Furthermore, digital maps illustrated structural differences in the sites; gradients and unique site characteristics could be identified. In sites 8, 9 and 10, the mixture of trees was high, with smaller tree clusters of the same species and few larger clusters. There was no gradient in tree species distribution. In the Slope sites 2, 3 and 5 the tree species followed a characteristic distribution. The trees grew in a pattern, which seemed to follow the increasing elevation and the proximity to the water source. The differences between the sites 8, 9 and 10 and 2, 3 and 5 were maybe a result of the exposure of the slopes or steepness of the slopes.

Those site-scale distributions, which formed the structure of the forest, were only visible when large areas were surveyed, and even better visible when canopy areas were marked. Even though only a small number of tree species were selected and their distribution and behaviour were analysed, different characteristics could be observed. The species distribution, together with the image analysis of orthomosaics was performed with ArcGIS, where every visible species could be analysed. With the provided maps and locations of the species, further field investigations were performed to support the image analysis with ground truth data, like soil analysis. It therefore helped to understand the forest composition and distribution better. This underlying information, which influences behaviours of tree species, can be combined in ArcGIS to analyse spatial characteristics in the data.

4.4.4.3 Evaluation of spatial pattern in the data

Image analysis provided information gathered in maps characterising tree densities and distributions. Reducing the amount of information contained in images is the task of image analysis, so that only information will be presented that highlight interesting aspects of the data. Otherwise, the characteristics, differences and similarities between 13 sites as well as the studies number of species could not be assessed with human capabilities. The discussion is separated into a site-scale evaluation of the data and a large-scale evaluation of the data, to provide the abilities of GIS analysis.

4.4.4.3.1 Site-scale analysis

When all sites were compared, the highest densities with the highest numbers of trees per cell were found in the Slope sites, while there was usually only one area with higher densities in the Riparian

sites. In Slope sites the clusters identified as hot spot regions were larger than in the flat Riparian sites. The higher tree densities were most probably a result of two main points. First the degree of the slope increased the density of tree stems in the images. Second, the layering of the forest and the degree of the slope allowed the growth of more trees in a small area, because more light can infiltrate the lower forest layers. The competition for light is therefore not as limiting as in flat sites and the tree numbers can be higher. The highest densities in riparian areas occurred mainly in monocultures, those trees grew close to each other without competition. Areas with *Juglans ailantifolia* trees were usually less dense, which means that the species dominates large areas and is therefore a stronger opponent when it comes to competition between tree species. Forest sites with a high number of tree species and a high mixture were also denser, as it was observed in sites 6, 11 and 12. Sites 8 and 9 had a mixed tree species distribution, where barely large species clusters were found, also visible in the count maps, where tree numbers variety was high. Sites with more even clustering of the same species, like *Magnolia obovata* in sites 2, 5 and 10 or *Juglans ailantifolia* in site 3, trees seemed to be more separated. This suggests that there were clusters like in sites 8 and 9, which occurred in small areas, in contrast to site 5, where the clusters distributed over a large area.

Monocultural areas were usually clearly identified as hot spot regions; however, the ones in sites 6 and 7 were less obvious. The hot spot analysis therefore provided that there was mainly a random distribution of trees in the forest, but some areas did have a structure. In site 12, a larger number of trees occurred with the proximity to the river, and in site 11 a hot spot was found in the north-west facing slope, which was also visualised in the density maps, even though the counts did not clearly show this characteristic. Here, the benefits of analyses like density measures and hot spot analysis are clearly shown, as they reduce a large amount of information and focus the perspective of the analyst on desired regions. In site 6, the count map as well as the density map did provide easily accessible information, while the hot spot analyses provided areas, which were significantly different. Another example was site 5, where cold spot regions were located at the eastern border of the site, where the count map provided tree numbers of one or two trees per cell. Site 4 had high densities in the monoculture, the distances between the other trees was comparably low. There should be irregular class category values to provide information about the less dense area. In site 6 the trees were distributed more equally, areas with slightly higher densities were already marked as high density spots (same colour as in site 4) while there were significantly fewer trees than in site 4. The density measure worked for most of the sites, but a comparison between the sites was not possible without errors, because high and low values as well as colour distributions were calculated and boundaries between colours changed with the site characteristic. Here, the count maps helped to give the colours a more specific value, and only spots with at least two trees were marked in the density map.

4.4.4.3.2 Large-scale analysis

Additionally, single tree species data were evaluated by summarizing and scaling them up, to identify large-scale pattern within the data. Single trees of *Pterocarya rhoifolia* were found in sites 2 and 5 at higher elevations, in areas, where water streams develop in the rainy season in summer and in the snowmelt season in spring. The trees are not well adapted to the dry conditions of the rest of the year, so these single trees can be seen as outliers. In sites 6, 11 and 12 the high occurrence of trees could only be explained by the small river crossing site 12. Additionally, in site 6 only small trees occurred in flat areas, where rain events usually kept the soil water content high. Interesting was the behaviour of *Juglans ailantifolia*, which did barely grow in east facing slopes. The river might be a valid reason, as the nuts are usually distributed by animals like squirrels, which do usually not cross the river. Sunlight could be a reason that the species did not distribute on east facing slopes, as the mountains shadow the slopes from the early afternoon. *Tilia* trees were infrequent, but in site 1 they occurred in a cluster. In the field old grown and juvenile trees were found in the same area, which might be disturbed before, so that the species could grow in the developing space. The distribution of small-leaved *Acer* was different in the southern and northern sites, which can be explained by the composition and steepness of the slopes. Sites 8, 9 and 10 had steeper slopes and the canopy cover was denser, which decreased the visibility of small-leaved *Acer*, being part of the understory layer. Therefore, the possibility is high that the trees were just not visible in the orthomosaics. The smaller slope angles in sites 2 and 3 were more suitable to identify *Acer* species. The diversity of tree species was low in site 2 and a high number of *Acer* covered the forest floor, which partially also happened in site 3, while in sites 8, 9 and 10 trees with a large canopy area occurred almost everywhere in the sites. *Larix kaempferi* is a tree, which usually occurs in high elevation areas, together with *Fagus crenata*, but in contrast to *Fagus*, *Larix* grew in Riparian sites. The reason is that *Larix* was planted in these areas. The only natural occurrence of *Larix* was in site 3, along the ridge.

The hot spot analyses were performed to test whether the tree species were distributed randomly or if they follow a pattern. In each site found hot and cold spots were found, when all trees were considered. In the analysis where tree species were analysed separately, most tree species did not follow a pattern and grew therefore randomly in the forest. Species like *Fagus crenata*, *Robinia pseudoacacia*, *Quercus Mongolia* and *Cornus controversa* occurred mainly randomly in the forests, while *Juglans ailantifolia*, *Acer* species, *Pterocarya rhoifolia* and *Salix* species followed some kind of patterns. Also, there were only some cells, which were identified as significantly different. Therefore, mixed forest grew mainly without a pattern, so that tree species occurred randomly in the forest. At least as long as they occur in their natural habitat, like *Salix* trees always grow in riparian forests. This randomness in the forest is based on their frequency of occurrence. Still, it was already figured out,

that tree species follow a pattern, but those must be then dependent on factors like water availability, light availability, disturbances and soil conditions, to mention a couple here. When there were hot spots, like in the case of *Salix* trees in site 4, *Pterocarya* and *Aesculus* trees in site 12, then there must be an underlying source, which increased densities of the tree species in those areas. At this point, the advantages of image analysis for forestry research become visible. The large amount of information, which was gathered from the images, was merged to generate an image of the whole forest area in the northern and southern part of the studies areas. Then the information was analysed to provide only the necessary and important information, giving a fast overview of the studied areas. The analyses further provided points in the forest, where distribution patterns were significantly different to the rest of the study site. This information can be used to explicitly research the reason for the distribution patterns in the field. Therefore, the time-consuming aspects of assigning research plots, classifying and locating tree species and collecting samples (soil samples, soil water measurements, nutrient evaluation, etc.) for the whole study site become unnecessary. Instead, the field work can be performed more precise in spots, which must have underlying properties and cause a specific distribution of the forest species.

Hot spot analyses reduced the amount of needed information to identify spatial pattern in the data. Therefore, depending on the site characteristics and the needed information, each of the measures can be performed, or even all of them to be able to access the data in the most efficient way. The benefit of this methodology is that the data basis (area shapefiles or point shapefile) only needs to be generated once and then all these analyses can be performed within minutes. The results and maps are furthermore easy to understand, underlying spatial information can be accessed and connected fast.

With such kind of information, differences related to spatial scales can be evaluated. As [Gong and Xu \(2003\)](#) pointed out, different scales allow analyses of influences on the forest ecosystem. At the tree level, they indicated biochemical and biophysical properties as the most influencing factors on forest compositions, leaf colour and size of trees. At the stand level, where structures of canopies are influenced by forest gaps or the horizontal structure. Or even on the larger scale, where the main influences are driven by human disturbances and climate change.

4.4.5 Conclusion

The results of this chapter provided unique insights into the forest composition, distribution and structure, which were mainly provided with maps and figures. The results summarised large amount of data, reduced to the necessary information for the reader. It could be seen that tree compositions

could be presented the best with counting statistics, which allowed a fast overview of the occurring tree species and the number of individuals. Distribution maps showed the location of trees and their canopy area, so that it was easy to address the dominating tree species and their characteristics. Structures could also be extracted from distribution maps. Further analyses, like density calculations, extraction from point information and hot spot analysis, indicated patterns in distributions and allowed to interpret the structure of the forest. Missing aspects were the vertical forest structures, which can only be assessed as long as the dominant canopy area had gaps. Evaluating vertical forest structures needs additional information from field surveys.

Remote sensing cannot replace field surveys and inventories, as some information cannot be gathered with images, especially concerning understory vegetations. Image interpretation is limited by field information. Information like site structures and characteristics, observations made in the field and a basic knowledge about the tree species or their occurrence in the forest are important, when image data are interpreted. Furthermore, effective and meaningful statements can only be provided with a good background knowledge about the forest ecosystem. Also, the settings for applications in GIS should have a fundamental background, so that analysis can be performed with realistic values.

Forests are a complex system and the provided analyses showed that they cannot be treated like homogenous patches, as each studied site had its own characteristics. Instead, image analyses allowed analysing single patches of forests, up to regional levels, with high resolution information. The performed analyses showed the effectiveness of gathering large amount of data and the possibility to access several aspects of the forest in a new dimension. One of the dimensions was that tree behaviours like competitions and aggregations could be evaluated on the scale of several sites with different characteristics. This study showed the effectiveness of image analyses and provided a couple of applications, which can be easily used in other forests.

Chapter 5 Semi-automatic counting of deciduous trees in images of a dense natural broadleaved forest – an evaluation

5.1 Introduction

Tree counting is an essential part of forest inventories and agricultural purposes, as they are used for plantations and environmental managements, as well as for biodiversity monitoring (Shafri et al. 2011). In forestry, manual interpretations of aerial images are commonly used to evaluate forests and forest plantations, regarding their species composition, structure and inventory. Several studies have been conducted using image processing methods to automatically detect and delineate individual trees. Especially for precision farming, like in Osco et al. (2021) or Santoro et al. (2013) tree counting was an essential part of managing the field efficiently. But even in forestry research, like Fromm et al. (2019), where conifer seedlings were detected, high accuracies were needed to estimate the recovery of the forest. In those studies, it was mentioned that tree detection depended on image resolution, densities of forests, considered tree species, canopy shapes e.g. All these aspects need to be considered when trees should be detected in forests.

As with the upcoming of remote sensing, airborne images and UAVs (Unmanned Aerial Vehicles), the possibilities of counting trees efficiently and at lower cost has become a suitable application in many studies, as it is much easier than evaluation on the ground. Culvenor (2003) extracted trees by identifying local maxima and minima in images and clustered pixels together. Erikson (2004) detected tree crowns comparing three methods: template matching and two region growth algorithms. Wolf and Heipke (2007) introduced the use of DSM and the extraction of tree crowns based on height information. Recent studies like Osco et al. (2021) used Convolutional Neural Networks (CNNs) to count and detect trees in plantations. They further mention that DL techniques are widely used in weed detection, counting of palm trees, citrus trees and tobacco plants in plantation, rice seedling detection and insect damages. Those study cases were all performed in open areas or plantations and did not consider counting in natural dense forests.

In natural dense forests, when they are additionally located in mountainous areas, research faces several challenges not only for DL application but also for image analysis with GIS (geographic information systems) and field surveys. In studies like Diez et al. (2019), Diez et al. (2020) and Nguyen et al. (2021) it was pointed out, that especially in Japanese mountain forests tree top detections are challenging and highly dependent on the terrain, where the data were gathered. Diez et al. (2019) pointed out that by taking different techniques as well as different forest densities and steep slopes into account, still tree top detections can achieve high accuracies. In Nguyen et al. (2021) a deeper

analysis of tree detection was performed, summarizing, that matching averages were lower for steeper slopes and when the rate of mixing was higher between broadleaved and coniferous trees. It was pointed out, that heterogeneities of the forest in terms of tree heights, age and tree species distributions influenced the detectability of tree tops. Especially smaller trees close to taller trees remained often undetected. This effect increased when only broad-leaved trees were evaluated. As the focus of the study (Nguyen et al. 2021) was on coniferous trees, there is a gap in knowledge, when it comes to the detection of broadleaved trees in natural mixed forests.

Additionally, the evaluation of the studies was usually done by comparing the results with manually labelled data. An evaluation of these ground truth annotations seemed not to be done. The question arose on how accurate those expert tree top annotations were. A study evaluating count methods for quantifying seed productions in a temperate broad-leaved forest, was presented by Tattoni et al. (2021) They compared two ground measurements with image counting. For seed counting they evaluated that using images is a reliable method.

Therefore, the aim of this study was to evaluate manual annotations for image tree top counting by comparing field data with counting performed on Digital Elevation Models (DEMs), as Wolf and Heipke (2007) already indicated the efficiency of elevation data for single tree detection. Furthermore, in this study the seasonality of the forest was used, while most studies focussed on the summer season to evaluate forests, only a couple used spring and autumn and rarely the winter season. The benefits of winter images of forests are the clear differentiation between evergreen and deciduous trees, as pointed out by Kentsch et al. (2020), but also the leafless deciduous trees can be identified well. Therefore, summer and winter images were used to further evaluate the performance of tree top counts from UAV acquired images and those will be evaluated in this study. To the best of our knowledge, this is the first study considering different techniques to count trees in images and evaluating the detection of tree tops by comparing them with manual field data. The following objectives were the basis of this study:

- vii. To compare tree counting with only DEMs and with DEMs together with orthomosaics
- viii. To compare tree counting in summer and winter images.
- ix. To compare the results with the gathered field data and to evaluate the accuracy.

5.1.1 Problem definition

In summer images, the canopy structure of deciduous trees is made up by several single canopies building a dense and large canopy area, in which single tree identifications are almost impossible (Figure 62). Furthermore, the automatic tree detections pointed out the problems of detecting trees

in natural mixed forests. Therefore, a suitable method was needed to count deciduous trees in the dense mixed forest. As Shonai area has high precipitation in winter, soil in the forest is covered by snow from December to April/May. The benefit of winter images is that the background of the orthomosaic is usually white, while the branches of the deciduous trees are in contrast to it, because of their grey and brown colours. Therefore, tree counting is enhanced with winter images.

5.2 Methodology

5.2.1 Study sites and field data

In the study of tree species classification, manual field surveys for the Riparian sites of YURF were prepared. The field surveys were conducted in autumn 2018 and summer 2019. To evaluate the accuracy of winter images, the four sites with the most accurate field data were chosen: site 1, 4, 6 and 7 (Figure 61). Site 1 was divided into three areas, to evaluate the counting accuracy in different kinds of mixed forests. As the southern part of the orthomosaic (S1a) is a monoculture of wingnut trees, it has a different characteristic and density than the rest of the orthomosaic. Furthermore, the island in front of the main building of the forest was chosen (S1b), as it showed a high variety of tree species characteristic for the riparian forest, and another mixed patch in the centre of the orthomosaic (S1c). A last part was chosen along a steep slope (S1d), as it was possible to gather field data in the slope. Site 6 was also divided into two areas to analyse the detectability of trees: a flat area in the centre of the orthomosaic (S6a) and the slope along the river (S6b). Regarding the areas selected in site 4 (S4a) and site 7, the centre part of the orthomosaics were chosen, as there were no distortions in the image and the fieldwork was the most accurate. Additionally, the monoculture of Salix trees (S4b) and the area around the larch trees (S4c) were analysed.

Finally, the centres of the sites 11 and 13 were selected to evaluate the counting possibilities in slope areas. The results of the fieldwork may not be complete due to the difficult access to some sites, but the results can be used to evaluate the counting in difficult terrain.

5.2.2 Data gathering

In order to evaluate counting possibilities in orthomosaics gathered in natural mixed forests, flights were performed in summer 2019 and from the beginning of the snowmelt season, which was in the end of February 2018 and 2019, when branches were snow-free. All images for the sites were taken a UAV, DJI phantom 4. An automatic flight protocol was used to perform the flights, so that all settings were the same for the cover area, flight height and overlap. The flight height ranged between the sites

from 80 to 120 m, as the elevation of the sites varied. The front and side overlap were always over 90 %. For the flights single images ranging between 200 to 350 images were gathered. As the forest is dense and parts of it inaccessible, ground control points could not be used.

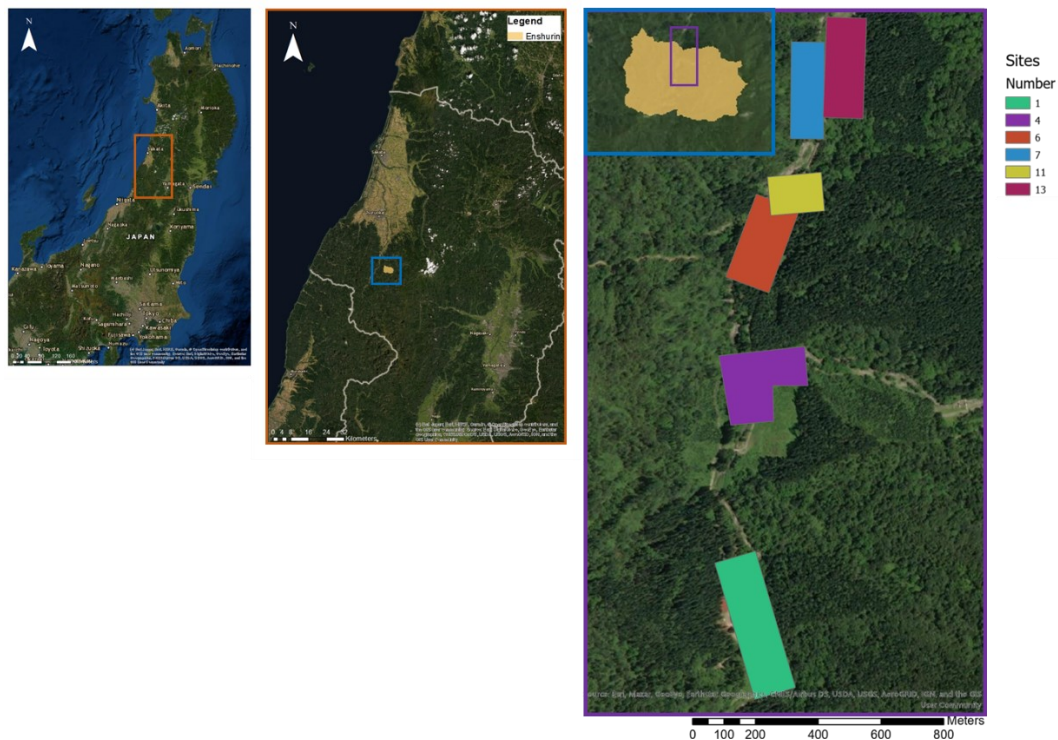


Figure 61 Location of the study area YURF. The left image shows the location in Japan, the middle image shows the location of YURF and the right image the study sites.

5.2.3 Data processing

Images were processed with Agisoft's Metashape, which merges single images to orthomosaics and DEMs (Figure 62). The resolution of the aligned images was between 2.75 cm/pix up to 3 cm/pix for the orthomosaics and 3.5 to 4.0 cm/pix for the DEMs. For the evaluation of the detectability of trees in images, two approaches were used, based on two sets of data. The basis were the same orthomosaics for both sets, but the area, which was selected for each approach, varied, as different tools were used. For the first approach one large area was selected in site 4 and for site 1 only winter images were analysed.

The use of DEMs with image processing software was not possible, as those software cannot read geoTIFF files. Therefore, the DEM needed to be transformed into JPEG format. With ArcGIS, the DEM can be transformed using the *Raster Calculator* and the tool *Copy Raster*.

The copied file can be exported as JPEG, containing the height information stored in different grey-values, whereby white represents high and black low values.

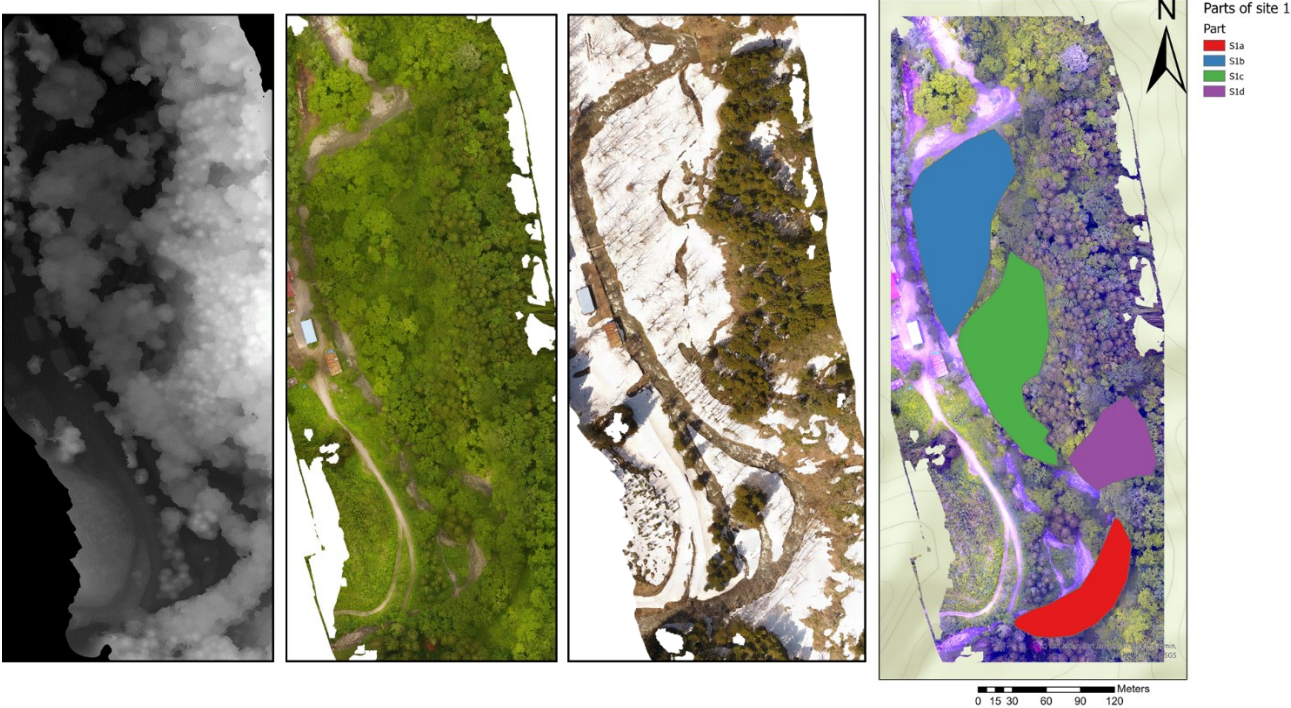


Figure 62 Example data (example site 1). From left: the DEM, the summer orthomosaic, the winter orthomosaic and the summer orthomosaic with the selected parts.

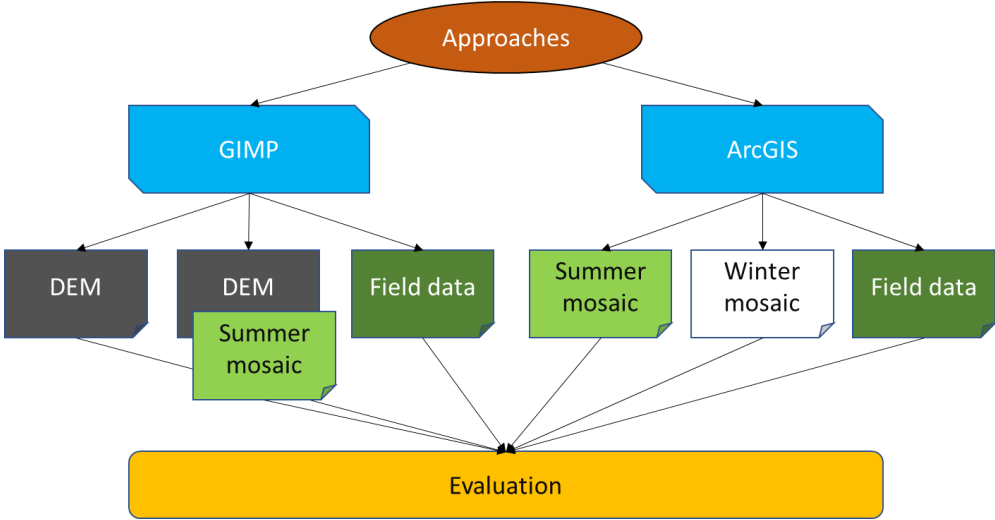


Figure 63 Workflow for this study

The first approach used GIMP and a python code to count black pixels in annotations (Figure 63). The first step was to annotate tree tops on the basis of DEMs, whereby binary images were created, which show black dots as the tree tops. A second set of annotations were created, where additionally to the

DEMs, orthomosaics were used to identify tree tops. The two sets of annotations were created for every site and area as well as for the summer. A simple top counting algorithm was used to count the tree tops in every annotated layer.

For the second approach, three point maps were generated: a field tree map, a summer tree top map and a winter tree top map (Figure 63). For the summer season only one set of annotations were prepared, mainly based on visual information. For the winter season, manual annotations were only done based on the orthomosaic, because Metashape did not produce good elevation models for leafless trees. ArcGIS pro was used to generate and visualise these maps. For each map points were annotated for the tree tops of deciduous trees and saved in a point shape file. In the corresponding table each tree top was assigned a label for the tree species. Additionally, polygon shapefiles were generated to reflect the different sites and areas, as presented in the section study sites and field data. The tree tops were marked and counted with the selection tool. Furthermore, maps were generated and exported, as well as counting diagrams, which counted the selected tree tops per species. All counted trees and shrubs were evaluated for both approaches.

5.2.4 Evaluation methods

Both approaches used a simple comparison between the actual counts in the field and the automatically generated ones.

$$Accuracy = \frac{Automatic\ counts}{Real\ counts} * 100$$

5.3 Results

5.3.1 Field observations

The considered study sites are old-growth forests, where the main species have already fully developed tree crowns. The crowns of different species grew usually together and built up a big canopy. The species occurring in the forest, like *Juglans ailantifolia* and *Pterocarya rhoifolia*, *Salix* species (*Salix serissaefolia*, *Salix jessoensis*) and black locust (*Robinia pseudoacacia*) reach similar heights in the considered areas. Between the adult trees, young trees grow, especially *Juglans* and *Pterocarya* trees. The juvenile trees grow mainly close to the adult trees or along the river, where the density of trees and shrubs is low. Sites 4, 6 and 7 have the highest number of young trees, in a range between 22 and 48 trees. Only in site 4 young trees grow in the middle of the site, as there was a small area only covered

with shrub vegetation. Sites 1, 11 and 13 are at higher elevations and therefore less disturbed. Hence, few young trees were found.

As the sites 1, 4, 6 and 7 are located along the river, they are characterised by a flat area, while the borders of the sites are already located at or on the slope. In comparison to these sites, 11 and 13 are located on the slope, whereby the elevation difference between the lowest and highest point is approximately 30 to 40 m depending on the site. These sites are characterised by terrace areas and steep slope parts. The density of the forest varied significantly with the steepness of the slope. The density of the sites 1, 4, 6 and 7 were similar and the distance between the trees was higher compared to the sites 11 and 13. The understory layer was in all sites dense and aggravated the preparation of surveys. Therefore, the forest can be described as a dense natural forest, composed of a dense canopy layer and a dense shrub layer. Surveys were completed for all mentioned sites, but for the counting evaluation only patches were chosen and trees were counted manually based on the surveys.

Regarding the field surveys of sites 11 and 13, it has to be considered, that the sites were difficult to access and field data could not be gathered area-wide. The lower part site 11 could be accessed well, therefore all layers in the forests were classified and georeferenced. On the higher slope and top part of site 11, mainly *Acer* and tree species belonging to the canopy layer were identified and detected, as the accessibility did not allow to localize and to determine small trees. In site 13, as the whole site was difficult to access, no understory vegetation was taken into account (except *Acer* species), while the field data were gathered. The characterization of the sites is provided, as it is assumed that the site conditions and tree densities had a strong influence on the counting accuracies.

5.3.2 Counting measures

The first approach aimed to provide information on the counting accuracies using DEMs and orthomosaic image information to detect tree tops. Therefore, only the DEM was used to extract tree tops based on local high points in the DEM. In large tree canopy areas local maxima could be identified, as these were the brightest spots in the canopy. Table 21 provides the results of the manual and the automatic counting. It can be seen, that the automatic counts were the lowest compared with the counts of DEM+orthomosaic and the winter counting. In total, 89 trees were missed in site 6a and 41 in part b, 78 in site 7 and 148 in site 4. The percentage of found trees was therefore between 35.5 % (site 6) and the maximum of 44.6 % in site 7. The accuracy for finding trees was slightly lower for site 6b. Regarding the bad results, young trees and shrubs were taken out of the counted number (Maple trees were still counted). Therefore, the counts decreased to 116 for site 6, 230 for site 4 and 121 for

site 7. The percentage of detected trees increased to 42.2% (site 6a), 47.5% (site 4) and 52.05 % (site 7). There was no change for site 6b as no young trees and shrubs were counted in the field.

It could be seen in the orthomosaic that large canopy areas often consisted of trees from different species, as the forest was mixed. The differences appeared in colour and shape of the leaves, which cannot be seen in DEM. In consequence, visual information gained from the orthomosaic can help to detect further tree tops by identifying maxima in canopies, which have the same or even lower heights than surrounding trees. This technique increased the accuracy of detection another 10 % for most of the sites, while the accuracy increased to 60.91 % in site 4. Using the counts without the young trees and shrubs, the accuracy of site 4 increased to 74.00 % and another 10 % for the sites 6a and 7.

Table 21 Results for the first approach, summarizing the automatic and real counts. (Orthomosaic=Mosaic)

<i>Season</i>	<i>Site</i>	<i>Automatic counts</i>	<i>Real counts</i>	<i>Accuracy</i>
<i>Summer</i>	Site6a DEM	49	138	35.51
<i>Summer</i>	Site6b DEM	32	73	43.84
<i>Summer</i>	Site6a DEM+Mosaic	70	138	50.72
<i>Summer</i>	Site6b DEM+Mosaic	46	73	63.01
<i>Summer</i>	Site4 DEM	95	243	39.09
<i>Summer</i>	Site4 DEM+Mosaic	148	243	60.91
<i>Summer</i>	Site7 DEM	63	141	44.68
<i>Summer</i>	Site7 DEM+Mosaic	75	141	53.19

In the second approach tree top annotations were done with ArcGIS. Three maps were generated and tree tops were identified on these. Table 22 provides the results of the tree detection performed with ArcGIS.

It can be seen, that for the monocultures in site 1a and site 4b, as well as in site 4c all trees were detected in winter images. For all other sites the accuracy ranged from 60 to 80 %. Interesting results were achieved in sites 11 and 13. The accuracy reaches almost 100 % in site 11 and exceeded the 100 % in site 13. As mentioned, no understory vegetation was classified in site 13 but were detected in the winter images.

In winter, 109 trees were detected, which could not be identified, as they were not included in the field survey. Furthermore, in winter images all visible shrubs were counted at the lower and upper slope, while in the field, as mentioned above, no shrubs were counted in the upper slope. The calculated high accuracy cannot be counted as good result, as it was most probably coincidence.

Table 22 Results for the second approach, summarizing the counting's in summer and winter images, as well as the comparison to the field counting.

Site	Winter counts	Summer counts	Field counts	ACC winter	ACC summer
Site 1a	72	53	72	100.00	73.61
Site 1b	88	68	145	60.69	46.90
Site 1c	111	170	135	82.22	125.93
Site 1d	48	48	70	68.57	68.57
Site 4a	89	53	117	76.07	45.30
Site 4b	114	96	114	100.00	84.21
Site 4c	24	20	24	100.00	83.33
Site 6a	119	90	162	73.46	55.56
Site 6b	37	38	57	64.91	66.67
Site 7	106	98	142	74.65	69.01
Site 11	315	154	316	99.68	48.73
Site 13	273	133	195	140.00	68.21

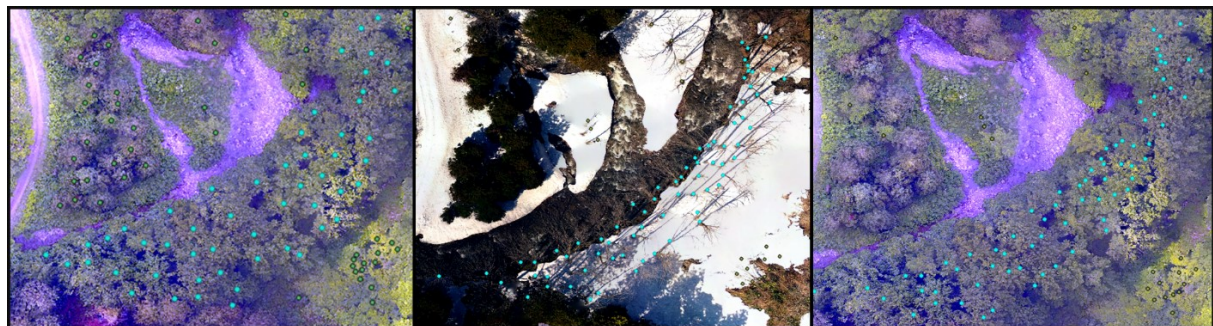


Figure 64 Tree top annotations for S1a. From left: Annotations based on the summer image, annotations based on the winter image and the field data overlaid on the summer image.

In comparison to the accuracy achieved with counting in winter, the summer accuracies were lower, with 15 % to 50 % less counts, which can be also seen in Figure 64. The only exemption was site 1c, where the accuracy was even higher than in winter with 125.93 %. In site 1c, the lower part of the slope was included in the counting. Along the slope, *Acer* species occurred with a high frequency and density. The number of individual plants was difficult to assess in the field because of the high density. Furthermore, in summer images, the structure of acer canopies was open and misled to count more acer trees as there were. Site 1d was, like site 13, located at a steep slope and because of the difficult access only canopy layer trees were counted.

In a second attempt, understory vegetation and young trees were excluded from the counting, as they would never be visible from above, when only RGB images were used and the forest structure was dense. Sites 1a, 1d, 4b and 4c were excluded from the analysis since they already reached 100 % in winter images or because there would not have been further improvements (Table 23).

Table 23 Counts excluding the understory vegetation and/or young trees, as well as the calculated accuracy for winter and summer images.

Site	Winter counts	Summer counts	Field counts	ACC winter	ACC summer
Site1b	88	68	88	100.00	77.27
Site 1c	83	68	89	93.26	76.40
Site 4a	69	53	69	100.00	76.81
Site 6a	119	90	100	119.00	90.00
Site 6a- y	119	90	122	97.54	73.77
Site 7	106	98	102	103.92	96.08
Site 11a	121	114	155	78.06	73.55
Site 11b	121	114	119	101.68	95.80
Site 13a	154	110	151	101.99	72.85

In site 1b, 57 shrubs and young trees were identified, which were *Alnus fauriei*, *Tilia japonica* and *Quercus mongolica* (Figure 65). They had a height of around 1 m, at maximum 2 m. Hence, trees and shrubs were not visible on the winter images under 3 m snow cover. Therefore, with excluding them from the counting, an accuracy of 100% was reached, while the summer accuracy reached a maximum of 77.27 %. It can also be seen, that the accuracy of identified trees in summer was around 75 % for most sites. In winter most sites have accuracies higher than 100 %, which was caused by the young trees, which were taller than 2 m and detectable in winter images. Site 6a showed 119 %, when the understory vegetation was excluded, but the percentage was slightly less than 100 % when young trees were still counted. In site 1c, *Acer* trees were excluded as they were miscounted in summer, which ended in reasonable results for this patch of the forest. Without the understory vegetation (also without *Acer* species) site 11 achieved 78.06 % and 73.55 % for winter and summer, respectively. As from the fieldwork is known, the site contained a high number of young Japanese wingnut trees, these were excluded from site 11b, too, and accuracies of approx. 101 % were reached.

5.4 Discussion

In this work, two approaches were studied, where tree tops were detected with different techniques and images. The first approach analysed the possibility of counting deciduous trees in summer images using first only DEMs and then additionally the visual information of the orthomosaic to identify tree tops. GIMP 2 and a tree top counting code were used to count the manual annotations. In the second approach, ArcGIS was used to create three maps: counting in winter images, in summer images and during a field survey. The first approach using only the DEM limited the counting possibilities because of the structure of deciduous trees. The tree crowns have a roundish shape generating an area of more than 30 m². In a dense natural forest this structure results in a dense crowded canopy area, where it is difficult to identify tree tops in a DEM. The even age of the forest trees and the limited number of tree species in the canopy resulted in a canopy area which has no significant differences in height. Therefore, only using the DEM was not successful to count trees in summer. Using additionally the visual information allowed to distinguish between species even when no significant differences in the DEM were visible. In comparison to coniferous trees, which have a cone shape and therefore a significant tree top in DEMs, the shape of deciduous trees will always be challenging in dense natural forests. The benefit of deciduous trees is that the seasonality can be used as they are losing their leaves in autumn. Furthermore, the climate of Japan with high precipitation in winter enhances the use of this season to count deciduous tree.

With the second approach, especially the use of winter orthomosaics was analysed. For some of the sites, high accuracies counting tree stems in winter images were reached. Especially in dense even-aged monocultures, the accuracy reached 100 %. In these areas, there was no understory vegetation found in the field. As in ArcGIS attribute tables give precise information about the species name of each point, it was possible to see where the differences between the field data and winter counting occurred. Furthermore, as the forest is seen from above, understory vegetations could only be detected when there were gaps in the canopy. The same problem occurred with young trees, as they are usually covered by adult trees, if they grow close together. Hence, excluding them from the analysis gave a better accuracy of tree counting. The accuracy reached 100% for almost all areas and did sometimes even exceed it (Table 23). The reason was that not all young trees grew close to adult trees and were therefore easy to identify in open spaces, if they have reached a height of more than 2 m.

The high accuracies indicate that using the seasonality and changes in temperate forests can help to achieve reliable information about the number of trees in a forest stand. Furthermore, it can be seen, that the accuracy in summer images reached at least 75 % for most of the site. Therefore, it can be stated that it seems to be normal not to find about 25 % of the trees in these dense forest conditions.

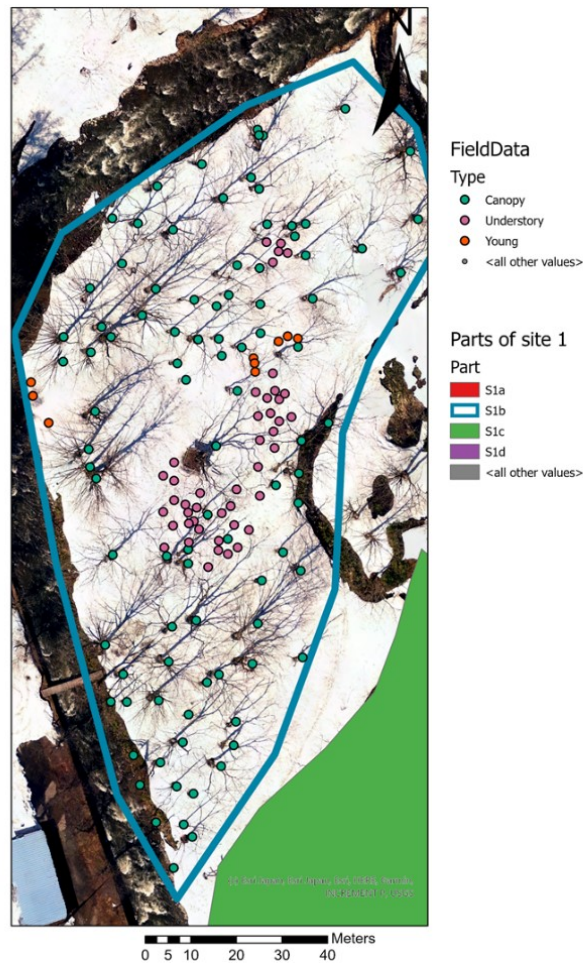


Figure 65 S1b with the annotations separated into canopy layer trees, understory and young trees.

5.4.1 Time and technique consideration

In recent years the development in UAVs, image analysis and computer vision offer another way to do forest research. While the use of computer vision and DL is already successful for classification of tree, detection of trees, forest health identification and biomass estimation, species it still requires expert knowledge to apply those techniques (Onishi and Ise, 2021; Safonova et al, 2019; Natesan et al., 2020). With this work, it is shown that there is already a lot of information in images, which can be extracted using easy techniques to count trees. The two presented approaches used different software. The first one used GIMP, which is an open-source software, where annotations can be done easily as the software is easy to use and it can further be connected with a graphic tablet. Hence, annotations can be provided fast, about one hour for a 1 ha forest patch. With the data gathering (10 min per 1 ha, depending on the flight settings) and preparation (Metashape and GIS 2h per 1 ha) a total time of around 3 h was needed to extract tree tops of summer images. The counting is therefore fast, while field work requires days and has a high demand in man-power.

Using ArcGIS (commercial software) takes longer time, as the annotations cannot be created as fast as in GIMP. Also, three point maps need to be prepared and the data need to be labelled for winter, summer and the field map individually, while a simple counting of the trees from the field was enough in the GIMP approach. On the other hand, GIS offers the visualisation of the data in the geographic environment and further allows the selection in the attribute table to exclude species. Therefore, in this approach it was easy to delete understory vegetation and/or the young trees without a lot of effort. ArcGIS offered a detailed and spatial analysis of the data, which cannot be provided by GIMP. Also, ArcGIS offers plenty of possibilities which help to speed up some of the tasks, like labelling the trees with the raster calculator. In the end, the work with ArcGIS might increase the needed time around 1 h per map but offers more options to analyse the data.

Both approaches showed a higher efficiency than manual field surveys. While ArcGIS offered more visualisation and useful tools, GIMP could provide the same results like ArcGIS in a fast a simple way (if only the canopy layer will be annotated and counted, which was not done in this work). Depending on the task and the needed information both approaches can be useful.

5.4.2 Observations and difficulties

In general, it could be realised, that counting trees in winter images can be done with a high success rate. The brown colour of the branches is significantly different to the white of the snow, which made the identification of tree stems easy. In the end of February, as the snow melting season already began, there were brown rings of soil around the tree stems, which increased the visibility of especially young trees. Difficulties occurred, when the alignment of the winter images did not work well. Then tree stems and branches were sometimes cut and dense areas, in this case tree stems could be hardly separated. Furthermore, trees were at the borders of the sites often covered by *Cryptomeria japonica* trees. The branches of *Cryptomeria* trees mainly cover stems and the effect of blurring at the borders of the orthomosaic further increased the difficulty for detection. Young trees, especially from *Juglans* and *Pterocarya* trees, usually grew close to the adult trees; hence big branches covered the small young trees. There were several conditions, when tree stems were becoming almost invisible: when they are covered by shadows or when the reflection of the snow was too high. On the other side, when the sun was shining, the shadows of tree stems could sometimes increase their visibility. Areas, where a lot of snow had already melted, the brown stems and the brown soil could not be separated. The barren soil areas were usually close to the river, where the dark colour of the water additionally increased the difficulty to find tree stems. Furthermore, in those areas, as they are influenced by several disturbances of the river, especially young trees grow and were even harder to detect. In site

1, the monoculture of *Pterocarya* trees, as all trees could be found in the images, provided a good example, because only adult trees grow there. On the other hand, several young trees were growing in site 6, which were missed during tree stem counting. At last, slopes increased the difficulty of detecting trees, as trees grew closer together or below each other, which made canopies denser and accurate counting impossible.

Even though there were difficulties, which could be identified, winter images provided the best possibilities to count trees in a deciduous mixed dense natural forest. Furthermore, young trees can be additionally identified as well as a high number of understory vegetation. Especially in areas, where the access is limited and field work cannot be done, the provided analysis offers a new way to efficiently count trees in forests.

5.5 Conclusion

The presented study shows two different approaches to do manual tree top annotations on forest images. Each technique provides benefits, which makes them useful for forest applications. While the GIMP approach uses freeware and annotations can be performed fast, it lacks in mapping and georeferencing applications. Annotations in ArcGIS need more time, therefore mapping, georeferencing and pre-processing of the data can be done easily.

Regarding the tree counting, broad-leaved trees make the approach challenging because of their canopy shape and structure, especially, when the forest is dense and naturally mixed. Considering only the canopy layer, around 25% of the trees could not be detected from the images. The use of manual annotations from summer images produces therefore unavoidable errors. Furthermore, young trees could usually not be detected on summer images, as well as understory vegetation. Hence, a better method to accurately count trees needs to be found. This study further indicated that the use of winter images for tree counting of deciduous trees is the most efficient approach for Japanese mountainous mixed forests, especially reaching a high rate of success when only the canopy layer is considered. The high performance exceeded all other presented annotations, using DEMs and also additionally visual information from summer images. Furthermore, understory vegetation could be indicated and young trees with heights of more than 2 m could be counted.

To sum it up, the annotations performed on winter images is an approach which was not used efficiently in previous studies but has the potential to achieve reliable tree counting for forest inventory purposes. The two introduced methods enhance analysis of UAV images in order to characterise forests and tree distribution in a time efficient and low-cost way.

Chapter 6: Deep learning tree species classification

6.1: Computer vision and deep learning techniques for the analysis of UAV-acquired forest images, a transfer learning study

6.1.1 Introduction

Forest ecosystems play an important role in water, carbon and nutrient cycling within the soil-vegetation-atmosphere continuum. In recent years climate change is exerting positive changes such as the early greening of forests in the northern hemisphere, shifting of forests to warmer environments northward (Chen et al., 2011) or negative ones, such as an increase of longer periods of drought (Esquivel-Muelbert et al., 2019), increase in the number of forest fires or extreme climate events (Kherchouche et al., 2019). Recent studies have focused on the ecological functions of mixed forests, since they show high resistance against insect outbreaks and a stronger capacity to recover from disturbances (Coll et al., 2018). Detailed knowledge about mixed forest structure and composition (Anderegg et al., 2019) is needed in order to properly understand current status and future changes.

Forests in Japan occupy approximately 68 % of the total territory, with most of them being natural deciduous broad-leaved mixed forests (Shimada, 2009). Natural forests are affected by climate change while man-made forest ecosystems such as coastal forests are affected by invasive species that diminish their functions as windbreak (Anderegg et al. 2019, Lopez et al., 2014). The distribution of each species within a stand, or the interactions between the different tree species (Coll et al., 2018) makes them ecologically complex, especially in comparison to monoculture forests (Grotti et al., 2019). Until very recently, forest research has been carried out using labour and time-consuming land surveys (Framer and Furnival, 1999). They are costly and demand a high degree of organization training and expertise. Moreover, the characteristics of Japanese forests make them particularly challenging for land surveys as they are often located in steep mountain slopes that are difficult to access. Thus, new tools are needed in order to efficiently gain an overall understanding of species interaction and their response to climate change in order to design the proper response policy to ensure the sustainability of forests.

UAVs are rapidly becoming an essential tool in forestry applications (Onishi and Ise, 2018, Natesan et al., 2019, Safonova et al., 2019, Fromm et al., 2019) and they represent an easy-to-use, inexpensive tool for remote sensing of forests as they can fly close to tree canopies, which results in high image resolution (with one pixel representing a few centimetres). That can be processed by computer vision algorithms. An example of such an application is the building of orthomosaics by aligning the images for visualization and coherent processing of specific forest areas encompassing several hectares.

Additionally, emerging technologies such as DL allow the incorporation of expert knowledge to the automatic processing of images, which together with the availability of larger amount of data, has the potential to radically change the way land surveys are done. Namely, the time-consuming (and sometimes dangerous), intensive field surveys will likely become unnecessary, while those tasks requiring expert human knowledge are expected to be greatly increased.

The main goal of this chapter is to study the use of DL to gain information on forestry applications. By dividing orthomosaics built using UAV-acquired images into regular patches and using two well-known DL architectures (ResNet and UNet), the following objectives were proposed (Figure 66):

- x. Develop an algorithm (that uses a ResNet50) to classify patches corresponding to tree species (MLP algorithm). Assess (a) Quality of the results obtained with the amount of data available (2800 images), and (b) Degree of improvement achieved by Transfer Learning.
- xi. Develop a semantic segmentation algorithm for tree species that is precise (DICE coefficient) and efficient (computation time), using three separate algorithmic approaches and two DL networks.
- xii. Evaluate the applicability of the MLP algorithm to another practical problem: Detection of an invasive tree species in a coastal forest.

For the first objective, a MLP classification algorithm was implemented using a ResNet50 architecture. The effects of learning rates (LR) on the output were studied: (a) Not using Transfer Learning (b) Transfer Learning from ImageNet (Krizhevsky et al., 2012) and (c) Transfer Learning twice, first from ImageNet, then from the Planet satellite image dataset (Planet). For the second objective three algorithms were used to obtain semantic (pixel-wise) segmentations of the deciduous vs. evergreen tree classes in winter orthomosaics: (1) The MLP algorithm as a standalone tool, (2) The MLP algorithm including a (non-DL) watershed segmentation refinement step and (3) A patch-based semantic segmentation algorithm using a UNet architecture.

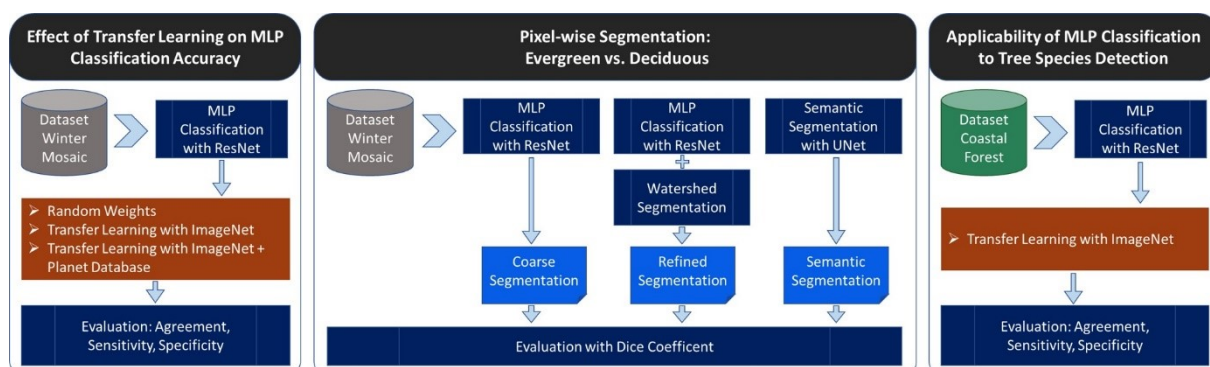


Figure 66 Overview of the contribution

6.1.2 Methodology

Most of the forests considered for this study are natural (i.e., unmanaged) and located in steep mountainous areas that make field surveys difficult. In addition, forests deal with invasive tree species which have a major impact on the structures, properties and function of forest ecosystems (Richardson et al., 2004). The abundance of precipitation in the climate of Japan makes data gathering with drone missions challenging which limits the amount of data. Furthermore, the problem of unevenly distributed trees made image recognition and segmentation tasks more complicated (previous studies of forests were performed mostly in plantations or well-managed forests located in flat areas see, for example (Abd Mubin et al., 2019)). Consequently, acquiring and annotating large datasets made up of millions of images such as ImageNet (Krizhevsky et al., 2012) was not feasible. The research was, thus, motivated by the reported capacity of DL networks to work with smaller datasets as well as it has benefits from Transfer Learning.

6.1.2.1 Data Acquisition

Having a sufficient amount of data is important for DL application. These study data were acquired using a DJI Phantom 4. For this chapter the seasonality in mixed forests was used, by collecting images in the winter season aiming at gaining information on the locations of the stands of evergreen and deciduous trees. Therefore, images were captured at three different dates in late winter 2018 presenting differences in illumination and tree age. Seven flights in five separate study sites were performed (Figure 67). For site 1, three flights were done, while of the other sites only one flight were performed, covering areas of 3 to 8 ha. In order to improve the Ground Sampling Distance (GSD), which is the distance between centre points of each image of the ground expressed in cm/px, two flight plans were performed in steeper slope areas. GSDs between 2.79 and 4.48 (cm/pix) were achieved. The following abbreviations for the sites were used: orthomosaics wm3, wm4 and wm5 belong to the site 1 while the rest are all from different sites (wm1 = site 3; wm2 = site2; wm6 = site 6; wm7 = site 4)

6.1.2.2 Problem definition

The first scenario was to classify the different parts of winter orthomosaics from mixed forests. Natural mixed forests are complex in ecological terms and present special challenges concerning research: The considered forests were located in steep mountainous areas that make field surveys difficult.

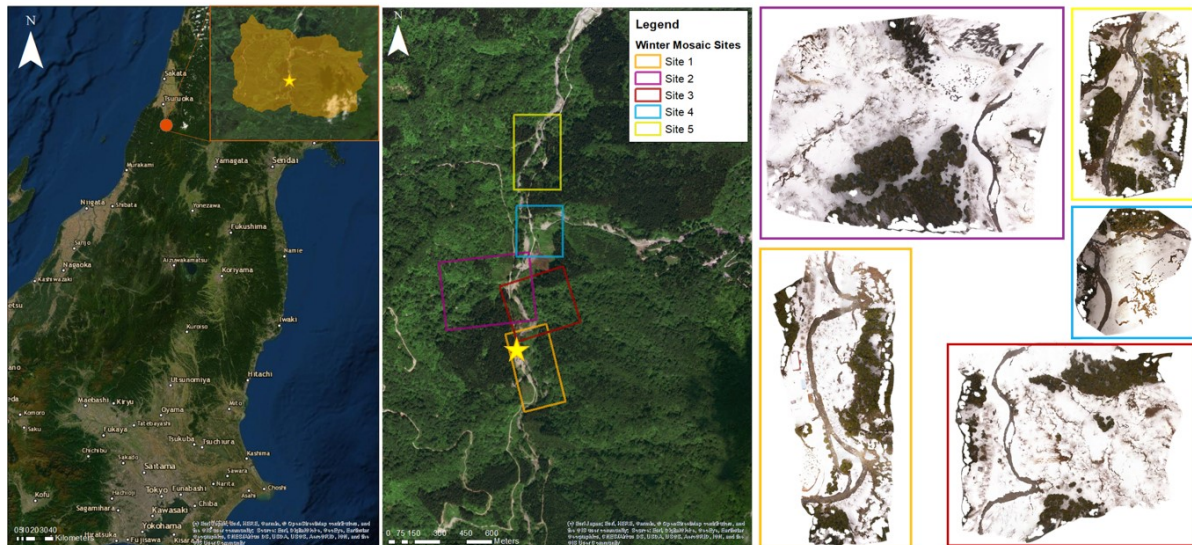


Figure 67 Location of the sites where data was acquired. The middle upper map shows the location of the study area in Japan, whereby YURF is marked as orange point. The map also contains the (orange) area of YURF. The five images at the right show representative orthomosaic for each site

Trees were distributed unevenly making image recognition tasks more complicated (previous studies of forests were performed mostly in plantations or well-managed forests located in flat areas see, for example (Abd Mubin et al., 2019)). The seasonality of mixed forests was used, by collecting images in the winter season aiming at gaining information on the locations of the stands of evergreen and deciduous trees. Knowing the distribution, composition or distance to water of the stands in large areas (such of those studied in this work) can improve the understanding of the overall composition of natural forests. The seasonal data provided additional information such as the number of deciduous tree stems.

6.1.2.3 Data Processing and Annotation

After alignment of the images with Metashape, the data were manually annotated. The annotation method needed 4 to 7 hours per orthomosaic and provided to be a simple, relatively fast way of annotating data for general applications. For the mixed forest winter orthomosaics five layers were annotated: River, Man-made, Uncovered, Deciduous and Evergreen (Figure 68).

Each of the orthomosaics were divided into axis-aligned, square patches of the same side length (hereafter size of the patch) (Figure 68). The annotations as well as the original data were considered, obtaining a set of patches along with patch-wise binary masks for each annotated class.



Figure 68 Example of a winter orthomosaic. Examples of patches each containing a single different class

Any algorithm used in a practical setting is heavily influenced by the characteristics of the data. In the studied case, the disposition of the forest prevented the use of Ground Control Points (GCP). GCPs are meant to be geo-localised easily distinguishable points that aid mosaicking software identify corresponding regions in different images during orthomosaic construction. Sites presenting dense and unmanaged forests prevent the placement of GCPs inside the forest making the use of GCPs impractical. Also derived from tree distribution, Figure 69 shows the difficulties to identify single trees. However, the use of winter orthomosaics (Figure 69) shows an image of the same area where stems are visible and their numbers can be counted. Furthermore, the orography of the forest made data acquisition limited in terms of the amount of data that could be gathered. All imaged sites include steep slopes that are common in this area, which increases the difficulty of identifying trees in this area. Picture C also shows deciduous trees in different conditions and frequently mixed with other classes. The understory vegetation present has the same colour of the deciduous tree and often appears mixed with them. A similar problem happens with the "River" class in. Another limitation likely resulting from not using GCPs is that Metashape produced some image registration artefacts (Figure 69). This increased the difficulty of automatically processing the images.

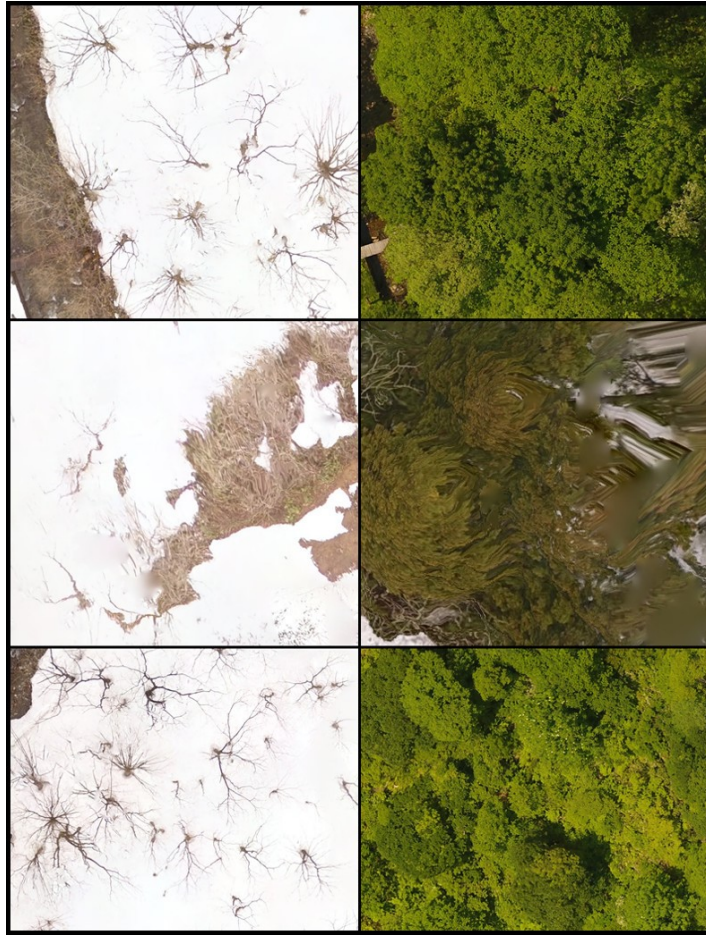


Figure 69 Example images of difficulties faced with the Data. Images are examples of the mixed forest

6.1.2.4 Problem Formalisation

The automatic division of the data and mosaic-level annotations into regular patches allowed to formalize problems in two different ways. First, the focus was on identifying what classes were present in each orthomosaic patch, which is known as multi-label classification. As a second formalisation the focus was on classifying each pixel in each orthomosaic patch. This problem is known as semantic segmentation (Guo et al., 2018). The aforementioned patch multi-label classification algorithm already gave an initial "coarse" approximation to this semantic segmentation. In order to refine it the classical watershed (Beucher and Meyer, 1993) image segmentation method was used. The UNet DL architecture (UNET) was also considered. A full pipeline of the work is provided in Figure 70, while Figure 71 (left) shows a patch of one of the winter orthomosaics. The central part of Figure 71 shows the manual annotation for this patch. Blue pixels are classified as the "Evergreen" class, yellow pixels to the "Uncovered" class and green pixels as the "River" class.

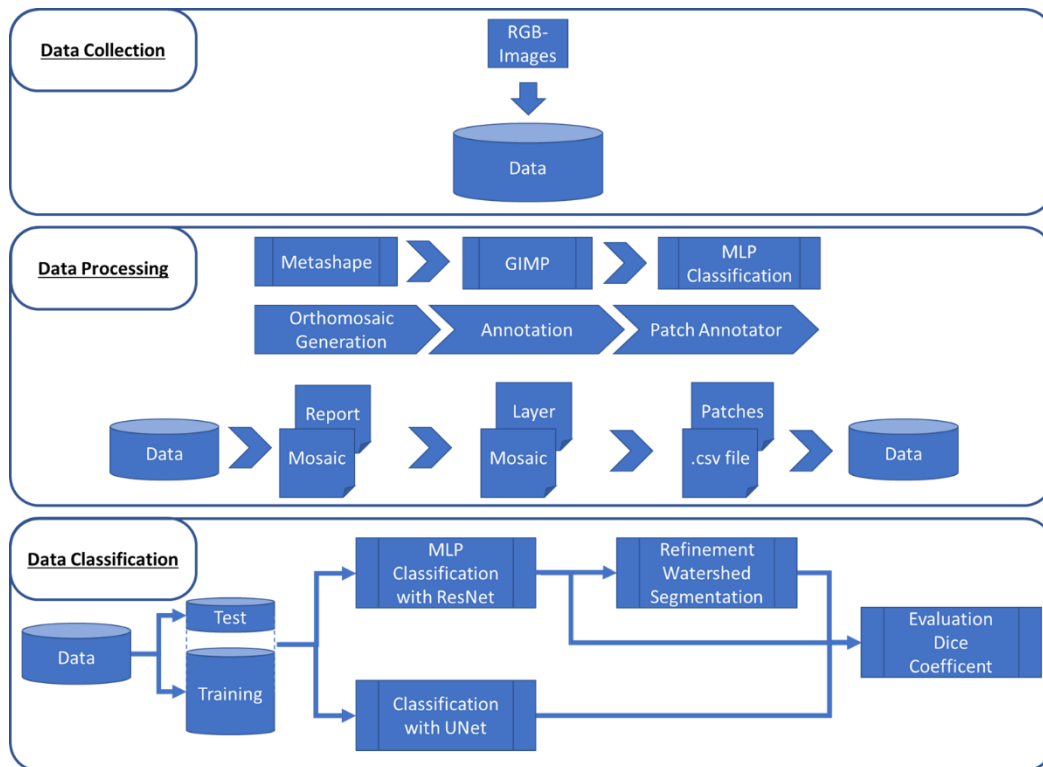


Figure 70 Algorithm Pipeline



Figure 71 A small section (patch) of a winter orthomosaic. Patch of an RGB Image as captured by the UAV (left). Mask with the annotations showing the class of each pixel (middle), in this case blue pixels belong to the "Evergreen" class, yellow pixels to the "void" class. This mask serves as the ground truth for the semantic segmentation formalisation. Superposition of the two previous images (right). Consequently, the ground truth for this patch was the list [river, uncovered, evergreen] for the multi-label classification formalisation.

6.1.2.5 Multi-label Patch Classification Using ResNet

Previous studies have shown the efficiency of DL networks to classify forestry images, specifically (Onishi and Ise, 2018; Natesan et al., 2019), because they relied on the ResNet architecture (He et al., 2016).

A ResNet variant with 50 layers was chosen, known as ResNet50. Although the aforementioned approaches used a tree crown segmentation step based on DEMs produced by the UAV. The data and annotations were used in form of patches, where each patch was assigned a class. For example, the list could contain the labels river, uncovered and evergreen. Thus, patches may belong to more than one class each, with a probability value for each patch. Given high enough probabilities in more than one class, the patch would be labelled repeatedly. Thus, this algorithm is referred to as the MLP based classifier. The ResNet50 network was trained to classify the created patches. A subset of the data was used for training, and the remaining data was used to validate the quality of the trained model at predicting the correct classes. 80 % of the dataset was randomly chosen for training and the remaining 20 % was used for testing.

DL architectures need less data than previous approaches, however, having sufficient data to produce results of satisfactory quality is still a problem in research areas such as forestry, where data acquisition is often problematic. Transfer Learning represents a way to improve the quality by initializing the weights of the matrices conforming the DL network to those obtained in the solution of a similar problem. In this study Transfer Learning is used as followed: (1) a general-purpose object classification problem codified in the ImageNet database ([Kizhevsky et al., 2012](#)) and (2) the closer problem of multi-label classification in satellite images of the amazon forests codified in the Planet dataset ([Planet](#)).

6.1.2.6 Segmentation Refinement using watersheds

The MLP classification algorithm generated an initial coarse segmentation. All pixels in any patch containing a class were considered to belong to that class. This patch-wise masks for all classes constitute a segmentation of the orthomosaic. The coarse nature of this segmentation produces two problems. First, over-segmentation: by assigning all the pixels in the patch to all the classes present, would also assign pixels to classes they did not belong to. These extra pixels make the masks of classes larger. Second, the coarse class masks therefore generated intersect. This is undesirable in the semantic segmentation problem as each pixel should be classified into one single class. In order to improve the initial segmentation a refinement step based on the watershed image segmentation algorithm ([Beucher and Meyer, 1993](#)) was implemented. This algorithm uses binary images representing initial masks consisting of doubtless labelled pixels. Parts of the image that could confidently assigned to the background were also determined. Any pixel not falling into any of these two cases were labelled as “unknown”. Labelled regions were visualised as ridges and unknown areas as basins. Then, water was pictured as expanding from the ridges into the basins until two of the growing ridges meet and watershed lines were determined. These lines defined the segmentation.

The starting point was the coarse segmentation of the “River” class. A binary image was generated by painting all pixel black that belonged to all patches where the river class had been predicted. All pixels out of these patches were marked as background. Then, this coarse mask was shrunk using a distance transform and pixels that had been deleted by this process were labelled as unknown. Further, all the connected components of the mask were computed and stored in a dictionary with their position and an identifier, along with the information that they belonged to the “River” class. Then, the second class, the “Deciduous” class, was considered. The previous process was repeated but storing the results from the previous step. Regions that previously formed the background were overwritten, regions that were unknown before or where two labels were assigned were labelled as unknown. The process was repeated for all classes and the images were partitioned into (1) Background (2) unknown and (3) initial regions. Each initial region had the information attached as to what class it belonged to. The watershed algorithm was subsequently run to create a finer segmentation without intersection between the different classes.

6.1.2.7 Forest Orthomosaic Segmentation Using UNet

The UNet DL architecture (Ronneberger et al., 2015) was originally developed for medical image segmentation (Funke et al., 2019) but has since then been used in a variety of applications. The UNet architecture is composed of two parts known as paths: the encoder and the decoder path. The encoder path extracts features using convolutional layers and reduces the size of the images using max pooling layers. At the end of the encoder path the images are greatly reduced in size and the transformations they were subjected to are stored in the weights of the matrices along the path. The decoder path, moves back to full size ones by replacing pooling operators with upsampling operators. High resolution features from the encoder path were combined with the upscaled output in order to localise them. Successive convolution layers learn to re-assemble the output more precisely based on this information. An algorithm was implemented using the UNet architecture to perform semantic segmentation of the winter orthomosaics. The data and pixel-wise-annotation patches described in Section Problem definition were considered and used to train a UNet network. Whenever a new orthomosaic needed processing, (1) it was divided in patches, (2) predicted the semantic segmentation of each patch using the trained UNet model and (3) joined all patch segmentations together to obtain a semantic segmentation for the whole orthomosaic.

6.1.2.8 Experiments

In the first experiment all seven winter orthomosaics were run with the Patch-Annotator. Randomly, 80 % of the patches were used for the training, the remaining 20 % for testing. The classifier was learning with the 80 % of patches and checking its own results with the .csv file, containing the correct labels of the patches outputting the mentioned values above. The results were evaluated on the remaining 20 % of the test images. The report of this approach focused on the patches. The classification accuracy of each patch was reported, as well as the misclassification.

For the second experiment six orthomosaics were processed by the Patch-Annotator and again the patches were divided into 80 % for training and 20 % for testing. In this case the last orthomosaic were taken and ran it on the Patch-Annotator. Those patches were used, after the training of the model, to run the Classifier again. The classification results were evaluated on the output of the model from the last orthomosaic.

6.1.2.9 Evaluation Methods

Several metrics were used to evaluate different aspects of the algorithm's performance. First, the capacity of the MLP algorithm to correctly predict the labels in every patch was evaluated:

- Full Agreement (FA)
- Full Agreement with False Positives (FAFP)
- Partial Agreements (PA)
- No Agreement (NA)

In order to target the predictive capacities of the algorithms patch labels for the MLP algorithm were considered and pixel labels for the semantic segmentation algorithm. For all of them the relation between predicted values and real values was considered with TP, FP, TN and FN. Furthermore, classification measures were computed on them:

$$Sens = \frac{TP}{TP + FN}$$

$$Spec = \frac{TN}{TN + FP}$$

$$ACC = \frac{TP + TN}{TP + TN + FP + FN}$$

$$DICE = \frac{2TP}{2TP + FP + FN}$$

6.1.3 Results

In this section, experiments were presented using real data corresponding to seven winter orthomosaics and one summer orthomosaic from the coastal forest covering a total area of 38.5 ha. Of the five winter orthomosaics from YURF, three corresponded to the same site on different days and under different lighting conditions. All the algorithms described throughout the paper were implemented using the python programming language. The ResNet and UNet DL architectures were implemented using the Fastai ([Howard et al.](#)) library. The watershed algorithm was implemented using the opencv computer vision library ([OpenCV](#)). All experiments were run in workstation using a Linux Ubuntu operating system with 10 dual-core 3GHz processors and an NVIDIA GTX 1080 graphics board. (For experiments 1 and 3 the data were randomly divided into (80 %, 20 %) training and validation/testing. For experiment 2 a leave-one-out approach was done with each of the seven winter orthomosaics using one for validation/testing and the other six for training.

6.1.3.1 Experiment 1: Transfer learning and multi-label patch classification

The data were randomly divided into (80 %, 20 %) training and validation/testing. The patch size was chosen to be 150, see Section Semantic segmentation for the effect of this parameter. With this parameter, the annotated patches contained the deciduous label in 52.26 % of the cases, the evergreen class in 39.33 %, uncovered in 28.29 %, river in 12.84 % and man-made in 1.26 %. Notice that, as patches often belong to more than one class, these percentages add to more than 100 %.

In order to assess the impact of Transfer Learning several "starting models" were built and trained using forest images. Each model was considered in two forms, frozen and unfrozen. When a frozen model was re-trained only the final layers of the model were changed. When an unfrozen model was re-trained, all of the layers were modified. The starting models that we considered were:

- Random: In order to test whether Transfer Learning was necessary, a model initialised with random weights were included. Only results of the unfrozen random model were presented as the frozen random model had poor results.
- RN50F, RN50UNF: We also considered a ResNet50 with preloaded ImageNet ([Krizhevsky et al., 2012](#)) weights. The inclusion of this model allowed us to study whether or not a general-purpose classification model could be fit to solve the problem using a relatively low number of images. This model was re-trained frozen (RN50F) and unfrozen (RN50UNF).
- RN50 + PLANET-UNFF, RN50 + PLANET-UNFUNF, RN50 + PLANET-FF, RN50 + PLANET-FUNF: The ResNet model was considered again and re-trained it using the PLANET dataset of satellite images of the Amazon rainforest ([Planet](#)). In order to assess whether better results could be

obtained when training from a problem (classification of satellite images of tropical vegetation) being more similar to the data. The ResNet model was considered frozen and unfrozen as before, RN50 + PLANET-F, RN50 + PLANET-UNF. These two models were subsequently retrained with images each considered frozen and unfrozen producing 4 models: RN50 + PLANET-UNFF, RN50 + PLANET-UNFUNF, RN50 + PLANET-FF, RN50 + PLANET-FUNF.

The learning rate of a DL model is a parameter that controls the step size of the optimizer that changes the weights in each iteration of the training phase. Various LR values were tested in all the different Transfer Learning approaches. In order to present a comprehensive picture, among all values tested Figure 72 was presented from 1×10^{-5} to 0.9 with 10 sampling points at each exponent value (1×10^{-5} , 2×10^{-5} ... 9×10^{-5} , 1×10^{-4} , 2×10^{-4} ...).

Agreement: Agreement results (TA, TAFP, PA) provided us with a general picture of the capacity to all the trained models to classify patches with all the possible labels (River, Deciduous, Uncovered, Evergreen and Man-made). The best TA results were obtained by the RN50+PLANET-UNFUNF model with a value of 81.58 at a learning rate of 4×10^{-3} . The first trend that could be observed in plots A, B, C in Figure 72 is that the learning rate that provides better result for a model is determined by whether the model was frozen or not. Specifically, the three unfrozen models obtained best results with smaller learning rates of around 1×10^{-4} while frozen models achieve their best results with learning rates of 0.04. This is consistent with previous results reported in (Onishi and Ise, 2018) where the best learning rate for a frozen model trained using ImageNet weights was 0.01.

The importance of Transfer Learning was indicated in the TA peaks of the different approaches. The model initialised with random weights peaked at 72.53 TA, a lower value than the other models. Frozen models achieved good results with models RN50F, RN50+PLANET-FF and RN50+PLANET-UNFF peaking at 79.51, 79.42 and 79.62 TA, respectively. This represented an improvement of 9.78% over the model with random weights. Similar trends could be observed for the accumulated TAFP and PA plots with peaks of 87.76 TAFP and 98.12 PA for the RN50+PLANET-UNFF model. Likewise, similar results could be observed with unfrozen models. Best results of RN50UNF, RN50+PLANET-FUNF and RN50+PLANET-UNFUNF peaked at 80.39, 80.98 and 81.58 TA. This was an improvement of 10.83 %, 11.66 % and 12.48 % over the random weights model. Best overall results were obtained from the model that was built using first an unfrozen version of the ImageNet model to train the Planet dataset and then leaving the resulting model unfrozen to train with the images. The general tendencies observed here were confirmed using difference of means hypothesis tests (t-tests as data size was > 25). Even models presenting smaller differences in the TA peak (like the difference between the performance of the RN50UNF and RN50+PLANET-UNFF) were found to present statistically significantly different means with significance level 0.05.

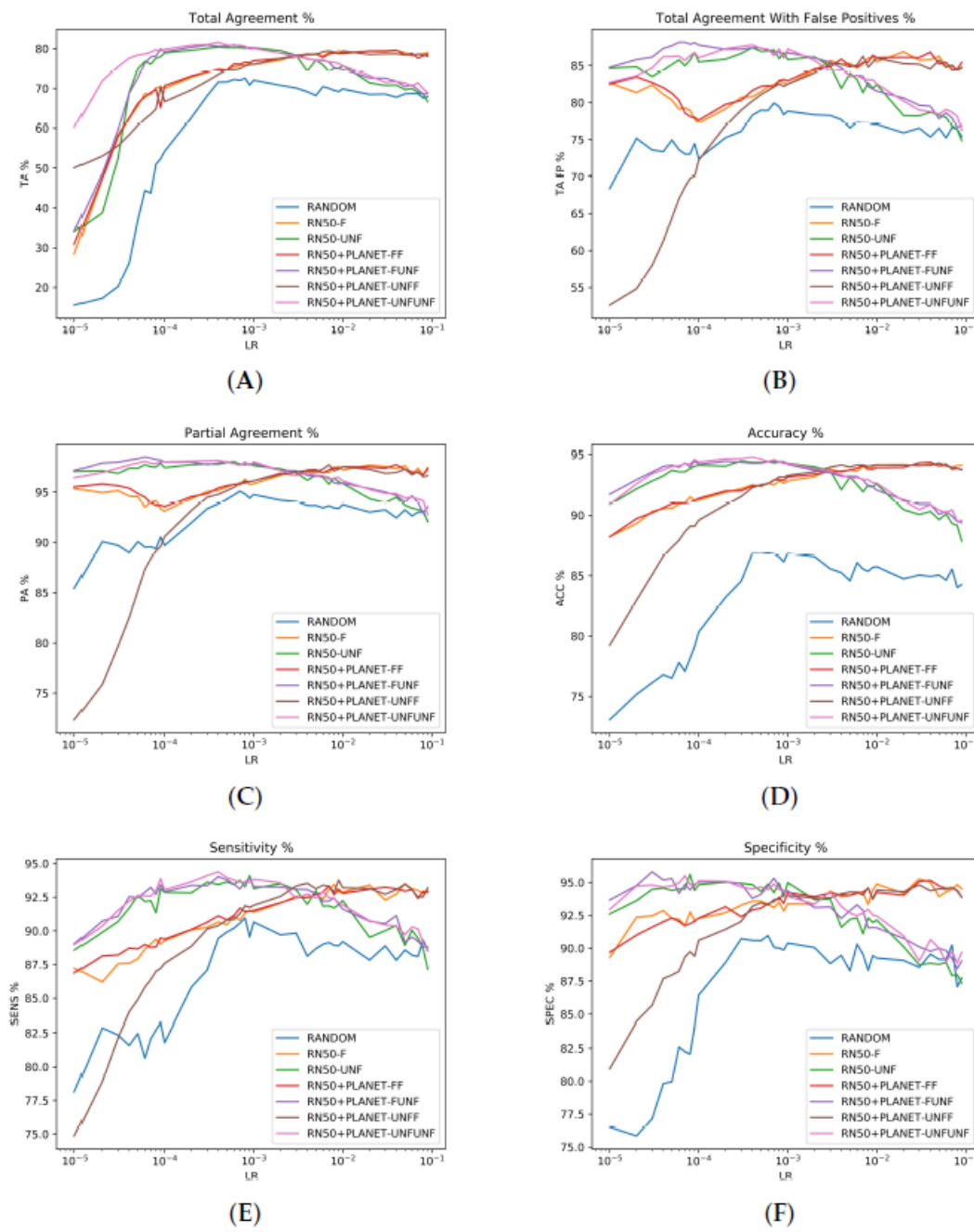


Figure 72 (A) Total Agreement (TA), (B) Accumulated value of Total Agreement with False Positives (TA FP), (C) Partial Agreement (PA), (D) Accuracy (ACC), (E) Sensitivity (SENS), and (F) Specificity (SPEC) for winter orthomosaic data. Patch Size is 150. Frozen models end with an F, unfrozen models with UNF

Classification of deciduous and evergreen classes: The best TA was obtained with the RN50+PLANET-UNFUNF and a value of 81.58 %. Patches without Total Agreement presented errors when classifying the three classes that were not of direct practical interest (river, uncovered, man-made). The number of patches containing them was low compared to patches presenting the other two classes (deciduous and evergreen. However, the results of the two classes of interest had high

sensitivity, specificity and accuracy values (plots D, E, F in Figure 72, average values for the two classes) when no data balancing was performed. Best average accuracy results between the two classes (94.80%) were obtained by the RN50+PLANET-UNFUNF model (that also obtained the top TA value). The clearly defined boundaries of evergreen trees resulted in an accuracy of 97.24 %, while the deciduous tree class presented less defined edges and obtained 92.36 %. Sensitivity and specificity values of the same model were also high with an average of 94.38 % (94.75 % Ev, 94.01 % Dec) and 94.50 % (98.73 % Ev, 90.27 % Dec). The larger difference appeared in specificity, where an 8 % difference was observed. This can be explained by misclassifications of the deciduous class into mainly the uncovered class. Still, the classification results were high with values of up to 97 %. This indicated that patch-dividing and classification approach using a multi-label ResNet DL classifier was successful with the amount of data available.

6.1.3.2 Experiment 2: Semantic segmentation

Results from three approaches were presented, the patch based coarse segmentation produced by the algorithm in Section Experiment 1, the refinement of that segmentation using watershed segmentation and the patch-based UNet algorithm. The first goal of this experiment was to test the performance of the algorithms in real-life conditions. The models were trained with data from six orthomosaics and validated (tested) with the one that had been left out. This approach relates to the use case where an already trained system receives a new orthomosaic for automatic classification. Of the seven orthomosaics three belonged to the same site. Consequently, in most cases (4/7), test images were of trees that the trained system had never seen before. In some other (3/7) images of trees previously seen under different conditions were used for testing. These two sets of results allowed us to discuss about the generalization power of the algorithm and the possibility of over-fitting. As a second major goal, the effect of choosing one problem formalisation or DL architecture over another were studied and insights were gained from the data.

Patch size and learning rate: The proximity of the multi-label patch classifier (seen as a coarse segmentation) output to the manual annotations depended on two factors: First, the accuracy of the classification model, where wrongly classified patches would result either in False Positive or False Negative regions in the coarse mask and second the size of the patches, which produced an approximation error that grew with the size of the patches. At the same time, smaller patches took longer to compute. Patch sizes from 500 to 25 for both ResNet Patch based classification (known as "coarse" segmentation) and the version with Watershed refinement (noted "Refined") were considered. The learning rate presented was the highest among all learning rates studied in Section

Experiment 1 for each patch size. The training time needed for the Resnet varied from under 10 minutes for patch size 500 to two hours fifty minutes for patch size 100 up to over 40 hours for patch size 25. Concerning the UNet, several patch sizes and learning rates were tested where the patch size of 500 led to better results. In this study only five illustrative examples of learning rates were presented.

Fehler! Verweisquelle konnte nicht gefunden werden. and

DICE coefficient: Concerning semantic segmentation for all sites, the best results for the UNet were (0.709, 0.893) DICE for (deciduous, evergreen) for LR=0.0005. The ResNet50 coarse segmentation obtained (0.790, 0.883) for patch size 25 with the refined version (watershed post-processing) reaching (0.733, 0.855). On the other hand, the UNet semantic segmentation achieved an average value of 0.893 for the "Deciduous" class, showing how its pixel wise approach adapts better to this class that presents less well-defined borders. The learning rates presented for the UNet show some representative examples of all the learning rates considered.

The refined ResNet algorithms, watershed post-processing helped to improve the coarse segmentation up to a certain patch size. For these models, the training time was the fastest among the three models and the results obtained were not far from the best obtained. This represents an example of specialized computer vision algorithms that can complement the knowledge gained by using DL. These algorithms, however, cannot easily be used by non-experts and require careful fine-tuning as exemplified by the failure of the watershed refinement to produce satisfactory results for small patch size. This was most likely due to small misclassified regions growing into larger regions due to poor parameter choice than actual limitations of the proposed approach. However, running the watershed refinement took less than a minute for any of the tested orthomosaics. Training time of the UNet network or any of the networks with smaller patch sizes was much larger than that.

The difference of the average DICE coefficient among sites were small. Orthomosaics 3, 4 and 5, representing site 1, show differences of 6% for the with UNet network defined "Deciduous" class. An improvement of 1% for the same orthomosaics and classes with the refined ResNet algorithm was attained.

Table 25 present the DICE coefficient for all the algorithm variants. The average training time of the UNet was of over 11 hours.

Table 24 Comparison of semantic segmentation approaches for the "Deciduous" class in winter orthomosaics (wM). The first half of the table contains the results for the UNet model, the second half contains results from the patch based multi-label ResNet classifier. The first column contains the size of the patches used. Rows marked "Coarse" use only the ResNet*

classifier while rows marked "Refined" also use watershed refinement. Last two columns are the average values (AVG) between all orthomosaics and between orthomosaics of site 1.

Deciduous		wM1	wM2	wM3	wM4	B	wM6	wM7	AVG	AVG Site1
UNet										
LR 0.3		0.253	0.222	0.000	0.402	0.254	0.329	0.397	0.265	0.219
LR 0.04		0.607	0.171	0.372	0.537	0.494	0.275	0.308	0.395	0.468
LR 0.003		0.650	0.631	0.571	0.448	0.429	0.254	0.326	0.473	0.483
LR 0.0005		0.824	0.772	0.797	0.609	0.596	0.664	0.699	0.709	0.667
LR 6×10^{-5}		0.792	0.740	0.784	0.591	0.637	0.639	0.620	0.686	0.671
Resnet										
Patches 500	Coarse	0.665	0.572	0.659	0.569	0.666	0.492	0.521	0.592	0.631
	Refined	0.704	0.597	0.695	0.501	0.583	0.510	0.568	0.594	0.593
Patches 300	Coarse	0.581	0.515	0.604	0.555	0.594	0.441	0.398	0.527	0.584
	Refined	0.585	0.505	0.501	0.552	0.666	0.450	0.449	0.530	0.573
Patches 200	Coarse	0.684	0.576	0.687	0.609	0.670	0.559	0.514	0.614	0.656
	Refined	0.720	0.613	0.708	0.510	0.597	0.555	0.616	0.617	0.605
Patches 100	Coarse	0.795	0.702	0.777	0.683	0.767	0.702	0.698	0.732	0.742
	Refined	0.796	0.703	0.780	0.681	0.764	0.707	0.704	0.733	0.741
Patches 50	Coarse	0.860	0.779	0.782	0.711	0.790	0.761	0.753	0.777	0.761
	Refined	0.667	0.614	0.514	0.570	0.670	0.432	0.509	0.568	0.585
Patches 25	Coarse	0.896	0.839	0.752	0.711	0.795	0.78	0.757	0.790	0.753
	Refined	0.706	0.6	0.448	0.562	0.611	0.494	0.488	0.558	0.540

DICE coefficient: Concerning semantic segmentation for all sites, the best results for the UNet were (0.709, 0.893) DICE for (deciduous, evergreen) for LR=0.0005. The ResNet50 coarse segmentation obtained (0.790, 0.883) for patch size 25 with the refined version (watershed post-processing) reaching (0.733, 0.855). On the other hand, the UNet semantic segmentation achieved an average value of 0.893 for the "Deciduous" class, showing how its pixel wise approach adapts better to this class that presents less well-defined borders. The learning rates presented for the UNet show some representative examples of all the learning rates considered.

The refined ResNet algorithms, watershed post-processing helped to improve the coarse segmentation up to a certain patch size. For these models, the training time was the fastest among the three models and the results obtained were not far from the best obtained. This represents an example of specialized computer vision algorithms that can complement the knowledge gained by using DL. These algorithms, however, cannot easily be used by non-experts and require careful fine-tuning as exemplified by the failure of the watershed refinement to produce satisfactory results for small patch size. This was most likely due to small misclassified regions growing into larger regions due to poor parameter choice than actual limitations of the proposed approach. However, running the watershed refinement took less than a minute for any of the tested orthomosaics. Training time of the UNet network or any of the networks with smaller patch sizes was much larger than that.

The difference of the average DICE coefficient among sites were small. Orthomosaics 3, 4 and 5, representing site 1, show differences of 6% for the with UNet network defined "Deciduous" class. An

improvement of 1% for the same orthomosaics and classes with the refined ResNet algorithm was attained.

Table 25 Comparison of semantic segmentation approaches for the "Evergreen" class in winter orthomosaics (wM*). The first half of the table contains the results for the UNet model, the second half contains results from the patch based multi-label ResNet classifier. The first column contains the size of the patches used. Rows marked "Coarse" use only the ResNet classifier while rows marked "Refined" also use watershed refinement. Last two columns are the average values (AVG) between all orthomosaics and between orthomosaics of site 1.

Evergreen		wM1	wM2	wM3	wM4	wM5	wM6	wM7	AVG	AVG Site1
UNet										
LR 0.3		0.856	0.822	0.364	0.576	0.708	0.785	0.620	0.676	0.549
LR 0.04		0.894	0.806	0.798	0.767	0.828	0.769	0.612	0.782	0.797
LR 0.003		0.855	0.802	0.803	0.626	0.761	0.763	0.648	0.751	0.730
LR 0.0005		0.931	0.896	0.906	0.815	0.897	0.928	0.876	0.893	0.873
LR 6×10^{-5}		0.914	0.857	0.859	0.794	0.866	0.896	0.818	0.858	0.840
Resnet										
Patches 500	Coarse	0.607	0.650	0.511	0.528	0.593	0.644	0.644	0.597	0.544
	Refined	0.676	0.710	0.548	0.375	0.604	0.700	0.729	0.620	0.510
Patches 300	Coarse	0.697	0.729	0.651	0.634	0.661	0.723	0.691	0.684	0.648
	Refined	0.804	0.345	0.744	0.708	0.676	0.800	0.809	0.698	0.709
Patches 200	Coarse	0.722	0.767	0.638	0.619	0.697	0.736	0.710	0.698	0.651
	Refined	0.845	0.850	0.759	0.722	0.769	0.807	0.721	0.782	0.750
Patches 100	Coarse	0.865	0.844	0.796	0.767	0.806	0.847	0.803	0.818	0.789
	Refined	0.887	0.869	0.884	0.689	0.873	0.907	0.877	0.855	0.815
Patches 50	Coarse	0.914	0.888	0.867	0.820	0.865	0.904	0.852	0.873	0.851
	Refined	0.844	0.744	0.880	0.514	0.523	0.865	0.735	0.729	0.639
Patches 25	Coarse	0.923	0.875	0.881	0.84	0.89	0.926	0.843	0.883	0.870
	Refined	0.424	0.529	0.621	0.514	0.55	0.656	0.675	0.567	0.562

6.1.4 Discussion

In the first experiment, the effects of DL were quantified concerning the problem of multi-label patch classification of winter orthomosaics. The available seven orthomosaics were an insufficient amount of data to reach high accuracies for tree species classification when training a ResNet network from scratch. Precisely, starting from random weights led to a TA value of 72.53. The experiments showed that Transfer Learning from ImageNet (a general-purpose dataset) was essential to obtain high quality results with a 9.78 % improvement in Total Agreement (up to 79.63 TA). Ref. (Fromm et al., 2019) reported a similar increase in conifer seedling detection metrics ranging between 3 % and 10 %. Additionally, a further 2.7 % improvement in Total Agreement (reaching 81.58 TA) was observed when Transfer Learning from the Planet dataset, which is more closely related to the images (Figure 72). Thus, Transfer Learning is necessary to obtain reliable results for the winter orthomosaics problem. Furthermore, the smaller improvement when Transfer Learning from the Planet dataset was performed (2.7 % over 9.78 %) suggests that dedicating too many resources to find closely related problems may not be cost-effective. Furthermore, these results indicated that making data and annotations from forestry-related DL research publicly available could speed up the development of this research area by decreasing the amount of data needed by future contributions.

In the last step of experiment 1 the focus was on the results of only evergreen and deciduous trees since tree species classification was the aim of this study. High accuracy, sensitivity and specificity values were achieved. Specifically, regarding sensitivity, evergreen trees reached values of 94.75 % and deciduous trees reached 94.01 %. Comparing these results to previous work is difficult as previous studies have used single-label (rather than) multi-label classification. Also, they have used different DL networks, applied in problems with different levels of complexity (Onishi and Ise, 2018, Natesan et al. 2019, Safonova et al., 2019).

Nevertheless, and for the sake of context, the obtained sensitivity values were presented with these previous works in Table 26. Specifically, Onishi and Ise (2018) and Natesan et al. (2019) reached average sensitivities of 89 % and 81 %, which were lower than the ones achieved in the experiment. Safonova et al. (2019) reached an average value of 91.84 %, which was close to the results but the single classes showed a high variability from 81.25 % to 100 %.

Table 26 Comparison with State-of-the-Art methods

Onishi and Ise 2018		Safonova et al. 2019		Natesan et al. 2019		Our results	
Classes	Sens.%	Classes	Sens.%	Classes	Sens.%	Classes	Sens.%
Deciduous broadleaf	95.83	Healthy	100.00	Red Pine	67.00	Deciduous	94.75
Deciduous coniferous	84.62	Colonized	86.11	White Pine	77.00	Evergreen	94.01
Evergreen broadleaf	68.00	Recently died	81.25	None Pine	97.00		
Chamaecyparis obtusa	91.95	Deadwood	100.00				
Pinus elliottii / taeda	94.12						
Pinus strobus	88.89						
Others	88.20						
Average	89.00		91.84		81.00		94.38

The second experiment focused on segmentation approaches of the "Deciduous" and "Evergreen" classes. Best DICE values for these two classes with UNet were (0.709, 0.893) and with ResNet (0.790, 0.883). These numbers showed that the best results were obtained by UNet for the "Evergreen" class while the "Deciduous" class was better detected by the MLP ResNet approach. The less-defined borders and the overlap between colours of the deciduous trees and the "Uncovered" class makes it difficult to properly segment the trees with the pixel-oriented UNet. In this sense, formalising the problem as a patch labelling problem allowed the gain some flexibility in the definition of the classes and identify the pixels belonging to this class more precisely. On the other hand, formalising the problem as a semantic segmentation problem allowed the use the internal coherence of the "Evergreen" class. In addition, the comparison between the DICE coefficients of all orthomosaics suggests that the algorithms were able to segment totally new orthomosaics as well as those that they had already seen under other lighting conditions. Overfitting, then, seems not to be present in the results and it could be confirmed that the algorithms can segment deciduous and evergreen trees in Japanese mixed forest with reasonably good results. Furthermore, the watershed-based refining step

provided a fast compromise between the two pure-DL formalisations. Consequently, using larger patch size with watershed refinement might be a solution in situations where training time is a limiting factor. This problem-specific computer vision algorithm illustrates the effect that a more sophisticated use of DL and computer vision techniques can have on forestry research.

6.1.5 Conclusion

In this work, the current role and development possibilities of DL were analysed to solve practical problems in forestry research. The study provided a simple pipeline based on drone-acquired images for classifying tree species. The experiments showed that Transfer Learning was essential to obtain good results for patch classification. Better results were obtained when a more closely related dataset was used.

The study obtained semantic segmentations for winter orthomosaics that reached high DICE values when compared to the ground truth. The effect of the DL model was made apparent by the fact that best results for the "Evergreen" class were obtained by UNet and for the "Deciduous" class by ResNet. Watershed post-processing could be used to reduce the computation time of the most cost-intensive algorithms.

Finally, the presented experiments also showed that DL provided valuable information about complex classification problems when used as a "black box". The patch-based classifier provided reasonably good results to find patches containing black locust trees in the black pine coastal forest orthomosaic. The methodology studied in this paper can, thus, be used to gain insight in other forestry applications.

6.2 Automatic tree species classification

6.2.1 Problem definition

Mixed forests were mainly classified using field plots and field surveys, to assess tree composition and tree distribution (Sakio, 2002; Fukumachi et al. 2020, Hedwall et al., 2018; Pyttel et al., 2013). The field plots were usually small (1 ha) or studies focussed on single tree species, while the relations of the sites to the whole forest were not considered. Field plots are time-consuming and demand high manpower. Image analyses are more convenient, as gathering in the field is fast and classifications or tree locations performed with the images are. While field data can be directly processed to maps, image data needs to be annotated first, where areas of different tree species will be marked. This step is usually done manually and can be as time-consuming as field inventories, when the forest has a high degree of mixture and density. Therefore, the need of faster annotations is high, which can be met using computers, which perform automatic classification. Recent developments in computer vision, as well as the increasing use of DL in forestry research, made automatic classifications attractive. First studies focussed on detecting trees in images (Mohan et al., 2017; Kattenborn et al., 2014; Malek et al., 2014) for counting purposes in plantations. Then, tree species classification gained more attention (Fujimoto et al., 2017; Morales et al., 2018; Kattenborn et al., 2020), where forests were composed of a small number of tree species or considered classes for tree species classification. Mixed forests can be composed of two tree species, but usually, there is a higher number of tree species, which occurs in the forest. Until now, a reliable methodology is needed to precisely classify several tree species, in natural mixed forests, on small scales, but also on large-scales. In Japan, two studies were conducted in an artificial coniferous forest (Fujimoto et al., 2017) and a managed forest composed of planted coniferous and naturally grown broad-leaved trees (Onishi and Ise, 2021). Both studies presented high accuracies using different versions of ResNet, but present methodological problems (Diez et al., 2021). Furthermore, they mainly classified coniferous trees, which were easier to identify because of their characteristic tree crown shape. The study of Schiefer et al. (2019) analysed 14 classes composed of nine different tree species, three genus-level classes and two other classes, being the only study with such a broad classification approach for tree species. The authors used semantic segmentation and considered trees as objects instead of assigning each pixel in the image to a category, reaching high classification results.

Detectability of trees, the use of the seasonality for image classification and image-resolutions were topics discussed in the previous mentioned studies. However, high class numbers and unbalanced classes are the most challenging aspects of tree species classification, which were identified when the accuracies were compared with single tree species results in Schiefer et al. (2019) and Onishi and Ise (2018). In natural mixed forests, the imbalance in tree species numbers and the occurrence of more

than two species is most likely, especially in Japanese mountainous forests. Achieving high accuracies for a high number of tree species is the basis for studying species interactions, like niche differentiation, facilitation and competition, which can help to understand forest interactions, provide management possibilities and even predict forest behaviours during changing climate.

Therefore, this study classifies tree species of a forest with a high degree of mixture, which helps to assess forest compositions and distributions on different scales. Therefore, the orthomosaics of the 13 study sites and the identified 41 species classes were used, first to fuse classes and then to:

- xiii. Automatically classify tree species in natural mixed forests of YURF using deep learning
- xiv. Perform semantic segmentation with the UNet architecture.
- xv. Assess the first results and evaluate the performance of the architecture based on experiences of manual annotation and faced challenges.

6.2.2 Methodology

Previous chapters focussed on assessing the forest with field work and images to evaluate tree species composition and distribution. It was expected that image analyses provided similar results to field investigations. Regarding the image analysis, the most time-consuming step was to prepare the manual annotation. Identifying every tree in all 13 sites needed time and precise colouring of the tree species. To avoid this time-consuming step, automatic classification was considered for this study.

6.2.2.1 Data collection and processing

Images were collected with the DJI phantom 4 UAV. The flight altitude ranged between 80 and 205 m depending on the imaged site, with the UAV flying a speed of maximal 3.7 m/s. Front and side overlaps between 90 and 97 % were chosen. Approximately 200 to 550 images were gathered per flight (Appendix A), which were processed for each site with Metashape, generating orthomosaics and DEMs. The pixel resolution ranged between 2.73 cm/pix and 4.5 cm/pix, while a standardized pixel size was set for each orthomosaic of 2,73 cm/pix. Images from summer 2019 were chosen and tree species were annotated, for each site one flight. In sites 1 and 3 flights were performed on the 20th of June 2019, in sites 9 and 10 the 10th of July and site 8 the 26th of July. For all other sites images from the 14th of June were used. The total imaged area was 61.9 ha with 31.48 ha located in the ROI.

6.2.2.2 Manual annotations

Manual annotations were done with GIMP, where each tree species was coloured black in separate layers. Furthermore, a tree top layer was generated and all layers were exported as JPEG files. In total 41 species layers were generated for 13 sites. Each tree species was assigned a species code starting from S01 and ending with S43 and a mixed class (note: there were species which were labelled with different codes, so that after the correction S29, S33 and S38 were empty classes). Species names and the assigned species codes can be found in Appendix C. After the evaluation of species with the Census code and a first test of the DL model, the classes were grouped together. Species with less counts and a small canopy area were grouped into a class 'Others'. After that step, the classes were only S01 to S09, S11 and Others, and the classification classes were named fused classes.

6.2.2.3 Semantic segmentation with UNet

In the previous chapters the main focus was on labelling regions with one or more labels, where usually bounding boxes or patches were used to identify single or multiple objects (Figure 73). Here, UNet performs semantic segmentation, it assigns each pixel in an orthomosaic a label with a given probability, which means that just pixels are considered, the object itself does not matter. The purpose is to create finer regions than the results gained, when ResNet is used. Compared to other approaches of automatic classification, UNet can be directly used, as identifying the object first is not necessary. However, tree counting cannot be performed with such kind of algorithm.

The approach used in this study was a multi-class segmentation, where more than two labels were assigned. The architecture used was UNet, which contained a feature extractor followed by a prediction block. Here, the prediction block was composed of convolutional blocks to provide an end-to-end prediction. The feature extractor followed a structure that was composed of an encoder and a decoder. First spatial information were compressed by the encoder into a low dimensional feature space, the gained feature was upsampled with the decoder and the output for the final segmentation was generated (Diez et al., 2021).

6.2.2.4 Evaluation

The evaluation was performed comparing the predicted values/pixels and real values/pixels provided with the ground truth. Each pixel was sorted into TP, FP, TN, FN. Based on this sorting, accuracy, precision and recall were calculated using the three calculations:

$$ACC = \frac{TP + TN}{P + N}$$

$$Precision = \frac{TP}{TP + FP}$$

$$Recall = \frac{TP}{TP + FN}$$

The accuracy assessed how many pixels were classified correctly out of all data. The precision represents a value for the correctly classified positives out of the predicted positives and the recall describes the correct classified pixels out of the actual positives.

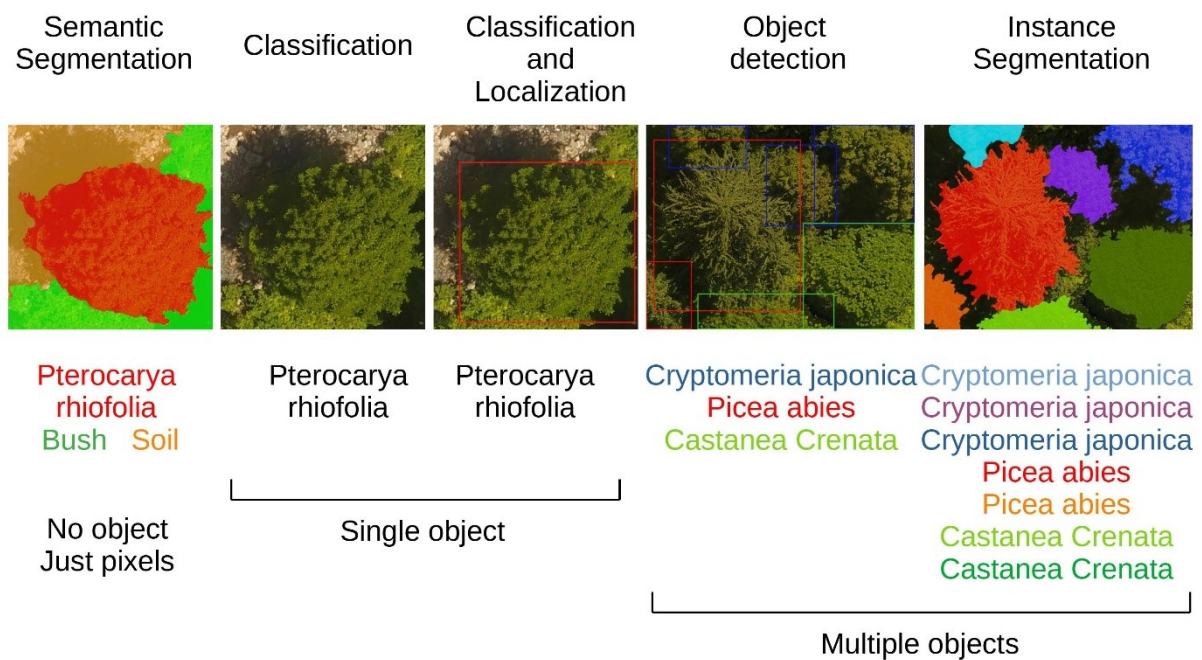


Figure 73 Examples of the different types of problems solved with DL (Diez et al., 2021)

6.2.3 Results

As pointed out before, DL classifications were performed with a small number of classes, while in the forest orthomosaics of this study 41 species classes were identified. In the previous chapters (field and image analyses) it was discussed that the data were imbalanced, with species dominating the areas and others with only a couple of individuals. This aspect challenged the automatic classification with DL. Preliminary, lower class numbers were considered based on the area calculation based on pixel counting. General analyses were performed to evaluate the area per species and their distribution along the sites. Note that the input for the DL classification was composed of two datasets: The one presented in this study with the sites 1 to 13 (S1 – S13) (hereafter set 1) and the ones on the top of the

mountain sites 14 to 17 (S14 – S17) (hereafter set 2). There were experiments separating the two datasets, but also experiments with a mix of all sites.

6.2.3.1 Initial experiments

The first approach was to understand the structure of the data in terms of pixels in the ROI, as the data distribution influences the results of a DL network. The class numbers were changed with the smaller class numbers as follows: Background: Sp00, S11 (*Acer mono maxim*): Sp10, S41 (*Acer japonica*, red): Sp11 and S01 – S09 (Table 27): Sp01 – Sp09. All other species classes were named Other with the label Sp12.

Table 27 Species labelling and area calculations of site ROIs

Species	Species lat. name	Area in ROI [%]	Area (S1-S13 only) [%]
Sp00	Background	32,59	30.17
Sp01	<i>Juglans ailantifolia</i>	16,84	16.14
Sp02	<i>Aesculus turbinata</i>	2,82	2.07
Sp03	<i>Cryptomeria japonica</i>	10,63	9.84
Sp04	<i>Pterocarya rhoifolia</i>	4,56	3.67
Sp05	<i>Quercus mongolica</i>	4,31	1.45
Sp06	<i>Larix kaempferi</i>	2,10	0.15
Sp07	<i>Fagus crenata</i>	2,00	0.15
Sp08	<i>Magnolia obovata</i>	5,20	4.28
Sp09	<i>Small-leaved Acer</i>	5,77	3.52
Sp10	<i>Acer mono maxim</i>	4,26	4.26
Sp11	<i>Acer japonica</i> (red)	0,06	0.06
Sp12	Other	8,89	8.12

The data indicated an unbalance towards the classes Background, *Juglans ailantifolia* and *Cryptomeria japonica*, while all other classes showed values lower than 10 % (Table 27). Furthermore, the orthomosaics 1 to 13 contained the main proportion for most classes, except Sp05 (*Quercus mongolica*), Sp06 (*Larix kaempferi*) and Sp07 (*Fagus crenata*).

It was further evaluated in which sites the species were concentrated, as there were sites with higher mixtures than others. Also, the differences between Riparian, Terrace and Slope sites were found to be different (**chapter 4.1 – 4.4 field and image analysis**). The results presented important insights, like

a leave-one-orthomosaic-out approach for the training influences the results significantly. The calculated values confirmed that the classes had varying proportions in the different sites. Species classes Sp04 (*Pterocarya rhoifolia*) and Sp11 (*Acer japonica*, red coloured) had significant imbalances, as 50 % of the canopy area of Sp04 was in site 1 and even 94 % of Sp11 in site 10. It is most likely, that a training of the network without site 10 would not allow automatic classifications of Sp11, as the number of training examples would be too low. Higher imbalances between the sites were observed for site 2, where Sp08 (*Magnolia obovata*) and Sp09 (small-leaved *Acer* species) had higher amounts, with 29 % and 28 %. In site 3, Sp05 (*Quercus mongolica*), Sp07 (*Fagus crenata*) and Sp09 (small-leaved *Acer*) inhabited more than 20 % of each species. Site 9 contained, with 29 %, a large area of Sp09, while in sites 14 and 15 large areas of Sp06 and Sp07 were accumulated. When the composition of the species was checked, sites 4, 6 and 13 were found to be mainly composed of the background, Sp01 and Sp03, while all other species classes had low percentages. Site 1 and 11 were similar, with high amounts of the background, Sp01, Sp03 and Sp04. Generally, the Slope sites had high proportions of Sp08, Sp09, Sp10 (*Acer mono maxim*) and Sp12 (Other), and also the mix of the species was higher than in the Riparian sites. The results showed that, even though classes were already fused, the imbalance was still high. The background and the species Sp01, Sp03, Sp08 and Sp09 were dominant species. The sites 14 to 17 were composed of Sp05, Sp06 and Sp07, which were minor species in sites 1 to 13.

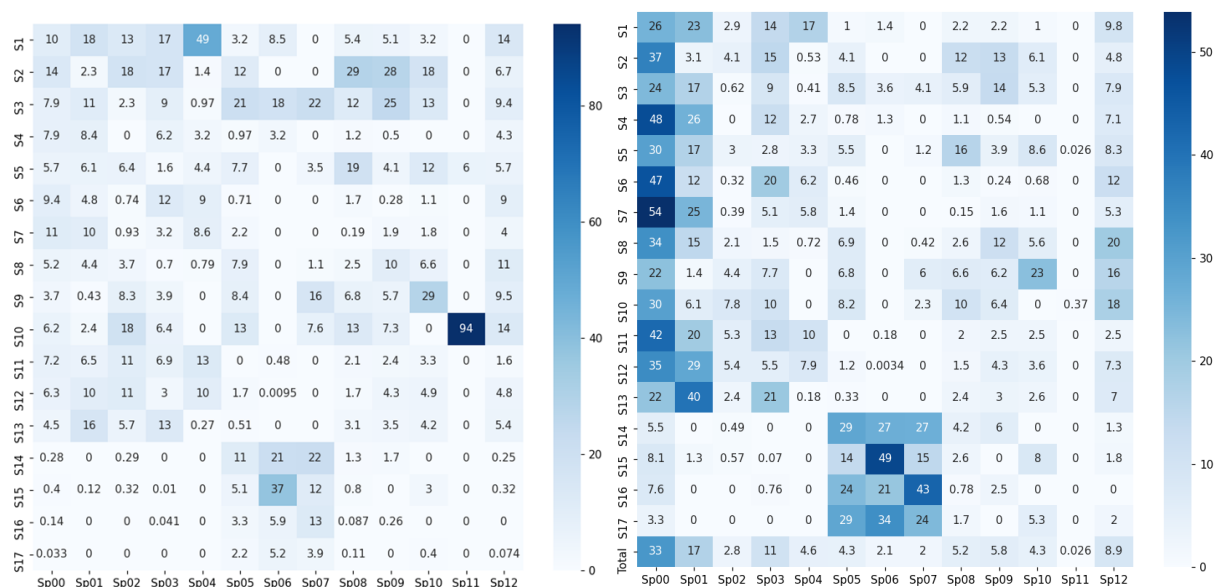


Figure 74 A) The following plot represents the distribution of the species per mosaic. Therefore, all columns should sum up to 100% B) The following plot represents the distribution of the species of a given mosaic (all lines should sum up to 100%)

6.2.3.2 Experiment with 13 classes

There were two experiments performed, one used all orthomosaics for training and testing, one where training was performed separately for the sites 1 to 13 and 14 to 17. For both experiments a leave-one-orthomosaic-out strategy was performed, so that the trees in the training and testing set were never the same and did therefore not belong to the same site.

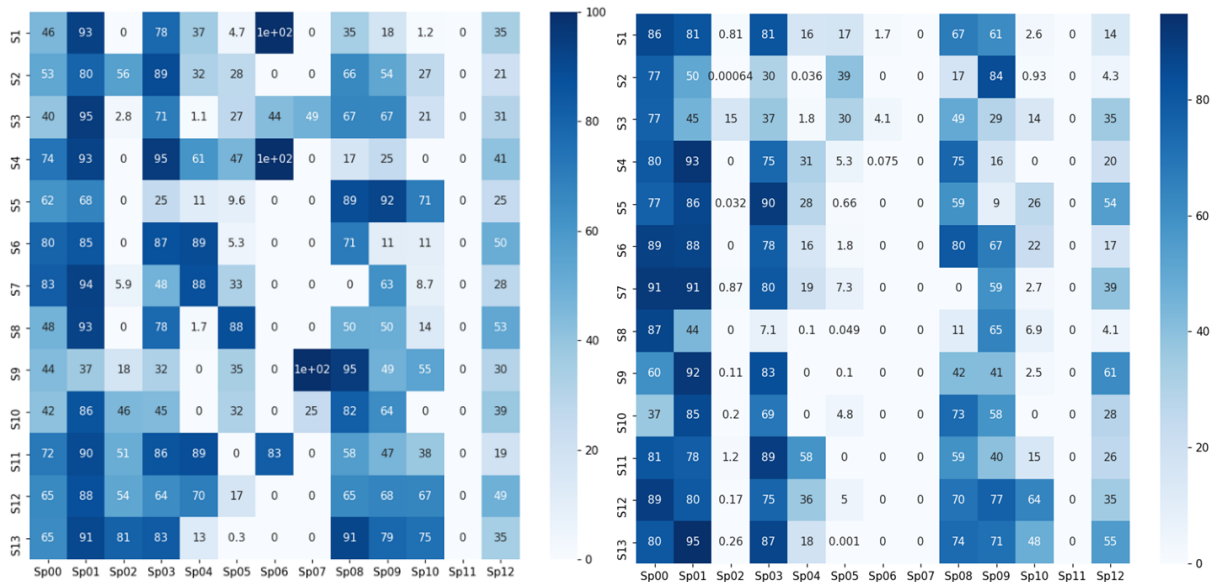


Figure 75 Precision Matrix A) all sites (left) B) specific sites (right)

The matrices (Figure 75) show that the precision was generally higher for the background, Sp01 and Sp03, when the training was performed only with the set 1 with a high recall value. When all sites were used, the recall (Figure 76) of Sp00 increased and the precision decreased, in comparison to the run where only 13 sites were used. Sp01 had no significant differences between both runs; therefore, the classification accuracy was not influenced by the number of sites used for training. The precisions were lower for species Sp02 and Sp04 and had higher recall values, when trained with set 1 only. The precision was low for the species Sp05, Sp06 and Sp07 when only trained with set 1. For all other species had high values when trained with all orthomosaics, and lower when training was performed with set 1 only. For species Sp08, Sp09 and Sp10 the values for precision and recall were relatively high, but it was observed that for sites with a high precision when trained with all sites, the precision was lower when trained with set 1 only and opposite.

Generally, low recall values occurred together with high precisions and recalls with low precisions for most of the species, while this phenomenon also occurred within a species row, when different sites were considered UNet provided results of the pixel classifications, which means that each class had a high number of pixels assigned to it. For a better readability, the number of pixels was divided by the total sum of pixels on the ground truth for each class. The values were therefore between 0 and 100 %.

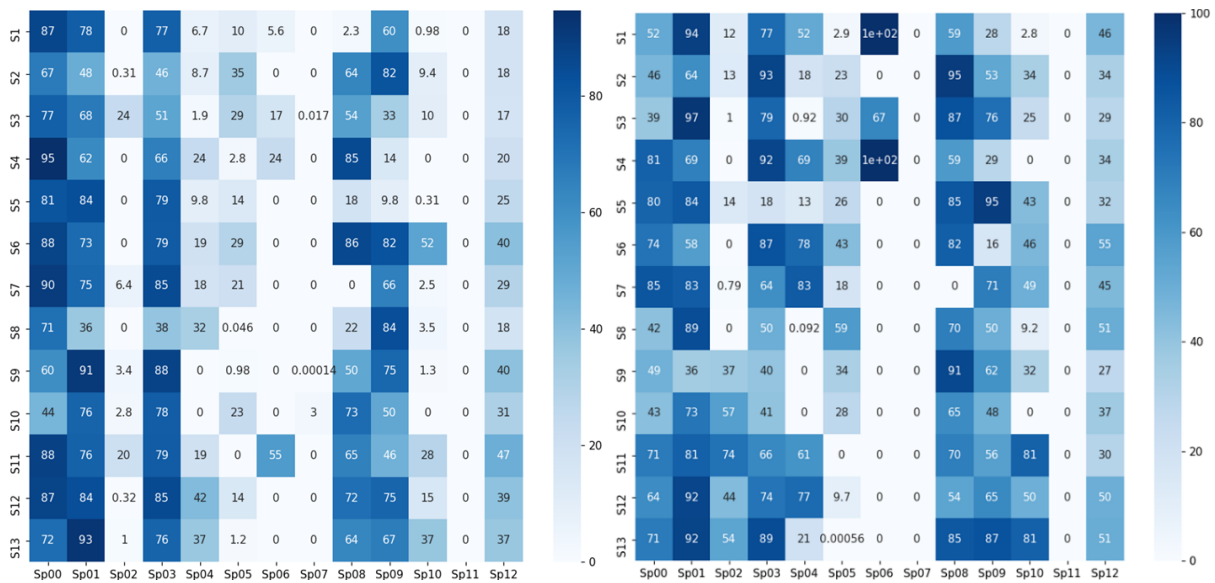


Figure 76 Recall matrix A) all sites (left) B) specific (right)

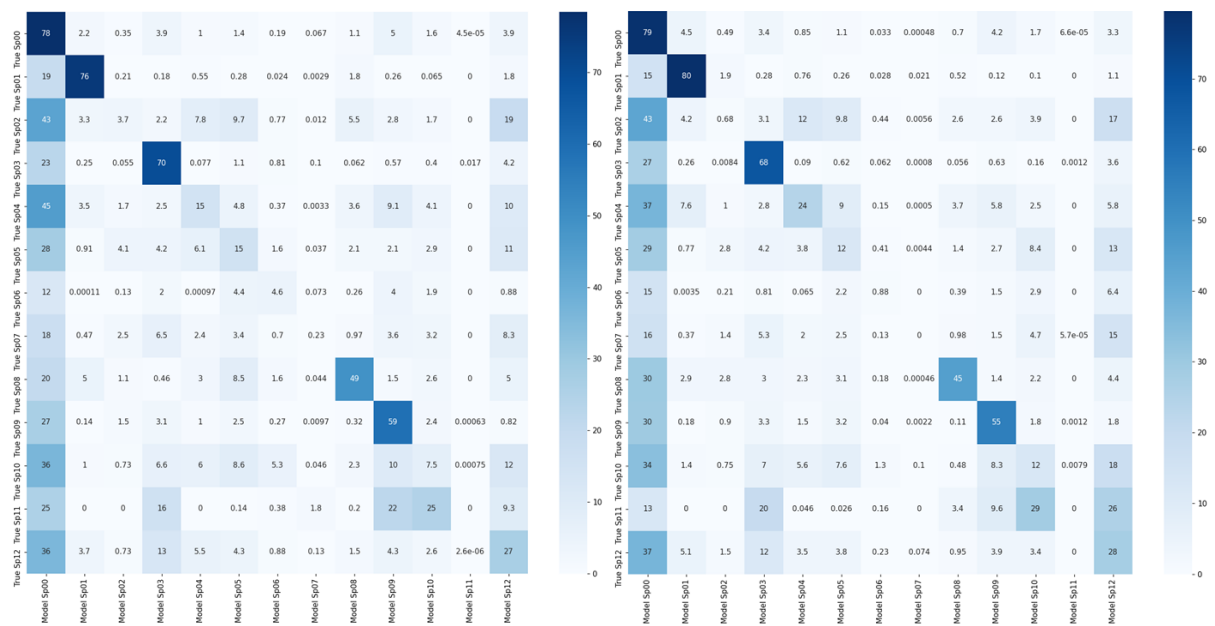


Figure 77 Confusion matrices only site 1 to 13 A) all sites (left) B) specific (right)

The confusion matrices show that the algorithm could predict the background, Sp01 and Sp03 with higher accuracies (Figure 77). Around 50 % of the species Sp08 and Sp09 could be detected. Furthermore, the matrices show that using all sites lead to better classifications for Sp03, Sp08 and Sp09, while the training with set 1 increased the classification percentage of the background and Sp01. Furthermore, the matrices show that most classes were confused with the background and Sp12. Species Sp11 could not be detected by the network and Sp06 and Sp07 were constantly misclassified with all other classes.

Table 28 Accuracies reached for the experiments

	13 classes	13 classes	6 classes
	Accuracy all	Accuracy (set 1)	Accuracy (set 1)
S1	55.23	59.28	66.27
S2	54.74	49.7	54.62
S3	47.57	42.75	57.26
S4	73.24	75.02	74.6
S5	47.59	58.07	58.75
S6	73.22	71.95	76.46
S7	75.63	80.15	81.51
S8	44.51	45.13	56.74
S9	36.2	36.66	72.48
S10	44.62	40.08	53.83
S11	69.91	70.24	76.91
S12	70.23	70.07	80.57
S13	75.47	82.18	82.17

The network achieved varying accuracies for the classification (Table 28). The highest accuracies were reached for sites 7 and 13 with 80.15 % and 82.18 %, when trained with set 1 only. The lowest accuracies were found for site 9, where the two training approaches did not influence the performance of the network. The overall accuracies were higher for sites 2, 3, 6 and 10, while all others achieved lower accuracies, but similar to each other. In site 5, the training with set 1 only provided the highest increase (10.48 %) of accuracy, the smallest was found for site 11 (0.33 %). Sites 1, 7 and 13 also benefited from the training with set 1 only, while sites 2, 3 and 10 showed a decrease in accuracy of around 5 %.

6.2.3.3 Level 1 Segmentation

This segmentation is still running, so the results, which were provided from the network until the date of the submission, are presented here. The first results showed that, even with the 13 classes, the data were unbalanced and influenced the classification significantly. Therefore, the dataset was fused by keeping the largest and fusing the rest:

Sp00 = background; Sp01 = S01 (*Juglans ailantifolia*); Sp02 = S03 (*Cryptomeria japonica*); Sp03 = S08 (*Magnolia obovata*); Sp04 (small-leaved *Acer*) and Sp05 (Other)

After fusing higher values of the Other class were found in sites 1, 3 and 10, while sites 17, 4 and 7 had low values for the Other class. The area of the Other class was more equally distributed over all sites.

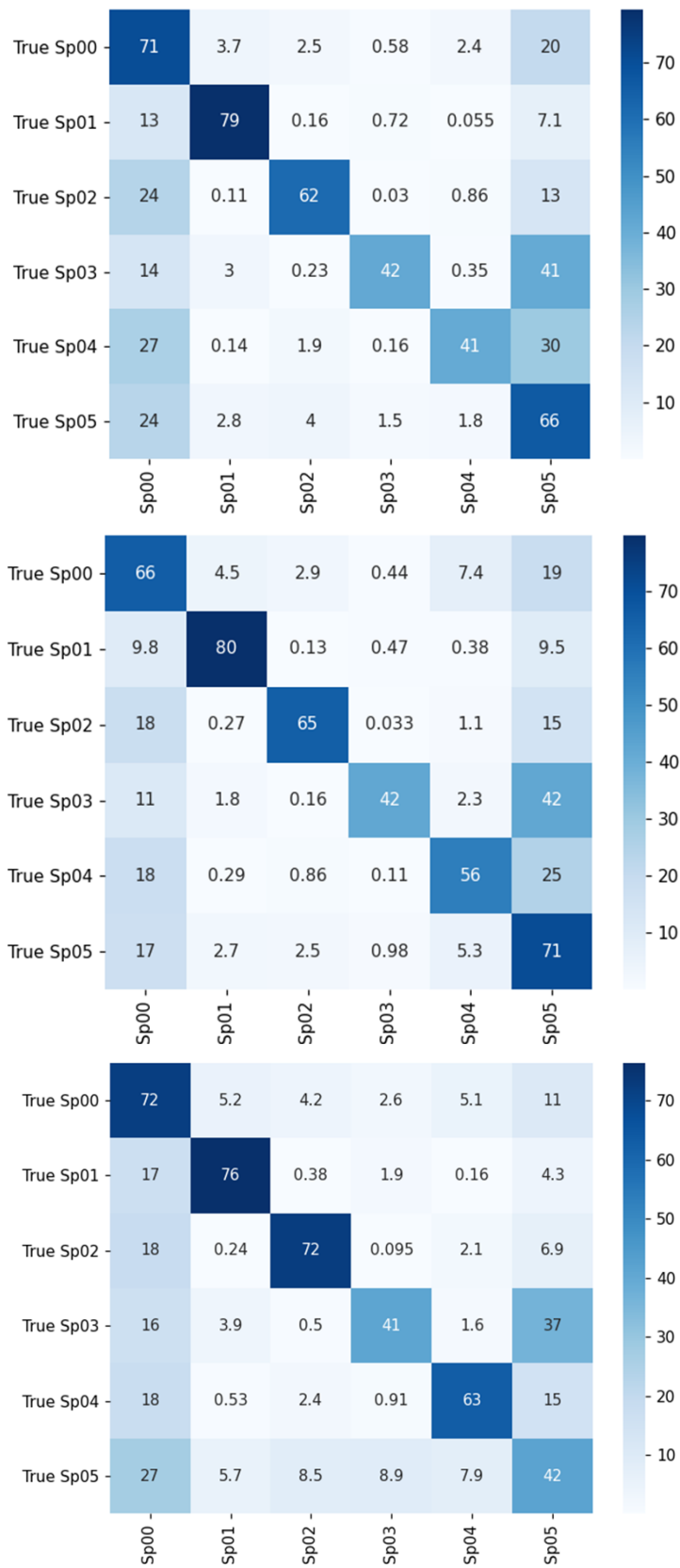


Figure 78 Confusion matrices A) training with 13 orthomosaics and 5 classes (top) B) training with all orthomosaics and 5 classes (middle) C) training with all orthomosaics and 11 classes (bottom)

In relation to all other species occurring in the different sites, the Other class occupied between 12 % and 56 % (highest in site 9), with lowest values in sites 4,13 and 7 (12 % to 14 %), medium values between 20 % and 30 % in sites 2, 6, 11, 12, 3 and 5 (increasing order) and highest for site 1,33 % and site 10, 37 %. The achieved accuracies ranged between 53.83 % (site 10) and 82.17 % (site 13), with less than 60 % accuracy for sites 2, 3, 5, 8 and 10, less than 70 % for site 1 and less than 80 % for sites 4, 6, 9 and 11. The lowest increases were observed in sites 5 and 7, with 0.68 % and 1.36 %. Best accuracies were reached for sites 13, 7 and 12 (82.17 %, 81.51 % and 80.57 %) (Table 28). The lowest accuracy was observed in site 10, with 53.83 %, while sites 2, 3, 5 and 8 reached slightly better accuracies. Compared with the 13 class experiments, the accuracies increased except for site 4 and 13, where the accuracy decreased slightly (by 0.42% and 0.01%), when trained with set 1. The highest increase of the values was observed for sites 9, 3, 10 and 8 with 35.82 %, 13.75 %, 12.23 % and 11.16 % increase.

The confusion matrices presented the results of three different training approaches: training with set 1 and five classes (A); training with all sites and five classes (B), and training with all sites and 11 classes (C) (note: Sp11 was left out, as the species was too small to be considered separately). The overall best classifications were reached using all sites for training; however, using five classes increased the accuracy of Sp01, Sp03 and Sp05 and training with 11 classes increased the results for Sp00, Sp02 and Sp04. Applying training (C) lead to the least misclassification of Sp03 and Sp04 with Sp05. When training method (A) was applied the confusions between Sp01/Sp03 with the background occurred less, while for all other classes training (B) lead to less misclassification.

6.2.3.4 Semantic segmentation

The network performs semantic segmentation, which means that each pixel was assigned a label. The results for site 13 can be seen in Figure 79. The classification of *Juglans* trees (red), as well as the one for *Cryptomeria* trees (blue) show already good results. *Acer* trees (green-brown) and the Others class provide less good classifications and is often mixed with the background (white). Note that the ground truth is only provided for the ROI, while the network provided a classification of all pixels in the image.

6.2.4 Discussion

The imbalance in the data influenced the classification, so that larger classes were predicted well, while small classes, which were not representative, had worse results. Therefore, the network was not able to classify *Acer japonica*, while *Juglans ailantifolia* and *Cryptomeria japonica* reached the highest

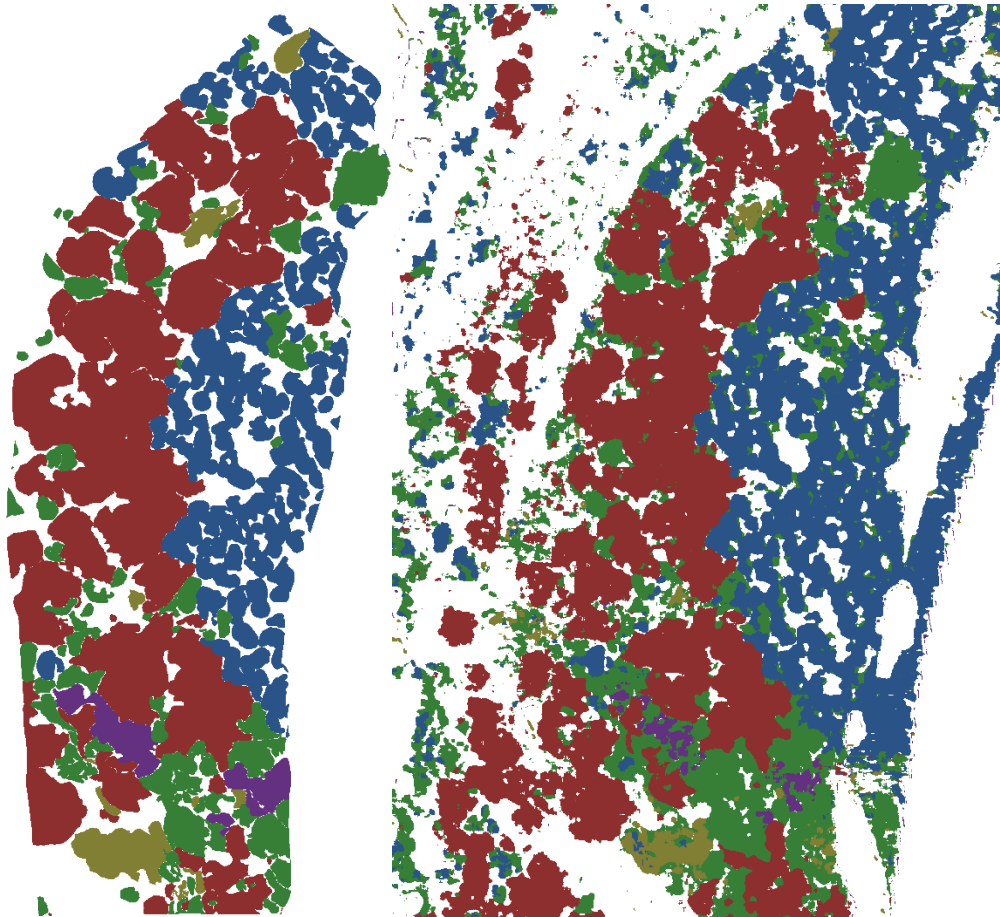


Figure 79 Ground truth (left) and segmentation result of the network (right)

values. The training, only using set 1, increased the accuracies for *Juglans ailantifolia* and *Pterocarya rhoifolia*, while for most classes the training did not seem to change the values significantly. There was an insignificant benefit for the species *Quercus mongolica*, *Larix kaempferi* and *Fagus crenata*. When the level 1 experiment was observed, the performance of the network increased for the smaller number of classes, which might be a result of less unbalanced data, as presented with the 13 classes.

The accuracy was compared with the distribution and composition of classes in the sites and evaluated relationships between classes. The highest accuracies occurred with high pixel numbers belonging to the background, *Juglans ailantifolia* and *Cryptomeria japonica*. The highest occurrences were found in sites 13, 7 and 4, with site 13 having high numbers for all three classes, while site 7 and 4 had a high number of background pixel values, but *Juglans ailantifolia* had half the number of the background, and *Cryptomeria japonica* had even less pixels. Lowest accuracies were found when the distribution of the classes was homogenous, *Juglans ailantifolia* pixel number was low and/or the main pixels were distributed in class Other. In the sites 2, 3, 5, 8 and 9 the number of *Magnolia obovata*, small-leaved *Acer* and *Acer mono maxim* were high, which were less frequent compared to *Juglans ailantifolia* and *Cryptomeria japonica*. Sites with high pixels numbers of background, *Juglans ailantifolia* or

Cryptomeria japonica reached generally the highest accuracies, while all other classes were infrequent. The accuracies in site 1 achieved medium accuracies, which can be explained by the homogenous distribution of the classes Sp00 to Sp04.

For the experiment level 1 segmentation, the following patterns were found. Highest accuracies occurred when the classes background, *Juglans ailantifolia*, *Cryptomeria japonica* and Other occurred frequently (sites 13, 7 and 12), while lowest accuracies occurred when the sites were mainly composed of classes *Magnolia obovata* and small-leaved *Acer*, which was in sites 2, 3 and 5. When mixtures occurred homogeneously, the accuracy values were on average. Another observed pattern was that when the distribution between the frequent classes was homogenous, the accuracy was also higher, as it was observed in site 13. Lower accuracies were found in site 7, where *Cryptomeria japonica* had low pixel numbers and site 12, where the background and *Juglans ailantifolia* had high numbers of pixels and the class other. The lower the distribution in classes 00, 01 and 02 the lower the accuracy. Homogenous distributions in all classes, except *Juglans ailantifolia* like in site 2 lead to low accuracies. High pixel values in the background and Other class caused the lowest accuracies.

The distribution and composition of the sites influenced strongly the achieved accuracy. When a site was composed of many small classes the overall accuracy was lower than in sites being mainly composed of large classes. Therefore, the imbalance in data hampered the classification ability of the network and needs to be overcome for increasing the performance of the network.

6.2.4.1 Misclassification

In this section, confusion matrices are evaluated to identify misclassified classes. The level 1 segmentation caused less misclassification of the single tree species, but there were misclassifications found between the single tree species and Other, as well as with background. The background class contained a mixture of understory vegetations, which had a high number of pixels and several different structures. The Other class contained a high number of pixels belonging to 37 tree species, which can have features similar to the four tree species Sp01 to Sp04. *Acer mono maxim* for example sometimes looked like small-leaved *Acer*, when the resolution was low. The training with all orthomosaics and the five classes provided the best accuracies for the Other class, while the one using 11 classes had significant lower values. The reason might be that there were confusions between the different species, when trained with 11 classes.

The confusion matrices of the training with 13 classes showed significantly different results. In general, the classification was found to be worse and some classes failed to be classified, while others had low accuracies. For all sites, tree species classes were mixed with the background and the Other class.

Compared with the level 1 experiment, tree classes were also mixed. *Aesculus turbinata* was mixed with *Pterocarya rhoifolia*, *Quercus mongolica* and *Juglans ailantifolia*. It is a tree species, which occurred with dark leaf colours but with a significant structure, which was different to most of the species it was mixed with. *Juglans ailantifolia* had a lighter green leaf colour, but with bad resolutions, the species had similar crown characteristics to *Aesculus turbinata*. *Pterocarya rhoifolia* was found to be mixed with *Juglans ailantifolia*, which was a result of similar leaf and canopy structures. *Acer mono maxim* was misclassified as *Pterocarya rhoifolia*, *Quercus mongolica* and small-leaved *Acer*. The similar colour might be a reason for the mixture with *Quercus mongolica*. *Fagus crenata* was wrongly classified as *Cryptomeria japonica*, *Larix kaempferi* and *Quercus mongolica*. Even though the leave colour of *Fagus* and *Quercus* trees was different, the structure of the canopy was similar. The reason why *Fagus* or even *Quercus* trees were found mixed with *Cryptomeria* and *Larix* trees cannot be explained, as the canopy structure and leave colour look different. *Acer japonica* (red) could not be classified and was classified as *Cryptomeria japonica*, small-leaved *Acer* or *Acer mono maxim*. The reason might be that *Cryptomeria japonica* had a reddish needle colour, easy to mix up with the red colour of *Acer japonica*. The confusion with the two *Acer* species can be explained by the similar canopy structure.

Most of the misclassifications can be explained with the phenological occurrences of the trees, varying image resolutions and the low number of example trees per species. [Schiefer et al. \(2020\)](#) discussed species abundances and errors in classifications. Species with similar features can cause problems, as less frequent species and abundant species are classified together from the DL network. Those misclassifications, but also no shared similarities can lead to poor classifications of less frequent classes. Sufficient amounts of data for rare species are therefore crucial ([Schiefer et al., 2020](#)) and for future training the data needs to be increased, which can be done with data augmentation, additional data or GANs. [Schiefer et al. \(2020\)](#) further pointed out that updating databases are an important aspect to accurately map species, especially when species are rare.

6.2.4.2 Over- and Underpredictions

Low recall values in combination with high precision values are an indicator for underestimation of trees, as it could be found for species *Quercus mongolica* and *Larix kaempferi*. Especially when all sites were used for training, the recall value decreased, indicating a large number of trees of each species which were not found by the algorithm. If a tree was found it was most likely classified correctly, as the precision value indicated. However, since the recall value was higher when only set 1 was regarded, the classifier worked better.

In contrast, *Aesculus turbinata* and *Pterocarya rhoifolia* had high recall values but low precision values, when trained with set 1. The low precision indicated that a large number of trees were classified wrong. The algorithm predicted species *Aesculus turbinata* or *Pterocarya rhoifolia*, even though it was a different species, explaining the high recall (low FN). In contrast, the precision value was low, indicating a high number of FP. This scenario is called overprediction of a class. While species *Aesculus turbinata* and *Pterocarya rhoifolia* seemed to be overpredicted, when trained with set 1, *Aesculus turbinata* was underpredicted in most of the sites, when trained with all sites. The high precision value indicated a low number of FP but the recall decreased dramatically, explained by a high number of FN.

The low precision and recall values for *Quercus mongolica* indicated that the algorithm can identify the species, but there was a lot of mixture. Only the background and species *Juglans ailantifolia* and *Cryptomeria japonica* were predicted with high recall and precision values, indicating that the algorithm could classify these species with high accuracies. For *Magnolia obovata*, small-leaved *Acer* and *Acer mono maxim* the over- and underprediction varied among sites, indicating that the algorithm was able to classify the species, when trained with different datasets.

Generally, the algorithm produced high numbers of FN and FP for the species which were less frequent, while only for the background, *Juglans ailantifolia* and *Cryptomeria japonica* high precision and recall values were found, with low numbers of FN and FP. In these classes, overprediction occurred more often, when the sites were mainly composed of *Juglans ailantifolia* or *Cryptomeria japonica*, which was in sites 1, 12 and 13 for *Juglans ailantifolia* and 4, 6 and 13 for *Cryptomeria japonica*. Furthermore, there seemed to be a trend that overprediction occurred more frequently, when the species was rare in the sites.

Overall, the algorithm was producing high FP and TP, especially when minor species were observed, indicating that the training examples were not enough to train the network to classify all classes with high accuracies.

6.2.5 Conclusion

The first sets of results gave useful insights into the tree species classification approach. The first results struggled to classify the tree species classes due to the imbalance in the data. The results of the 6 classes approach reached significant higher accuracies than the one with 13 classes, which indicated that reducing the classes and focusing on the large classes helped to overcome data imbalances. While these results indicated that the automatic classification is possible, the data need to be balanced for sufficient network behaviour. Less frequent classes, which showed similar characteristics to other classes, need to be overcome.

Chapter 7 Invasive species - Two application examples of image analysis and deep learning

7.1 Introduction invasive species

Recent changes in global climate conditions influence species composition and increase the impact of invasive plant species on natural environments. Invasive species are known to spread rapidly outside their native range and with a rapid and effective adaptation to new environments (Prentis et al., 2008). In Europe more than 11,000 alien species occur, while more than 50 % are terrestrial plants (Rabitsch and Genovesi, 2012). The spread of invasive species does often benefit from ecosystem changes and habitat disturbances, weakening the natural species and opening ecological niches for the invaders. Hence invasive species can have an influence the biodiversity by vanishing some species due to the higher occurrence of invasive species, and this could lead to ecosystem degradation (Pyšek and Richardson, 2010). Didham et al. (2005) pointed out that not only invasive species have an impact on native plants, but there are often several factors interacting with the environment, which need to be considered and studied, influencing species distributions. Still, it is known that invasive species influence nutrients, water resources and fluxes in natural environments, changing the ecosystem's life-cycle (Nentwig et al., 2018). In recent years, the need to precisely understand the ecological impact of invasive species in ecosystems has become a key requirement when designing and prioritizing natural resource management approaches (Pyšek and Richardson, 2010). Especially, since one of the challenges of invasive species is that their distribution and spread increase over the time, which requests a rapid eradication (Keller et al., 2011). Pimentel et al. (2005) claimed that 42 % of threatened or endangered species in America are in danger because of invasive species. In Europe, 11 % of the 12000 identified species cause damage to the economy, society and the environment (Caffrey et al., 2014). In the work of (Rabitsch and Genovesi, 2012) it is stated that hundreds of invasive species find their pathways to natural environments and the linear increasing trend of invasive species numbers (from 1970 to 2007) indicates higher impacts of invasive species in the future. Furthermore, there is a high number of invasive species finding their pathways into natural environments through horticulture, agriculture, transport etc.

Discussions about invasive species include often the impact and abundance, the awareness and the costs of them. The fast adaption to multiple stress factors of environments could also lead to a replacement of native species and can increase economic costs due to losses in agriculture and forestry (Pimentel et al., 2005). In Europe, costs caused by the damage and the control of invasive species exceed 12 billion Euros (Rabitsch and Genovesi, 2012). They provided a detailed analysis of the budgets spent, dealing with invasive species, showing an increase from 5 million (1995-1997) to 40 million (2004-2006), indicating a further increase in the future. Especially, since from 1990 the number of

established terrestrial invasive species increased constantly to 4,000. These numbers are one of the reasons for an increasing the demand of a management strategies because without an effort to control those species their numbers will continue to grow (Keller et al., 2011). Land use and nature conservation management approaches need to be dealt with low costs and high efficiency for the prevention, early detection and reduction of invasive species. However, existing studies are limited in time and area due to the use of costly and labour-intensive field surveys (Pyšek and Richardson, 2010). Even though many studies have been conducted, the quality of published data is highly variable because quantitative and experimental data are in some cases impossible to gather (Gurevitch and Padilla, 2004). Therefore, a second challenge is often to deal with the missing information to control invasive species, which increases the difficulties for management approaches (Keller et al., 2011). Gathering information about which conditions lead to invasions and the long-time lag between an introduction of a terrestrial invasive species and their wide spread, further arises difficulties when working on invasive species (Keller et al., 2011).

Therefore, the examination to find a method to control invasive species is a complex problem (Allendorf and Lundquist, 2003), since the behaviour and consequences of invasive species is still not studied (Pimentel et al., 2005; Rabitsch and Genovesi, 2012). The need of an updated methodology is discussed (Rabitsch and Genovesi, 2012) and aims at managing and preventing the introduction and spread of invasive species (Caffrey et al., 2014). Further, an appropriate monitoring is necessary to prevent new invasions, decrease spreads and to analyse the impact of invasive species (Caffrey et al., 2014). The developed methodology for tree species classification and detection in this study was found to be a useful technique to apply it to invasive species examples. Therefore, the objective was:

- xvi. Assess the use of deep learning techniques to detect invasive species in natural environments

7.2 State-of-the-Art

In recent years remote sensing studies were applied to various natural environments. Their purpose was to reduce in-situ measurements by increasing studies using remote sensing methods (Mahdavi et al., 2018). This method already proved its efficiency to cover large areas and the acquired data can be directly used and processed within GIS (Mahdavi et al., 2018). Joshi et al. (2004) proposed the potential of GIS as a synthesising tool in invasive species management approaches. In addition, studies presented by Wu (2018) and Twumasi and Merem (2006) pointed out the benefits of GIS applications for environmental studies. Two application studies using GIS and remote sensing data are Rebelo et al. (2008) and Meera Gandhi et al. (2015). Rebelo et al. (2008) used the Maximum Likelihood Algorithm,

mapping and spatial analyses, they finally refined and confirmed with ground data. Their approach provided detailed analysis and reached 86 % accuracy. GIS in combination with remote sensing data was found to be an effective methodology to investigate wetlands. [Meera Gandhi et al. \(2015\)](#) detected changes in the vegetation by image interpretations, based on NDVI, carried out using ERGDAS IMAGINE software. The study provided information about the lowest decrease in the forest area by 6 %, while agriculture land increased the most by 19 %.

In comparison to satellite images, which were used in ([Rebelo et al., 2008](#); [Meera Gandhi et al., 2015](#)), UAV images provide a higher resolution. Higher resolution images acquired by UAVs allow higher accuracies of image interpretations and feature extractions ([Dronova, 2015](#)). Therefore, they appear to be more suitable for wetland investigations, especially with focus on invasive species. This can be concluded from the variety of studies in agriculture ([Grenzdörffer et al., 2008](#); [Raparelli and Bajocco et al., 2019](#)) and forestry ([Natesan et al., 2019](#); [Kentsch et al., 2020](#); [Gambella et al., 2016](#)). Several studies using UAVs in wetlands have already been carried out ([Wan et al., 2014](#); [Boon et al., 2016](#), [Dvořák et al., 2015](#)). [Dvořák et al. \(2015\)](#) developed a method to detect and map invasive species with UAVs. The authors acknowledged UAVs as suitable to monitor eradication efforts in wetlands. [Boon et al. \(2016\)](#) realised the higher efficiency in gathering valuable and accurate information in comparison to field studies, when using UAVs and computer vision techniques to enhance classifications and health assessments in wetlands. [Wan et al. \(2014\)](#) and [Mafanya et al. \(2018\)](#) used UAV gathered images to classify invasive species. [Wan et al. \(2014\)](#) analysed the spread of *Spartina alterniflora* in Beihai in the years 2009 and 2011, using high resolution images acquired by UAVs. A total accuracy of 94.0 % could be achieved and hence provided information about an increasing spread of 19.07 % from 2009 to 2011. Moreover, the image analysis provided the opportunity to identify areas with different levels of densities. Therefore, drones were considered as sufficient tool for this study.

Capturing large areas and the demand of precise classification results smoothed the way for DL applications in natural environment studies. The use of DL and segmentation to process large data sets is common use. [Sun et al. \(2017\)](#) used images taken with a mobile phone to identify ornamental plant species. Their database consists of 10,000 images from 100 different species. ResNet networks were compared and used to classify the 100 plant species. The best recognition rate was archived by ResNet26 with 91.78 %. A recent study of [Rezaee et al. \(2018\)](#) used a fully trained and fine-tuned CNN with a limited amount of data to classify wetlands. A comparison of the CNN with Random Forest was performed to evaluate the capacity and classification accuracies of CNNs. The CNN outperformed Random Forest and an overall accuracy of 94.82 % was achieved, varying between 76.65 % and 98.74 %. Deep Convolutional Neural Networks were developed by [Liu and Abd-Elrahman \(2018\)](#) to classify wetlands from UAV imagery. Image segmentation was done with Trimble's eCognition by first

segmenting objects, then extracting features and finally train and implement a classifier. The results of the study showed the advantages of deep CNN reaching accuracies of 82.02 %, when multi-view images were used, and with lower accuracies when orthomosaics were used (71.69 %). A similar approach was done by [Ashqar and Abu-Naser \(2019\)](#), who used a dataset containing 3,800 images of the Brazilian National Forest (Kaggle dataset). The authors used data augmentation and three models: VGGNet, DenseNet and Inception, which were pre-trained with ImageNet. Accuracies of 97.6 % were reached.

7.3 Coastal Forests

Coastal forests cover shore lines all over the world and are often used for disaster prevention, especially in Japan, where coastal forest extends approximately 30,000 km long covering a 100,000 ha area ([Kudoh, 1985](#)). Most of them are plantations that started in the 17th century ([Ohta, 2013](#)). Coastal forests were intentionally planted to protect the inland from Tsunamis because of their capability to reduce the force, depth and velocity of tsunamis and therefore their damage. Especially after the earthquake of 2011, coastal forests reduced significantly the mortality and damage rates ([Nateghi et al. 2016](#)). In general, coastal forests have the function of preserving the environment by protecting it from strong winds, sand movement, waves and fog ([Kudoh, 1985](#)). ([Kudoh, 1985](#)) identified coastal forests for Hokkaido, Honshu, Shikoku, Kyushu and Okinawa and specified the forest area in windbreak, tidal waves shifting, sand control and fog prevention forests. Hokkaido has the largest area of coastal forest with 95,984 ha, from which approximately 50 % are fog prevention forests and 40 % wind protection. The main island Honshu has a total of 25,777 ha coastal forest with 12,863 ha to protect the area from tidal waves, 9,867 ha to decrease the wind speed and a small part to protect the inland from moving sand. The planted black pine trees (*Pinus thunbergii*) were chosen because of their ability to grow on the soils in coastal areas with poor nutrient supply and the trapping activities of their needles ([Ohta, 2013](#)). Nowadays, coastal forests have additional functions for relaxation, recreation, conservation of biodiversity and their forest products.

7.3.1 Methodology

7.3.1.1 Study site coastal forest and problem definition

The study site is located in the north of Yamagata prefecture at the coast of the Japan Sea (38°52'35''N 139°47'54''E). The site is found south of Sakata and part of an approximately 115 ha wide coastal forest. The forest has a length of around 5.9 km, a minimum width of 140 m and a maximum width of 350 m.

The coastal forest is a black pine (*Pinus thunbergii*) plantation with high tolerances to acidic and alkaline soils as well as drought conditions (Ito et al., 2004, Lisein et al. 2015). Since the early 1990s this forest has been invaded by black locust trees (*Robinia pseudoacacia*), a fast-growing species growing in gaps in the black pine forest. It is known for its rapid invasion and high biomass production with a high impact on the structure and function of tree communities (Richardson et al., 2004). However, the influences on the function of the coastal forest are unknown but it is expected to weaken its windbreak potential. Invasive tree species have a high impact on the structures, properties and functions of natural ecosystems (Moran et al., 2000; Coll et al., 2018). Therefore, it is necessary to detect and identify black locust trees in order to provide information about their distribution and density to support the strategies of forest management practices.

7.3.1.2 Data processing

A UAV flight was performed in summer 2019, collecting approximately 1,000 images at a flight altitude of 30 m, covering an area of 2.8 ha. The raw images were processed using the software Metashape to generate one orthomosaic. Afterwards, a manual annotation process was done using GIMP. The classes were divided by objects/characteristics that were able to be identified on the images. Four layers were annotated for the coastal forest mosaics: "Black locust", "Soil", "Other trees" (especially black pine trees) and "Man-made" (Figure 80). The orthomosaic, as well as the manual annotations, were divided into axis-aligned, squared patches with a side length of 150 pixels.

7.3.1.3 Deep learning methods

In this approach the MLP classifier was applied, where the data and annotation patches were labelled for each respective class. Since one patch can contain more than one class, the problem was defined as multi-label classification. The network used to perform the patch classification was ResNet50. The network was pre-trained with ImageNet weights and considered as frozen or unfrozen.

The network was retrained with the coastal forest dataset, whereby a subset of the data was used for training and the remaining data was used to validate the quality of the trained model at predicting the correct classes. 80 % of the dataset was randomly chosen for training and the remaining 20 % was used for testing.



Figure 80 Example of the coastal forest mosaic. Examples of patches each containing a single different class

7.3.2 Results – Detection of invasive tree species in the coastal forest

The MLP algorithm was trained for pine trees with green-yellowish leaves and black locust, presenting a light green broad-leaved. The shape of the leaves was visible on the mosaic but it was difficult to differentiate between the species (Figure 81). The main interest in this practical application was to detect the occurrence of black locust. This is a complex problem in image classification terms as the differences between these "Other trees" and black locust were minor. Moreover, the distribution of the invasive species within the forest was irregular and often made up of very small patches, sometimes including single trees (Figure 81).

The results with the highest accuracy were obtained with the unfrozen model. Figure 82 shows representative examples of the results obtained. A 75 % rate of True Positives (TP) for black locust and less than 10 % False Positives (FP, 90.826 % True Negative rate) were achieved (Figure 82, right side). At the same time, the other trees were detected with over 95 % TP rate and about 10 % of FP. The results indicated that by using DL tools in a more sophisticated approach or complementing it with computer vision algorithms, these insights could be improved.



Figure 81 Example of the coastal forest. Mosaic with marked black locust areas (left); Example of Japanese black pine trees (middle); Example of black locust trees (right)

For example, a learning rate of $2 \cdot 10^{-3}$, obtained a high Total Agreement (TA, 90.8 %) with only 62% sensitivity for the black locust class. This version of the classifier presents low FP, recognizing values for both classes and thus, high accuracy without considering the black locust class, which was less frequent (Figure 82). The TA value in this case (42.78 %) was low, but the sensitivity value of the black locust class was the highest during the whole experiment, reaching almost 85 %. This resulted in a high confusion between the black locust and other trees classes, with the specificity of the black locust class dropping to about 65 %.

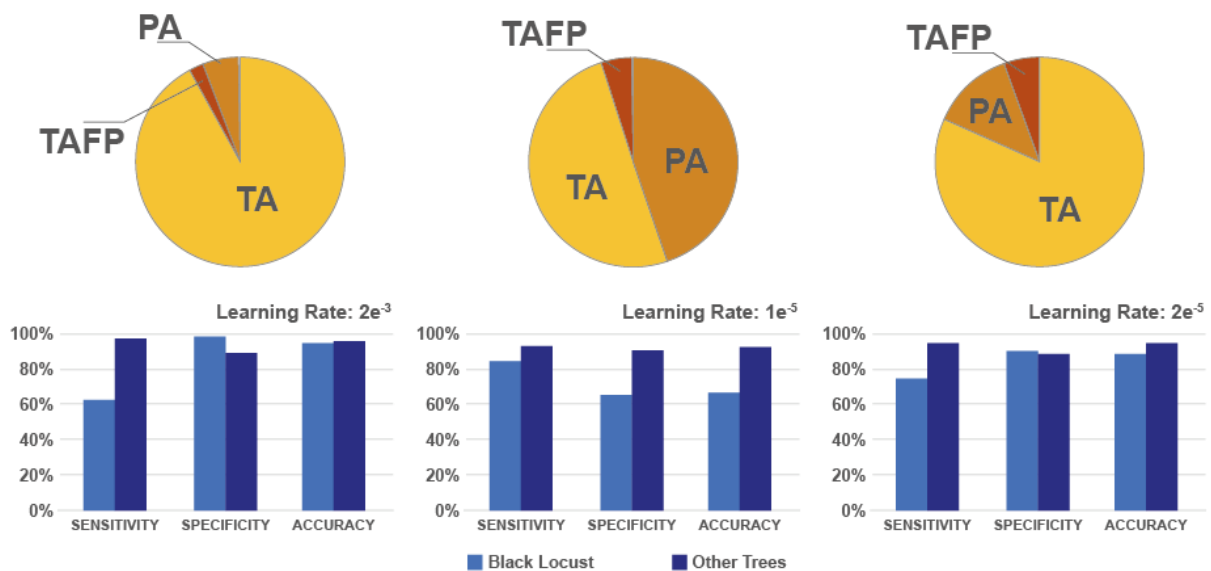


Figure 82 Results for the MLP classification of the Coastal Forest Mosaic for three learning rates (LR). Pie charts show, Total Agreement (TA), Total Agreement with False Positives (TAFP), Partial Agreement (PA). The bar charts show classification measure for the "black locust" and "other trees" classes: Sensitivity or True Positive rate (SENS), Specificity or True Negative Rate (SPEC) and Accuracy (ACC).

7.3.3 Discussion

7.3.3.1 Data imbalance

In the coastal forest experiment the performance of a simple patch-based approach was assessed for solving practical problems. A 75 % rate of TP was obtained for the black locust class with under 10 % of FP while simultaneously obtaining (95 % / 10 %) values for the other trees class. This showed that DL can provide valuable information about complex classification problems even when used as a "black box". The results of the first dataset indicated that the amount of data for black locust was not enough to train a DL network. Moreover, the data were imbalanced regarding the classes Others and black locust, which can be improved by increasing the dataset, suggesting that using techniques such as data re-balancing (oversampling/down-sampling) or computer vision post-processing steps could improve the results even further by reducing the rate of FP. [Onishi and Ise \(2018\)](#) already confirmed that statement showing an increase of their sensitivity results from an average of 83.1 % to 89 %. [Safonova et al. \(2019\)](#) showed an increase of 12.1 % in their average sensitivity data since their data were less unbalanced than [Onishi and Ise \(2018\)](#). Based on these studies, data re-balancing has the potential to improve the classification results for the coastal forest. In Japan, black locust trees are mixed with other tree species, which makes it difficult to get images from pure black locust stands. Nevertheless, since the invasion of the tree species is a problem in forests all over Japan (e.g. [Srivastava et al., 2014](#); [Tanigushi et al., 2007](#)) images of black locust trees in mixed forests can be easily collected.

7.3.3.2 Effects of coastal forests

Coastal forests have an important purpose and it has been proven that management is important to preserve their capabilities. Both tree species, black pine and black locust, are well adapted to coastal conditions. The invasion had changed the monoculture plantation into a mixed forest, which might be an enhancement of forest resilience since several studies have pointed out the benefits of mixed forests under climate change. [Tinya et al. \(2019\)](#) suggested that mixed forests showed more stability to stress and disturbances. The study of identifying invasive species has the potential to analyse their influence on coastal forest functions. Those functions are known from studies like [Kudoh \(1985\)](#) and [Forbes and Broadhead \(2008\)](#), which focussed on the requirement of forests.

[Kudoh \(1985\)](#) studied the role of the black pine coastal forests and their potential to protect the environment, while [Forbes and Broadhead \(2008\)](#) explained the functional attributes of a forest, especially related to tsunami protection, like forest width, tree density and age. [Kudoh \(1985\)](#) explained that sea water droplets can be trapped 25 times of the forest tree height and therefore filter the salt. Already 2 m high trees in two planted rows covering 11 m along the coast can capture a large

amount of sand, according to (Kudoh, 1985). Further, the author calculated the reduction of the destructive power and height of tsunami waves. Forbes and Broadhead (2008) identified the width of the forest as most important factor. The authors pointed out that a coastal forest with a width of 200 m reduces the power of a 3 m tsunami by at least 80 %. Forbes and Broadhead (2008) indicated that a black pine forest with a width of at least 20 m is needed to withstand a tsunami with a wave height between 1 and 3 m. The minimum width of the Shonai coastal forest is 140 m and it has therefore the potential to effectively absorb the energy of a tsunami.

The density of the forest is another important factor and closely related to the vertical structure of the forest (Forbes and Broadhead, 2008). The black pine trees in coastal forests grow their first branches at a height of 3 m. Hence, the protection potential of a pure black pine forest is significantly lower than a mixture of black pine trees with deciduous trees like in the Shonai coastal forest. Kudoh (1985) indicated that black locust trees have a high potential to increase the mixture of the plantation even better and to positively influence on the forest ecosystem. The moderate density, which is generated by the mixture, will have the highest protection potential, according to Forbes and Broadhead (2008). The black locust in the Shonai coastal forest is subdominant as well as part of the understory vegetation.

The mixture of coastal forests is not well studied; therefore, a first analysis of the mixture would already provide essential information to indicate the potential or the threat of black locusts in black pine forests. The whole classification of this mixed forest and discussion was only possible because of the developed image analyses. Even though black locust trees can have positive effects on the coastal forest, negative influences need to be discussed as well. Since black locust trees are deciduous, they might create wind tunnels in the winter season.

7.3.3.3 Study assumptions and limitations

The proposed methodology is a tool for forest management practices since it can provide fast and reliable information about forests. In particular, the coastal forests with their function as wind and tsunami breaker could benefit from a more automated management system. Further, the Ministry of Environment in Japan has called for the urgency of management of black locust (Taniguchi et al., 2007). Since most of the forests are unmanaged and dense, this study provides a simple tool for forestry to assess the spread of black locusts and to detect invasive trees. Fieldwork in this area showed that the amount of black locust is higher than the 10 % coverage in the orthomosaic, which can be explained by smaller tree height (12 - 18 m) in comparison to black pine trees (up to 40 m). The smaller black locusts are often covered by the black pine canopies, only visible in forest gaps and cannot be easily identified from above. The true distribution and number of trees is still unknown, since not all trees

were visible on the images. Therefore, further fieldwork needs to be conducted to evaluate the accuracy of the model.

7.3.4 Conclusion

The method studied with coastal forest data showed its limitation regarding the visibility of smaller black locust trees. Still, the methodology indicated a high potential which needs to be pursued further. The results show the benefit of this technique since they provided a fast overview of the study area and facilitated management approaches.

7.4 Analysis of UAV-acquired wetland orthomosaics using GIS, computer vision, computational topology and deep learning

7.4.1 Wetlands

Defining a wetland is difficult in terms of their high variability in size, location and hydrology (Mahdavi et al., 2018). They are often characterised as forming a transitional zone between terrestrial and aquatic zones, showing characteristics of both (Mahdavi et al., 2018). The water content in wetlands is usually changes between different seasons, creating therefore different conditions depending on the location. A common definition is giving by the Ramsar Convention, summarizing marsh, fen, peatland and water into natural or artificial wetlands. The water content can be static or flowing, it can be brackish or salty (Mahdavi et al., 2018).

Wetlands have a high economic value because of several advantages for the environment. Wetlands are known for their purification of water and their protection against flooding and their high filtering potential that reduces pollutions and sediments significantly. They are habitats for plants and animals, including some threatened species (Kingsfor et al., 2016). Wetlands are a natural sink of carbon and have therefore a direct relation to climate change. Further they have a significant influence on all nutrient cycles (Mitsch and Gosselink, 2000).

Mitsch and Gosselink (2000) estimated wetland areas to cover around 4 to 6 % of the terrestrial surface, while (Kingsford et al., 2016) estimated 5 to 10 %, whereby more than 70 % might be already destroyed. In the past, wetlands were often drained for agricultural land or urban space, especially in Europe and the USA. Also, further anthropogenic influences like air pollution, groundwater extraction and land irrigation affect wetlands (Mitsch and Gosselink, 2000). Changing climate conditions increased pressures on the natural habitats because of drought conditions and salination (Mahdavi et al., 2018). Natural threats are known to be diseases or invasive species, which are further causing a biodiversity loss (Mitsch and Gosselink, 2000).

The loss of wetland area and the acknowledgement of their great potential increased the pressure to conserve wetlands. As conservation actions mitigation of threats, risk assessment and management possibilities are pronounced (Mitsch and Gosselink, 2000). The determination of wetland status needs to be done by inventory assessments. Thus, collecting information about the current status and the changes within a wetland requires monitoring (Mitsch and Gosselink, 2000). Therefore, primary threats can be identified and protection, mitigation and rehabilitation can be established for management practices.

7.4.1.1 Problem definition Blueberries

In the past two decades an explosive spread of North American blueberry hybrids (*Vaccinium corymbosum* x *angustifolium*) has been observed in several moors of the northern German Geest area, endangering the natural development of these protected raised bog areas (Hollenbach, 2014). Starting point of the spread were almost exclusively existing or former commercial blueberry plantations (Scheppker and Kowarik, 1998; Stieper, 2018), which are located in the area or in the immediate vicinity of bogs or former peat extraction areas due to the good soil conditions. Most of the recipient habitats are pine forests and bogs in various stages of de- and regeneration. Particularly in bogs, spontaneously growing blueberries are displacing valuable species indigenous peatland fauna such as *Erica tetralix*, *Eriophorum vaginatum*, *Empetrum nigrum*, *Andromeda polifolia*. Because of these characteristics, the American Blueberry (*Vaccinium angustifolium* x *corymbosum*) was classified as a potentially invasive neophyte by the Federal Agency for Nature Conservation (Nehring et al., 2013). This work is focused on a natural environment defined as an "ombrotrophic s for bog", i.e., a wetland hydrologically isolated from its environment receiving both water and nutrients only from precipitation. After the degradation of wetland areas due to anthropogenic activities protection programs were issued for the conservation and development of rare animal and plant communities in these areas called "Moorschutzprogramm", established by the state government of Lower Saxony (Deilmann et al., 1990). Furthermore, activities that threaten the goals of the protection program are prohibited, which increases the difficulty of corresponding field studies (Deilmann et al., 1990). However, maintenance and development measures are needed to rehabilitate wetland areas, especially nowadays, where the invasive blueberry species (*Vaccinium corymbosum* x *angustifolium*) migrates into protected, comparatively sensitive ecosystems. In 2011 stands of spontaneously growing blueberries were known from 20 counties in Lower Saxony. The tendency to spread continues: practically every cultivated area has experienced a spread over time if suitable biotopes occur in the immediate vicinity (Starfinger and Kowarik, 2011). The potential area occupied by spontaneously growing blueberries can reach several square kilometres within a few years (Starfinger and Kowarik, 2011). Studies from Scheppker et al., (1997) and Schiefer (2018) used grids in the field to plot the distribution of blueberries in wetlands. Both studies focused on areas near blueberry cultivation, as the biggest spread was found in close proximity to the blueberry plantations (Scheppker and Kowarik, 1998).

Still, it is unclear how widespread the blueberries have already become, as well as in which areas they occur. In order to take effective measures on these areas and to minimise disturbance of the usually sensitive biotopes, it is necessary to localise the individual blueberry plants as accurately and early as possible. In addition, the following questions arise: Does a displacement of natural species take place and where should what measures be taken against a continuing invasion? According to Scheppker et al.

(1997) and Essl (2004) counter measures with little efforts can lead to good results and prevent a further spread, especially when blueberry bushes are identified early. Therefore, a suitable method for recording stock development and distribution is needed, which is associated with low human impact.

Locating the small single blueberry bushes from the ground in large distribution areas is difficult and has not been done before, to the best of our knowledge. UAV-supported methods therefore offer an efficient possibility to discover individual young plants on a large scale and to detect propagation hotspots at an early stage. Driven by the urgent need to detect the blueberry species and given the latest developed technologies allowed to formalize the following objectives:

- xvii. To classify wetland vegetation and
- xviii. To detect invasive blueberry species with DL techniques
- xix. To quantify the classification results achieved using data augmentation and loss function weighting
- xx. The effect on the classification results based on the use of different DL architectures
- xxi. To map and analyse the distribution and properties of the invasive species

The main goal was to explore the use of UAV-acquired images to analyse large parts of the sensitive ecosystem, studied here. The gathered high-resolution images were used together with techniques from different study fields (ecosystem analysis, image processing, DL and computational topology) to produce informative and accurate maps, which will help to manage areas affected by blueberries.

7.4.2 Study area

The chosen study area "Lichtenmoor" is in a natural environment defined as wetland and is located about 60 km northwest of Hanover, Germany (52°43'06.2"N 9°20'41.5"E) (Figure 83). The Lichtenmoor is an upland moor complex of national importance for the protection of upland moors. The Lichtenmoor lowland is located in the central region of Lower Saxony, northern Germany, predominantly in the district of Nienburg/Weser. The total extent of the wetland complex is 38 km² (Schneekloth and Tuexen, 1975). The central area of the studied wetland is characterised by past industrial peat cutting. As a subsequent use, some former peat cutting areas are rewetted with the aim of regenerating raised bogs. In the surrounding area parts of the Lichtenmoor were designated as nature reserves; at the edges and in parts of the nature reserves there are former hand peat cutting sites. The remaining area is dominated by agricultural areas, mostly grasslands, dry to moist moorland forests, scrubby heather and moorland degeneration stages, pioneer stages of moorland rewetting and peat extraction areas under cultivation. The case study area covers a total area of 62 ha and is located in the central part of the Lichtenmoor complex. In the northeast it borders on a pine plantation,

in the southwest current peat extraction areas are adjacent. Blueberry plantations can be found throughout the Lichtenmoor, especially on the outskirts of the localities Lichtenhorst, Heemsen, Sonnenborstel and Steimbke.

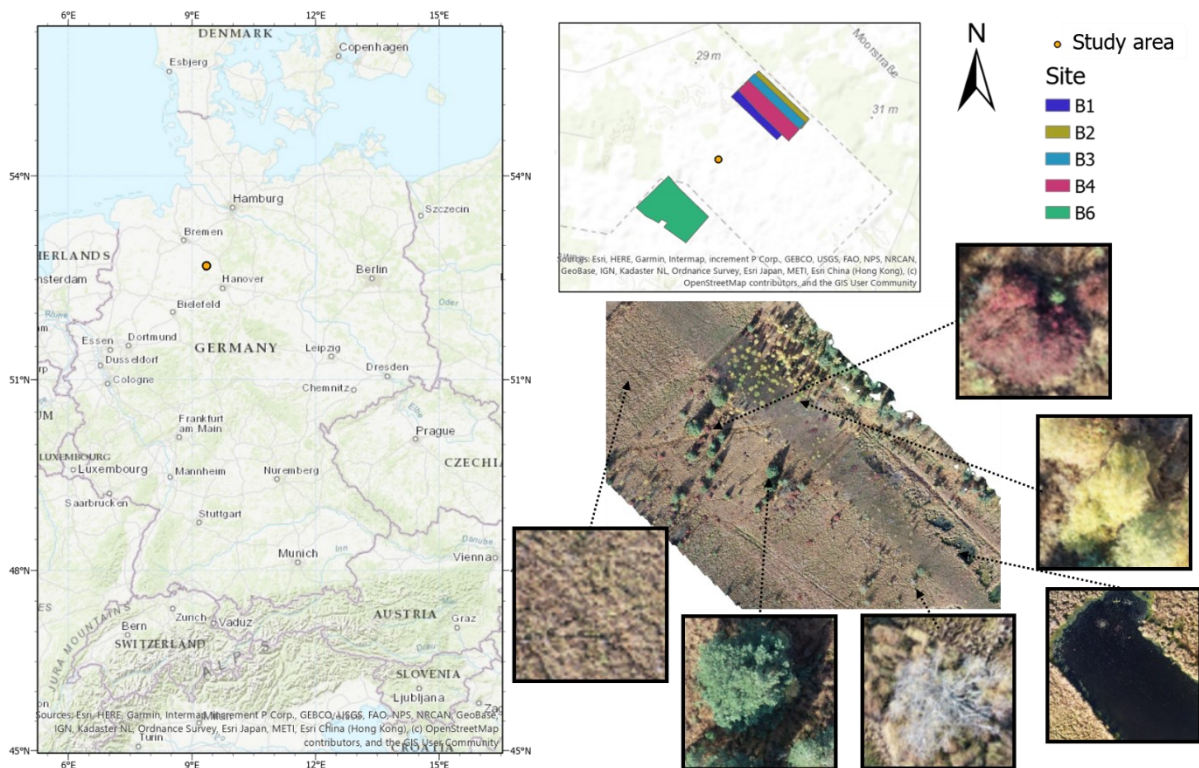


Figure 83 Location of the study area in the north of Germany. In the upper right part of the figure the study sites are marked with different colours. The bottom right part an example orthomosaic is shown with detail of the different classes

7.4.3 Description of the blueberry species

Blueberries have been cultivated in commercial plantations in Lower Saxony since the early 1930's (Schepker et al., 1997). Since then, the area under cultivation has increased steadily. In 2005 the area under blueberry cultivation in Lower Saxony was about 1,400 ha (Starfinger and Kowarik, 2011). In nature, blueberries are mainly distributed by birds and small mammals, which spread the seeds. Once established, plants can spread in the vicinity by colonial growth and the high regeneration potential of the blueberry favours the strong spread (Stieper, 2018). Thus, blueberries are increasingly becoming wild in neighbouring areas. Schepker et al. (1997) and Schepker and Kowarik (1998) found a correlation between the density of blueberries and the distance to blueberry plantations, a maximum distance of 1,700 m was recorded. Near the cultivated areas, the feral blueberries form dense shrub stands with height up to 2-3 m and ground coverage of up to > 60 %. With increasing distance, the degree of coverage decreases rapidly (Schepker and Kowarik, 1998; Starfinger and Kowarik, 2011, Hollenbach, 2020). Since these studies took place already in the last millennium, a larger distribution must be

expected today. Stieper (2018) describes a distribution of blueberries over 4 ha in the “Krähenmoor”, where the maximum distance to the plantation was marked at 100 m. The species prefers acidic locations, such as pine forests or wetlands. Especially raised bogs in their degeneration stage provide ideal habitat conditions for the invasive blueberries (Schepker et al., 1997). Increasingly, shallow individuals, which can reach a height of 60 cm, but also tall bushes can be represented, which can reach a height of 3 m (Stieper, 2018). In the course of the increased growth and the dense shrub structures, ground vegetation is displaced, since it cannot exist under the shade of the blueberries. Other presumed effects of blueberry cultivation are reduced evaporation rates and an influence on nutrient cycles in bogs, which in turn can have an impact on existing species. Therefore, human interventions are necessary to protect the sensitive and rare structures and plants of wetlands (Stieper, 2018).

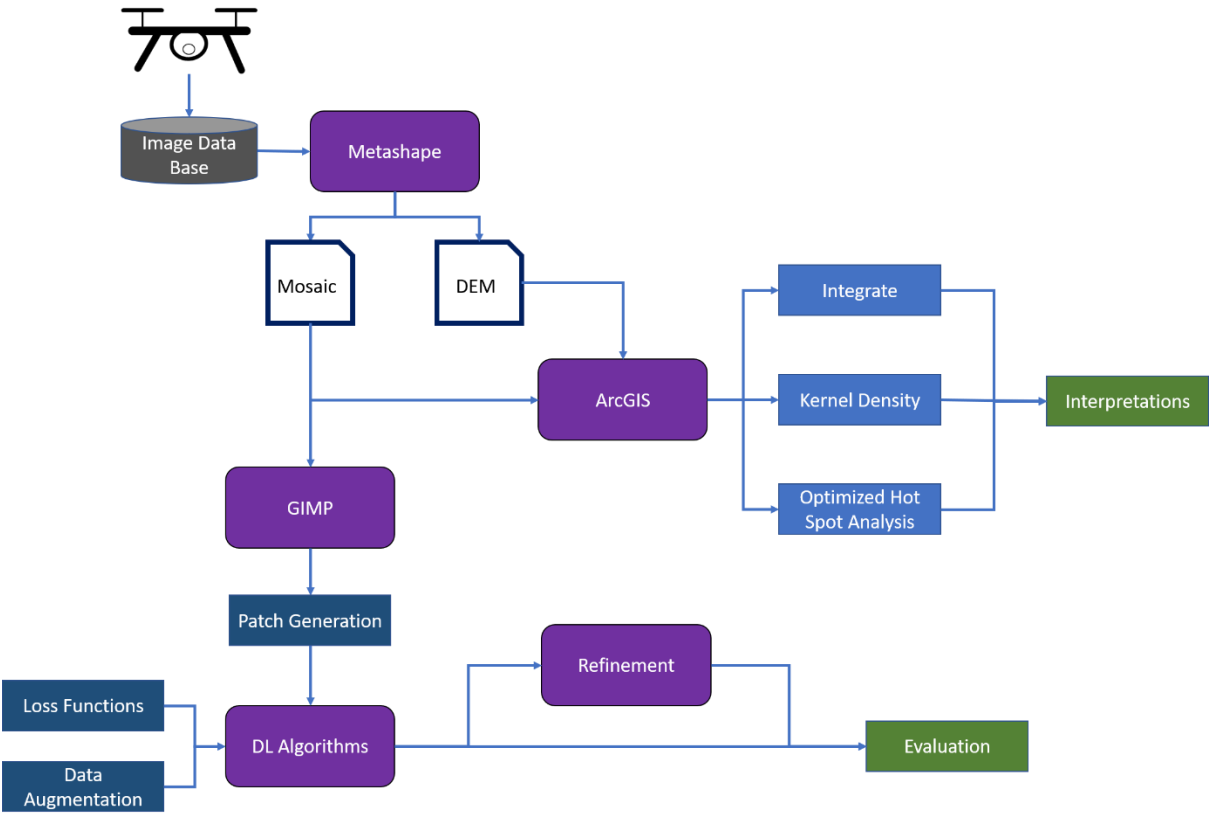


Figure 84 Workflow of the chapter. Gray is the data base; purple boxes show software/programs used in this study; white boxes with a blue outline are generated files; dark blue are processes used for the DL classification and detection; light blue are tools in ArcGIS

7.4.4 Data collection and pre-processing

Image collection was performed by using a DJI phantom 4 UAV in autumn 2018 due to the seasonal red colouring of the blueberry leaves. For the sites B1 to B4 490 to 584 images were collected, while 1,346 images were taken for B6. The flight height was 50 m and front and side overlaps of 80 % were chosen.

All images were aligned with Metashape and obtained orthomosaics were annotated with GIMP. For three of them (B1, B2 and B3) the whole orthomosaic was annotated and each pixel was given one of the following 6 labels: Blueberries, trees, yellow bushes, soil, water and dead trees. The class trees contain pine trees (*Pinus sylvestris*), the class yellow bushes were defined by shrubby birches (predominantly *Betula pubescens*, secondary *Betula pendula*). Binary layers for each of the six classes were created for each of the three orthomosaics using the pixel-level labels. These annotations were based on colour, shape and context information contained in the orthomosaics. In the last two mosaics (B4 and B6) only blueberries were annotated.

In order to train a model capable of predicting all the possible different classes, orthomosaic with all the possible label annotations were needed, therefore only B1 to B3 were used. The orthomosaics, as well as the annotated binary layers were divided into axis-parallel patches of side length (referred from now on as patch size = 100). Given the size of the blueberry bushes, ranging from 20 to 100 pixels in radius it was decided to use $s = 100$ pixels for all the experiments presented. Patches of 100 x 100 pixels were used as an input for the DL network. In the first step of the network, each patch was resized to fit the size needed by each feature extractor. The classes present in each patch were stored in a separate label list. In general, patches contained more than one class and therefore the problem was defined as a multi-label patch classification problem.

7.4.4.1 Data processing using ArcGIS

This section deals with data processing performed with ArcGIS and python coding (Figure 84). The processing helped to visualise and identify parts of the mosaic containing blueberry bushes. Further analyses were performed to gain knowledge about the blueberry bush properties.

In this context, points were marked manually and stored in a shapefile to identify the position of the invasive species within the five orthomosaics. Furthermore, analytical tools were used to extract useful information about the problematic species. With the tool *kernel density*, kernel functions were used to calculate the magnitude-per-unit area from the blueberry points. A smaller search radius was used to show a detailed density raster. The tool *integrate* was used to group blueberry bushes which fell

into a specified distance. These specified distances were 3 and 6 m, respectively. With the tool *collect events*, the points, which were integrated before, were summarised in a new layer. These steps were necessary to perform an *optimized hot spot analysis* with the blueberry point shapefile. The hot spot analysis identified significant differences between the proximity of a feature in comparison to the extent of the respective study area. Is the value of a feature significantly higher, then it is considered as a hot spot and the tool outputs a feature map with three levels of confidence (90 %, 95 % and 99 %). The input file was the result of the collect events and as analysis field counts were chosen. Furthermore, it also indicates the significant lower features. Additionally, the optimized hot spot tool was used to identify the hot spots, where larger blueberry bushes were located.

On the basis of the annotations made for all orthomosaics, several simple python codes and ArcGIS were used to perform image analysis. Pixels were counted for all mosaics, as well as for all annotated layers. The numbers of black pixels in the annotated layers were specifically counted to get the percentage and area in square metres per class. Additionally, the overall area, presented in mosaics, was calculated in a hectare basis. Since the focus of this work was on the blueberry bushes, several statistical values were generated. The number of blueberry bushes were counted and the number of blueberries per ha were calculated for each mosaic. Additionally, the total area and also the area per blueberry bush were computed in square metres. Furthermore, the proportion of blueberries in relation to the vegetation was calculated in percent. Finally, height values were computed on the basis of DEMs, annotations of the blueberries and annotations of floor points per site. Floor points were annotated close to blueberry bushes to increase the accuracy of the computed height. Maximum height values were estimated in a first analysis and the median height in a second.

Finally, persistent homologies were computed on the annotations of the blueberry bushes. Persistent homology is an algebraic method to identify topological features of data (Carlson, 2020). The tool connects nearby points to get a trivial topology behind discrete points. In this study the idea behind this complex mathematical idea is used to observe changes in the data using an increasing threshold. 0d persistent homology was used, which can be explained by circles growing around points, simultaneously (Koplik, 2019). The aim was to connect all points by increasing the radius of the growing circles. When two circles intersected each other, the points were connected into the new component, so they were fused. When points were fused, they created a point in the persistent homology diagram. The growing of the circles continued until all points were connected. Points, which were close to each other connected quickly, while further ones needed a larger radius and therefore more time to be connected (Koplik, 2019). Persistent homology computes numbers, which describe the clustering and separation of data. The original output was used to generate the radius needed to fuse 1, 10, 50 and 90% of the points contained in the orthomosaics.

7.4.5 Deep learning techniques

DL is a trending field of machine learning that focuses on fitting large models with millions of parameters for a variety of tasks, such as image classification and segmentation. These approaches have been rapidly gaining attention in computer vision tasks due to their increased accuracy.

DL models commonly learn from examples in a supervised manner: First, *architecture* or a graph of connected nodes is defined. These nodes are often grouped in *layers* that perform a specific operation and the combination of a large number of *layers* is referred to as a DNN. The typology of the nodes, the number of nodes per *layer* and the connections between them determine the behaviour of the network. In general, two main types of nodes are used: linear nodes, expressed as matrix multiplications and nodes that introduce non-linear functions (such as the sigmoid function). The weights in linear nodes are usually initialised with random values following a specific distribution. Afterwards, the network is given samples of the data, known as *training samples*, that contain instances of the problem (i.e. image intensities) with their corresponding solutions (i.e. labels). These samples are iteratively run through the network to evaluate its current accuracy and the weights are updated following an optimization process.

The approach was based on a patch classification model that uses the patches of 100 x 100 pixels. A patch of mosaic B1 and B3 covered therefore 700 x 700 cm and a patch of mosaic B2 500 x 500 cm. For each patch, a list containing the class labels was created from the binary maps for each class. This classification style is usually referred as multi-label, since each input patch might contain different labels (i.e. a part of the patch may contain soil, while other parts of the same patch could also contain bushes or blueberries).

7.4.5.1 Deep learning architectures

In this work, DNNs were used to locate and identify the six classes defined in section. DNN have two major components for classification: a feature extraction stage and a prediction stage. On the first stage, convolutional operators are trained to extract salient and meaningful features (such as texture) while on the second stage these features are used to predict the final labels for the given input patch or image. In order to train general and robust feature extractors a large pool of heterogeneous images with different properties (light conditions, colour, view, etc.) is needed, to capture all the possible image variability. During the process of the working with the blueberry data, it was recognized that the data were challenging to run them with a DL network, as the data were unbalanced and similar challenges to the Black locust data occurred. Therefore, the work was split into a DL part, which is presented in detail in [Cabezas et al. \(2020\)](#) and [Kentsch et. al \(2020\)](#) and in the application part

(Kentsch et al., 2021). In this chapter the important aspect of the study (Cabezas et al., 2020) are included to understand the DL part of the blueberry classification. One part of the CNN is the feature extraction, which was performed with the following architectures:

1. AlexNet (Krizhevsky et al., 2012) is a widely used CNN architecture, that uses Rectified Linear Units (ReLU) and consist of eight layers, five convolutional layers and three full connected ones.
2. The VGG (Simonyan and Zisserman, 2015) uses small receptive fields together with three ReLU units, which increased the decision function. In this work a VGG version with 19 layers (1 x 1 convolutional layers), including batch normalization, was considered.
3. ResNet (here used: ResNet50, ResNet152) (He et al., 2015) has an increased deepness, which provides higher performances of the network, with the additional use of identify shortcut connections and ReLU functions (Fung, 2017).
4. The Squeezenet (squeezenet1_0) (Iandola et al. 2016) uses an architecture with 1 x 1 filters and 1x1 convolutional layers. The benefit of the network is the high accuracy which can be achieved, even with few parameters (Tsang, 2019).
5. DenseNet (densenet161) (Huang et al., 2016) uses dense connection, few parameters and achieves high accuracies. The DenseNet, used in this work, contains 161 layers and is built up by pre-activation, batch normalization, ReLU and finally the 3x3 convolutional layers.
6. Wide ResNets (wide_resnet101_2) (Zagoruyko and Komodakis, 2016) has modifications, which allows the network to be shallower than the ResNet, without losing accuracy. Wide ResNets allow adding more feature maps in each layer, which enables the possibility to reduce the depth of the network (Zaguroyko & Komodakis, 2016).
7. ResNeXt (resnext101_32x8d) (Xie et al., 2017) is another modification of the ResNet network. The network uses the split-transform-merge paradigm. The cardinality, introduced with this network, influences the performance of the model (Fung, 2017).

7.4.5.2 Data augmentation and transfer learning

Proven by previous work (Kentsch et al., 2020, Cabezas et al., 2020), transfer learning is a useful tool for image analysis applications, where the training dataset is too small to properly train these feature extractors from scratch. So, transfer learning with ImageNet was applied to initialize the weights of the DL network to increase the performance of the network, as only three different orthomosaics were available.

In order to obtain a higher detection rate for the blueberry class, two main approaches were used:

- ❖ Data augmentation is a commonly used strategy in DL that can increase the size of the training datasets without the need to collect new data. In this case, data augmentation was used to generate new synthetic patches of the blueberry class, which was the less frequent class. Six image transformations to augment the data were used, which were implemented with the `imgaug` library:
 - Rotations: the original image is rotated with a random angle, which can be compared with a UAV collecting the data from the same object imaging it from different directions and angles.
 - Flips: Flips are applied on the x- and y-axis by turning the image up or down, left or right. Furthermore, the image can also be mirrored.
 - Gaussian blurring: The artificial blurring is applied by a kernel moving over the image, simulating movements, sensor malfunctions or distance effect during the data acquisition or the data processing, when orthomosaics are produced.
 - Linear and small contrast changes: Data acquisition is accompanied with different illumination conditions and shadows in the images, which can be also applied as augmentation technique.
 - Localised elastic deformation: This kind of deformation can be used when there are intra-species differences between the single bushes imaged for this study.
- ❖ Loss functions are used to compute the accuracy of the network and update their parameters. By giving different weights to different classes, their importance can be changed during training. In this study, two loss functions were used. The first function checked if a patch contained a blueberry bush or not, while the second one checked the fraction of blueberry pixels inside the patch. For this work the optimal training settings following ([Cabezas et al., 2020](#)) was used.

7.4.6 Evaluation

In order to assess the predictive power of the algorithms, labels were used for all the patches and the relation between 1) Predicted values resulting from the algorithm and 2) Real values as stated in the manually-annotated ground truth. All patches were following broken into the usual classification categories TP, FP, TN, FN with TP predicting the contained Blueberry class, which is also marked in the ground truth as containing them.

In order to summarise the occurrences of the four categories, the two following metrics were used (True Positive Rate or Sensitivity, False Positive Rate and Accuracy).

$$Sens = \frac{TP}{TP + FN}$$

$$FPR = 1 - SPEC = \frac{FP}{TN + FN}$$

$$ACC = \frac{TP + TN}{TP + TN + FP + FN}$$

The algorithm was finally modified to present the results in a way that was convenient for end-users. The 100 x 100 patches used for prediction managed to capture most of the occurrences of the Blueberry class. However, those rather large patches also included large areas not actually containing any blueberries. While expert users could easily use these results as a starting point to quickly identify the exact location of blueberry bushes, a refinement using smaller patches would make their work faster while also providing clearer information for non-expert users. Consequently, each of the predicted 100 x 100 patches were divided into sixteen 25 x 25 patches, re-sampled to the image size used by the DNN and re-classified. This resulted in a refined result made up of 25 x 25 patches. This process had the downside that if errors were made some of the originally correctly predicted Blueberry pixels might be lost, to evaluate this issue the TP, FP, TN, FN status of each pixel in each patch were considered and the percentage of Positive pixels covered by the predicted patches was measured. Further was the dice coefficient an indicator for the relative weight of Blueberry pixels inside the predicted patches:

$$DICE = \frac{2TP}{2TP + FP + FN}$$

7.4.7 Results

This section is divided in two parts: The first part of the analysis focused on the manual annotations of the wetland vegetation and especially of the blueberry bushes. GIS, computer vision and persistent homology were used to describe and quantify the characteristics of the blueberry invasion in all test sites. In the second part results of DL techniques are presented. The goal was to assess to what extent these technologies can be used to automatically generate the annotations that were used in the first part to characterise the invasion. The general workflow can be seen in Figure 85.

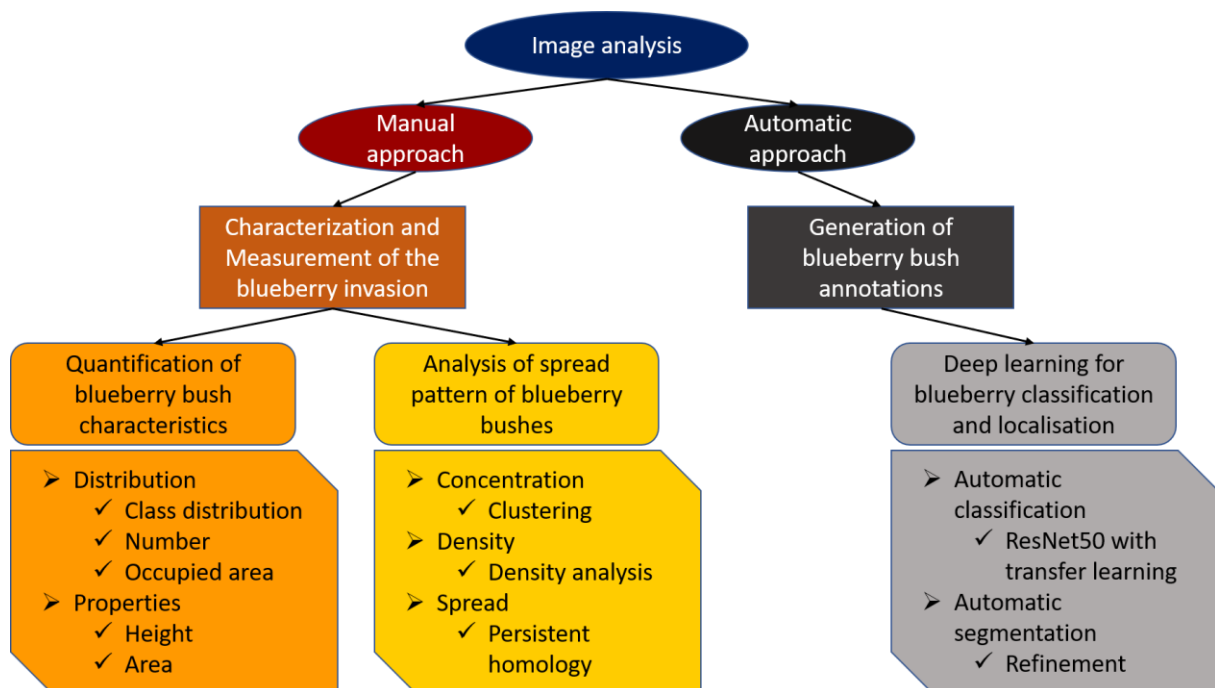


Figure 85 Image analysis workflow. Consists of two parts, the manual approach using manual annotation, GIS and persistent homology and the automatic approach using DL and segmentation to analyse the blueberry invasion

7.4.7.1 Quantitative analysis of the blueberry invasion

In this part of the study the focus was on characterizing and measuring the dimension of blueberry invasion of the wetlands.

The distribution of the classes in the images (blueberries, trees, yellow bushes, soil, water and dead trees; was analysed and the state of the invasion was assessed by gathering information about the areas of the sites, the numbers of blueberry bushes and the average area per bush.

One important aspect was to calculate the area of blueberry bushes within the orthomosaics. The area covered by the orthomosaics varied between 10.6 and 12.5 ha, only B6 was larger with 15.5 ha (Table 29). Together with the annotations made for B1 to B3, the area of every class was calculated (Figure 86). The main part of the image represented soils (Figure 86). This was validated by the area calculations: with 76 % of the orthomosaic B2 and 89 % of B3, soil represented the highest proportion of all classes. The second smaller pie shows the living vegetation varying between 4.7 % in B1 and 18.6 % in B2. Out of the living vegetation, 8.2 % (B2), 15.0 % (B3) and 21.1 % (B1) are blueberry bushes. In most of the orthomosaics blueberries were the least frequent class (with 1 to 1.5 %).

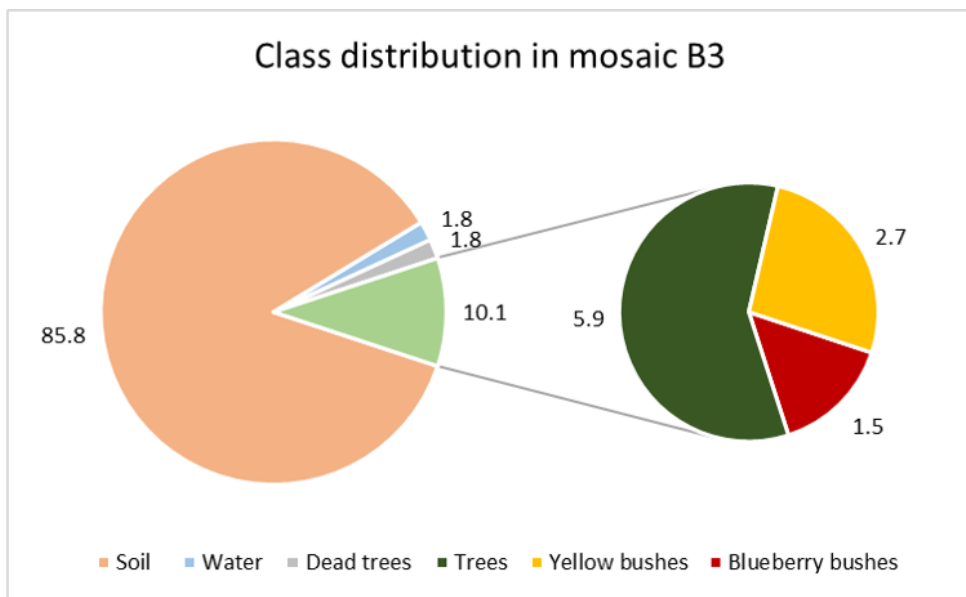
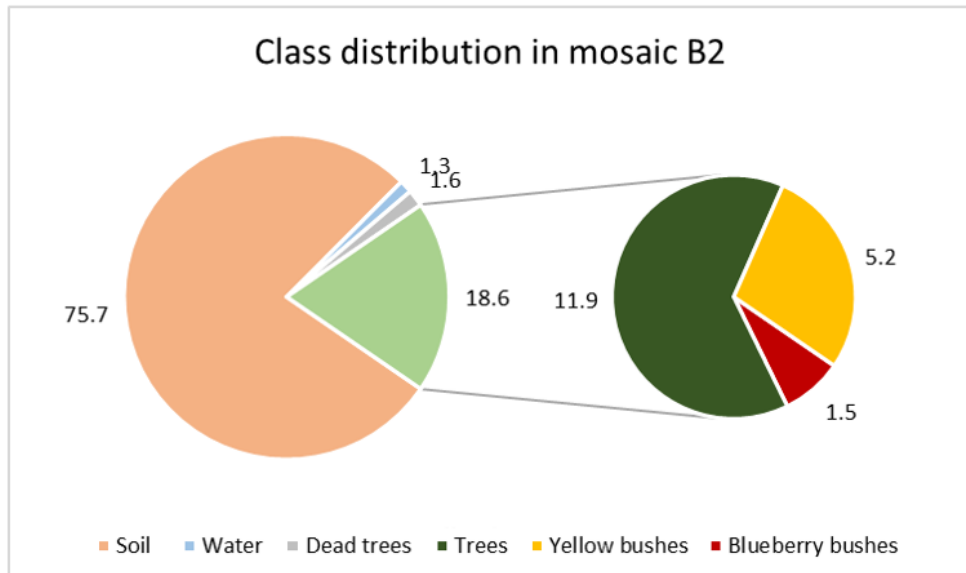
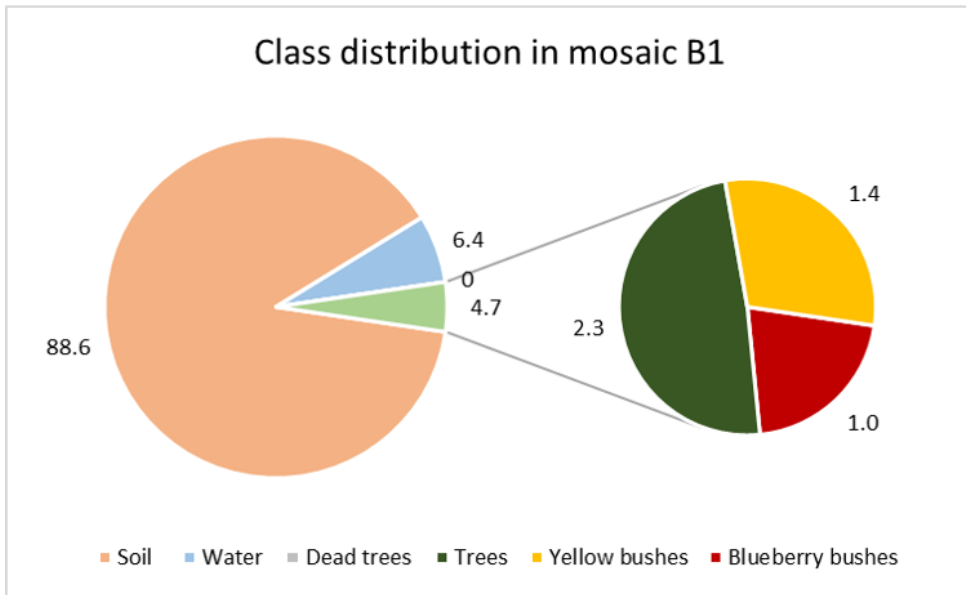


Figure 86 Distribution of annotated classes for the orthomosaics B1 to B3

The number of blueberry bushes varied from 235 in orthomosaic B6 to 687 in B2 (Table 29). The site areas of orthomosaic B1, B3 and B4 were similar, while orthomosaic B6 was the largest site containing the least blueberry bushes, in contrast to orthomosaic B2, which contained the highest number of blueberry bushes in the smallest area. The ratio could be confirmed by calculating the blueberry bushes per ha (Table 29). In another step annotations were used to calculate the total area covered by blueberry bushes. In orthomosaic B6 an area of 278.07 m² was covered with blueberry bushes, which represents the smallest area and resulted in an area of 1.18 m² per blueberry bush. The largest area, covered by blueberry bushes, was found in B2 with 1885.51 m². The average size of the bushes was similar for B2 and B3. In site B1 the average size of blueberry bushes was the highest with 3.55 m², while the covered area was third lowest with 1331.41 m².

Table 29 Area and counting measures of blueberry bushes detected in the orthomosaics

	Orthomosaic area in ha	Number of blueberry bushes	Blueberry bushes per ha	Blueberry bush area in m²	Area per blueberry bush in m²
B1	11.64	375.00	32.21	1331.42	3.55
B2	10.64	687.00	64.55	1885.51	2.74
B3	12.47	566.00	45.40	1470.24	2.60
B4	12.44	405.00	32.54	870.33	2.15
B6	15.14	235.00	15.53	278.07	1.18

Since the covered area and the average size of the bushes could be calculated, the next point of interest was the area and height per blueberry bush (Figure 87). Since the percentage of blueberries decreased towards larger cover areas, bushes were grouped into the intervals 6 to < 10 m² and > 10 m². B1 and B2 had approximately 30 bushes between 6 and 10 m², which was the maximum for all sites. Mean areas were computed for all orthomosaics, indicating that B1 had a high number of large bushes with a mean area of 3.57 m². The smallest blueberry bushes could be found in orthomosaic B6 indicated with a mean value of 1.18 m². In general, most of the blueberry bushes showed areas up to 2 m², a lower amount distributed between 2 and 4 m² and the lowest numbers distributed in areas greater than 4 m². B1 was an exception with around 10 % per class over 4 m². The highest areas calculated range between 17 to 25 m², with B1 containing 4 bushes in that range and 27 with areas of more than 10 m². The smallest areas were found to be less than 10 m² for B1/B4 and approximately 15 m² for all other orthomosaics.

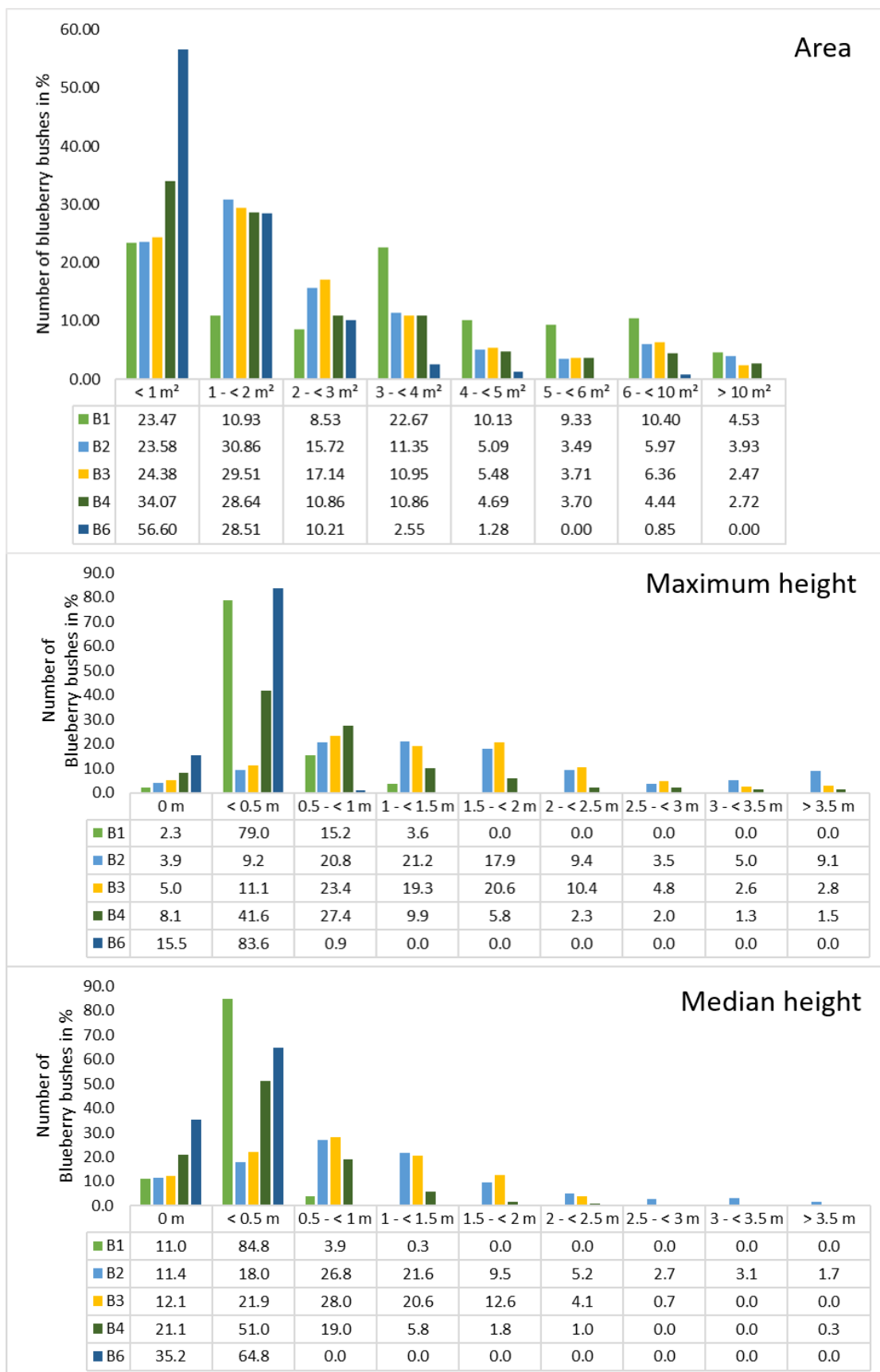


Figure 87 Distribution of the area and height values of blueberry bushes. From top to bottom: area, maximum height and median height

A similar distribution can be seen in Figure 87, where the number of blueberry bushes was plotted against the height. Classes were chosen for every 0.5 m height, starting with 0 m up to less than 3.5 m and more than 3.5 m. This distribution was chosen due to the characteristics of shallow blueberry bushes that reached 60 cm and tall species that reached 3 m. Regarding the maximum height, no height was computed for 2.3 % (B1) up to 15.5 % (B6) while the numbers were higher when the median height was considered (11.0 % for B1 up to 35.2 % for B6). In general, the median height values were higher for the classes 0 m and 0.5 m in comparison to the maximum height, while the values are lower from 0.5 m. The lowest height values started from 0.01 m (B6), 0.03 m (B1), 0.07 m (B3/4) and 0.1 m (B2) for both maximum and median height. In general, the maximum and the median height distributions of the orthomosaics were similar. Almost all of the blueberry bushes in orthomosaic B6 were within the class < 0.5 (83.3 %). In B1 the number of blueberry bushes in this same class was 79 % and 15.2 % was between 0.5 and < 1 m, which was similar to B6. Orthomosaic B2 to B4 showed a Poisson distribution, whereby B2 had the highest number in 1 < 1.5 m with 21.2 m, while 41.6 of the blueberry bushes in B4 had the highest value in < 0.5 m. Furthermore, in B2 and B3 more than 50 % of the blueberry bushes reached heights between 1 m and 3.5 m (57 % and 57.7 %).

It has to be considered that the area was calculated based on the shapefiles in ArcGIS, while the developed python code was used to calculate the height of the blueberry bushes. Since the input for the code were the annotations of the blueberry bushes, stored as PNG file, bushes which were close together were grouped. Therefore, the height values were not always calculated for an individual bush, which resulted in a different number of blueberry bushes per site: 309 (B1), 519 (B2), 461 (B3), 394 (B4) and 219 (B6).

7.4.7.2 Analysis of spread patterns

In a second step of the quantitative analysis of the blueberry invasion, the concentration, density and the spread patterns were examined. GIS and persistent homology were used to assess these issues. Characterisations of concentrations and densities can indicate the number of blueberry bushes within a given region of the orthomosaic, which exceeds a simple location because the distribution of the bushes can be analysed precisely. Clustering bushes and mapping densities further increase the understanding of the distribution. Together with the persistent homology and hotspot analysis the spread could be defined for all orthomosaics, which helped to characterise the invasion.

The first step was to cluster blueberry bushes by using specified distances, of which 3 and 6 m were chosen, due to the calculated area of the blueberry bushes. The average diameter was considered to be 2 m for the different sites, and therefore a diameter of 3 m was found to be appropriate to

especially group blueberry bushes which were close to each other. The results of both distances were listed and compared (Table 30). When blueberry bushes were located in a range of 3 m, they were clustered with the following results. From orthomosaic B3 to B1 35.51 % to 39.87 % were clustered. The highest number of clustered bushes was 33 in B3, followed by 25 in B2 and 10 in B1. In comparison to B1 to B3, B4 and B6 had around 28.3 % clusters with 3 and more blueberry bushes. The highest number within a cluster was 9 for B4 and 13 for B6. After increasing the range to 6 m the number of blueberry bushes clustered in the group 3 or more bushes increased to 69.57 %, which is more than 30 percentage points. B1, B3 and B4 had a similar increase of around 15 percentage points and reached 56.63 % in B1, 50.43 % in B3 and 44.35 % in B6. With less than 10 percentage points, 37.68 % of the blueberry bushes were grouped together with more than 3 bushes.

Table 30 Clustering results based on point shapefiles of the sites

	3 m clustering			6 m clustering		
	grouped 3 or more (in %)	number of single bushes	of highest counts (group)	grouped 3 or more (in %)	number of single bushes	of highest counts (group)
B1	39.87	89	10	56.63	18	25
B2	36.82	87	25	69.57	23	50
B3	35.51	98	33	50.43	36	50
B4	28.34	92	9	44.35	39	22
B6	28.28	51	13	37.68	28	21

Based on the GIS point shapefiles of the blueberry bushes, density maps were generated to see how the bushes were distributed within the site. Figure 88 provides three examples of the orthomosaics B1 to B3. Areas with a high density were marked in red and low densities in dark green. Orthomosaic B1 has one high density spot in the north-western part of the map, while the density decreased with only single or paired bushes in southeast direction. Orthomosaic B2 showed four density spots. Two smaller ones were located in the northwest; a larger spot was in the middle of the orthomosaic, and a last one in the southeast. The space between the middle and southeast spot was covered with blueberry bushes, which was similar to the distribution of B3. In orthomosaic B4 nearly the whole area was dominated by green to reddish colours. There were three dense spots in the northwest, two spots in the middle and one in the southeast. In comparison to B2 and B3 the spots were smaller. Orthomosaic B6 covers a larger area than all other orthomosaics, but only three density spots could be identified in the middle of the orthomosaic. There were smaller groups of blueberry bushes along the borders of the orthomosaic, and single ones were found close to the groups of bushes.

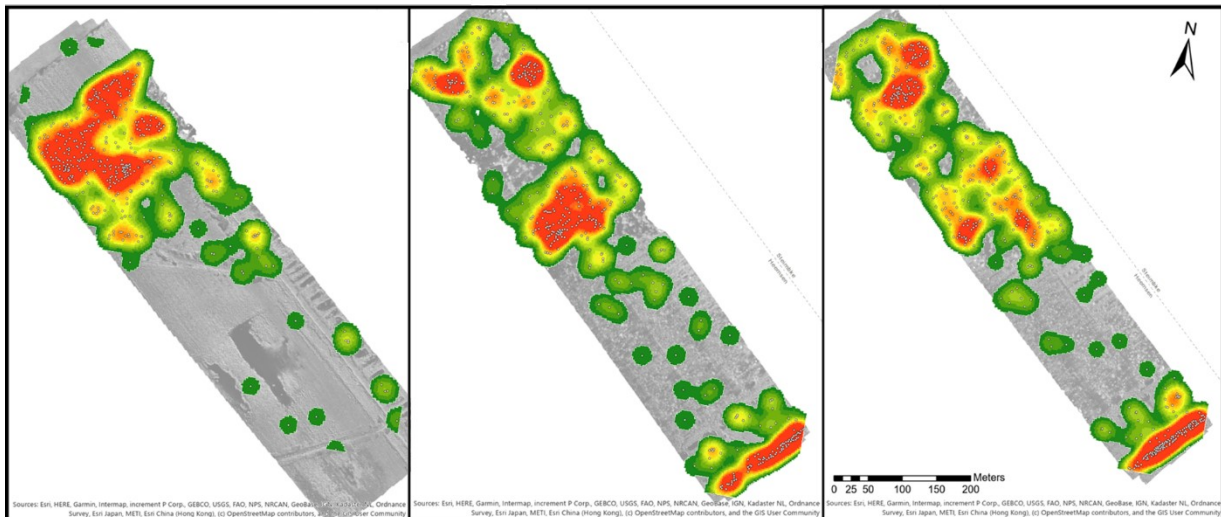


Figure 88 Density map for the blueberry species for the sites B1 to B3. Areas of low densities are marked in green and high densities are red coloured. A gradient between green and red represents values of medium density. White points mark the location of the blueberry bushes

In order to analyse the spread of the blueberry species, another analysis focused on the point analysis to generate a map of hotspot areas. The point analysis used the manually marked blueberry bushes to identify where the proximity of the bushes was significantly different (hot and cold), and to quantify those that were not identified as significantly different. In B1, two hotspots with 90% confidence interval were found in the north. 21 clusters were identified to be to 90% significantly different from the study area. The hotspots in B2 were concentrated in the south-easternmost part of the orthomosaic. 26 clusters (out of 220) were significantly different to the study area with a confidence interval of 99%. These points contained all bushes located in the south-easternmost part of the orthomosaic. In B3 16 out of the 214 clusters fell into the 99% confidence interval, all located in the south-east of the orthomosaic. The same characteristic was found in B4. 23 clusters out of 248 were found to be significant with a 99% confidence and seven points with 90% to 95% confidence. B4 was the only orthomosaic containing two points considered as cold spots with 90% confidence in the centre of the orthomosaic.

Finally, the persistent homology was performed. As it can be seen in Figure 89 the radius was plotted against the fused region. The orthomosaics B2, B3 and B4 showed a similar trend, while B1 and B6 followed a different trend, but similar to each other. B2 was the first orthomosaic, where 1% of the blueberry bushes were fused with a radius of 386 and B1 needed the largest radius with a value of 497. The necessary radius to fuse up to 10% of the blueberry bushes was similar to values between 415 and 557. There was a small gap of approximately 150 between B3 (945), B6 (998) and B1 (824), B2 (768), B4 (831) when 50% of the blueberry bushes were fused. The radius needed to fuse 90% for B1 and B6 are 3,279 and 3,611, while for B2 to B4 it is 1,610 to 1,709.

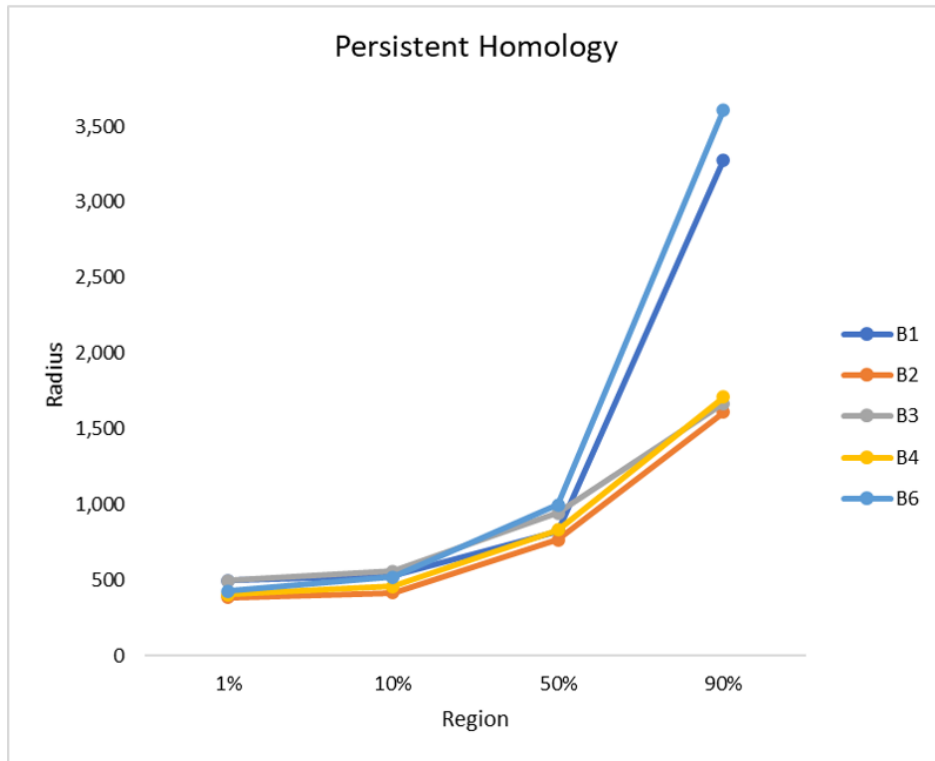


Figure 89 The persistent homology is plotted by radius against the region. Four fused regions were considered: 1 %, 10 %, 50 % and 90 % and all sites are plotted

7.4.7.3 Deep learning results

Experiments were presented using three orthomosaics containing the invasive blueberry species. The algorithms were implemented using the python programming language and the pytorch Library. All experiments were run using a Linux Ubuntu operating system with 10 dual-core 3 GHz processors and an NVIDIA GTX 1080 graphics board (Cabezas et al. 2020).

A leave-one-orthomosaic-out strategy was applied, whereby two orthomosaics were used for training, while the third one was used for testing. Every orthomosaic was used once for testing, but no orthomosaic was used for training/validation and testing at the same time.

The three folds used for the experiments are presented in the following enumeration:

- The first fold and testing: Orthomosaic 1 used for testing with 6,400 patches of which 2.53 % contain blueberry bushes; Training: Orthomosaics 2 and 3 (22,562 patches with 2.66 % blueberry)
- Second fold and testing: Orthomosaic 2 used for testing with 14,641 patches of which 2.58 % are blueberry bushes; Training: Orthomosaics 1 and 3 (14,321 patches with 2.68 % blueberry)
- Third fold, testing: Orthomosaic 3, 7,921 patches, used for testing and contains 2.53 % blueberry bushes; Training: Orthomosaics 1 and 2 (21,041 patches with 2.57 % blueberry)

The averages for TPR, FPR and accuracies were used to present the results of the blueberry class for each testing. Even though the focus of the study was on the blueberry bushes, the training with all classes improved the network performance, especially, because tree, yellow bushes, water and dead trees were as infrequent as the blueberry bushes. The soil class caused that the TPR were high and accuracies low, because of their high frequency in the dataset (Cabezas et al. 2020).

7.4.7.3.1 Experiment 1: Assessment of deep learning architectures and settings

Data balancing and transfer learning: Imbalance in data, with only 2.5 % of the patches containing blueberry bushes, influence the performance of the architectures significantly. Classes, which are infrequent will be classified with lower accuracies, therefore an adjustment of the network and data need to be performed. The combination of different DL techniques will be analysed here.

In a first step, the ResNet50 network was initialised with the ImageNet database (Krizhevsky et al., 2012) and with frozen and unfrozen weights to assess the importance of network settings on the performance of the network. Two kinds of data augmentation were performed to identify the influence of the amount of data augmentation. The TPR and accuracies vary in the different training sets and provide useful insights into the network performance (Figure 90), while details on the settings can be found in Cabezas et al. (2020). Best TPR results were obtained with the settings unfrozen, high weights (value of 8) on the blueberry class and an intensive use of data augmentation, while low results were obtained when the network was frozen and loss function weighting was applied with a value of 6 for the blueberry class. For the accuracy most of the network settings reached high accuracies, while the unfrozen networks had slightly higher results (Cabezas et al., 2020). Initialising the network with ImageNet weights did not increase the results significantly and the identification of the blueberry class was not increased (Cabezas et al. 2020).

7.4.7.3.2 Experiment 2: Comparison of different networks

In the precious studies, ResNet50 and UNet were assessed in order to classify evergreen and deciduous trees (Kentsch et al., 2020). A comparison with other networks (presented in section: deep learning architectures) is necessary to test which network provide sufficient results for the application. The networks were tun with limiting effects of randomness, discussed in Cabezas et al. (2020), to ensure that the networks run under the same conditions, with the same data distribution and the same testing set.

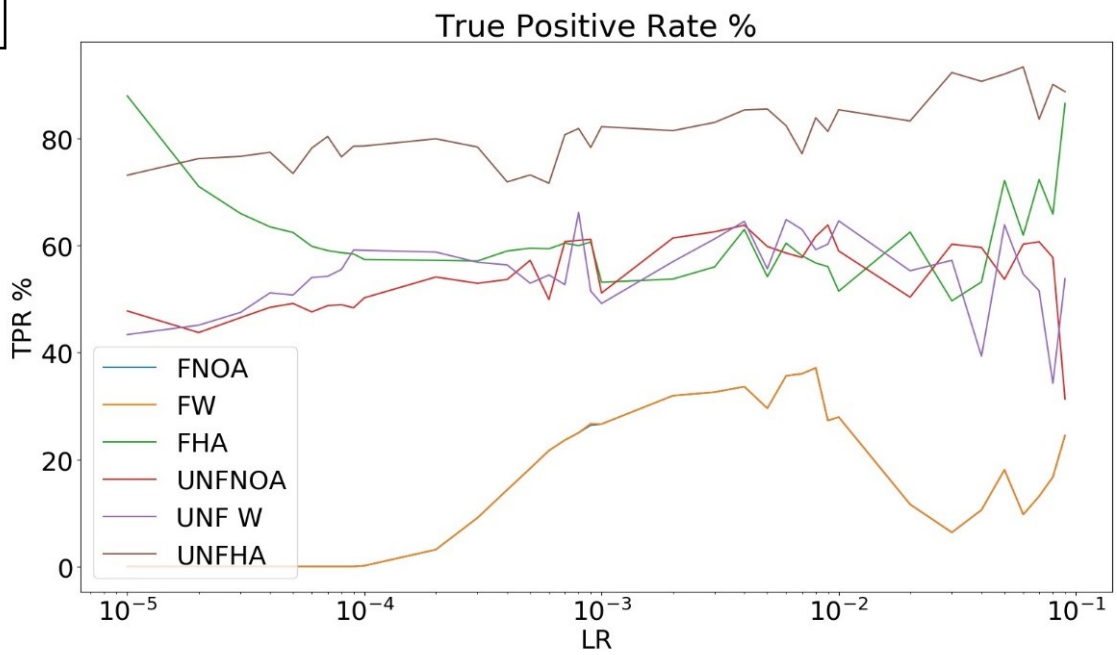
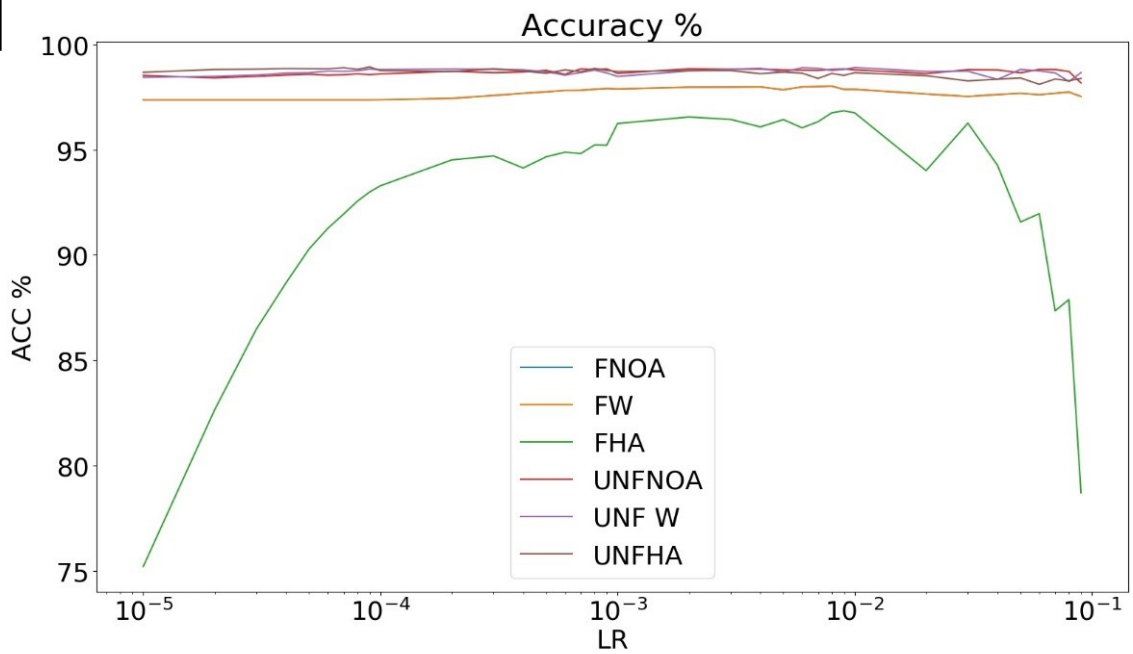
A**B**

Figure 90 TPR (A) and accuracy(B) results of different tests for the blueberry class with F = Frozen and UNF = unfrozen network settings. Additionally: data augmentation or loss function weighting with FNOA and UNFN OA and with loss function weighting, FW and UNFW, with function weighting and intensive use of data augmentation, FHA and UNFHA (Cabezas et al. 2020)

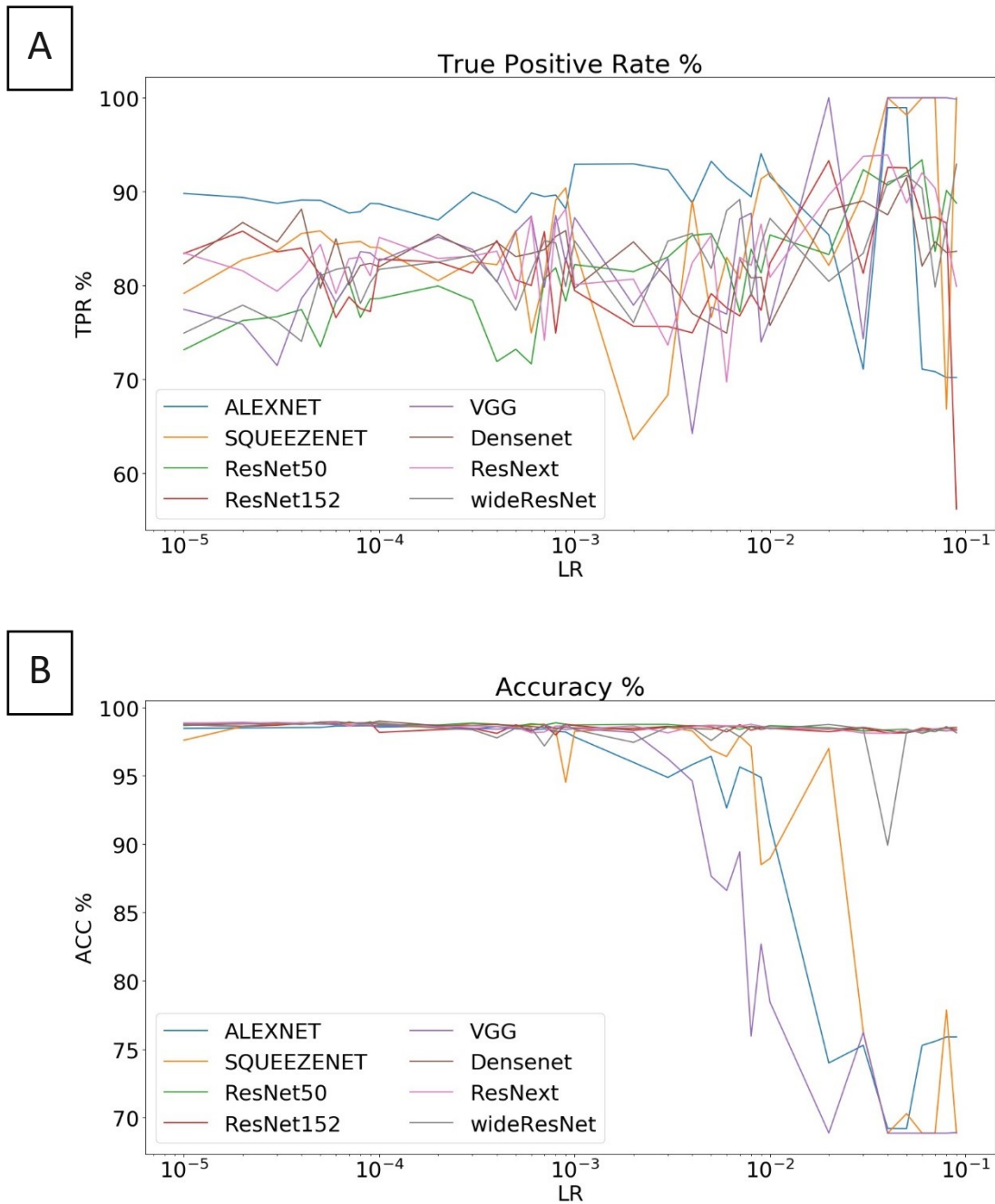


Figure 91 TPR (A) and accuracy (B) results of the network comparison. Networks: AlexNet, ResNet50, ResNet152, VGG, Densenet, ResNeXt, wideResNet (Cabezas et al., 2020)

Insufficient results were obtained by AlexNet's, Squeezenet's and VGG's, while wideResNet performed only well for some LR, which might be a result of the data imbalance (Figure 91). Densenet and the ResNet-based networks reached high TPR and accuracies (Figure 92) with only TPRs presented here to provide insights of the best results, as the accuracies were varying insignificantly between 98.90 % (ResNeXt) and 98.98 % (Densenet). The imbalance in data indicated that the TPR need to be higher than 98% to successfully identify blueberry bushes. Best results were therefore found in ResNeXt (TPR=93.75, Acc=98.11) ResNet50 (93.39, 98.10) and ResNet152 (92.54, 98.13) (Cabezas et al., 2020).

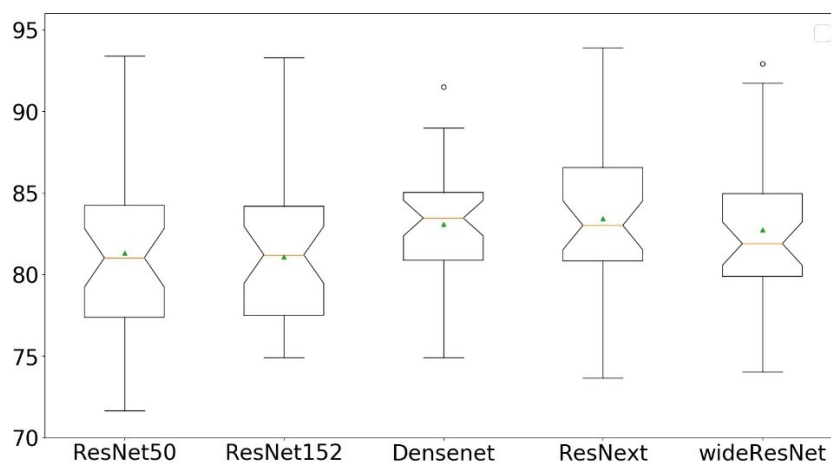


Figure 92 Comparison of ResNet50, ResNet152, VGG, Densenet, ResNext, wideResNet TPRs

7.4.7.3.3 Experiment 3: Deep learning application

After assessing the different architectures and settings, the best working model was applied to produce results for the application.

ResNet50 was found to show the best overall performances on the giving dataset with transfer learning and unfrozen weights, so a training of all layers and updating weights after each learning step. The data imbalance was addressed by weighting blueberry patches of the soil class eight times and four times of all other classes. With data augmentation the 12 new samples were created for each patch to increase the number of training data, while 50% of the soil patches were removed from the original number of patches. The average results for TPR and the accuracy of the three testing stages were presented for each testing stage.

When no data augmentation was applied a TPR value of 63.8 % was reached, while with data balancing the value increased to 93.4 %. The overall accuracy was in both cases similar, with 98.8 % and 98.1 %. The network used with frozen weight failed because it reached only 37.1 % without the use of data augmentation, but a high overall accuracy of 98.0 %. However, the use of high data augmentation with frozen weights resulted in the best TPR value of 88.0 %, while the overall accuracy dropped to 75.2 %. These results showed that transfer learning with ImageNet weights can be used, but data augmentation is needed to increase the accuracy in detecting blueberry bushes.

The refinement step concentrated on the segmentation of the blueberry patches. The classification can be used as a coarse first segmentation, which is only able to predict large patches in which blueberry bushes can be found. The refinement step aimed to locate the bushes more precisely. It can

be seen, that the refinement step provided segmentations, which were closer to the manual annotations (Figure 93). Still, the refinement missed some of the blueberry bushes, which can be seen in Table 31. The Dice coefficient evaluated the overlap and the number of non-GT pixels contained in the predicted patches. The coarse mask provided low values around 0.2, while the refinement significantly improved the results to values of 0.5 to 0.6. The ratio of GT pixels covered is higher for the coarse mask with 0.88 to 0.95, than for the refinement (0.78 to 0.87).

Table 31 Numerical evaluation of the refinement step of the DNN. The rows marked "refined" stand for the algorithm after refinement while the rows marked "Coarse" correspond to the algorithm without refinement for each of the three studied mosaics. The Dice coefficient as well as the ratio of blueberry pixels in the Ground truth covered by each of the two masks is presented

	Mask type	Dice	GT cover
B1	Coarse	0.187	0.953
	Refined	0.526	0.860
B2	Coarse	0.264	0.949
	Refined	0.624	0.874
B3	Coarse	0.223	0.884
	Refined	0.587	0.789

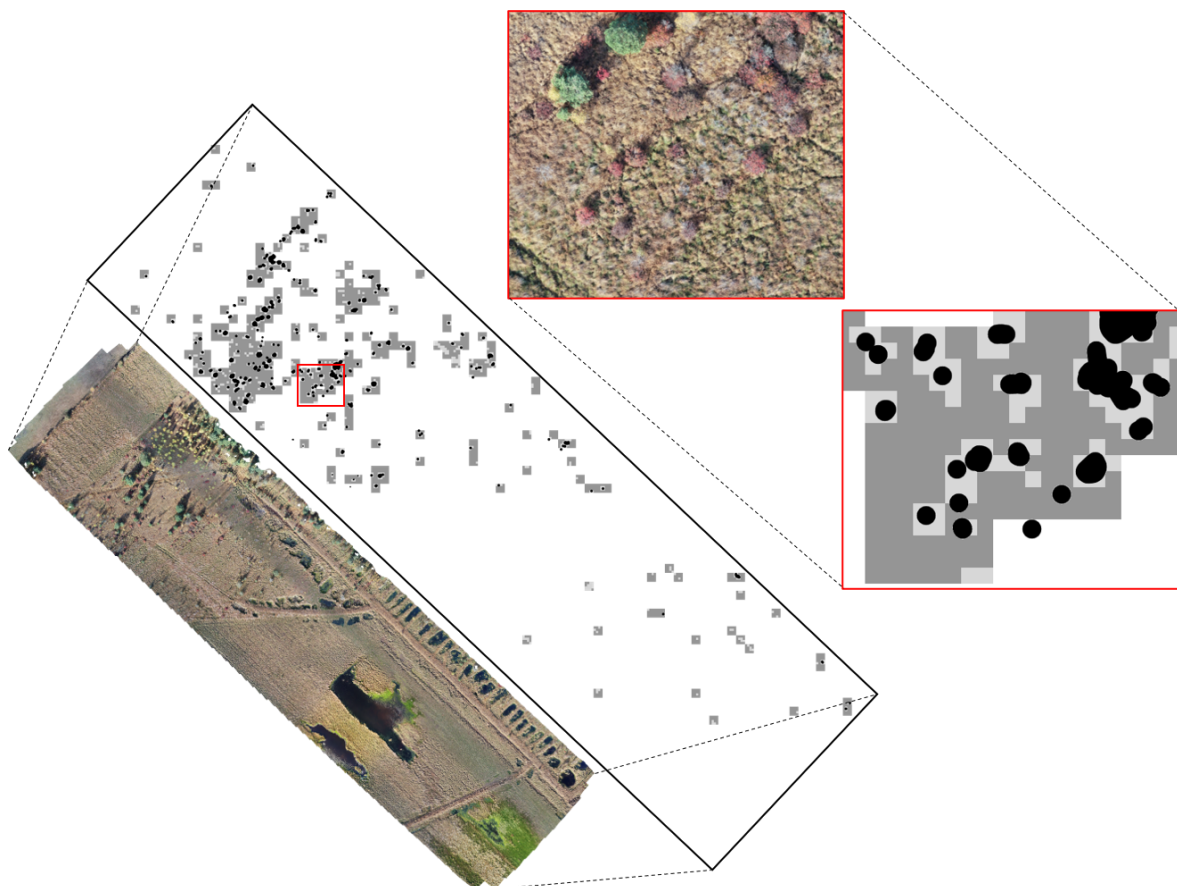


Figure 93 Orthomosaic B1 is imaged with a combination of the manual annotations (black marked spots), the coarse mask (dark grey) and the refined mask (light grey). The red box was zoomed in to show a detailed view on the image and masks

7.4.8 Discussion

The applied methodology used UAVs to gather information in a restricted access area. Techniques from several research fields were applied to gain knowledge about the distribution and properties of the bushes of the invasive blueberry species. The presented results are interpreted in this section in order to assess the stage of the invasion in each of the mosaics.

7.4.8.1 Difficulties with data

Blueberry plants show a characteristic red leaf colour in autumn, which makes them easily recognisable and identifiable in comparison to other classes of vegetation. However, partly visible soil with reddish tones constrained blueberry identification. This problem was especially critical for small blueberry bushes. In autumn the leaf colours can vary between red, red with a yellowish tone and partly black. This caused challenges for the annotations and for the DL algorithm, since the number of blueberry images was already low in comparison to the other classes and made the colour approach not usable for this study. Further complications were given by light conditions during image taking. When the blueberry bushes had brighter red colours due to sun light, it was difficult to distinguish them from the ground. Bushes, which were located in the shadows, especially the ones which had a predominately black colour were hardly recognisable.

The analysis presented some difficulties in the calculations of the height and surface area of the blueberry bushes. The main problems during the determination of the bush height were occlusions due to nearby trees and difficulties due to dense floor covering vegetation.

As the cluster analysis showed, the high density of blueberry bushes in some areas and their proximity increased the possibilities that bushes were partly covered and the whole bush area was not visible, as already pointed out by [Stieper \(2018\)](#). Furthermore, bushes were often located close to trees which have canopies that can cover most of a blueberry bush. The areas calculated for the blueberry bushes, exceeding 4 – 5 m², indicated that there has to be more than one bush, which was difficult to identify in the images, as well as for calculating the height. Wetland regions, imaged in the orthomosaics, are grassland and covered with dense hassocks. Therefore, the soil was often not visible and the ground annotations often represent the height of the hassocks, which resulted in values of 0 m maximum height and even more bushes showed a value of 0 m, when the median height was calculated for smaller bushes, especially in B4 and B6. Therefore, it is assumed that the hassocks can reduce the real height of the bushes by 30 cm. However, the calculated height values exceeded 3 m, which is unusual for the blueberry species studied here. There were errors produced when the annotations contained parts of an overlapping tree canopy, which increased the maximum height. The median height was

resistant to outlier values. When parts of the ground were annotated, the median generally decreased the height values, especially for small bushes. Annotations of the ground needed to be set carefully, since the wetland was uneven and depressions could increase the height values of the blueberry bushes. Furthermore, the differences between the maximum height and the median height can be influenced by the structure of the bush canopy. Due to these difficulties, a correlation between height and area values of blueberry bushes was not considered, but a comparison of the distribution of these values showed that the distribution was similar and that the bush area was larger than the height.

Even though these values are estimations, the applied methodology gave a good overview over a large study area, which cannot be done otherwise by extensive field measurements due to wetland protection regulations. Therefore, despite the difficulties, the achieved results emphasised the following discussion of applications and the qualitative use of the introduced methodology.

7.4.8.2 Application in landscape management

The collection of high-resolution images and the gathered information can help to map and visualise the findings of this study. This information can be used to easily establish management measures against the further invasion of blueberry species into the wetlands as already pointed out in several studies ([Wan et al., 2014](#), [Mafanya et al., 2017](#)).

The area occupied by blueberry bushes was low in comparison to the total studied area (covering 1 to 1.5 %), which is lower than the identified 3 to 5 % in ([Essl, 2004](#)). However, when only the living vegetation was considered, the number of blueberry bushes was found to increase from 8.2 up to 21.1 %. These percentages can be considered to be very high due to the fact that the species is invasive and does not belong to this sensitive ecosystem. B6 has the largest area and contained the smallest number of blueberry bushes, with the lowest height and area values measured. The invasion seems to be therefore in an early stage and should be easier to manage. Nevertheless, as shown by the persistent homology and the high number of single bushes after clustering, bushes were widely spread, which increases the area where measures against the blueberry bushes need to be considered. The hotspot analysis and the density map of B6 indicated that there are some bushes, which are concentrated in a dense spot in the middle of the area and distributed from there homogeneously. These findings allowed the conclusion that the progress of the blueberry bushes into this site is low.

B1 has a similar distribution, while the number of blueberry bushes per hectare is doubled in comparison to B6. The density map showed high densities in the northern part of the orthomosaic and a gradual decrease of blueberry bushes in the southern direction, which was confirmed by the hotspot analysis. The density of the bushes was higher than in B6, but, as indicated by the persistent homology,

the spread was greater. This meant that the blueberries invaded but did not reach every region of the site. Furthermore, the blueberry bushes in B1 had the largest bush area within all studied sites. The identified bushes maturity suggested that the blueberry species had invaded the area a long time ago. Since the density map provided the information that the blueberry bushes were mainly distributed in the north, there have to be conditions in the south which prevented a further spread.

In comparison, B2, B3 and B4 showed a high spread in the southern direction, because blueberry bushes of various sizes were found everywhere and there were higher concentration areas and several spreading centres. These findings can be confirmed with the persistent homology and the density map, indicating a high progress of the invasion. The three orthomosaics seemed to have a homogeneous distribution and a gradual change to lower numbers in southern direction. However, the significant differences found by the hotspot analysis indicate that there are conditions which influenced the distribution of the blueberry bushes as in site B1. In addition, all three orthomosaics showed an area with a small density of bushes, which can probably be explained by the high water content in the soil correlated with unsuitable conditions for plant growth. The invasion of the blueberry species was characterised as such and far advanced for B2 to B4. Only B4 had smaller bushes covering a smaller area, which means that the invasion was less advanced than for B2 and B3. The spread will probably increase there in the following years.

Furthermore, the distribution of the blueberry bushes can be connected to the proximity of trees, especially in B1 to B3, where the bushes were mainly found around pine trees and shrubby birches, since birds use these as rest areas and distribute seeds mainly where they rest. An exception was B4, where the trees were located next to depressions filled with water, which confirmed the unsuitable living conditions for blueberry species. In general, it seems that more blueberry bushes occurred when the density of the living vegetation was higher, which can be explained by better living conditions and a better distribution through birds.

To sum up the results and interpretations, it was found that B6 showed an early stage of invasion. B1 showed an advanced stage of invasion with limitations in the south, while B2 to B4 showed a critical, advanced stage of invasion, since blueberry bushes were found in the whole study site. The methodology used here helped to assess the stages of invasion.

This study introduced a method to help to preserve a sustainable and adaptive conservation. Together with further expert interpretations, a deeper understanding of wetland ecosystems can be achieved ([Dronova, 2015](#)). The calculated properties, height and area, are indices which can be used for plant growth monitoring and therefore provide useful information for the practical management of wetlands.

7.4.8.3 Automatic masks generation

DL techniques were used to assess whether DNN can be used to automatically detect the presence of blueberry bushes. Since the manual annotation of the blueberry bushes is the most time-consuming step of this workflow, this has the potential to greatly extend the range of studies. The results in section DL results showed that the ResNet50 network succeeded at the classification tasks associated to this problem and that the best results were obtained by re-training the whole network. In this respect, relying on pre-trained weights from ImageNet to solve the problem after minor re-training of the last layer is suboptimal. A dataset must be large enough to re-train the full networks. In this case, it meant using images taken from three mosaics covering a total of 33 ha. Still, the benefit of transfer learning was that it stabilized the network behaviour, as shown in smaller variances in achieved accuracies and statistically significantly smaller accuracies were reached according to [Cabezas et al. \(2020\)](#).

At the same time, the results also quantified how a data unbalance may result in a network that classifies most patches correctly even if the blueberry bushes were mainly misclassified. This shows that a balanced dataset is needed, when practical problems need to be solved, as the aim was to identify the blueberry bushes in the images. The solution was to apply techniques like data augmentation and loss function weighting, which increased the amount of blueberry bush examples and decreased the amount of soil examples in the dataset and at the same time assign weights to each class depending on their importance. This helped to reduce bias of the training towards the correct classification of blueberry bushes. High TPR with FPR lower than 1 % needed to be achieved to be applicable for different use cases.

The results of the automatic classification were used to map the invasive species, which was an important first step, whereby a refined segmentation was vital to effectively determine the exact location of plant invasions ([Mafanya et al., 2017](#)). The DL applications used classified images, and a refined mask provided the blueberry bush locations. The refinement step was necessary in this application since most of the blueberry bushes were small. Hence, the refined mask offered a more precise localisation of the blueberry bushes. Even though not all bushes were found and some soil areas were misclassified as blueberry bushes, the refined mask could significantly reduce the time of manual annotations and provide maps of the studied area. Increasing the amount of blueberry data can help to optimize the classification accuracy and the localisation of blueberry bushes. This will be considered in future research. The generation of automatic annotation masks, as performed here, will further allow large scale studies with a minimum of disturbances in the studied environment.

Therefore, UAVs and image analysis provide accurate and cost-effective surveys which are needed when studying invasive species (Wan et al., 2014). The used techniques provided more information than gathered by previous field surveys in wetland areas (Schepker et al., 1997, Stieper 2018}.

7.4.8.4 Contribution to invasive blueberry studies in wetlands

The studies done in Germany were mainly fieldwork approaches. To the best of my knowledge this was the first study applying image analysis and especially DL techniques to investigate the species. Studies presented by (Schepker and Kowarik, 1998, Schepker et al., 1997) discussed invasive species in general with a special focus on the blueberry species. They already pointed out that the spread of the blueberry species has to be a concern. Especially (Schepker et al., 1997) studied the invasive species close to 13 plantations. They estimated the distribution area by looking for the blueberry bush which was the furthest away and stated that its distance was the maximum spread. This approach was inaccurate and the differentiation between different cover areas was insufficient. The area they researched was 12.5 km², but the authors stated that most numbers of studied areas and areas covered by blueberries were estimations (Schepker et al., 1997).

Another study focussed on the invasive blueberry species was presented by (Essl, 2004) studying an area of 4.7 ha, which is nine times less compared to the area studied in Lichtenmoor. Also, (Essl, 2004) stated that a complete detection cannot be guaranteed. The estimated coverage area was between 3 and 5 %, which is comparable with the presented study. The identified high number of young blueberry bushes was identified as future source of spread but no further information was provided. With the results presented in this study, small bushes could be identified and future spread centres were further interpreted with hot spot analysis.

A more recent study was presented by (Stieper, 2018), who already provided detailed information about the properties of blueberry bushes studied in a small area of the “Krähenmoor”. The author pointed out, that there are difficulties to estimate the distribution of blueberry bushes because of their different properties and their strong scrub encroachment, which were also identified on the presented images of this study. However, it was pointed out that most analysis were done on a subjective grading of blueberry bush coverage with taken images in the field. In comparison the provided objective grading, presented in this study, were necessary to compare invasive status in different sites. Furthermore, (Stieper, 2018) stated a high possibility in identification losses during the fieldwork because of the density of bushes in some areas and only areas were analysed close to former blueberry plantations. The limitations of study areas, when fieldwork need to be conducted, are high, as can be seen in (Stieper, 2018), where they studied the region for ten days. Using UAVs, an area of 62 ha could

be covered in one day. In comparison to all previous studies, the whole area can be covered with UAVs and all blueberry bushes can be identified. Coverage areas can be calculated in each image accurately. Further the methodology presented in this study allows to monitor the area and to provide maps of change detection. Therefore, the success or failure of measures against the invasive species can be directly monitored and user friendly presented with the help of ArcGIS.

7.4.8.5 Deep learning studies

Wetland classifications were performed by (Rezaee et al., 2018) and (Liu and Abd-Elrahman, 2018) identifying 4 and 6 classes, reaching overall accuracies of 94.82 % and 82.02 %. Transfer learning, which was only applied in (Rezaee et al., 2018), showed the effectiveness of these technique for natural environment studies, when the dataset is large enough. The best result of (Liu and Abd-Elrahman, 2018) was observed when using multi-view images, which might be an interesting approach for future studies. A similar approach to detect invasive species was used by (Ashqar and Abu-Naser, 2019). Their approach applied DL with data augmentation and transfer learning. Their highest accuracies were 97.6 %, which was slightly less, compared with the overall accuracies of 98.83 % and 98.10 % found for Lichtenmoor. It has to be considered, that in the approach of Ashqar and Abu-Naser, (2019) the dataset mainly contained images of the invasive species, while only 2.64 % of the generated patches of B1 to B3 contained the invasive species. This shows that with the application of loss functions and data augmentation it was possible to achieve high accuracies (Ashqar and Abu-Naser, 2019).

7.4.9 Opportunities, limitation and future works

The appearance of invasive species shows generally an increasing trend. Studies were conducted to increase the knowledge of impacts, abundance, threatening to biodiversity and costs caused by invasive species. There were no generalized methodologies to study invasive species, which increased the demand of a new and generalized methodology. Connections between different study areas need to be established and accepted to gain further knowledge and increase the possibilities to tackle the problem of invasions. Studies were mainly conducted when invasive species were established in a region. Therefore, most studies failed to study the pathways invasive species have and how they are introduced. Regional differences and small-scale studies increase the variables why invasive species choose specific pathways and why they are introduced.

The presented work provided the methodology to analyse the invasive species from UAV images. Nevertheless, there were limitations regarding the data. The autumn season seemed to be a good time

for image taking, but the difficulties regarding the varying colour of the blueberry bushes should be taken into account more carefully. Image taking could be done when the weather is cloudy and not windy as suggested in previous studies (Zmarz 2014; Wierzbicki et al., 2015).

The chosen flight altitude of 50 m resulted in high-resolution images, which created heavy orthomosaics. The resolution was reduced to 5 to 7 cm/pixel to be able to use image processing software. This led to difficulties of identifying blueberry bushes and their properties. For the future different flight settings can be tested, as presented in (Dandois et al., 2015; Falkowski et al., 2018), especially smaller flight areas and a reduced flight height can help to increase the resolution and the results of blueberry bush properties. Additionally, the accuracy of the DL algorithm can be improved when the blueberry bushes are larger on the images. The amount of blueberry bush data was limited, which caused challenges for the DL algorithm. That can be overcome by the collection of more blueberry bush images. Since blueberry bushes were often planted for blueberry production, those fields offer a good opportunity to collect images. Therefore, the detailed mapping of this study can further improve the results of the current status of the blueberry species invasion. A repeated data collection in the same area, as planned, will provide a year-to-year comparison in order to monitor and analyse the invasion, the development in the wetlands and the further spread. Changes will be easily detectable within the wetlands and the studied blueberry species without disturbances of vulnerable plants, animal species and habitats, as already mentioned by (Dronova, 2015, Mafanya et al., 2017).

7.4.10 Conclusion

In this paper a multi-disciplinary methodology to quantitatively evaluate the role of plant species in ecosystems, including invasive species were introduced. The use of UAVs makes the approach applicable even in restricted access areas and increases the total area that can be studied, greatly exceeding the range of existing field studies. This methodology was used to gather information about wetland vegetation. Simple and time-saving methods were applied to classify vegetation and to provide information about the properties of the invasive blueberry species found in the study site. The distribution of blueberry bushes was analysed in terms of their density, clustering and spread. The relative importance of blueberries in the wetland was analysed (number of bushes, bush area and bush height). This information was transformed into location, density and hotspot maps to provide advanced visualization tools. DL techniques were used to automatically detect and segment blueberry bushes, opening the possibility to further extend the range of similar studies.